

- *J. T. Henderson, *President*
- Yasujiro Niwa, *Vice-President*
- *W. R. G. Baker, *Treasurer*
- *Haraden Pratt, *Secretary*
- *D. G. Fink, *Editor*
- *J. D. Ryder, *Senior Past President*
- *A. V. Loughren, *Junior Past President*

1957

- J. G. Brainerd (R3)
- J. F. Byrne
- J. J. Gershon (R5)
- A. N. Goldsmith
- A. W. Graf
- W. R. Hewlett
- R. L. McFarlan (R1)
- *Ernst Weber
- C. F. Wolcott (R7)

1957-1958

- II. R. Hegbar (R4)
- E. W. Herold
- K. V. Newton (R6)
- A. B. Oxley (R8)
- F. A. Polkinghorn (R2)
- J. R. Whinnery

1957-1959

- D. E. Noble
- Samuel Seely

*Members of Executive Committee

George W. Bailey,
Executive Secretary

- Evelyn Benson, *Assistant to the Executive Secretary*
- John B. Buckley, *Chief Accountant*
- Laurence G. Cumming, *Technical Secretary*
- Emily Sirjane, *Office Manager*

EDITORIAL DEPARTMENT

- Alfred N. Goldsmith, *Editor Emeritus*
- D. G. Fink, *Editor*
- E. K. Gannett, *Managing Editor*
- Helene Frischauer, *Associate Editor*

ADVERTISING DEPARTMENT

- William C. Copp, *Advertising Manager*
- Lillian Petranek, *Assistant Advertising Manager*

EDITORIAL BOARD

- D. G. Fink, *Chairman*
- E. W. Herold, *Vice-Chairman*
- E. K. Gannett
- Ferdinand Hamburger, Jr.
- T. A. Hunter
- A. V. Loughren
- W. N. Tuttle

Authors are requested to submit three copies of manuscripts and illustrations to the Editorial Department, Institute of Radio Engineers, 1 East 79 St., New York 21, N. Y.

Responsibility for the contents of papers published in the PROCEEDINGS OF THE IRE rests upon the authors. Statements made in papers are not binding on the IRE or its members.



Change of address (with 15 days advance notice) and letters regarding subscriptions and payments should be mailed to the Secretary of the IRE, 1 East 79 Street, New York 21, N. Y.

All rights of publication, including foreign language translations are reserved by the IRE. Abstracts of papers with mention of their source may be printed. Requests for republication should be addressed to The Institute of Radio Engineers.

PROCEEDINGS OF THE IRE®

Published Monthly by

The Institute of Radio Engineers, Inc.

VOLUME 45

November, 1957

NUMBER II

CONTENTS

Scanning the Issue	1456
Poles and Zeros	1457
W. R. G. Baker, Treasurer, 1957	1458
6247. Engineering Education: A View Ahead	John D. Ryder 1459
6248. Future Circuit Aspects of Solid-State Phenomena	Edward W. Herold 1463
6249. High-Frequency Semiconductor Spacistor Tetrodes	H. Stutz, R. A. Pucel, and C. Lanza 1475
6250. The Utilization of Domain Wall Viscosity in Data-Handling Devices	V. L. Newhouse 1484
6251. Correction to "Prediction of Semiconductor Surface Response to Ambients by Use of Lewis Acid-Base Theory"	C. G. Peattie and J. R. Macdonald 1492
6252. IRE Standards on Reference Designations for Electrical and Electronic Equipment, 1957	1493
6253. Design of Transistor Regulated Power Supplies	R. D. Middlebrook 1502
6254. Correction to "Theory and Experiments on Shot Noise in Semiconductor Junction Diodes and Transistors"	W. Guggenbuehl and M. J. O. Strutt 1509
6255. A New Technique in Ferrite Phase Shifting for Beam Scanning of Microwave Antennas	F. Reggia and E. G. Spencer 1510
6256. Slalom Focusing	J. S. Cook, R. Kompfner, and W. H. Yocom 1517
6257. Bip periodic Electrostatic Focusing for High-Density Electron Beams	Kern K. N. Chang 1522
6258. The Equalization of Base-Band Noise in Multichannel FM Radio Systems	Charles A. Parry 1527
6259. Theory of a Wide-Gap Emitter for Transistors	Herbert Kroemer 1535
6260. Shot Noise in Transistors	G. H. Hanson and A. van der Ziel 1538
Correspondence:	
6261. Spectrum Analyzer for Whistlers	Raymond R. Nelson 1543
6262. Long Life Microwatt Batteries	Cyril F. Elwell 1543
6263. Masers and Reactance Amplifiers—Basic Power Relations	Bernard Salzberg 1544
6264. Very Narrow Base Diode	B. R. Gossick 1545
6265. The Use of Surface Weather Observations to Predict the Total Atmospheric Bending of Radio Rays at Small Elevation Angles	B. R. Bean and B. A. Cahoon 1545
6266. Arc Prevention Using P-N Junction Reverse Transient	William Miller 1546
6267. On Higher Order Approximations to the Solution of Nonuniform Transmission Lines	Laszlo Solymar 1547
6268. Unilateralized Common Collector Transistor Amplifier	Lucio M. Vallese 1548
6269. Improvement of Impedance for Microwave Reflector Feed	M. W. Scheldorf 1548
6270. A Simplified Procedure for Finding Fourier Coefficients	Jean A. Develet, Jr. 1549
6271. On the Universal Standard of Time and the Velocity of Light	Reinhold Gerharz 1549
6272. Propagation of a Pulse Across a Coast Line	James R. Wait 1550
6273. Yttrium Garnet UHF Isolator	F. R. Morgenthaler and D. L. Fye 1551
6274. Radio Observations of the Russian Earth Satellite	R. R. Brown, P. E. Green, Jr., B. Howland, R. M. Lerner, R. Manasse, and G. Pettengill 1552
6275. Radio and Radar Tracking of the Russian Earth Satellite	A. M. Peterson and Staff 1553
Contributors	1555
IRE News and Radio Notes:	
Calendar of Coming Events and Authors' Deadlines	1558
Professional Groups	1560
Sections and Subsections	1561
6276. Abstracts of IRE TRANSACTIONS	1566
6277. Abstracts and References	1568

ADVERTISING SECTION

Meetings with Exhibits	6A	Notes	56A	Membership	74A
News—New Products	16A	Professional Group		Positions Open	133A
IRE People	28A	Meetings	58A	Positions Wanted	136A
Industrial Engineering		Section Meetings	66A	Advertising Index	181A



THE COVER—Resting on a finger at the right is a tiny cryotron, a super-conductive computer switching element. The impact of this and other new solid-state devices on future circuitry is typified by the "Megacoder" on the left, an experimental decoding device for a pocket-size radio paging system which can select one of over a million coded signals on the same wavelength. This array of transistors, ferrite cores, and other elements, embedded in plastic and mounted on a printed wiring board, is a first step towards the eventual development of components which will combine in a single solid the functions of many components and wires, as discussed in the review of future solid-state circuits on page 1463.

Cryotron photo—Arthur D. Little, Inc.
"Megacoder" photo—RCA Laboratories

Scanning the Issue

Engineering Education: A View Ahead (Ryder, p. 1459)—In this age of rapid scientific progress, unless our educational system goes much further in teaching engineering as a science and less as an art, the engineer of the future will be left with a training that will become obsolete as rapidly as the particular devices and practices he learned about in college. The engineering curriculum of the future, says this noted educator, must have as its primary objective the study of the fundamental sciences of nature; the teaching of "hardware" should be left largely to the industrial employer. If this timely warning is not heeded, new fields of engineering will fall by default to better equipped professionals in other fields of science.

Future Circuit Aspects of Solid-State Phenomena (Herold, p. 1463)—The host of solid-state developments of the past decade have already changed the basic character and behavior of many present-day circuits. Just how far-reaching these changes will be in the future is set forth in this stimulating review of the newest solid-state device ideas now under consideration and development. Among the topics considered are superconductivity, molecular amplification, magnetic effects in semiconductors, and nonlinear capacitance in junctions. The author describes, in a manner that will appeal to all readers, the basis of operation of several new devices utilizing these phenomena, and points out a number of intriguing possibilities for future applications. Especially significant is the author's suggestion of employing controlled inhomogeneity in solid-state devices of all types to produce totally new circuit elements which combine in one solid the functions of many present components and associated wiring.

High-Frequency Semiconductor Spacistor Tetrodes (Statz, *et al.*, p. 1475)—This paper presents the first full technical description of an important new type of semiconductor device which received considerable public attention when it was announced last summer. Like the depletion layer transistor discussed here last month, the basic idea is to inject electrons into the high-field space-charge region of a reverse-biased junction to obtain shorter transit times and higher operating frequencies. This device is distinguished by having two contacts in the space-charge region: an injection contact and a second contact which modulates the injection current. The result is a device that offers not only important improvements in high-frequency response but also many of the attractive features of a vacuum tube, especially with regard to high input and output impedance and very low coupling between input and output circuits.

The Utilization of Domain Wall Viscosity in Data-Handling Devices (Newhouse, p. 1484)—Some new and potentially important observations are reported on the behavior of magnetic materials when subjected to extremely short pulses in the millimicrosecond region. It has been discovered that magnetizing pulses much larger than the normal limit can be applied without permanently changing the state of magnetization of a material, provided the pulses are short enough. This phenomenon is explained in terms of the elasticity and viscosity of the walls of the magnetic domains in the material, and is shown to offer much-improved methods for very high speed switching and for nondestructive read-out of storage devices.

IRE Standards on Reference Designations for Electrical and Electronic Equipment (p. 1493)—This Standard, a revision of a previous one issued in 1949, establishes the methods of designating some 200 kinds of components and parts on diagrams, parts lists, and on the equipment itself, in a manner compatible with existing military standards.

Design of Transistor Regulated Power Supplies (Middlebrook, p. 1502)—A new form of transistor series regulated power supply is presented which boasts an extremely low output resistance, excellent transient response to sudden

changes in load, and yet simple and economical circuitry. The design will find widespread application to high-current low-voltage power supplies such as are employed in a wide variety of laboratory equipment.

A New Technique in Ferrite Phase Shifting for Beam Scanning of Microwave Antennas (Reggia and Spencer, p. 1510)—This paper discloses a new design for a phase shifter which affords a simple electrical means of beam scanning with a stationary antenna at X-band frequencies. By placing a small ferrite rod inside a rectangular waveguide and subjecting it to a longitudinal dc magnetic field, phase shifts in excess of 300° per inch can be obtained with relatively small applied fields. If the phase shifter is placed in one arm of a two-element antenna, the direction of the antenna beam can be varied by small changes of control current. Because of its simplicity, small size and light weight, this development promises to be very useful for rapid-scanning antennas.

Slalom Focusing (Cook, *et al.*, p. 1517)—An ingenious method is proposed for electrostatically focusing high density electron beams by which a sheet-shaped beam is made to weave sinusoidally through an array of positive rods or wires placed midway between two negative plates. In addition to providing a unique type of focusing scheme for traveling-wave devices, the arrangement may find application in beam switching devices; if one of the center wires is driven negative the course of the beam will be altered. Moreover, if two wires are driven negative, the portion of the beam between them can be trapped and made to slalom back and forth for a time until released, thus suggesting a new type of storage device.

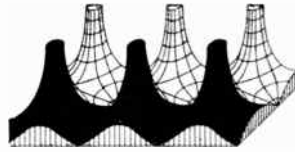
Biperiodic Electrostatic Focusing for High-Density Electron Beams (Chang, p. 1522)—This is the second paper in this issue to deal with electrostatic focusing of high-density beams. The subject is significant because the extremely large forces required to focus a high-density beam have not heretofore been realizable by electrostatic methods, and electrostatic systems have thus been confined to low-density applications. This paper presents a noteworthy solution to the problem by employing two periodic fields, counteracting each other, instead of only one field. The fields are produced by two periodic structures that are coaxial to each other, with the hollow electron beam flowing between them.

The Equalization of Base-Band Noise in Multichannel FM Radio Systems (Parry, p. 1527)—Noise which falls in the channels of a multichannel fm radio system increases with frequency. Consequently, the noise is greatest in the upper channels. In order to redistribute this noise more evenly among the channels, pre-emphasis and de-emphasis networks are commonly employed to emphasize the higher-frequency transmissions. This paper presents an excellent analysis of the effects of these equalizing networks on signal-to-noise improvement, and provides a practical method of adjusting a system having these networks for maximum improvement.

Theory of a Wide-Gap Emitter for Transistors (Kroemer, p. 1535)—This paper points out that a significant increase in the performance capabilities of transistors is possible by using an emitter material with a higher energy-band gap than the base material. The greater activation energy that results causes an improvement in the injection efficiency of the emitter; which in turn prevents a fall-off of the current amplification factor at high current levels. Equally important, it reduces the amount of emitter doping usually required, resulting in a much lower emitter capacitance. This effect can be utilized either to increase frequency range or power capabilities.

Shot Noise in Transistors (Hanson and van der Ziel, p. 1538)—This clear, well written account presents experimental verification of a previously published and important theory that describes the generation of noise in transistors.

Poles and Zeros



Solid. E. W. Herold has prepared, as one of a series of invited reviews, a paper (this issue, p. 1463) which brings together two traditionally separate subjects in electronic technology, circuit concepts, and the physical properties of solids. Ed Herold has spent over thirty years in the vacuum tube arts (his second job was with E. T. Cunningham) and he has been in the thick of electron tube development throughout that time. He was, therefore, an engineer who had some mental habits to rearrange when the transistor and its cousins came along. He has negotiated the transition with conspicuous success, as his paper shows.

He says this of the future of solid-state devices: "We may look forward to the day when the synthesis of an improved compound, its technology of use, or the discovery of a new effect in solid materials can do more to revolutionize the performance of an electric circuit than all the classic ingenuity of the circuit designer." The paper explains from first principles such effects as superconductivity, molecular resonance, the Hall effect, depletion in semiconductor junctions and charge carriage in crystal lattices, and it relates these phenomena to the remarkable circuit properties of gyrators, masers, semiconductor capacitors, drift transistors, and other latter-day devices which are radically changing the course of electronics. Since the paper is not only authoritative and comprehensive, but also highly readable, we commend it to all PROCEEDINGS readers.

Backtalk. Passed on herewith is an account of conversations held at the M.I.T. Lincoln Laboratory between the TX-2 electronic computer and Mr. Jack Gilmore. The TX-2 machine has a $2\frac{1}{2}$ million-bit internal high-speed memory in which it is feasible to store standard inquiries and responses concerning the current state of a program or computation. It was a simple, if somewhat frightening, step to arrange these questions and answers to print in plain English on the electric typewriter, rather than in the more usual (and admittedly more efficient) numeric or mnemonic code symbols. Mr. Gilmore is thereby able to commune with the machine in a manner calculated to astound the uninitiated on-looker.

Example: Mr. Gilmore types in the word "prince."

This brings into play a standard utility printout program and the machine responds, "Do you want the vertical column layout?" Gilmore chides the machine gently with "Be brief." The machine responds equably, "Yes sir" and waits for the answer to its question. Gilmore answers "No." The machine then asks (briefly, as advised) the relevant questions for the printout and receives answers: TX-2 Instructions? / *Gilmore No* / TX-2 First? (what is the first memory register to be printed?) / *Gilmore 2* / TX-2 Last? (what is the last memory register to be printed?) / *Gilmore 7* / TX-2 15 740000 626600 740000 200015 200013 (the contents of the requested registers) / TX-2 More? / *Gilmore No* / TX-2 Finished.

Mr. Gilmore is talking to himself, of course, since he set up the utility program in the machine in the first place, and he couldn't afford much of this plain language business if customers were lined up waiting to use the computer. But, for all that, it's not mere whimsy. Much communication is thus stylized (including many an inquiry from engineering to accounting). It is, we think, highly significant that expert programmers like Gilmore and his associates find that such direct "on-line" communication with the machine is a valid technique for testing programs and machine operations under many conditions. This effort at Lincoln is, as W. N. Papian has advised us, "part of a serious long-term effort toward improving one of the weak areas in the digital-computer field, the man-machine relationship." For all this worthy purpose, we won't be surprised if one of these days TX-2 gets mad and tells Gilmore off, at length, when advised to "be brief."—D.G.F.

Sputnik. On the assumption that the Russian earth satellite will still be with us, at least in memory if not in substance, when this issue reaches the membership, we have hastily inserted two letters to the editor on the subject. They report the first results of attempts to determine the satellite's velocity, altitude, and path by radio and radar observations during the week following its appearance on October 4. We trust that our interest in these early reports on Sputnik's peregrinations, and on the use of the tools of our trade to decipher them, will be shared by our readers.—E.K.G.



W. R. G. Baker

TREASURER, 1957

Walter R. G. Baker was born November 30, 1892 in Lockport, N. Y. He received his bachelor's degree in 1916 and his master's degree in 1918, both from Union College. Later in 1935 that same institution presented him with an honorary Doctor of Science degree, and in 1951 Syracuse University honored him with a Doctor of Engineering degree.

Dr. Baker joined General Electric's Research Laboratory in 1917 and forthwith became engaged in the development and testing of radio apparatus for military mobile vehicles. In 1924 he assumed the responsibility for the design of all radio products and in 1926 he was given complete charge of development, design and production. He oversaw the design of the pioneer broadcasting stations KOA in Denver, KGO in Oakland, and WGY and the radio developmental laboratory in Schenectady. The latter maintained communications with the early Byrd Antarctic expeditions.

When RCA was founded in 1929, Dr. Baker joined its staff. He became head of its production and later its vice-president of engineering and manufacturing.

In 1935 when General Electric renewed radio-receiver activities in Bridgeport, Conn., Dr. Baker returned to the company. He became managing engineer in 1936, and in May, 1939 he was named manager of General Electric's radio and television department.

In October, 1941, Dr. Baker was elected a vice-president and his departments were fused into the Electronics Department which produces radio, radar, television and similar electronics equipment. The present Electronics Park at Syracuse, N. Y. is the culmination of Dr. Baker's dream. He has been serving as vice-president and consultant to C. W. LaPierre, executive

vice-president of the Electronic, Atomic and Defense Systems Group.

Under Dr. Baker's chairmanship of the first National Television System Committee, standards for monochrome telecasting were developed, recommended and adopted by the Federal Communications Commission, and his leadership of the second NTSC resulted in the development of its proposed color television standards. Under his supervision as chairman of the Radio Technical Planning Board, recommendations for frequency allocations of all broadcasting services were formulated.

In 1953 the U. S. Army presented Dr. Baker with its Medal of Freedom for his application of electronics to Army research and development problems. The Electronics Industries Association (formerly the Radio-Electronics-Television Manufacturers' Association) bestowed its Medal of Honor upon him during the same year. He is now president of the EIA.

Dr. Baker became an Associate of the IRE in 1919 and a Fellow in 1928. He has been an IRE Director for the past eleven years, President in 1947, and Treasurer since 1951. He has served on a host of IRE and technical committees, and he is the present chairman of the Professional Groups Committee. He was chairman of the Philadelphia Section in 1930-31, and secretary of the Connecticut Valley Section from 1938 to 1940. From 1948 to 1952 he also served as IRE Representative on the ASME Glossary Review Board.

The IRE has rewarded his activities with the award of its Medal of Honor, given in 1952. He will be further honored at the annual banquet of the IRE National Convention next March, when he will be presented with the IRE Founders Award.

Engineering Education: A View Ahead*

JOHN D. RYDER†, FELLOW, IRE

Summary—The forces acting on engineering education are discussed, and it is shown that all these seem to point to a need for further movement away from technician training, and toward much further study of the fundamental sciences of nature in the education of all engineers for the future years. The place of mathematics in a computer age is also reviewed, and it is mentioned that the importance of the "physical model" decreases as the use of mathematics increases.

A simplification of the definition of engineering is proposed which places emphasis on the separation of science and art, showing the former to be the duty of a university, the latter of the industrial employer. The basis for an electrical engineering curriculum to treat the subject as a science is outlined and discussed as now being applied at one school.

THE IMPACT of electronics, nucleonics, and other new growth fields on engineering education has been a major factor in indicating some of the shortcomings of past educational practices and in pointing out the necessity for study of a future path which might be followed by technical education. Terman [1] previously discussed these effects and the necessity for clarification of our educational objectives. This paper is an attempt to rationalize some of the trends and to present a plan which, it is hoped, looks well into the future of engineering education.

In all that follows, it is only the technical aspects of the program which are being considered. It is assumed that the broader social aspects will also be investigated, made consistent with the general plan, and certainly not reduced in scope or magnitude.

THE TREND IN ENGINEERING EDUCATION

Engineering education probably began about the middle of the eighteenth century with the training of apprentices by the early builders of roads and steam engines. From this early beginning, in training for what was then a trade, has come our modern system of engineering education, exemplified by the engineering schools of the United States.

Among the early apprentices were a few who stood out from their fellows and were curious as to the "why" behind the devices, methods, and materials which they were using. These men learned from the work of the early physical and chemical investigators and added their own discoveries, so that through the nineteenth century the most curious individuals of each generation added to the store of knowledge. They learned why the early rule of thumb or empiricism worked, and gradually progressed to the development of a considerable knowl-

edge of basic scientific fact as it exists on this earth. This trend to fundamental scientific fact has continued and accelerated throughout the whole lifetime of engineering education.

BREADTH OF THE FIELD

The movement from the elements of a tradesman's knowledge to those of a scientist has been augmented since the last war by a realization of the tremendous breadth of opportunity existing to graduating engineers in the modern scientific age. Added to this is a realization that knowledge, based on purely temporal devices, may be of little value unless it is truly basic in its concern with our physical world. It is no longer practical or intellectually honest to prepare narrowly a graduate of a university for a specific field of work, because during this graduate's lifetime the field of work may become obsolete. This is well demonstrated by much engineering training of the early part of this century which was based on the steam engine. It may not be too far afield to assume that training based on the steam turbine may likewise be shown as obsolete in an age already concerned with jets and rockets. In fact, we may be in the last century of the life of the steam turbine since some developments of the nuclear engineering field hold considerable promise for the future attainment of electrical energy directly from the atomic nucleus. Certainly with only the presently available fuel resources of the earth, we cannot afford much longer the tremendous waste inherent in our use of the heat cycle. In any case, it is this continuing and rapid progress into new fields, and the utilization of new devices, that makes dangerous the education of our present engineering graduates in terms of the things or the "hardware" of the present or past.

In a day when our economy was based largely on raw materials and their production, the engineering student could be narrowly trained to the relatively few jobs available in such an economy. Today, with an economy based on manufactured goods, and with the variety of fields and the difficulty of problems much enhanced, it is no longer possible to predict safely that a given graduate will work in a given narrow field. For instance, in the 1920's an electrical engineering graduate was faced with the prospect of preparing for ultimate work in the field of electrical or communication utilities, electrical machinery, and to an extremely limited extent, radio receivers and transmitters. Today, these fields still exist, but in terms of engineering employment are far exceeded by the fields of electronics, including radar navigation, computers, feedback control and system design, solid-state electronics, nuclear engineering, and the like. A narrow program could certainly be justified in

* Original manuscript received by the IRE, July 22, 1957; revised manuscript received, August 28, 1957.

† Dean of Eng., Michigan State University, East Lansing, Mich.

1920 because the graduates were headed for work very largely in the production of the raw materials of the electrical industry. Today, it is extremely difficult to see how any form of an applied program could be suited to the breadth of the field. Similar breadth is apparent in most of our other engineering instructional fields as well.

COMPETITION BETWEEN FIELDS IN SCIENCE AND ENGINEERING

There is another factor also working in this same direction, but it has not been so apparent. This is the competition between existing fields of science and engineering. This competition is very real and of the roughest dog-eat-dog sort. If your portion of the profession does not do a really good fundamental job of solving its problems, someone else from another field may come along and do the work for you, because the present state of activity in science and engineering is not going to allow an important problem to remain long unsolved. If individuals in their own portions of the profession are not prepared to find the solutions, then individuals from other scientific or engineering fields will supply the answers. This threatens a high rate of obsolescence among fields of engineering which are not prepared to solve their fundamental scientific problems and to move into the new areas of knowledge as they are discovered.

Several fields can be cited as examples of this, one of them certainly being that of mining engineering, which now represents a minor field in engineering education. In the early days, the ore deposits were easy to find on the surface of the earth, and the mineral compounds were relatively easy to break. Later, as the surface deposits were worked out, the geologist was called in and aided in predicting where the ore or oil bodies might be found. The purification of the more complex ores and the petroleum products required help from the chemical engineer or the metallurgist. For example, in the eighteenth century, copper ores of less than 18 per cent copper were considered impractical, today many areas are working with copper ores of less than 1 per cent copper. Much work in the field has been taken over by the geologist, the metallurgist, and the chemical engineer, and the relative importance of mining as an engineering educational field has declined. Apparently someone else has done a better job in solving the critical and complex problems of today.

Sanitary engineering is a similar field, now reduced to less than 20 graduates annually in the United States. Its problems have become more complex and are being solved by the chemical engineer and the bacteriologist. What may happen to a mechanical engineer trained in the utilization of steam in an era of direct translation from nuclear processes to electricity?

The problems facing the engineer of tomorrow are more difficult and complex than those faced by his predecessors of 50 years ago. The easy problems have been solved and the work is at higher orders of difficulty.

Design of steam generators working at 4500 pounds and 1100° temperature is certainly more of a challenge than the design of a 200-pound, 450° boiler of a preceding generation. The problems present in the design of an airborne collision warning device for airplanes are of a totally different order of magnitude from those involved in the development of earlier forms of power-system protective devices.

ENGINEERING SCIENCE, A BASIS FOR THE FUTURE

In looking ahead, it first seems desirable to look back and to recognize the significance of 1) the trend toward more usage of the knowledge of the science of nature, 2) the breadth of the modern engineering field, and 3) the implications of the competition between the sciences and the engineering fields. Engineering education needs a common denominator to meet these challenges and to shape itself for the future. Because of its continuance as a basic trend, because it seems to furnish a satisfactory answer for technical education for a broad field, and because it provides for meeting competition from other fields, the fundamentals of physical science as given to us by nature on this earth seem to be that common denominator. Nature is not noted for the frequency of reversals of such long-time trends, whereas man-made applications or particular devices and methods are very likely to change in the future. Thus it seems a safe assumption that the road of more and more basic science is the highway along which engineering education will progress in the future.

The question of what is "basic" in the training in science is a natural one. The engineering field is a broad continuous spectrum of knowledge, which spans the field of the electrical engineer on one hand, through the other fields of the mechanical, chemical, and metallurgical engineer, to that of the civil engineer dealing in construction or the industrial engineer working with automation problems.

It is difficult to see any group of physical science areas as broadly necessary and basic for all, and it may be more important to study certain science areas in depth than to study all areas in breadth. The use of the scientific rather than the applicational viewpoint may give a greater gain than mere coverage of area. We should not overlook our basic energies and modern concepts of materials, but we also should not be preoccupied with things or "hardware" as against ideas and information. The latter areas open up the possibility of extending man's mind, and are exemplified in all engineering fields by aspects of communication, computation, and control. These areas may well furnish the major impetus in the next great step in the evolution of our civilization. Can we overlook the science areas fundamental to them?

IS MATHEMATICS A FUNDAMENTAL?

It seems generally accepted that mathematics is a true fundamental of all engineering education, and in

most schools all engineering students do take the same mathematics sequence. However, even here, as a student becomes more advanced, it is found that no one mathematical area can ideally suit the requirements of all engineering work.

This situation is a result of our trying to use mathematics to fit the physical world as we find it. As has been pointed out, the early engineers were little better than mechanics and certainly knew little mathematics. As a substitute, the accent was on observation of the physical model or actual system as a means of study and understanding. Thus came the early emphasis on engineering laboratory, or having "things" there which the student could "see."

As the mathematical training of the engineer has increased, he has found that mathematical prediction and analysis is a faster and much cheaper means of gaining new knowledge and understanding of our world. Thus he has learned to place more reliance on mathematics and has reduced his usage of the physical model and of the laboratory. This statement, however, applies only to those areas in which mathematics has been developed which will yield *answers*, the end result of engineering thinking.

Two areas of mathematics seem broadly basic to engineering; namely, the calculus as used in the linear constant-coefficient differential equation and the partial differential equation, and statistical theory. The linear differential equation is a general form, useful in engineering because we can obtain answers from it. Therefore, where this form applies to the physical world, the use of mathematical prediction is increasing over the experimental approach. Next is the area of the partial differential equation, rigorously solvable in only a few special cases although approximation methods exist. Here the laboratory must still be depended upon for many solutions where analytic methods are not yet fully available.

These types are suited to continuous variables, or at least finitely discontinuous ones, and thus mathematics based on these forms is fundamental to those areas of engineering where variables of continuity occur, such as in electricity and hydraulics.

Where the variables occur in discrete packages, as in traffic or in production, or probably in any field in which the human factor is evident, the basic mathematics must recognize this lack of continuity, and the fundamental mathematical form is of statistical nature. Thus the basic mathematics for electrical engineering, much of mechanical and chemical engineering and related fields, may not be entirely the same as that basic for much of civil engineering or the human related fields. (Information here appears as human related!)

No question is raised here of the necessity for education of the engineer in mathematics suited to both continuous and discontinuous variables. Mathematics as a training in sound scientific reasoning alone amply justifies its place as an engineering fundamental. Its applica-

tions to engineering problems represent further justification. However, the realization that there is a difference in the form of mathematics the engineer may *use*, in practice in various fields, seems to accentuate the point that the physical knowledge he will use will also differ, and that no list of over-all basic physical sciences can really be suggested with much hope of satisfying the needs for all types of work. He should be taught the basic knowledge needed for his field, and through sufficient mathematical training, he should be able to acquire additional breadth as needed.

WHAT IS ENGINEERING EDUCATION?

The above is intended to emphasize that the future duty of engineering education is the teaching of the science of nature in considerable depth rather than in an over-all coverage of all physical science. To further the understanding of this duty, it appears desirable to modify and simplify one of the definitions of engineering. This modified definition may be stated as: "*Engineering is the science and art concerned with the utilization of materials, energy, and men.*" This adds nothing fundamentally new, but by the removal of modifying adjectives, is offered as a clearer statement of purpose, especially for the engineering educator.

First, it retains the broad field of materials and phenomena found in nature, which have always been the areas of interest to the engineer, and it elevates the management of men in engineering concerns to an equal position, certainly a move justified by the increasing importance of engineers in modern management of industrial organizations.

Second, and of much more importance to the engineering educator, it emphasizes that engineering is both a science and an art. An art teaches "how to do" through qualitative understanding and past experience, whereas a science teaches "why" through mathematical correlation and physical models. If it is asked which of these should be the duty of the university, it appears unquestioned that the teaching of science should be given first importance in our educational pattern. Universities were originally organized and set up to conserve and disseminate knowledge. A science is a body of knowledge and therefore it is appropriate that the engineering universities so conserve and disseminate engineering knowledge. It is appropriate also by reason of the training and interest of their staffs, and by the fact that this places engineering in a position which is consistent with the other colleges on our campuses. If there is a job in the education of the engineer for the engineering college, this certainly must be part of it.

The art of engineering includes not only many aspects known as skills, but also other methods of analysis or short cuts in procedure, or the methods by which our goods are manufactured. It is this area in which industry is most interested and it is in industry that the arts of engineering most often originate. They are developed on the frontier of our industrial progress and industry is

on that frontier. Also, if the so-called arts of engineering are to be treated in the university, it requires that the faculty in the university be aware of the frontier progress in industry. All too often such people lose contact upon joining a university, and therefore their teaching is based upon dated procedures, sometimes back-dated many years.

The above argument supports the proposition that the education of an engineer should be split into two parts, 1) the science which is definitely a duty of the university, and 2) the arts which may best be taught in industry. Under some circumstances the latter duty may be shared with the university, which through its off-campus activities can conduct its share of educating within the profession for the arts of the profession. It seems extremely doubtful that the arts, concerned as they are with the most recent advances, apparatus, equipment, or hardware, should be taught in any detail upon the university campus. This is really a basic duty of industry to be undertaken after the young engineer chooses his own segment of the profession, since such hardware teaching is always a narrowing process, possibly too narrowing to be justified as part of a curriculum, prior to the young graduate's selection of his field of work.

Thus, the training in the many skills and arts of engineering is made a responsibility of industry, where it can be directed specifically to the methods, processes, and practices of the particular employer. This seems well in line with the desires of many industries, and with their performance in setting up training courses and schools for young graduates.

It seems reasonable, then, to base an engineering educational philosophy not only on engineering science, but also on providing of time for better teaching of that science by subjugating the teaching of applications or hardware to a secondary position, to the end that at a reasonably near date the applications may be almost completely eliminated from the usual engineering curriculum.

AN EXPERIMENT WITH THIS PHILOSOPHY

Numerous universities are experimenting with new methods of engineering education, some pointing in this same general direction. One such experiment in educational philosophy is being undertaken in electrical engineering at Michigan State University. As broad rules of application of the philosophy, the following may be stated. First, that the objective of the curriculum is the teaching of engineering science. Second, that any teaching of hardware, or apparatus, or application is secondary and is introduced purely to illustrate the basic science theory; it is not an end in itself. The teaching of such a field as an engineering science can rest on a decision as to what areas of this science are important,

interesting, and challenging. This represents a departure from past years when a curriculum was based on decisions as to what the student needed to hold his first job. It actually represents the use of a form of liberal arts approach to the problem, in that we are asking only what topics in the field will produce a well-rounded engineer of the future.

The philosophy has been carried out by the selection of network theory as the core, around which are added mathematics, electronics, electromagnetic fields and circuits of distributed constants, and electrodynamic systems. The electrical portion of the curriculum consists of only four course sequences and seems adequate for the training of an electrical engineer for the needs of the future.

The adoption of network theory as a core is the key to this program. This selection appears logical since if required, all of our known electrical phenomena and ideas may be analyzed as circuits, and while the circuit idea may not be employed in all cases, it is available when needed. Definitely employed is the philosophy that basic material should be taught first and taught correctly in the circuits and networks course, with the timing such that it is ready for use whenever required in the parallel sequences. This timing calls for a considerable amount of cooperation among the staff and this in itself is valuable. Through such cooperation and coordination it appears possible to increase the efficiency of teaching by a major amount, and to obtain a definite time gain through teaching a topic once and teaching it correctly. This gain, it already appears, may amount to as much as one half of a scholastic year.

As a corollary experiment, not bearing upon the major premise, all laboratory work has been removed from each of these courses. This work is accomplished in one paralleling laboratory course in which integration of ideas and material from these several courses is achieved in an atmosphere of exploration. This in itself is turning out to be extremely valuable in its enforced review of both the philosophy and the achievement which is obtainable in laboratory work.

Through application of this philosophy, it is believed that graduates can be produced who are well oriented to future needs in research, development, and systems design. It is hoped that graduates will have reached a level of attainment well beyond that of the usual bachelor of science degree, and that this will carry on into improved graduate work, and greater personal success twenty or more years after graduation.

BIBLIOGRAPHY

- [1] Terman, F. E. "Electrical Engineers Are Going Back to Science!" *PROCEEDINGS OF THE IRE*, Vol. 44 (June, 1956), pp. 738-740.
- [2] American Society for Engineering Education, *Report on Evaluation of Engineering Education*. Urbana, Ill.: University of Illinois.

Future Circuit Aspects of Solid-State Phenomena*

EDWARD W. HEROLD†, FELLOW, IRE

Summary—Future electric circuits will depend more and more on new solid-state phenomena and on solid devices which perform increasingly complex circuit functions. This paper discusses several specific phenomena of interest to circuit and device engineers, namely, superconductivity, molecular amplification, magnetic effects in semiconductors, and nonlinear capacitance in junctions. The paper concludes with a presentation of the potential advantages of controlled inhomogeneity in all types of solid-state devices. It is indicated that, by departing from uniform, homogeneous materials, it is possible to produce new effects and improved performance. Ultimately, controlled inhomogeneity may lead to solid devices which combine the functions of many conventional components and associated wiring.

INTRODUCTION

ELECTRIC circuits were once largely confined to the use of conductors, insulators, and magnetic metals, in combination to produce inductors, capacitors, and resistors, and dependent on the electron tube for amplification and nonlinear effects. In the last decade, a myriad of solid-state materials and effects have been used to obtain gyrators, switching devices, memory elements, amplifiers, electro-optic transducers, and thermoelectric devices. We may look forward to the day when the chemical synthesis of an improved compound, the technology of its use, and/or the discovery of a new, useful effect in these solid materials, can do more to revolutionize the performance of an electric circuit than all the classic ingenuity of the circuit designer. There will be a dependence on new solid materials and devices which will be even greater than the circuit man's earlier dependence on better and different electron tubes to advance his art. Furthermore, the trend toward a merging of circuit and device, which started with microwave tubes, is now found in more and more applications, at all frequencies.

A review of the solid-state phenomena which affect electronic circuits must include such a wide variety of subjects that completeness is hardly possible in a single paper.

In Table I a partial list is given which indicates the scope of the field. The present paper is concerned with some selected topics from the column labelled "Electrical Only." A point of view is taken which is intended to stimulate interest in several phenomena not yet widely utilized by circuit and device engineers. Among the

topics considered are superconductivity, molecular amplification, magnetic effects in semiconductors, nonlinear capacitance, and last but not least, the utilization of controlled inhomogeneity to extend the electrical performance of known materials.

TABLE I
SOME SOLID-STATE PHENOMENA OF INTEREST IN CIRCUITS

Electrical Only	Energy Conversion
A. Conduction Processes	A. Mechanical—Electrical
1) Normal Metals	1) Piezo-Electrical Effect
2) Superconductors	2) Electro-Striction
3) Semiconductors	3) Magneto-Striction
a) Thermistors	4) Strain Effects
b) Junction Devices	
c) Hall Effect Gytrators	
4) Photoconductors	
B. Dielectric Phenomena	B. Thermal—Electrical
1) Normal Dielectrics	1) Ohmic Heating
2) Ferro-Electrics	2) Thermoelectric Effects
a) Electrets	a) Generation of Electricity
b) Modulators	b) Heat Pumping and Cooling
c) Storage Devices	
C. Magnetic Behaviors	C. Radiation—Electrical
1) Conventional Magnetic Metals	1) Photo-Voltaic Effect
2) Ferrites	2) Electroluminescence
a) Storage Devices	3) Recombination Processes
b) Gytrators	4) Particle Bombardment
3) Other Spin Resonances, Masers	a) X-Rays
	b) Cathodoluminescence

CONDUCTION IN METALS

The conducting solids used in passive circuit elements are usually copper, silver, gold, or aluminum. Their conductivities differ from one another by considerably less than an order of magnitude, and one may tend to ignore this area of circuitry in thinking of solids. The future, however, may see increasing use of low temperatures, both on the earth, by artificial cooling, and in space, where low temperatures can be achieved quite naturally. It is appropriate to examine both conventional (*i.e.*, normal) conductivity and superconductivity to determine their potential utility in circuits.

Let us first consider the dc resistance of a nonsuperconducting metal, and a typical superconductor. Copper, gold, and silver behave much alike, so we may look at any one. There are more data available on gold, so it has been chosen for illustration. The superconductors are also somewhat alike but white tin has been studied so extensively that it is here chosen for the typical superconductor. In Fig. 1 a log-log plot of the resistivity data

* Original manuscript received by the IRE, June 20, 1957; revised manuscript received, July 23, 1957. Portions of this paper were presented at the Symposium on "The Role of Solid-State Phenomena in Electric Circuits," Polytechnic Institute of Brooklyn, Brooklyn, N. Y., April 23, 1957.

† RCA Labs., Princeton, N. J.

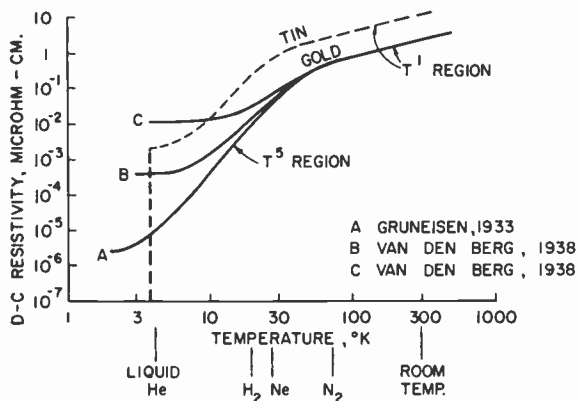


Fig. 1—Resistivity of three samples of gold, and one of tin, vs temperature.

reported by various investigators is shown.^{1,2} Around room temperature, the lattice scattering of the charge carriers causes a linear dependence of resistivity with temperature. In solid-state language, this is the region in which kT is greater than the phonon energy corresponding to maximum lattice vibration frequency; the temperature is said to be above the Debye temperature.³ Solid-state theory indicates that the resistivity should be linear with temperature until, below the Debye temperature, the lattice scattering begins to diminish rapidly and the resistivity then drops as the fifth power of the temperature. Each charge carrier has a longer and longer mean free path as the temperature drops, which is of importance in skin effect at high frequencies, as we shall see. In a perfect crystal lattice, the resistivity should disappear at zero temperature. In practice, this has not been found. Instead, one finds, in ordinary metals, a low-temperature residue of resistance which never disappears and, in superconductors, a disappearance of all resistance at a temperature which is not zero.

Most ordinary metals show a residual resistance which is about two to three orders of magnitude below the room temperature value, but in the purest and most perfect crystals, this can be lower. The gold sample, A, of Fig. 1, measured by Gruneisen in 1933, has the lowest residue commonly quoted in the literature; *i.e.*, six orders of magnitude down, but this is rather exceptional; the other two gold samples are more typical of gold and also of copper and silver. The residual resistance has been definitely linked with imperfections and dislocations in the crystal lattice, and with impurities. The sample of tin has a superconducting transition at about 3.7° K and, below that temperature, its dc resistance is so low

as to defy measurement. This transition point and the effects below the transition point are much less sensitive to impurities and crystal properties.

Let us now consider passive circuit effects and, particularly, what happens with high-frequency alternating currents. The skin effect formula⁴ indicates that the skin depth of a conductor is given by

$$\delta \approx 5000\sqrt{\rho/\mu f} \text{ (cm)}$$

where ρ is the resistivity in ohm-cm, μ the relative permeability ($\mu = 1$, for air), and f the frequency in cps. In terms of the surface resistance, R_s ; *i.e.*, the resistance of a square piece of conducting surface, this may be written

$$R_s \approx 2 \times 10^{-4}\sqrt{\rho\mu f} \text{ (ohms per square).}$$

Both of these formulas would lead us to believe that the hf resistance at low temperatures could be determined by taking the square root of the dc values of Fig. 1. Thus, gold sample A, with its 6 orders of reduction of resistance, might have 3 orders-of-magnitude reduction at high frequency. Measurements fail to show this, and for a very obvious reason. As the mean-free path of the charge carriers begins to get longer and longer at low temperatures, they soon get longer than the skin depth and begin to hit the surface, which behaves as a scattering source of great potency. Known as the anomalous skin effect, this scattering is found to greatly increase the hf resistance of all normal metals at low temperatures.⁵ In the gold sample A, the bulk mean-free-path, which is of the order of a millionth of an inch at room temperature, becomes over half-an-inch at 4.2° K! As a result, for normal metals, the hf resistance at low temperatures becomes quite *independent* of the bulk mean free-path (which determined the dc resistance) and *dependent* on the surface conditions.

In Fig. 2 data at 1200 mc of the surface resistance of gold are shown. It is seen that the very best reduction in resistance which is achieved is about 3 times, a long way from the anticipated result! Furthermore, it is found that the high-frequency residual resistance is substantially independent of the dc resistance caused by impurity and crystal imperfection scattering, and is affected chiefly by surface smoothness and contamination. This surface resistance varies as the $\frac{2}{3}$ power of the frequency, rather than the $\frac{1}{2}$ power of the conventional skin effect. We conclude that low-temperature operation of *conventional normal metals* will not be highly advantageous at ac until either a surface condition, or a technique of operation, can be devised which takes full

¹ For a bibliography on normal conductivity, see D. K. C. MacDonald, "Electrical Conductivity of Metals and Alloys at Low Temperature," in "Handbuch der Physik," vol. 14, "Low Temperature Physics I," Springer-Verlag, Berlin, Germany, 1956.

² For a bibliography on superconductivity, see D. Shoenberg, "Superconductivity," Cambridge University Press, Cambridge, Eng., 2nd ed., 1952.

³ This is a temperature which when multiplied by the Boltzmann constant, gives the maximum phonon energy.

⁴ F. E. Terman, "Radio Engineers' Handbook," McGraw-Hill Book Co., Inc., New York, N. Y., pp. 34-35; 1943.

⁵ A comprehensive survey and bibliography is contained in A. B. Pippard, "Metallic Conduction at High Frequencies and Low Temperatures," in "Advances in Electronics and Electron Physics," Academic Press, New York, N. Y., vol. 6; 1954.

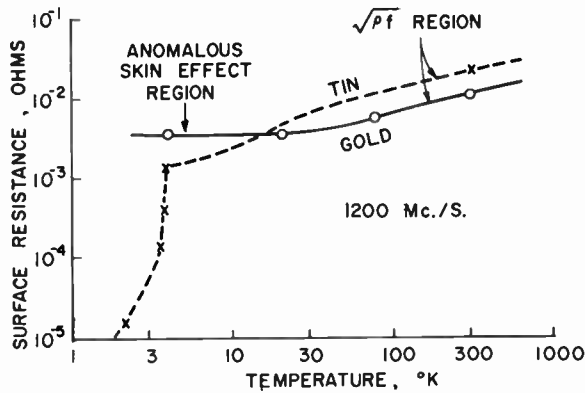


Fig. 2—HF surface resistance of gold and tin at 1200 mc, plotted against temperature.

advantage of long mean-free paths for the charge carriers. We also can see that no new nonsuperconducting metal of lower ac resistance is likely to be achieved by reduction of lattice scattering alone.⁶ These conclusions provide challenges to the solid-state physicist which we may hope will not go unanswered.

The ac surface resistance of a superconductor behaves quite differently from the normal conductor and is much more advantageous to the circuit engineer.⁵ This is particularly true if the temperature can be reduced well below the transition point. For example, we see in Fig. 2 that tin at 2°K, has 3 orders of magnitude less resistance at 1200 mc than our best room-temperature conductors. The circuit man may indeed be tempted to use such a behavior in specially important areas of his field. His temptations will increase if thermoelectric cooling can be employed to assist the liquid-helium methods, but this does not appear to be “just around the corner.”

In Fig. 3 the frequency dependence of the ac resistance of gold and tin is shown. It is clear that tin is very advantageous, even at high microwave frequencies.

As a potential application, let us consider the short doublet, or dipole, antenna. A half-wave dipole has a radiation resistance of around 70 ohms, and a capture cross section of about $\lambda^2/8$, where λ is the wavelength.⁷ It is sometimes forgotten that an extremely short dipole, much less than a half-wavelength, also has about the same large capture cross section, and about the same directivity pattern as the half-wave case.⁷ Unfortunately, it has such a low radiation resistance [it varies as $(l/\lambda)^2$ where l is the length and λ the wavelength], and such a high reactance, that it is difficult to match it to a load without excessive ohmic losses. However, if the high Q can be tolerated, it would seem

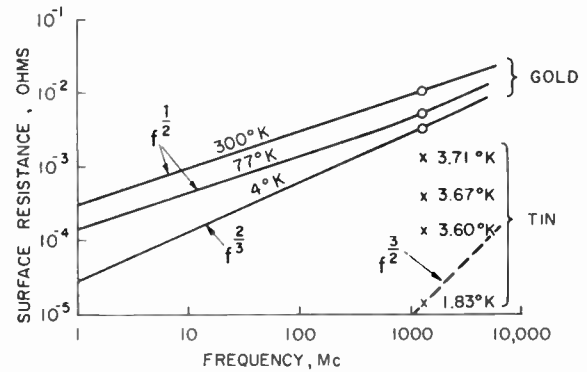


Fig. 3—Frequency response of hf surface resistance of gold and tin at various temperatures.

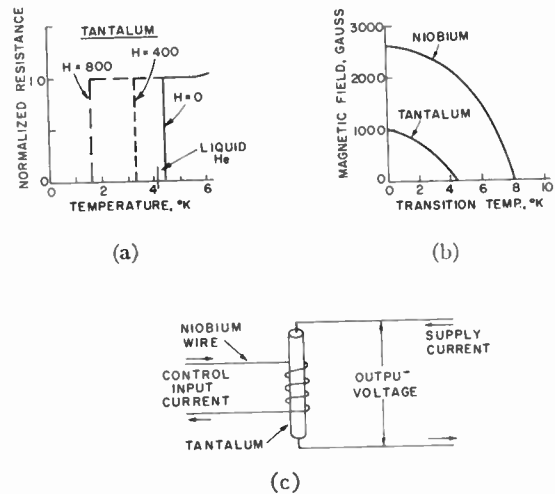


Fig. 4—The cryotron, a superconductive amplifier at 4.2K.

possible to overcome ohmic loss by a superconductor. In other words, a 100-mc antenna an inch or so long is potentially capable of as much interception or transmission of narrow-band electromagnetic radiation as the 5-foot half-wave dipole. With more complicated arrays, it is (in theory) even possible to make highly directive antennas of small over-all area. The problem of matching a few milliohms of radiation resistance by a superconducting transformer device will be left to the engineers of the future. It will surely come sooner if solid-state scientists can make a superconductor with a somewhat higher transition temperature.

It is now appropriate to discuss another application of superconductivity which has been exciting computer engineers recently, the cryotron.⁸ This clever little device makes use of the fact that a magnetic field affects the superconducting transition temperature. In Fig. 4 is shown in two ways how the transition temperature of tantalum varies with magnetic fields. Niobium has a much higher transition temperature and, therefore, will be unaffected by fields which will change the tantalum

⁶ An exception is the case of high-temperature operation, *i.e.*, temperatures well above the Debye temperature of conventional metals. In such instances, the scattering is so great that it is conceivable that substantial improvement would result from a new material, even without an increase in the number of conduction electrons.
⁷ Terman, *op. cit.*, pp. 787-791.

⁸ D. A. Buck, “The cryotron—a superconductive computer component,” *Proc. IRE*, vol. 44, pp. 482-493; April, 1956.

transition. Below the curves of transition temperature shown in Fig. 4(b), the materials are superconducting; above them they are "normal." At 4.2°K, liquid helium temperature, it is seen that an increase in magnetic field will convert tantalum to its normal state, while leaving niobium unaffected. A cryotron is made as in Fig. 4, with a coil of fine niobium (Nb) wire around a small tantalum (Ta) wire. The input is the current through the Nb wire, which requires no voltage and hence no power. The output is the voltage across the Ta wire. As the control current is increased, at the critical magnetic field, the Ta begins to develop its normal resistance, and a voltage drop occurs across it.

The cryotron is almost an exact dual of a grid-controlled triode electron tube, as can be seen from a comparison of the characteristics. In Fig. 5 a triode tube is shown, whose grid voltage, E_c , controls the anode current, I_b , through a load, R_L . If the load is shorted and the supply voltage, E_b , is varied for different values of E_c , we obtain the familiar plate characteristic shown.

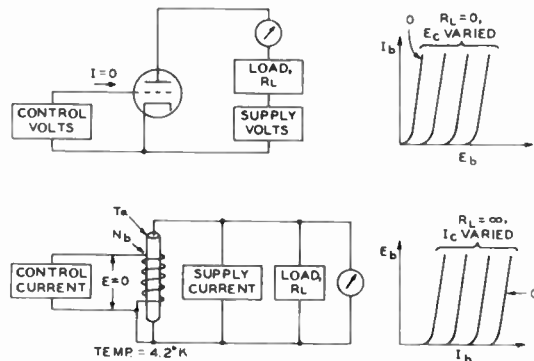


Fig. 5—The cryotron is shown to be the dual of a triode electron tube.

Now let us consider the cryotron. Its control current, I_c , through the niobium wire, controls the voltage, E_b , across the tantalum wire and across the load, R_L . If the load is open-circuited, and the supply current, I_b , is varied, the tantalum wire has either no resistance, corresponding to no output voltage, or its resistance begins to increase so that E_b varies with I_b as shown. Thus the characteristics are like those of a triode, except that every current is replaced by a voltage and every voltage is replaced by a current.⁹ The even spacing of the curves is purely schematic and does not imply linearity, nor does the parallelism.

If there is no control voltage in the triode, the curve marked with a zero in the triode characteristics of Fig. 5 is applicable. This is the result of the anode voltage alone, controlling its own current; note that it is the left-hand curve. In the cryotron, if there is no control current,

the curve which applies is again marked with a zero. It is the result of the supply current which, through its magnetic field, removes the superconductivity at a definite point and then controls the voltage.

However, in the cryotron, the curve marked zero is the right-hand curve of the group. There is one other difference; in the triode all the curves at high currents eventually merge into the limiting one (not shown) determined by the emission capability of the cathode; in the cryotron the curves merge at high voltages into the Ohm's-law curve for normal tantalum at the temperature concerned. In practice also, the cryotron may vary its temperature slightly due to heating by the supply current, and the curves will thereby be modified. For the details of how the cryotron is used in a computer, reference is made to the published literature.⁸

We may now leave the field of conduction in metals and turn to some of the solid-state circuit effects in other materials.

SOLID-STATE MASERS

It is an abrupt jump from a consideration of conductivity in metals to the exciting new field opened up by the demonstration a few years ago of a molecular amplifier. Such a jump is indicative of the breadth of solid-state effects and one must be prepared to make such rapid changes in thinking again and again. For those not completely familiar with the term, maser represents the title "molecular amplification by stimulated emission radiation." It is applicable to a class of microwave amplifiers and generators which do not require electric charges or currents, as in the electron tube or transistor. To the circuit man, this new concept is apt to be so unfamiliar that some slight introduction is in order.

In the field of gas discharges, we are all familiar with the light produced by gas atoms or molecules whose internal energy has been raised by an electric discharge. Many years ago, it was believed that the light came from recombination of free electrons and positive ions, but this hypothesis was quickly disposed of by the measured discrepancy between ionization energy and the much lower-energy light quanta emitted. It was then shown that internal energy states were responsible and, by adding energy to a gaseous system, a wide variety of electromagnetic radiations could be produced when the gas molecule returned to its equilibrium state. The energy levels involved were several electron volts, and the tendency for the molecule to return to its ground state was very great, so the light emission occurred spontaneously and immediately. To a circuit man, the system has a very low Q , or a wide bandwidth. As we might expect, the radiation resembles the thermal noise of such a circuit; *i.e.*, it is incoherent and relatively insensitive to external stimulation. The large energy changes represent radiation far above the radio spectrum.

⁹ The duality also applies to high frequencies, in that the triode includes three capacitive susceptances in input, output, and coupling paths, while the cryotron includes three inductive reactances.

A number of years ago, Weber pointed out to the radio fraternity¹⁰ that, of the many other internal energy states in molecules, some had very small differences in energy, corresponding to radiation at radio frequencies, rather than in the visible light range. Furthermore, there appeared the possibility that there were systems which would retain their excess energy state long enough to be highly sensitive to external stimulation; this property is described by atomic physicists as due to a long "relaxation time." Thus, if a system of molecules could be put in the higher energy state, an incoming signal of the correct frequency could trigger off the available radiation in proportional fashion and in phase synchronism, so as to produce amplification. The first problem lay in a suitable means to excite the molecules to the correct higher energy state, since there are ordinarily a very large number of possible excitations. Gordon, Zeiger, and Townes reported that ammonia vapor could be so excited,¹¹ and used for amplification. A second problem, which was apparent from the start, involves the amount of output power obtainable. The total energy available from a single molecular transition at radio frequencies is only 10^{-5} electron volts (10^{-24} watt seconds) or less. It requires, therefore, a tremendous concentration of excited molecules to produce an appreciable output power; a solid material is clearly desirable. In a solid, the excitation means again becomes critical but we are fortunate in having several possibilities.

A rather complete review article has recently been published,¹² so we will content ourselves with a hasty survey of three possible excitation methods. Fig. 6 is the customary energy level diagram showing possible internal energy states. Also pointed out is the small energy associated with transitions at microwave frequencies. Let us suppose we have a material with three energy states shown. At thermal equilibrium, the number of molecules in the energy state W_3 is greater than that in W_2 which, in turn, has more molecules than state W_1 . Thus, an incoming radio wave of angular frequency, ω_{32} , can be absorbed by promoting transitions from W_3 to W_2 . At high excitations, the population of state W_2 builds up to a new equilibrium value, until it equals that of state W_3 at which point the power absorbed is a constant depending on the original inequality. If we could find a way of artificially increasing the population of state W_2 to exceed W_3 in the first place, then we would have a possible *release* of energy rather than an absorption. When there are three or more energy states, we require an increase in population of

any higher state and we have a greater variety of choices as to excitation means.

A suitable solid material consists of a host crystal with the desired atoms or molecules (whose resonances we wish to use) homogeneously dispersed throughout as an impurity. It has been found that one of the most useful molecules is a paramagnetic atom; in the presence of the host crystal and a magnetic field, a single degenerate energy level is split into a number of closely-spaced levels. Since the splitting is partially due to the magnetic field, the system is "tunable"; *i.e.*, the useful frequency can be adjusted. For a two-level system, arsenic-doped silicon has been used;¹³ the three-level system recently worked upon at Bell Telephone Laboratories used gadolinium in a lanthanum ethyl sulphate host lattice.¹⁴ To remove interaction with thermal lattice vibrations, both require low-temperature operation. The apparatus to build an amplifier is quite simple, since it requires only a microwave cavity loaded with a piece of the doped material and placed in a cryostat between the poles of a magnet.

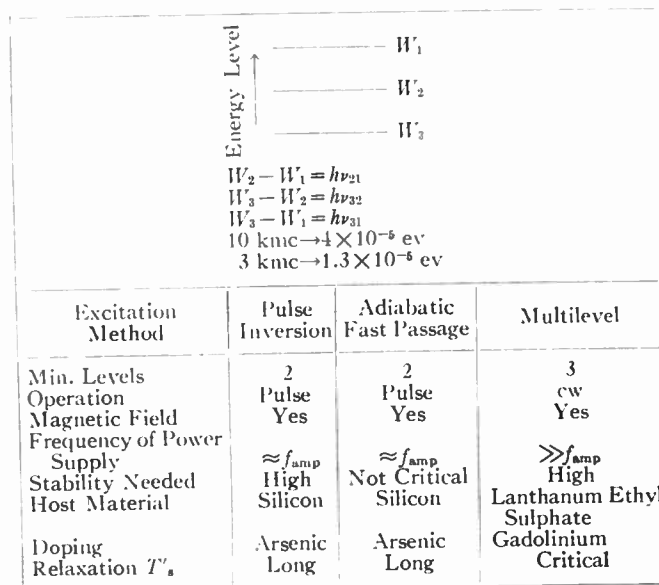


Fig. 6—Solid-state masers; a table of excitation methods.

The three best known excitation methods are shown in Fig. 6. For all three, the input power must be supplied at radio frequency. With pulse inversion, the rf supply is pulsed and, by resonant absorption, the molecules of level W_3 , for example, are excited to level W_2 ; *i.e.*, their populations are inverted. When the supply power is removed (between pulses), the system is ready to amplify or oscillate at the same frequency. If the magnetic field is also shifted slightly, the amplification

¹⁰ J. Weber, "Amplification of microwave radiation by substances not in thermal equilibrium," IRE TRANS., vol. ED-3, pp. 1-4; June, 1953.

¹¹ J. P. Gordon, H. J. Zeiger, and C. H. Townes, "The maser—a new type of microwave amplifier, frequency standard and spectrometer," *Phys. Rev.*, vol. 99, pp. 1264-1274; August 15, 1955.

¹² J. P. Wittke, "Molecular amplification and generation of microwaves," *Proc. IRE*, vol. 45, pp. 291-316; March, 1957.

¹³ J. Combrisson, A. Honig, and C. H. Townes, "Use of spin resonance for an oscillator or amplifier at hyperfrequencies," *Compt. Rend. Acad. Sci., Paris*, vol. 242, pp. 2451-2453; May 14, 1956.

¹⁴ H. E. D. Scovil, G. Feher, and H. Seidel, "Operation of a solid-state maser," *Phys. Rev.*, vol. 105, pp. 762-763; January 15, 1957.

can be at a slightly different frequency. The magnetic field and excitation frequency must be reasonably stable to assure proper operation and, of course, a long relaxation time is essential.

Another pulsed system uses what is known as adiabatic fast passage. In this system, either the power supply frequency, or the magnetic field, is swept from one side to the other of the desired resonance point at a relatively fast rate compared to the relaxation time. Immediately after the sweep, the populations have become inverted and the system is "ready" to amplify. The method shares the characteristics of pulse inversion except that the rf supply and magnetic field are no longer critical.

In the third system, outlined in a paper by Bloembergen,¹⁵ continuous operation is feasible, and there are other advantages as well. The material is extremely critical, however, since it is necessary to have both short and long relaxation times between levels. The frequency of the power supply is selected to correspond to the W_3 transition. The population of W_1 then becomes equal to that of W_3 . The intermediate state, W_2 , now has either a smaller or a larger population than its neighbors, W_1 and W_3 . If it is smaller, amplification occurs at W_{21} , the upper transition. If its population is larger, amplification can occur at W_{32} . To obtain a maximum of population difference, it is necessary to have one short and one long relaxation time in the $W_1 - W_2$ and $W_2 - W_3$ transitions. Thus the relaxation times, as well as the frequency differences for a desired application, make the choice of material critical. At Bell Telephone Laboratories, an oscillator was made to operate at around 9 kmc, using a 17.5-kmc power supply and a 3000-Gauss field; gadolinium was used in a lanthanum ethyl sulphate crystal.¹⁴ A little cerium was introduced, and a proper orientation of the magnetic field was provided to promote an interaction with one transition to decrease its relaxation time.

Bandwidths of solid-state masers are expected to be from 1 to 10 mc, with an upper limit of around 100 mc. The operating frequency will lie above 1 kmc, in general. The noise factor is expected to be of the order of zero db, since the low temperature and absence of moving charges eliminate internal noise sources. A magnetic field and microwave power source are needed and, with the multiple-level excitation method, a multiply-tuned microwave cavity is also needed.

SOME SEMICONDUCTOR DEVICES USING THE HALL EFFECT

The Hall effect occurs when a current-carrying conductor is placed in a transverse magnetic field. The force on the current, given by Ampere's law, is such that the current paths are pushed in a direction at right angles to themselves and to the magnetic field. If the

charge carriers are positive, a transverse emf is set up of one polarity. Negative charges give an opposite emf. The emf known as the Hall voltage is a measure of the sign and mobility of the charge carriers, and is one of the important tools in studying semiconductors. The Hall effect also has practical value in devices for use in circuits, and we will describe three of them.

To those of us trained in classic circuit theory, the gyrator has seemed a strange and remarkable circuit element. Since the ferrite gyrator works only at microwave frequencies, we are still prone to ignore the gyrator as a circuit element applicable, for example, to a doorbell wiring system. Perhaps this is a practical point of view to take. Nevertheless, the Hall effect provides an extremely simple nonreciprocal, passive four-pole circuit element which works from dc up to very high frequencies. Fig. 7 shows the classic Hall effect experiment and how it was used by Mason and his co-workers to make a gyrator.¹⁶ Referring to Fig. 7(a), when a current, I , is passed through an n-type semiconductor in a transverse magnetic field, H , a voltage appears across its two sides, given by

$$V = RIH/W$$

where R is the Hall constant, proportional to the mobility divided by the conductivity, and W is the thickness. In practical units, R is in volt-cm/amp-oersted. The polarity of the Hall voltage is as shown.

If one now builds a symmetric square, with four side contacts, as shown in Fig. 7(b), it is seen that, in a magnetic field, electrode A can be thought of as having a resistive connection to B , and C to D . A battery poled as shown; *i.e.*, positive, terminal to A , produces a positive output on terminal B to the load resistor. The source current into a terminal is deflected clockwise and the upper end of the load is positive. Now let us reverse the battery and load resistor as in Fig. 7(c). The source current now flows into B , is deflected clockwise, and the positive output terminal is now the *bottom* end of the load. This is the property of a gyrator and it is seen that the output of the four-pole used in one direction is 180° out-of-phase with the output used in the other direction.

Let us look at the circuit equations. For a resistive four-pole, we may write

$$V_1 = I_1 R_{11} + I_2 R_{12}$$

$$V_2 = I_1 R_{21} + I_2 R_{22}$$

Ordinarily, all passive reciprocal networks have $R_{12} = R_{21}$. The determinant of the resistance matrix is

$$\Delta = R_{11}R_{22} - R_{12}^2$$

which can be made zero, if

¹⁶ W. P. Mason, W. H. Hewitt, and R. F. Wick, "Hall effect modulators and gyrators employing magnetic-field independent orientations in germanium," *J. Appl. Phys.*, vol. 24, pp. 166-175; February, 1953.

¹⁵ N. Bloembergen, "Proposal for a new type solid state maser," *Phys. Rev.*, vol. 104, pp. 324-327; October 15, 1956.

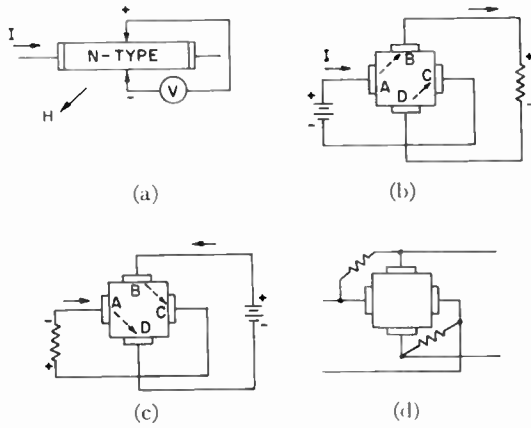


Fig. 7—The Hall gyrotor. (a) Hall effect, (b) gyrotor, forward direction, (c) gyrotor, back direction, (d) isolator.

$$R_{11} = R_{22} = R_{12} = R_{21}.$$

Thus, in a transmission system, it is easily shown that the minimum insertion loss is also zero; *i.e.*, zero db.

The Hall gyrotor, on the other hand, has $R_{12} = -R_{21}$. As a result, the matrix determinant is

$$\Delta = R_{11}R_{22} + R_{12}^2$$

and cannot be made zero. If one puts¹⁷

$$R_{11} = R_{22} = R_{12}$$

in the insertion loss formula, using image-resistance matching, it is found that the minimum loss is 7.7 db. This is the chief disadvantage of the Hall gyrotor, as compared with ferrite gyrotors, which are reactive in nature, and can have almost no transmission loss.

To make a gyrotor into an isolator, it is only necessary to couple reciprocal resistance elements across the terminals, as shown in Fig. 7(d). The effect on the circuit equation is to add a positive resistance to both R_{12} and R_{21} , so that one of the diagonal terms is reduced to zero. Transmission in one direction only is now permitted, and the minimum theoretical loss is decreased to about 6 db. In practice, best results are obtained with such high-mobility semiconductors as indium-antimonide. It is possible to achieve a forward-direction loss of about 10 db and a backward direction loss of 70 db. The actual devices can be very tiny, though the magnetic field required is substantial (the higher, the better). Where an isolator is a necessity down to low frequencies, and the amplifying action plus isolation of an electron tube is ruled out of consideration, the insertion loss of the Hall gyrotor may be tolerable, and can probably be made to approach the theoretical values more closely than presently achieved.

The Hall effect can also be used as an amplifier,¹⁸ as shown in Fig. 8. It is found that an input magnetic field can be applied, with a load resistance in the transverse

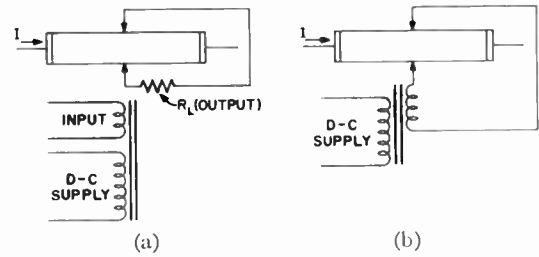


Fig. 8—Hall-effect amplification. (a) Amplifier, (b) regenerative feedback.

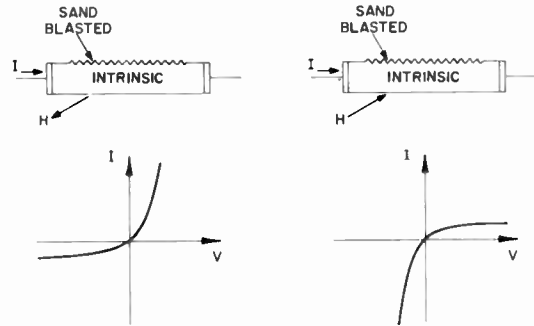


Fig. 9—The magnetic rectifier, a bulk effect.

connections, to give power gain. In a feedback arrangement, also shown, negative resistance effects have been obtained.

Another outgrowth of the Hall effect is a novel semiconductor rectifier, first described in print by Weisshaar and Welker.¹⁹ In distinction to all other rectifiers, this device uses a bulk effect, rather than a barrier or contact. Fig. 9 shows a slab of approximately intrinsic semiconductor, with a transverse magnetic field. One surface is sand-blasted, the other has a very low recombination. A sand-blasted surface is a high recombination surface, and (in equilibrium) is also a high carrier-generating surface. When a voltage is applied, with the left-hand terminal positive, the holes and electrons generated at the upper surface and in the bulk are driven downward in the drawing, toward the low recombination surface. As a result of very little recombination there, a high carrier concentration results and a high current can flow. Upon reversing the voltage, the carriers are driven to the sand-blasted surface, which has an extremely high recombination rate. Since there is no other generating surface to supply carriers, the concentration becomes small and little current flow results.

By reversing the magnetic field, the rectifier is reversed in polarity, as shown. This rectifier is an extremely interesting and unusual device from the circuit point of view and will undoubtedly find use in special applications. As with other Hall-effects devices, advantage can be taken of the extremely high mobilities of the so-called 3-5 compounds, particularly indium antimonide and indium arsenide.

¹⁷ R. F. Wick, "Solution of the field problem of the germanium gyrotor," *J. Appl. Phys.*, vol. 25, pp. 741-756; June, 1954.

¹⁸ H. Weiss, "The back-coupled Hall generator," *Z. Naturf.*, vol. 11a, pp. 684-688; September, 1956.

¹⁹ E. Weisshaar and H. Welker, "Magnetic barrier layers in germanium," *Z. Naturf.*, vol. 8a, pp. 681-686; November, 1953.

A SEMICONDUCTOR VARIABLE CAPACITOR

Many circuit investigators have explored, in a modest way, the utility of the depletion-layer capacitance of a point-contact or junction rectifier. It is quite well understood that, when such a diode is biased in the reverse direction, an insulating, charge-free layer builds up, whose thickness depends on the reverse dc voltage. This layer is a relatively low-loss dielectric, since any charges generated there are quickly swept out and produce no ac effect up to rather high frequencies. The junction can be considered as a capacitor whose value depends on the dc voltage applied to it, as shown in Fig. 10(a). Typical capacitance changes in a germanium p - n junction are a 3:1 change in capacitance for a 15-volt bias change.

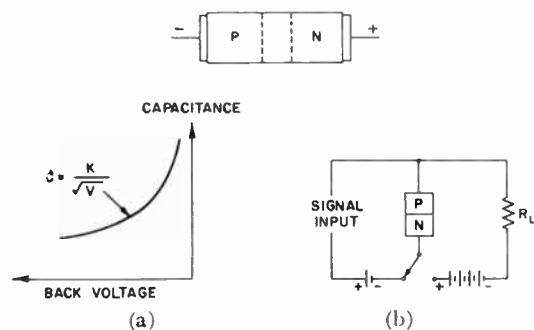


Fig. 10—The p - n junction as a variable capacitance.

Unfortunately, commercial diodes are not made for this purpose and the losses are high compared with good circuit components. It is not a difficult matter to design the device with low series resistance, so that a reasonably high- Q capacitor results; this was done by Giacoletto and O'Connell.²⁰ There are many uses for this simple, low-cost device. As an fm modulator, one finds a capacitance change of around 10 per cent per volt. Thus, for the 100-mc fm band, it is only necessary to apply a modulating signal of 14 mv, rms, to obtain the 200-kc modulation. This is easily obtained from a microphone. A separate diode is not necessary, since the collector capacitance of a junction transistor can be used to modulate its own frequency. In fact, such an arrangement was used in a color tv subcarrier generator, which automatically locked itself to the burst signal, all with only one transistor.²¹

As a nonlinear capacitor, various switching devices, dividers, mixers, and harmonic generators can be devised. It is significant that such a diode capacitor is substantially independent of temperature and has no hysteresis loop up to frequencies of many thousands of

megacycles. It is, therefore, different from the ferroelectric dielectric device in major respects.

An amplifier can be made of ferromagnetic and ferroelectric materials, and amplification can also be obtained from the junction capacitor. The same general principles apply; *i.e.*, the power supply must be at a higher frequency than the frequencies to be amplified. However, it is much easier to understand the junction capacitor because of its lack of a hysteresis loop. An accurate picture of amplification in such a nonlinear reactance may be obtained if the input signal is assumed to modulate the high-frequency power supply;²² a rectifier is used to recover the signal frequency in the output. Since the depletion layer capacitance is a majority-carrier phenomenon, its change with voltage is extremely rapid, and amplification is possible (in principle) well into the microwave range. If there are no losses in the variable capacitor, the noise is also potentially low.

Another point of view which may be taken of the junction diode as an amplifier is that portrayed in Fig. 10(b). The switch is assumed to alternate from one position to the other at a very high frequency. It is seen that, in the input position, the capacitance has a high value since the back bias is small. It is then charged up by the input signal, to a charge determined by the time and the series resistance. The switch is then thrown to the high-voltage condition, and the capacitance drops to a lower value. Since the charge injected by the signal remains constant, the voltage corresponding to it must rise in inverse proportion to the capacitance. Thus additional output power is available for the load, and the system has a power gain. The gain is small since the capacitance changes are ordinarily less than an order of magnitude. Much higher gain is possible, at the expense of frequency response, by use of minority-carrier storage.²³ Under such operation, the input-position battery is connected in the forward direction, and a very high current of minority carriers flows. Before equilibrium is approached, the switch is thrown to the output position, and the minority carriers are swept out again. The equivalent capacitance change for such operation is several orders of magnitude, so the power gain is correspondingly higher. However, since minority-carrier flow is now used, the upper frequency limit is imposed by a transit time similar to that of junction transistors. In practice, of course, a fast switch is not available, and one uses a high-frequency oscillator and a blocking diode connected in the output, so that this circuit arrangement is seen to be substantially the same as that of the modulating amplifier described above, and the principle of operation may be thought of in the same way also.

²⁰ L. J. Giacoletto and J. O'Connell, "A Variable-Capacitance Germanium Junction Diode for VHF," in "Transistors I," RCA Labs., Princeton, N. J.; 1956; also published in *RCA Rev.*, vol. 16, pp. 68-85; March, 1956.

²¹ L. J. Kabell and W. E. Evans, "A transistor subcarrier generator for color receivers," *IRE TRANS.*, vol. BTR-1, pp. 9-13; July, 1955.

²² J. M. Manley and H. E. Rowe, "Some general properties of nonlinear elements—Part I. General energy relations," *PROC. IRE*, vol. 44, pp. 904-913; July, 1956.

²³ A. W. Holt, "Diode amplifiers," *Electronic Design*, vol. 2, pp. 24-25; October, 1954.

CONTROLLED INHOMOGENEITY IN SOLIDS—OR HOW TO COMPROMISE WITH NATURE

Technology makes its advances by compromise, in which a result is achieved by using nature's gifts as they are, rather than a waiting eternally until an ideal is reached. Thus the theoretical scientist makes assumptions which allow a solution, even when they do not exactly fit the problem. The transformer designer accepts a nonideal conductor (such as copper), and a non-ideal magnetic core material. (such as silicon steel) and proceeds with the best compromise design for a given result. And so it is with other electric circuits, which are made up with the "best" conductors, separated by the "best" insulating dielectrics, none of which are quite perfect. The elements of the periodic table, and the compounds, alloys, and mixtures which can be made with them, never provide ideal materials. Each year improvements are made, but the result is always a compromise.

Solid-state technology has now reached a stage where the method of compromise can be extended well beyond simple choices of the "best" material *A* juxtaposed to another "best" material *B*. Consider, for example, a simple mechanical illustration involving a weight-carrying steel beam, shown in Fig. 11. Given the span, and the weight to be carried, we may go to a table of structural steel characteristics and find an alloy and I-beam size which meets the requirements. Is this going far enough? The metallurgist may suggest a better or cheaper alloy, while the structural designer may suggest a nonuniform cross section, to equalize stresses. Both reach a practical compromise, which is ultimately the result of limiting their choice to a homogeneous material.

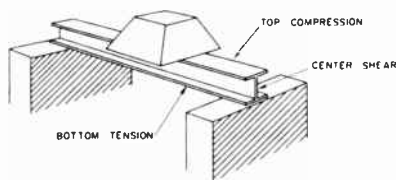


Fig. 11—A beam, carrying a weight. Stress varies from end to end. Best results require a continuous variation in material properties.

Let us look at the problem more fundamentally. The top of the beam is in compression, the bottom is in tension, and the central web must resist shear; each of these stresses varies along the length of the beam. Thus, each region of the beam has a somewhat different requirement for the material in that region. Why then should the same alloy composition be chosen from one end to the other and from top to bottom? In fact, a careful choice of *nonhomogeneous* material, from end to end and top to bottom may lead to an equally strong beam with less material, or with cheaper material. The illustration is, of course, an impractical one in today's

economy and the state of technology of structural metals. But it illustrates a point.²⁴

Fortunately, in electronic solid-state devices, one is able to take a very advanced point of view. Relatively little material is needed, so that we can afford the luxury of such rare chemical ingredients as selenium, germanium, gallium, and the like. In piezoelectric and semiconductor materials, we can even afford single crystals of a high order of perfection. An auspicious start has been made, in the transistor field at least, on optimization by use of inhomogeneity. This is sufficiently striking to justify detailed discussion. The ordinary transistor is based on the *p-n* junction. Here a material containing a *p*-type impurity is joined to one containing an *n*-type. One may contend that this is a case of inhomogeneity; it is actually an abrupt junction between homogeneous regions. Although more complex, it isn't too different in kind from those junctions which have been used in electric circuits where a copper wire is abruptly joined to its plastic insulating covering, or soldered to the end of a resistor. As we shall see, one can do better.

The transistor is undoubtedly a marvelous device, but it has its shortcomings. The most outstanding is its high-frequency response, which is limited mainly by the finite mobility of the charge carriers, the electrons and holes. Although one would like a semiconductor which gives good operation at room temperature or higher, and substantially infinite mobility, the elements of the periodic table, and the compounds we can form from them, seem to thwart us. For example, the materials which show mobility orders of magnitude higher than germanium will not work even as high as room temperature. In the last two years, however, nearly an order of magnitude improvement in frequency response *has been achieved in transistors at room temperature*, by an application of a continuous and controlled inhomogeneity in the semiconductor material. In the first publication, by Kroemer, this radically improved structure was called the drift transistor.²⁵ It has also been described in terms of the technique employed to obtain the result; e.g., diffused-base transistor,²⁶ and grown-diffused transistor²⁷ are terms also in use. We shall call it the drift transistor.

In the drift transistor, advantage is taken of a specially chosen nonuniform distribution of impurities in the base region to create the effect of an internal electric

²⁴ A more practical illustration is the cutting tool of a lathe, whose working edge is heat treated differently from the main body. Another illustration is the case-hardened, wear-resistant exterior of a ball bearing or other machine part, whose interior has the requisite toughness or other required bulk property. The latter is of particular interest because it can be achieved by the type of solid-state diffusion also used to obtain nonhomogeneous base regions in the drift transistor, to be mentioned next.

²⁵ H. Kroemer, "The drift transistor," in "Transistors I," RCA Lab., Princeton, N. J., pp. 202-220; 1956. The first publication of the principle was in *Naturwiss.*, vol. 40, p. 578; November, 1953.

²⁶ C. A. Lee, "A high-frequency diffused-base germanium transistor," *Bell Sys. Tech. J.*, vol. 35, pp. 1-22; January, 1956.

²⁷ Texas Instruments, Inc., Dallas, Texas.

field. This field speeds up the charge carriers from emitter to collector by a substantial factor, and leads to an equally startling improvement in frequency response. Fig. 12 shows schematically the original, homogeneous-base transistor and the drift transistor, with its base of nonhomogeneous impurity distribution. Because the donors in the base region act as fixed positive charges, by piling them up near the emitter, and thinning them down near the collector, one can "build in" an electric field which propels the holes from emitter to collector at many times their normal diffusion speed. In theory, the optimum impurity distribution is exponential with distance and leads to an order-of-magnitude improvement. In practice, solid-state diffusion of impurities leads to an error-function distribution which is close enough to optimum to produce about a 5-fold, rather than a 10-fold improvement.²⁸

Let us notice that the circuit man was relatively limited with the original homogeneous-base transistor. He could not, as in a vacuum tube, produce an internal field and speed up the charge carriers by an increase in voltage. The fixed donor impurity centers, which made the transistor possible in the first place, also held all effect of voltage to the depletion-layer region of the collector junction. It is clear that the solid-state physicist was called upon to "build in" an effect in the solid which, in turn, produced a greatly improved result in the circuit. The drift transistor principle is now a basic part of all the highest-frequency transistor designs; it was done by recognizing the advantage of not dividing the world of semiconductor junctions into two sharply different but homogeneous parts.

The drift transistor is, of course, not the only device in which advantage can be taken of controlled inhomogeneity of impurities. The principle has already been suggested to change the characteristics of a semiconductor variable capacitance,²⁹ to maximize the breakdown voltage of a semiconductor rectifier,²⁹ and to improve sweep-out of minority carriers in semiconductor switching devices.

We may now allow our imagination to roam further into the possibilities of the future. In semiconductors, it has been shown that a nonhomogeneous crystal lattice can lead to a nonuniform band gap with distance.³⁰ If this is done in a controlled way, it is possible to produce in a solid, not the simple electric field of the drift transistor, but a force which acts on electrons and holes *in the same direction*, even though their electric charges

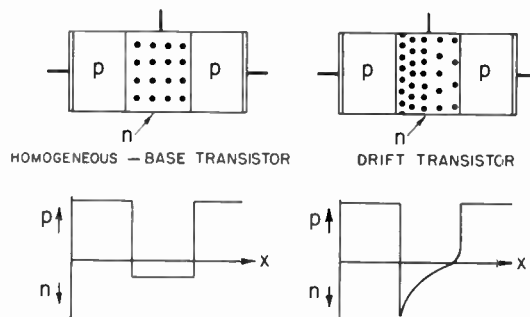


Fig. 12—The ordinary transistor and the drift transistor; the latter uses controlled inhomogeneity of impurities in the base to achieve a 5 to 10-fold better high-frequency performance.

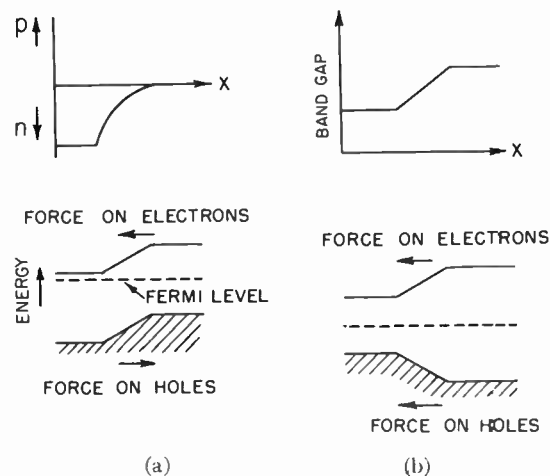


Fig. 13—Two types of controlled inhomogeneity in semiconductors. The energy level diagram shows the force on electrons and on holes. (a) Impurity density varied, (b) band gap varied (intrinsic material).

are opposite. Fig. 13 shows the difference between the electric field produced by an impurity change with distance, and a band-gap change. (Of course, when there is no emf across the material, this electrical force is exactly counterbalanced by the diffusion force which comes from the progressively higher hole-electron density in the lower band-gap regions.) Still further, it can be shown that another type of lattice change can produce a quasi-magnetic field which is quite different from any we can simulate by coils and magnets.³¹ Since these fields act on electrons and holes differently from ordinary electric and magnetic fields, they are called quasi-electric and quasi-magnetic.

It may be necessary now to dispel the charge that these notions of controlled inhomogeneity are highly speculative. Let us look at some results of the past few years on alloys of germanium and silicon, shown in Fig. 14. Although it was known that germanium and silicon were miscible in all proportions, it was found only recently that single crystals could be grown with as much

²⁸ A. L. Kestenbaum and N. H. Ditrick, "The design, construction and high frequency performance of drift transistors," *RCA Rev.*, vol. 18, pp. 12-23; March, 1957.

²⁹ L. J. Giacoletto, "Theoretical junction capacitance and related characteristics using graded impurity semiconductors," *IRE TRANS.*, vol. ED-4; July, 1957.

³⁰ H. Kroemer, "Band structure of semiconductor alloys with locally varying composition," *Bull. Amer. Phys. Soc.*, ser. II, vol. 1, p. 143; March 15, 1956.

³¹ H. Kroemer, "Quasi-electric and quasi-magnetic fields in non-uniform semiconductors," paper to be published.

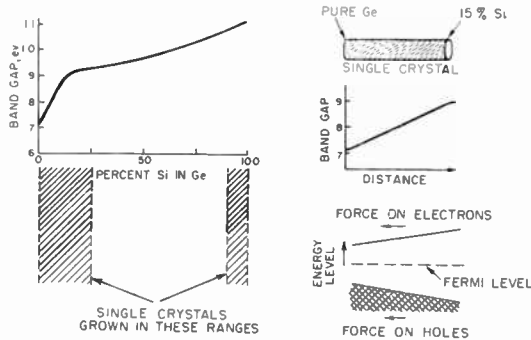


Fig. 14—Characteristics of alloys of germanium and silicon.

	III	IV	V
	Al Ga In	Si Ge Sn	P As Sb

	Band Gap (ev)	Mobility		Lattice Constant
		Electron	Hole	
Si	1.1	1900	500	5.42
AlP	3.0	—	—	5.44
Ge	0.7	3900	1900	5.62
GaAs	1.4	7000	300	5.62
Sn	0.1	10,000	—	6.46
InSb	0.2	80,000	1200	6.46

Fig. 15—Table of data on 3-5 semiconducting compounds compared with their column-4 neighbors.

as 25 per cent silicon in germanium, and 10 per cent germanium in silicon.³² Even more important, as shown in the right of Fig. 14, a single crystal was grown, an inch or two long, which was pure germanium at one end, and merged gradually into a 15 per cent silicon alloy at the other end.³² The characteristics of Ge-Si alloy materials are seen to vary gradually from one composition to the next. In principle, then, a quasi-electric field has been achieved in the most difficult structure to work with, a single crystal. Germanium and silicon are not the only semiconductors with which this may be done. In the table of Fig. 15, are data on that very remarkable class of compound semiconductors, called 3-5 compounds. For each semiconducting element in column 4 of the periodic table, there is a binary material made of a column 3-column 5 combination, which has almost exactly the same lattice constant, and the zinc-blende crystal structure. The zinc-blende crystal is the binary analog of the diamond-like crystal lattice of germanium and silicon. It is evident that a merging of gallium arsenide into germanium, or aluminum phosphide into silicon, is not prevented by any mismatch of crystal lattice, although there may well be other difficulties. There is hope that the next few years will see some of these new

³² S. M. Christian, "The growth and properties of single crystal Ge-Si alloys," paper to be published.

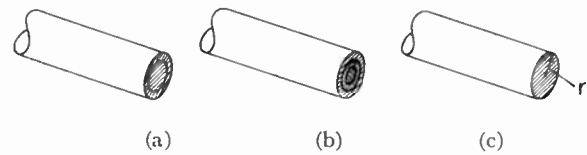


Fig. 16—High tensile strength electric conductors using abrupt and continuous inhomogeneity. (a) Copper-clad or aluminum-clad steel wire, (b) two layers over steel core, (c) continuous change in composition, $C=f(r)$.

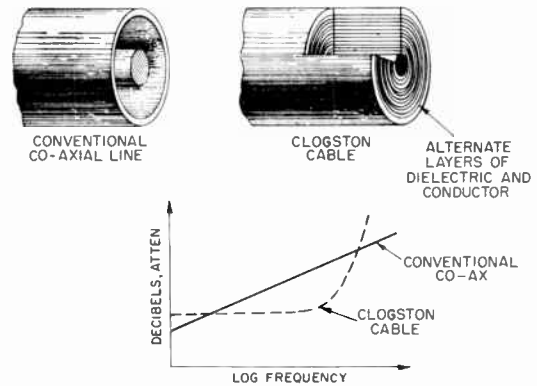


Fig. 17—Clogston cable is a successful attempt to fill the space between inner and outer conductors of a coaxial line with something more useful than air or dielectric.

materials provide additional tools for the achievement of controlled inhomogeneity in advantageous fashion.

Clearly, controlled inhomogeneity is much more easily obtained when single crystallinity is not necessary. So, let us leave semiconductors and consider a few other circuit elements for illustration. A trivial illustration, in the field of conductors, is a copper-clad or aluminum-clad steel wire as shown in Fig. 16. Because alternating-current flows mainly on the surface, a copper or aluminum-clad steel wire is a compromise which gives the tensile strength of the steel core, and the ac conductivity of the outer conductor. At the sharp transition between the core and the high-conductivity surface layer, too little current is carried to justify the copper, and too much current to justify the steel. A better compromise would use two layers over the core, selecting an intermediate layer of higher tensile strength than copper, and higher conductivity than steel. The compromise of a gradual change in composition from center to outside, which is even better, may not be practical or economic today, but it is clearly possible in principle.

The laminated Clogston cable of Fig. 17 uses alternate layers of conductor and insulator to achieve a high-frequency cable loss much less than common air-dielectric coaxial cable of the same diameter.³³ Although this novel cable uses abrupt transitions from conductor to dielectric throughout, it is clearly an attempt to fill the space between inner and outer conductors with

³³ A. M. Clogston, "Reduction of skin effect losses by the use of laminated conductors," *Bell Sys. Tech. J.*, vol. 30, pp. 491-529; July, 1951.

something more useful than air or dielectric. Its success, in principle, is another example of useful compromise with nature's limitations by a controlled inhomogeneity.

Another illustration of a compromise with nature lies in the field of ferrite magnetic materials. By choosing the composition of a ferrite, a wide variety of magnetic properties can be achieved.³⁴ In a magnetically "soft" ferrite, one composition achieves a high permeability but with a low Curie temperature and a low resistivity; in another composition, one gets high Curie temperature and resistivity at a sacrifice in permeability, as shown in Fig. 18. A first compromise, for a transformer core, is the simple one of a single homogeneous material with a finite boundary. However, it is clear that we would not normally expect the flux to be constant throughout the ferrite and, if there are copper losses, the temperature will also vary over the core. A better compromise will be achieved if the ferrite composition is changed to be more nearly optimum for each portion of the core, as in Fig. 18.

In a ferrite loop antenna, Fig. 19, one may find it advantageous to change composition between the portion under the coil, which should have the highest μQ product, and the remote ends, which could be made of a ferrite having highest permeability. Since the ends are present to enlarge the effective capture cross section of the antenna, but contribute somewhat less to the losses, one can achieve an advantage in this way without increasing the core diameter. The table in Fig. 19 gives some typical published data.³⁴

There is not enough space to go into other illustrations, but ferrite switching cores, magnetostriction devices, gyrators, piezoelectric crystals, ferroelectric devices, thermistors, photoconductive devices, etc., all have their special problems. By use of controlled inhomogeneity, the designer and device technologist can often build into his device a circuit performance which could otherwise not be achieved with available materials. For the circuit engineer, in turn, a result is attained which would not have been possible by years of painstaking circuit variations using less-refined devices and

³⁴ C. D. Owens, "A survey of the properties and application of ferrites below microwave frequencies," *Proc. IRE*, vol. 44, pp. 1234-1247; October, 1956.

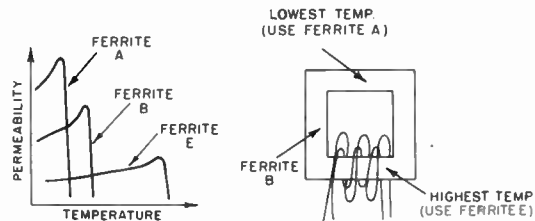
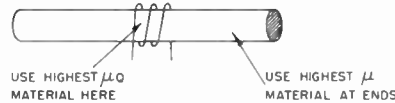


Fig. 18—A transformer core, in which copper loss produces a non-uniform temperature, can advantageously use ferrites of corresponding nonuniform Curie point.



	Ferrite	
	A (NiZn)	B (MnZn)
μ	4000	1500
μQ (1 mc)	1600	10,000

Fig. 19—In a ferrite loop antenna, a judicious choice of inhomogeneous material composition can improve the effective pick-up without increasing size.

components. The ultimate extension of the general principle of inhomogeneity may produce a very complex single solid which performs a multiplicity of functions by virtue of the difference in molecular structure from point to point.³⁵

CONCLUSION

The future developments in new solid-state phenomena in conductors, dielectrics, semiconductors, and magnetics will lead to circuit behaviors which cannot otherwise be achieved. Above all, it appears that controlled inhomogeneity in solids will produce both new and unusual phenomena and, ultimately, a single, solid, circuit element which combines the functions of many conventional components and associated wiring.

³⁵ A summer course, "Molecular Engineering," was given at Mass. Inst. Tech., August 20-31, 1956. This course, organized by Prof. A. R. Von Hippel, emphasized future engineering design, starting with molecular structure and ending with a desired circuit element.



High-Frequency Semiconductor Spacistor Tetrodes*

H. STATZ†, R. A. PUCEL†, MEMBER, IRE, AND C. LANZA†

Summary—The basic idea in these devices is to achieve a good high-frequency response by using processes which are localized in the high-field region of reverse-biased p - n junctions. Structures have been proposed previously which use one injecting contact in the space-charge region. These devices have disadvantages which may be overcome by going to devices with two contacts in the space-charge region. These latter devices have been successfully built and tested. Electrons are injected into the space-charge region of a reverse-biased junction. The injection current is modulated by another nearby contact. This modulating contact is a small alloyed p -type region which is biased in "reverse" and consequently draws negligible current. Its function, in a sense, is analogous to the grid in a vacuum tube. In such a device, the second contact has the additional function of shielding the injecting contact from voltage changes across the main p - n junction. The high degree of shielding already achieved in the first few experimental units reflects itself in the fact that the output impedance is of the order of 30 megohms. The measured input impedance is, at present, also about 30 megohms. The input impedance can probably be made even higher. The first experimental devices show a low-frequency power gain at least as high as that obtained with our present-day transistors. The input and output circuits are coupled only through a low interelectrode capacity. Additional interesting features of these new devices are their low capacities and the independence of their operation on the minority carrier lifetime of the semiconducting materials used. In analogy to previously proposed structures, the name "spacistor tetrode" is suggested.

INTRODUCTION

THE basic idea, underlying this new class of devices, is the avoidance of limitations imposed by the relatively slow diffusion of minority carriers through the essentially field-free base regions of transistors. Though the base regions of diffused transistors have a built-in field, the total voltage drop across this region is limited, in principle, to at most one-half the energy gap of the semiconductor material used. In practice, this upper limit is never reached and in most devices this drop corresponds approximately to 0.1 or at most to 0.2 volt. The possible gain in cutoff frequency as compared to a transistor with equal base width and no built-in field is therefore approximately four- to eight-fold.

Very much higher field strengths, however, are found in the space-charge regions of reverse-biased junctions and, as is well-known, one easily obtains the highest fields that can, in principle, exist in semiconductor bodies before breakdown mechanisms set in. At the same time, the thickness of the space-charge region can be made arbitrarily small. Therefore, we have attempted to make amplifying devices which utilize these high fields

to obtain very short transit times for charge carriers.

Early work indicated¹ that oscillating and amplifying devices could be built utilizing one injecting contact in the space-charge region in conjunction with the avalanche multiplication of the injected carriers in the region of high field. In subsequent unpublished experimental work, the negative resistance diodes proposed by Statz and Pucel,¹ actually were built. It was necessary, however, to maintain very close tolerances in the dimensions and the resistivities of these devices in order that just the right amount of avalanche multiplication resulted. In addition, because of the high applied voltages necessary and other reasons to be discussed below, perfect surface conditions were also required. Thus the emphasis of further work was shifted to devices which did not require any avalanche multiplication. In the meantime, a device had been suggested² which used one injecting contact in the space-charge region (just as in the above-mentioned negative resistance device) but no avalanche multiplication. The operation of the device depends critically upon the requirement that the injecting contact is very close to one boundary of the space-charge layer; for example, for an electron injecting contact this is the boundary between the space-charge layer and the neutral p region. In biasing the contact to inject the desired type of carriers, the space-charge region is deformed such that for even very moderate currents the contact might no longer remain in the space-charge region, and hence, the postulated high-frequency performance of the device might be impaired. This leads to the result that the power-handling capacity decreases with increasing power gain.

Another undesired effect occurs which is connected with the surface condition and which will be discussed further below. Some other possible objections, such as the fact that the device has no current gain and that the input and output are coupled, also are worthy of mention. It will be shown, however, that these last objections can be overcome by a different mode of operation, one which shares some of the features of the device to be described in this article.

The question may arise as to how the devices which utilize injection of carriers into space-charge regions

* Original manuscript received by the IRE, July 9, 1957; revised manuscript received, August 15, 1957.

† Raytheon Mfg. Co., Waltham, Mass.

¹ H. Statz and R. A. Pucel, "The spacistor, a new class of high-frequency semiconductor devices," *Proc. IRE*, vol. 45, pp. 317-324; March, 1957; "New High Frequency Semiconductor Devices Utilizing Injection of Carriers into Space-Charge Regions," presented at the IRE-AIEE Semiconductor Device Res. Conf., Purdue Univ., Lafayette, Ind.; June, 1956.

² W. Gaertner, "A New UHF Transistor," presented at WESCON Convention, Los Angeles, Calif.; August 21-24, 1956.

differ from the so-called field-effect transistor.³⁻⁵ In the field-effect transistor, the cross sectional area of an n - or p -type ohmic conducting "channel" is varied by surrounding space-charge regions produced by a "gate." The current flowing through this channel causes a potential gradient along this channel; however, the field strengths reached are limited by the heat generation due to this current and are orders of magnitude smaller than those obtainable in space-charge regions.⁵ A similar comment applies to the so-called analog transistor.⁶ Actually the analog and the field-effect transistor are very similar, the only essential difference, for example, being the use of intrinsic material in place of lightly doped n -type material for the region between the "source" and the "drain." The frequency limitations of the two transistor types are also closely related. In order to have a high electric field, for example, between the analog grid and analog cathode a large current must flow between the analog cathode and the analog plate. Thus, comparable heating effects will limit the obtainable electric fields. This state of affairs is to be contrasted to the devices described here in which no current is necessary to establish the high electric fields and thus no excessive power has to be dissipated in order to obtain a good high-frequency response (short transit time).

PRINCIPLES OF DEVICE OPERATION

Because of the difficulties in the above mentioned devices, a new approach was made. The resulting device is shown schematically in Fig. 1. A p - n junction is biased in reverse. The resulting space-charge region is indicated by the shaded area. A suitable electron-emitting contact C is placed into the space-charge region. (Later both injecting and noninjecting contacts in space-charge regions will be considered and experimental results discussed.) The contact C is connected to terminal A through a battery which biases the contact negatively with respect to the potential of the underlying space-charge region. Note the potential of point C is still positive with respect to A . Electrons are emitted from this contact into the space-charge region. The electrons flow to the n side, through the load, and back to point C . The emission of the electrons from contact C will be space-charge limited^{7,8} for most cases to be discussed.

A second contact D is placed between the emitting contact and the n region. It is essential that this contact

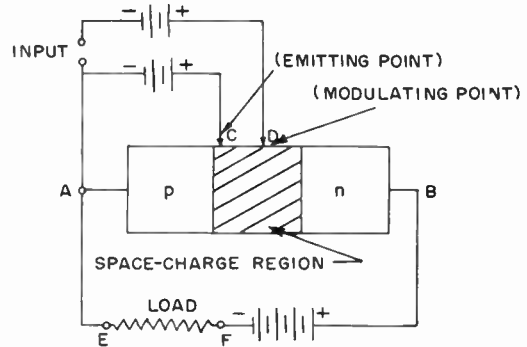


Fig. 1—Schematic presentation of new high-frequency semiconductor device.

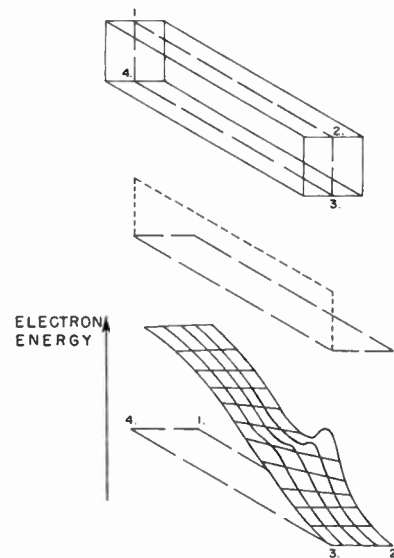


Fig. 2—Electron energies in a section through space-charge region with modulating contact.

be rectifying when situated in the space-charge region. Point D should be biased in reverse with respect to the underlying space-charge region in order that it draw negligible current. As will be shown below, a p -type alloyed contact will perform this function. In operation of the device, the bias potential of modulating point D will always be positive with respect to the potential of the underlying space-charge region. In spite of this fact, none of the electrons emitted by C will be collected by D . The reason for this may be seen partially from Fig. 2 where the potential in a longitudinal cross section through the space-charge in the vicinity of point D is shown. Contrasting to a vacuum tube where the electrons can gain kinetic energy in their flight from cathode to plate, in a solid the electrons constantly collide with the lattice. Consequently, the direction of the current is always in the direction of the electric field. Thus, by biasing point D negatively with respect to the potential of the underlying space-charge region, no net electron current will flow into the point. Since the point D is placed in the space-charge region, the field produced by it will penetrate throughout this region. The field extends to the boundaries of the space-charge region where it is shielded out by a

³ W. Shockley, "Unipolar 'field-effect' transistor," *PROC. IRE*, vol. 40, pp. 1365-1376; November, 1952.

⁴ G. C. Dacey and I. M. Ross, "Unipolar 'field-effect' transistor," *PROC. IRE*, vol. 41, pp. 970-979; August, 1953.

⁵ G. C. Dacey and I. M. Ross, "The field effect transistor," *Bell Sys. Tech. J.*, vol. 34, pp. 1149-1189; November, 1955.

⁶ W. Shockley, "Transistor electronics: imperfections, unipolar and analog transistors," *PROC. IRE*, vol. 40, pp. 1289-1313; November, 1952.

⁷ W. Shockley and R. C. Prim, "Space-charge limited emission in semiconductors," *Phys. Rev.*, vol. 90, pp. 753-758; June, 1953.

⁸ G. C. Dacey, "Space-charge limited hole current in germanium," *Phys. Rev.*, vol. 90, pp. 759-763; June, 1953.

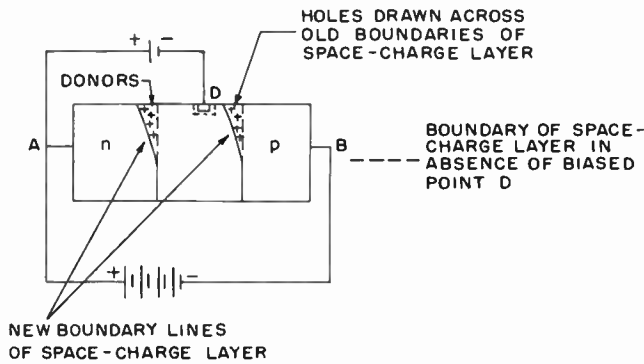


Fig. 3—Diagram illustrating effect of negatively biased point in space-charge region.

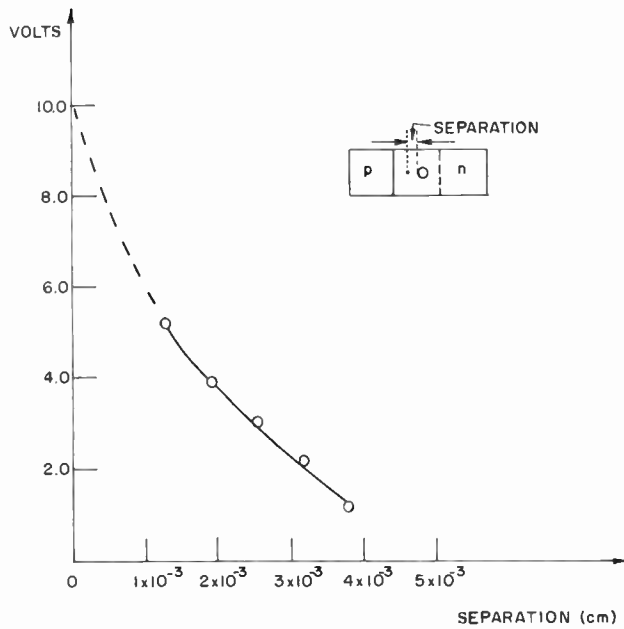


Fig. 4—Diagram illustrating how voltage applied to point *D* alters potential in space-charge region.

deformation of these boundaries, as shown in Fig. 3. One can easily measure how the potential in the space-charge region is altered by the presence of the biased point *D*. For this purpose a 10-volt alternating voltage was superimposed on the bias of point *D* and with a tungsten point, the ac voltage on the surface of the space-charge region was measured at various points. In Fig. 4, the results are shown for a germanium device with total applied direct voltage of 220 volts across a 1.2×10^{-2} cm wide space-charge region. The function of contact *D* is two-fold. First, by superimposing on its dc bias an alternating voltage, one can vary the emission of the emitting contact. This is so because the field strength in the vicinity of point *C* will be altered and the space-charge-limited emission will be modulated. The degree of modulation, of course, depends critically on the geometric arrangement of the two contacts—in particular on their spacing, and also on the magnitude of the bias current flowing. To discuss the modulation quantitatively, it is convenient to use vacuum tube

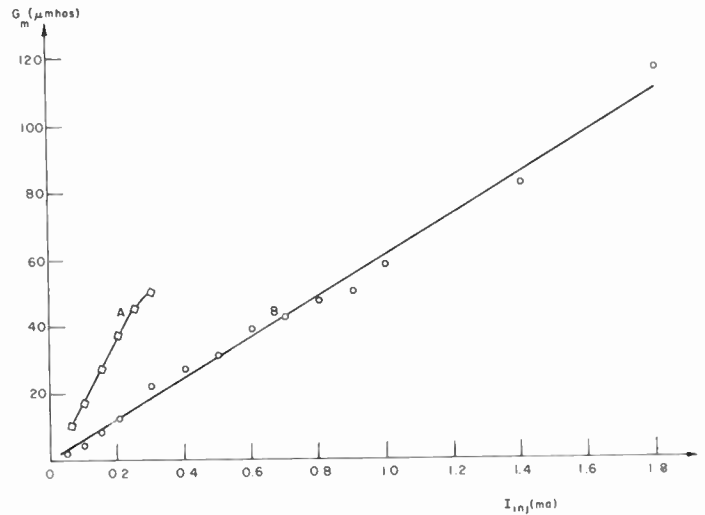


Fig. 5—Transconductance for two devices as a function of injected current.

terminology and define a transconductance g_m as

$$g_m = \frac{\partial I_{out}}{\partial V_{mod}} = \frac{\partial I_{inj}}{\partial V_{mod}} \quad (1)$$

In (1) I_{out} is the load current and I_{inj} the injected current, V_{mod} is the potential of the modulating point *D*. Transconductance is plotted in Fig. 5 for two typical germanium devices as a function of the injected bias current. It is seen that g_m increases approximately linearly with the bias current. The modulating contact was a *p*-type gold alloyed dot approximately 5×10^{-3} cm in diameter. The injecting contact was a tungsten point approximately 1.2×10^{-3} cm away from the edge of the modulating contact. This latter distance is very difficult to estimate because etching of the device causes some of the germanium to be removed under the gold dot. This is also the reason that devices with distances substantially smaller than 1.2×10^{-3} cm have not yet been investigated. In the above devices, a total voltage of 205 volts was applied and the width of the space-charge was approximately 10^{-2} cm. The position of the tungsten point is in practice always chosen to lie between the *p*-type region and the modulating point *D*. It might be added that if the injecting contact *C* sits side by side with contact *D*, a lower g_m is obtained for comparable separations. A more detailed consideration of geometries will be given below.

The second function of contact *D* is to reduce the influence of voltage changes across the load on the emission of *C*. To illustrate how this comes about, the potential across a space-charge region without any points is shown for two applied voltages in Fig. 6(a). The position which the emitting contact *C* usually has is indicated by a dashed line. From Fig. 6(a), one can see that the potential of this position depends upon the applied voltage across *A-B* (Fig. 1). In Fig. 6(b), the potential across the space-charge region near the surface is shown for two applied voltages, but with contact *D* present and biased

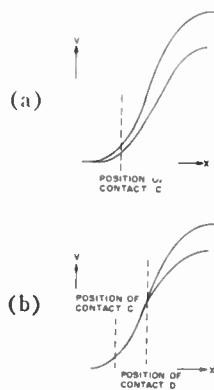


Fig. 6—Diagram illustrating the shielding effect of a biased point D in space-charge region.

with a constant voltage with respect to A (Fig. 1). In Fig. 6(b), it is seen that at the position where contact C will normally be placed, there is almost no variation in the potential of the underlying semiconductor; therefore, the bias of contact C with respect to the space-charge region will be almost independent of the applied voltage across $A-B$. From this, one may expect that the emitted current will be independent of the voltage across $A-B$ and thus that the output impedance of the device will be very high. Also one can look upon the shielding action of the contact D in a somewhat different way. The field strength determining the space-charge-limited emission of contact C depends partially on the voltage applied across $A-B$ and partially on the potential of the contact D . A high output impedance means that the field in the vicinity of C is essentially independent of the bias across $A-B$ and depends only on the potential of contact D . It is obvious that high transconductance and good shielding action of contact D go in parallel. A realistic way of measuring the output impedance so as not to be disturbed by leakage currents is measuring the change in injected current for a change in the voltage across the output $A-B$. In measuring the unit for which the g_m values are shown as curve A in Fig. 5, an impedance of approximately 30 megohms for $I_{inj} = 0.3$ ma is found. The output impedance decreases with increasing injected bias current. It is seen that even with a small contact, efficient shielding can be obtained.

CONTACTS IN SPACE-CHARGE REGIONS

As has been argued, it is necessary to make good injecting and rectifying contacts in space-charge regions. For the device to have high-power gain, it is particularly important for the modulating contact to have a good reverse characteristic. In our search for suitable contacts, tungsten points and small fused bonds have been investigated experimentally. In these investigations, the current-voltage relationship was measured, using the circuit shown in Fig. 7(a). No current will flow when the potential of the contact essentially equals the potential in the underlying space-charge region. In the experiments, the voltage applied to the contact is

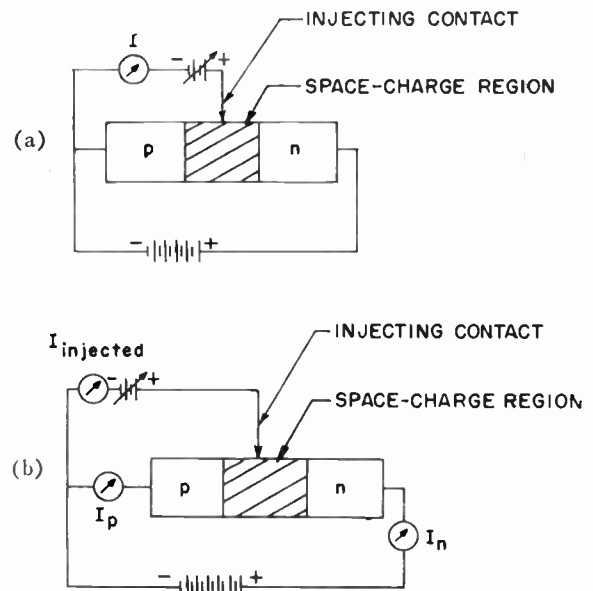


Fig. 7—Diagrams of circuits for measuring current-voltage relationship and injection efficiency of contacts in space-charge regions.

measured relative to the above mentioned potential so that for $I=0$, $V=0$. By measuring the currents, as shown in Fig. 7(b), one can determine what fraction of the injected current consists of electrons or holes.

Consider first the experimental results obtained with a tungsten point. In Fig. 8(a), the current-voltage characteristic of a typical tungsten point in the space-charge region is shown. The interesting result is that practically no rectification takes place.⁹ The forward impedance is approximately the same as the reverse impedance. The result is quite different from what is found for points on neutral n - or p -type material. In Fig. 8(b), the hole and electron currents, I_p and I_n respectively, are plotted as a function of I_{inj} . It is seen that for voltages in which the point is biased positively with respect to the underlying space-charge, the injected current consists mainly of holes. In the space-charge region the holes flow to the p side; the current is recorded by the meter labeled I_p in Fig. 8(b). For opposite polarities, the injected current consists mainly of electrons which flow to the n side; the resultant current is recorded by the meter labeled I_n . From the results of the above experiments one arrives at the conclusion that a tungsten point is biased in "forward" for either polarity relative to the potential in the underlying space-charge region. These experiments also show that there are small changes in I_n with I_{inj} when mostly hole current flows, and in I_p with I_{inj} when mostly electron current flows. In order to draw general conclusions concerning these small changes, more, and very accurate, measurements need to be made. The decrease of I_p with I_{inj} to the left of the origin in Fig. 8(b) is what one would normally expect. Some of the holes

⁹ W. G. Matthei and F. A. Brand, "On the injection of carriers into a depletion layer (L)," *J. Appl. Phys.*, vol. 28, pp. 513-514; April, 1957.

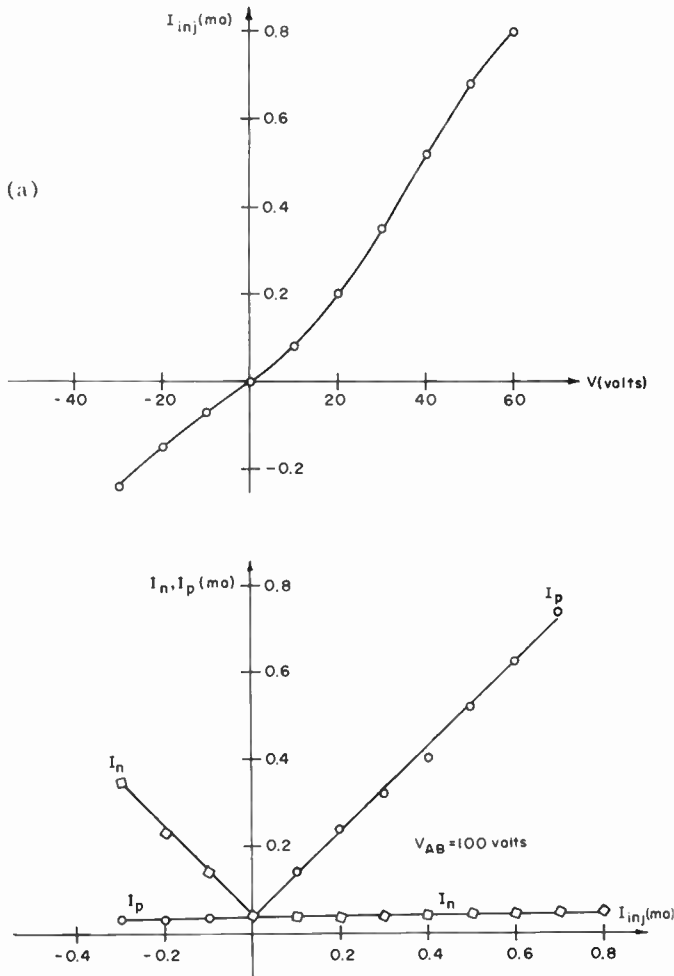


Fig. 8—(a) Current-voltage relationship of tungsten point in space-charge region. (b) Electron and hole currents injected by tungsten point.

generated in the space-charge region or in the *n* side approximately within one diffusion length of the space-charge region are collected while flowing by the tungsten point. Thus I_p is expected to decrease the more negatively the point is made with respect to the space-charge region. By the same reasoning, however, one would also expect I_n to decrease with increasing I_{inj} to the right of the origin, contrary to observation. Several reasons may account for this observation. For example, because of injection the junction may become heated sufficiently so that the reverse current of the main diode is increased; or the field strength may be large enough so that some of the injected electrons induce avalanche multiplication; or, small leakage currents across the surface may account for the observed effects.

A plausible explanation of the main features of the behavior of the contact will be given below. In Fig. 9, the metal is shown in contact with the semiconductor. Surface charges have been ignored since if they are not large enough to cause inversion layers, they will not affect the argument. In the semiconductor there are virtually no holes in the valence band and no electrons in the conduction band, because the high field in the

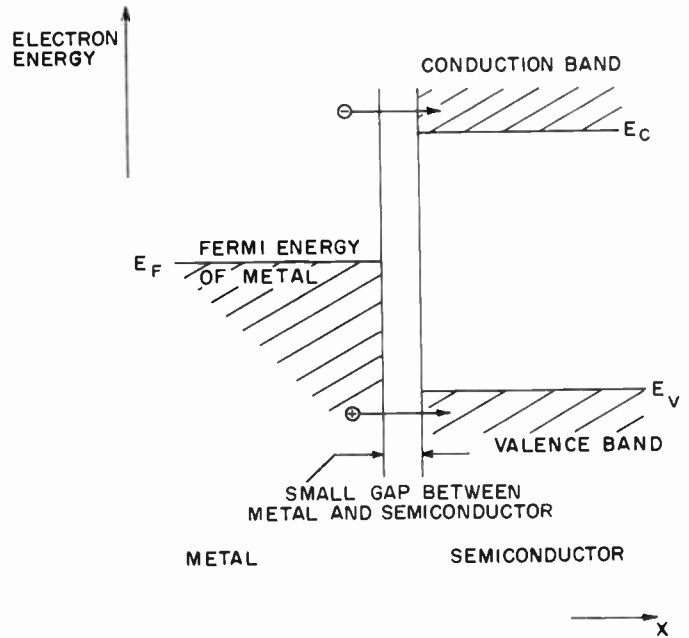


Fig. 9—Diagram illustrating contact of metal in space-charge region of reverse-biased junction.

space-charge region sweeps out all carriers. Electrons from the metal will flow into the conduction band. The magnitude of this current will be

$$I_n = I_{no} \exp \frac{-(E_c - E_F)}{kT} \quad (2)$$

In (2) I_{no} is a constant which is related to the area of the contact, the probability of transition for an electron from the metal to the conduction band in the semiconductor, and other factors. The Boltzmann factor in (2) takes into account the number of electrons that have enough thermal energy to make the transition into the semiconductor. The quantity E_c is the energy of the conduction band edge of the surface and E_F is the Fermi energy in the metal, k is Boltzmann's constant, and T , the absolute temperature. Similarly, electrons will make transitions from the valence band of the semiconductor into the metal or, what is the same, holes will go from the metal into the valence band of the semiconductor. The hole current I_p will be of the form

$$I_p = I_{po} \exp \frac{-(E_F - E_v)}{kT} \quad (3)$$

The quantity I_{po} is related to the area of the contact and to the probability of transition of a hole from the metal into the semiconductor. The energy of the valence band edge at the surface is denoted by E_v . Thus the net current I out of the contact into the semiconductor is

$$I = I_p - I_n = I_{po} \exp \frac{-(E_F - E_v)}{kT} - I_{no} \exp \frac{-(E_c - E_F)}{kT} \quad (4)$$

If the contact is floating, E_F will take on a value E_{F_0} , for which $I=0$. From (4)

$$\exp \frac{E_{F_0}}{kT} = \sqrt{\frac{I_{p0}}{I_{n0}}} \exp \frac{E_c + E_v}{2kT}. \quad (5)$$

If a voltage V is applied between the metal and the semiconductor, most of the potential drop will occur in the space-charge region; however, because of the finite spacing between the metal and the surface, a small fraction of the voltage will appear between the metal and the surface. Let this fraction be c . Thus, for an applied voltage V , the Fermi energy of the metal will shift with respect to the energy bands at the surface from E_{F_0} to

$$E_F = E_{F_0} - qcV \quad (6)$$

where q is the charge of an electron. Inserting (5) and (6) into (4) gives

$$I = 2\sqrt{I_{n0}I_{p0}} \exp \frac{E_v - E_c}{2kT} \sinh \left(\frac{qcV}{kT} \right). \quad (7)$$

The experimental curves exhibit the main features of (7). However, it must be considered that the validity of (7) is limited to small currents and voltages. As the current increases, the concentration of electrons or holes in front of the contact increases. As a result, the assumptions of negligible concentrations of electrons or holes in the semiconductor break down. Also, these electrons or holes reduce the electric field near the point and c decreases, or in other words, the space charge starts to limit the emission from the point. Thus, there is a transition from the current-voltage relationship of (7) to one corresponding to space-charge-limited emission. For completeness one may mention one other reason for c to be a slowly varying function of the applied voltage. For large enough applied voltages, the boundaries of the space-charge region are deformed, causing a change in the fraction of the applied voltage that appears between the metal and the semiconductor surface. However, the above derivation shows why there is no rectification and why for positive and negative biases, holes and electrons are injected respectively.

From the above discussion, it is concluded that a tungsten point contact can be used for injecting either electrons or holes. However, a tungsten point is completely useless for the modulating contact D . For this application it might be anticipated that doped contacts would show the desired rectifying characteristics. Turning now to such contacts, consider a heavily doped p -type contact. If biased positively with respect to the potential of the underlying space-charge region, holes are emitted into the space-charge region. This emission may be considered to be space-charge limited.^{7,8} If biased in reverse, the holes in the p -type contact cannot flow into the space-charge region. However, there are some electrons in the p -type region. Their concentration

will be zero at the boundary between the p -type contact and the space-charge region. Thus, there will be a concentration gradient in the electron distribution from inside of the contact to the above mentioned boundary layer, giving rise to a small direct current. The magnitude of this current may be of the order of 10^{-7} amps for germanium and will be orders of magnitude less for silicon. This current will not depend on the applied bias as long as this bias is larger than a few tenths of a volt, and thus the differential impedance will be infinite. No electrons can flow into the contact from the space-charge region because of the reverse bias. The p -type region can, however, in principle, collect some holes which have been thermally generated in the space-charge region or in the neutral n -type region within approximately one diffusion length of the space-charge region. The number of holes collected will depend slightly upon the reverse bias, and thus this contribution to the current will give rise to a finite differential impedance. In materials with large energy gaps and reasonable lifetime, the rate of carrier generation will be much smaller and their contribution to the input impedance will be reduced. Experimental curves corresponding to those of Fig. 8(a) and 8(b) are shown in Fig. 10(a) and 10(b). It is seen from Fig. 10(a) that the reverse impedance varies with bias somewhat but is of the order of 30 megohms. The same order of impedance has been measured in the operating devices where such a bond has been used as a modulating contact. From Fig. 10(b) it can be seen that in the forward direction, the injected current consists almost entirely of hole current. In the reverse direction, no measurements were made because of the very small current involved, but it is believed that the reverse current consists predominantly of collected holes and possibly is contributed to by surface leakage.

TRANSCONDUCTANCE

Of considerable importance in the operation of the device is its transconductance, g_m . It would be quite valuable to get some theoretical estimates of the magnitudes that can be obtained. It is felt that the geometry of two point contacts on the surface is not advantageous for obtaining high g_m values. A device using line contacts, for example, is expected to be much better [Fig. 11(a)]. In addition, geometries may be used in which the modulating contact is on the other side of the semiconductor body [Fig. 11(b)]. Many other configurations can be given. The following discussion, however, is restricted to the case of point and line contacts. It is exceedingly difficult to calculate accurately characteristics of these devices though it could be done by using relaxation methods. An estimate of the upper limit for g_m can be found by using rather idealizing assumptions.

Consider the case of the line contacts in Fig. 11(a). By applying a certain voltage to the modulating contact, the potential along the surface of the modulating

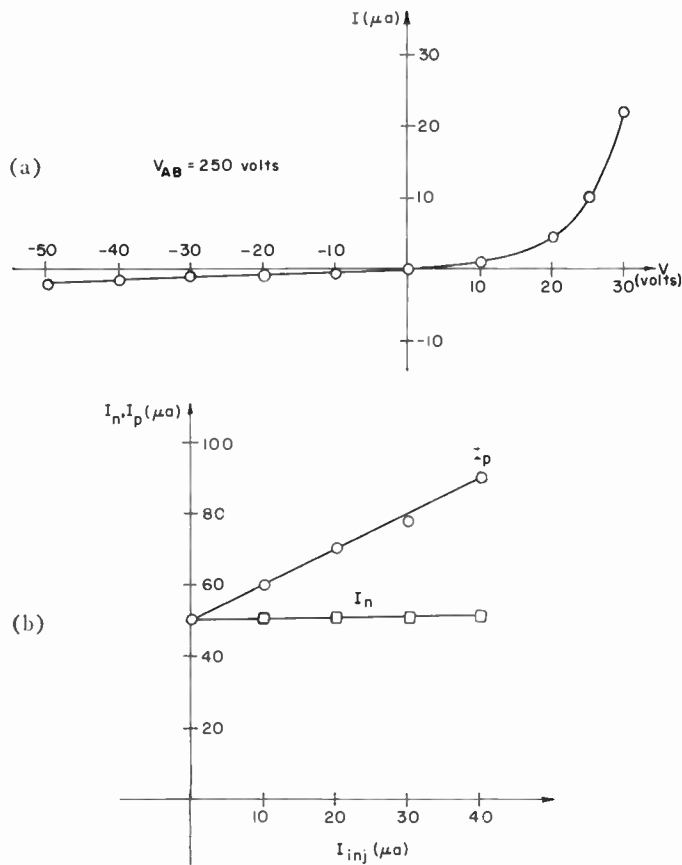


Fig. 10—(a) Current-voltage relationship of alloyed *p*-type contact in space-charge region. (b) Electron and hole currents injected by alloyed *p*-type contact.

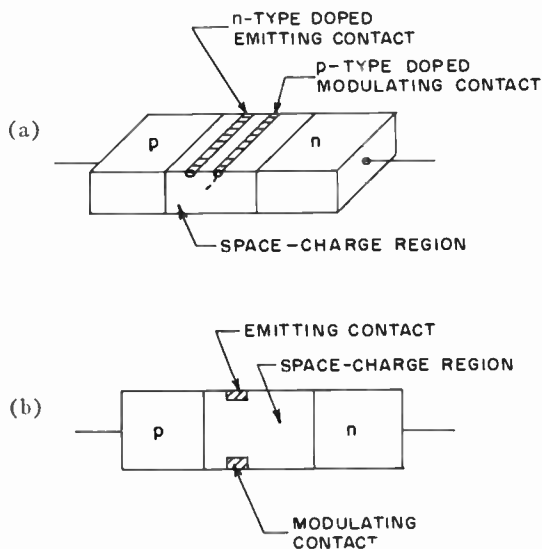


Fig. 11—Alternate geometries for device.

contact in the space-charge region assumes this value. This causes the potential, and thus the electric fields, to change throughout the space-charge region. In order to obtain an over-all cylindrical symmetry it is assumed that the potential along a one-eighth section of a cylinder takes the value of the modulating contact, as indicated in Fig. 11(a) by a dotted line. It is further assumed

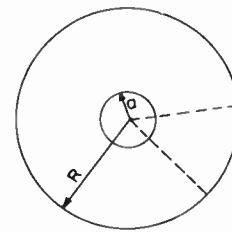


Fig. 12—Diagram used in simplified calculation of space-charge-limited emission.

that the current flow is cylindrically symmetric in that portion of the cylinder. By this idealization, the effect of the modulating contact will be overestimated very probably by a factor less than 10. The problem now becomes one of calculating the space-charge-limited emission (Fig. 12) from an *n*-type cylinder of radius *a* into a *p*-type region with an acceptor charge density ρ_a . The potential is prescribed as $V(R)$ on a cylinder of radius *R*. Poisson's equation for cylindrical symmetry may be written

$$\frac{d^2V}{dr^2} + \frac{1}{r} \frac{dV}{dr} = -\frac{1}{\epsilon} (\rho_a + \rho_n). \quad (8)$$

In (8), V is the potential, r the radial variable, ϵ the dielectric constant, ρ_a the acceptor charge density and ρ_n the charge density due to electrons. By neglecting diffusion,⁶ ρ_n may be written as

$$\rho_n = \frac{j}{\mu E}. \quad (9)$$

In (9), j is the magnitude of the electron current density, μ is the electron mobility and E is the radial electric field. Since the total current per unit length J is assumed to flow in one-eighth of a cylinder, then

$$\rho_n = \frac{4J}{\pi r \mu E} = -\frac{4J}{\pi r \mu} \frac{dV}{dr}. \quad (10)$$

Inserting (10) into (8) one obtains

$$\frac{d^2V}{dr^2} + \frac{1}{r} \frac{dV}{dr} = -\frac{\rho_a}{\epsilon} + \frac{4J}{\epsilon \pi r \mu} \frac{dV}{dr}. \quad (11)$$

For most purposes, it will suffice to assume $\rho_a = 0$ since in practical devices the contacts will be situated in almost intrinsic material. It may be mentioned at this point that there is still another reason to suspect that the inclusion of fixed charges in (11) will not improve the estimates of g_m . In the device, the modulating and emitting contact may be located in regions of the space charge where ionized donors predominate. In the model, the latter case is meaningless because it would correspond to a heavily doped *n*-type region in contact with a slightly doped *n*-type region. Thus, letting $\rho_a = 0$, one obtains from (11) the solution

$$V(R) = a \sqrt{\frac{4J}{\epsilon\mu\pi}} \left\{ \sqrt{\frac{R^2}{a^2} - 1} - \cos^{-1} \frac{a}{R} \right\}. \quad (12)$$

As boundary conditions it has been assumed that $V=0$ and $dV/dr=0$ at $r=a$. In this model

$$g_m = \frac{dJ}{dV} = \frac{\sqrt{J}\sqrt{\epsilon\mu\pi}}{a \left\{ \sqrt{\frac{R^2}{a^2} - 1} - \cos^{-1} \frac{a}{R} \right\}}. \quad (13)$$

Suppose we consider germanium and use for an example: $J=10^{-3}$ amps/cm (J is current per unit length of emitting contact); $\mu=10^3$ cm²/volt sec; $a=5 \times 10^{-4}$ cm; $R/a=2$; then, $dJ/dV=6.1 \times 10^3$ μ mhos/cm. If one assumes $R/a=3$, then $dJ/dV=2.6 \times 10^3$ μ mhos/cm. In (13), μ has been assumed constant and independent of the field. Some account of the reduction of the mobility due to the field has been made by assuming an electron mobility smaller than its low-field value. The value of g_m is a rapidly varying function of the spacing of the line contacts. It appears that values of the order of 1000 μ mhos may be obtained if the devices are operated at higher currents. If, in the model, a ρ_a different from zero had been assumed, the values for dJ/dV would have come out larger.

Using similar simplifying assumptions, one can calculate g_m for a point contact structure. In this case the emission from a sphere of radius a is considered. Fig. 12 shows the cross section through the sphere. In analogy to the cylindrical case, the current may be considered to flow within a segment of a sphere of solid angle $4\pi/8 = \pi/2$ (one-eighth of the sphere). The expression corresponding to (13) is

$$g_m = \frac{dJ}{dV} = \frac{\sqrt{J}\sqrt{3\pi\epsilon\mu}}{\sqrt{a}f\left(\frac{R}{a}\right)}. \quad (14)$$

where

$$f\left(\frac{R}{a}\right) = \int_{x=1}^{x=R/a} (x^{-1} - x^{-4})^{1/2} dx.$$

The values of this integral are tabulated in Table I. Assume $J=10^{-3}$ amps; $\mu=10^3$ cm²/volt sec; $a=2 \times 10^{-4}$; $R/a=6$. These values correspond roughly to the experimental units of Fig. 5, with the exception that the emitting contact was not a doped bond but a tungsten point. With the above numbers, $g_m=97$ μ mhos. This value is remarkably close to the experimental results. It should be pointed out, however, that this is rather fortuitous since, according to (14), g_m should vary as \sqrt{J} , whereas the experimental findings show a more nearly linear behavior, except that curve *A* shows some bending over at the highest J value. One reason for this discrepancy certainly lies in the fact that a tungsten point will behave differently than a doped contact.

TABLE I

R/a	$\int_1^{R/a} (u^{-1} - u^{-4})^{1/2} du$
1	0
2	0.62
3	1.236
4	1.766
5	2.236
6	2.662
8	3.418
10	4.085
20	6.705
50	11.302

SURFACE EFFECTS

In general, the surface properties of semiconductors can be understood in terms of the interaction of several sets of surface states with the underlying semiconductor material. Of great importance for the operation of the transistor is the surface-states-induced surface recombination velocity and minority carrier lifetime in general. For the present device, surface recombination velocity is of little importance. Of some concern, however, is the fact that the surface states may have a net charge. As is known, this leads on neutral semiconductor material to a bending of the bands and, for large charge densities of the proper sign, to inversion layers.¹⁰ The situation for surfaces on space-charge layers is somewhat different. The surface states are located on a region which is not in thermal equilibrium and their occupation will depend upon their capture cross section for electrons and holes and, of course, also upon their energy. In thermal equilibrium the occupation of a state depends only upon its energy and not upon capture cross sections. In this paper, the physics of surface states in space-charge regions will not be discussed further, and we proceed to consider the effects of surface charges. Consider, for example, a space-charge region with a net positive charge on the surface. The field of this charge will penetrate into the space-charge region, and the space charge will be distorted, as shown for three cases in Fig. 13. In the case *c*, such a large surface charge has been assumed that an inversion layer is formed. The art of controlling the surfaces has progressed sufficiently so that inversion layers can be readily prevented. However, small surface charges as shown in Fig. 13(a) may occasionally occur. They will exert little influence on the operation of the above described device. This may be seen as follows: a change in the surface charge will cause the emitting and modulating contacts to be located at a slightly different place in the space-charge region. If the modulating contact is biased sufficiently in reverse, the modulating point will remain in the reverse bias condition regardless of any small changes in the space-charge region. On the other hand, for a good device, the emission of contact *C* depends almost completely on the voltage difference of

¹⁰ "Semiconductor Surface Physics," University of Pennsylvania Press, Philadelphia, Pa., 1957.

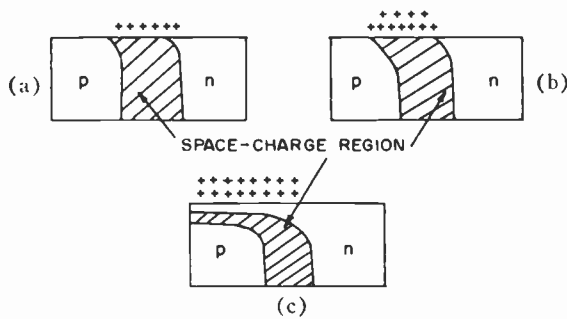


Fig. 13—Effects of surface charges on space-charge regions.

contact *C* and contact *D*, and thus is insensitive to small changes in the surface charge. This relative independence of emission on surface charges can be further strengthened by biasing the emitting point with a stiff direct current source which is shunted by a capacitor. The capacitor clamps the emitting point at a fixed potential relative to ac signals and permits modulation of the emission current. In devices in which the injecting contact has to be very close to one edge of the space-charge layer,² small changes may bring the contact out of the space charge or too far into the space charge, depending upon the sign of the surface charge.

DISCUSSION

Before entering into a discussion of the device with two contacts in the space-charge region, it should be mentioned that some of the advantages of the present device could, in principle, be realized using only one contact in the space-charge region by choosing the input terminals somewhat differently than Gaertner² (Fig. 14).

In comparing the above-described device with the transistor, the frequency response is of prime interest. By the frequency response of the transistor one usually means the dependence of power gain on frequency. Actually, for our device it is not meaningful to consider the power gain, because of the insignificant input power. However, as a matter of interest, the low-frequency power gain for one of the experimental units is calculated below. The input is

$$P_{in} = \frac{V_{in}^2}{R_{in}}$$

where V_{in} is the input voltage and R_{in} the input resistance. The power dissipated in the load is

$$P_{out} \approx V_{in}^2 g_m^2 R_L$$

where R_L is the load resistance. The low-frequency power gain is

$$\frac{P_{out}}{P_{in}} \approx g_m^2 R_L R_{in} \tag{15}$$

With the measured values $g_m = 10^2 \mu\text{mhos}$, $R_{in} = 30$ megohms, $R_L = R_{out} = 30$ megohms, where R_{out} is the output resistance of the device, one obtains a power amplification of approximately 9×10^6 or 70 db. At

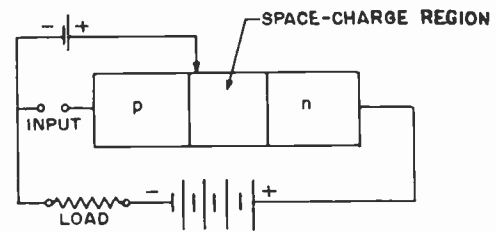


Fig. 14—Alternate choice of input for device with only one contact in space-charge.

higher frequencies, of course, the gain is lower. For example, when the transit time through the space-charge region becomes comparable to the inverse frequency, g_m will decrease. At higher frequencies there will be an additional power consumption at the input arising from the capacitive coupling between the modulating contact and the load. However, the capacities in question will be quite small (of the order of $1 \mu\mu\text{f}$), since the contacts are situated in a rather wide space-charge region.

If the input impedance is extremely high, it is more appropriate to consider voltage gain than power gain. The ratio of the output voltage to the input voltage at low frequencies is approximately equal to $g_m R_L$ if $R_L \ll R_{out}$. With the above value of g_m and $R_L = R_{out}$, this corresponds to a voltage gain of 3×10^3 . Though a load resistance of this magnitude is unreasonable at low frequencies it can be approached by use of high Q tuned circuits at the higher frequencies. Therefore, useful voltage gain will be obtainable up to frequencies corresponding to the inverse transit time of the carriers, at which point g_m starts to decrease rapidly. As is well-known, the output capacity, *i.e.*, the capacity of the reverse-biased main *p-n* junction, is related to the amplification bandwidth. Consider, for example, a parallel *RLC* circuit. If $R \ll R_{out}$, then, at the resonant frequency, the voltage gain is $g_m R$. If one defines the bandwidth $\Delta\omega$ as the frequency interval in which $|Z| \geq R/\sqrt{2}$, where Z is the impedance of the tuned circuit, then this bandwidth becomes $1/RC$ and the gain-bandwidth product is g_m/C .

Another property of interest is that in the above-described device the output and input circuits are only loosely coupled through a small interelectrode capacity. Thus, the device is well suited for the design of multi-stage amplifiers.

It appears that the above device has many of the attractive features of a vacuum tube and may not only extend the frequency response of present-day transistors but may also find useful applications in medium- and low-frequency circuits.

Another attractive feature is the fact that minority carrier lifetime has practically no influence on the operation of the device. Hence, new semiconductor materials with large energy gaps suitable for high temperature operation may more readily be used for the manufacture of this device than for the transistor.

The Utilization of Domain Wall Viscosity in Data-Handling Devices*

V. L. NEWHOUSE†, MEMBER, IRE

Summary—The investigation of the switching behavior of metal tape rectangular loop cores in the millimicrosecond region has led to the discovery of a group of phenomena associated with elastic switching. These effects can be explained in terms of the existing theory of magnetic domains and appear to be associated with the elasticity and viscosity of motion of the domain walls involved in the magnetization process.

Various digital circuit applications are described. These include a technique of continuously displaying the contents of magnetic shift registers and means of operating random access memories an order of magnitude faster than present current coincidence types without an increase in the amount of equipment required, and without the use of extra windings or of a special core geometry.

THE MAGNETIC EFFECTS

Experimental Account

DURING the investigation of the high-speed switching of 1/8-mil grain-oriented 4-79 Molybdenum Permalloy tape, a group of effects were discovered which do not seem to have been previously described in the literature. They appear to be associated with the viscosity of the magnetic domain boundaries. The author has demonstrated these effects in ferrites as well as in Molybdenum Permalloy. The present report will be concerned with the description and utilization of the effects in 4-79 Molybdenum Permalloy as it is this material which has been chiefly investigated to date. The effects can be described under three headings.

Elastic Switching: This effect has been demonstrated in 1/8-mil and 1/4-mil grain-oriented tape made of 4-79 Molybdenum Permalloy. It was found that the application of magnetizing pulses much larger than the coercive force did not give rise to permanent changes of magnetization provided that the duration of the pulses was sufficiently short. This effect, which is a type of nondestructive read-out, is demonstrated in Fig. 1, which shows the waveforms resulting from the application of a 10-ke train of 0.1-microsecond half sine-wave current pulses through five-turn magnetizing windings to a toroid consisting of five wraps of 1/8-mil material. The coercivity of this material was approximately 0.07 oersted. The peak height of the magnetizing pulses shown in Fig. 1 is 0.63 oersted. This is close to the maximum amplitude of 0.1- μ sec half sine-wave pulses which can be applied to this material without significantly affecting the permanent state of magnetization.

* Original manuscript received by the IRE, April 12, 1957; revised manuscript received, July 10, 1957. This paper was presented in abbreviated form at the Western Joint Computer Conference, Los Angeles, Calif., February 27, 1957.

† Radio Corp. of America, Camden, N. J.

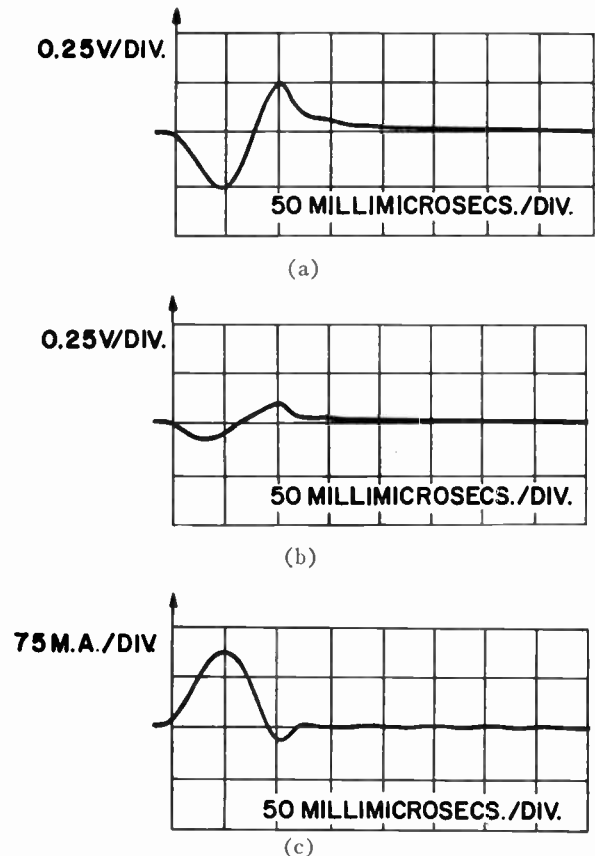


Fig. 1—Nondestructive read-out in 1/8-mil 4-79 Molybdenum Permalloy. Core construction: five wraps of 1/8-mil tape, 3/2 inch wide, ceramic bobbin, 1/2-inch outside diameter. (a) Voltage across five-turn sense winding, core at negative remanence. (b) Voltage across five-turn sense winding, core at positive remanence. (c) Negative magnetizing pulse, repetition rate 2 kc.

Size Anomaly of the Elastic Flux Change: The minimum amplitude of 0.1- μ sec pulses required to completely switch the core under discussion was 2.8 oersteds. Waveforms accompanying complete switching are shown in Fig. 2. Comparison with Fig. 1 shows that the reversible magnetization changes occurring during nondestructive read-out consist of a relatively large fraction of the total magnetization change obtainable on completely switching the core. The output signals for nondestructive read-out are approximately symmetrical about the base line in 1/8-mil material and their amplitude is strongly dependent on the state of remanence. In a representative case such as that shown in Fig. 1, the ratio between the peak amplitudes of the "one" and "zero" output signal when hit with the standard interrogation pulse is of the order of 3:1, and the peak of the output voltage pulse associated with the nondestructive

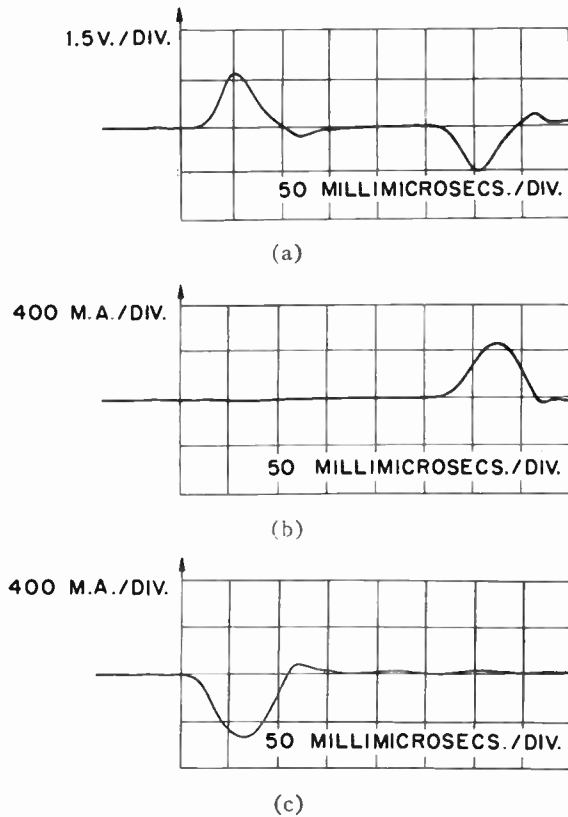


Fig. 2—Complete switching of $\frac{1}{8}$ -mil 4-79 Molybdenum Permalloy Core construction: as in Fig. 1. (a) Voltage signal across five-turn sense winding. (b) Set pulse (minimum amplitude required for complete switching). (c) Reset pulse.

read-out in the “one” state is as high as 17 per cent of the voltage pulse associated with complete flux reversal.

Quasi-Elastic Switching Using Symmetric Excitation: In the type of core described above having a coercivity of approximately 0.07 oersted, the maximum amplitude of 0.1- μ sec pulses which do not cause a permanent change of flux is of the order of 0.63 oersted. The pulse amplitude required to completely switch a core of this type in 0.1 μ sec is 2.8 oersteds. It has however been found that pulses of 1 oersted can be applied without causing a permanent change of state, provided that each pulse is followed by an opposite polarity pulse of similar amplitude. Alternatively, a pair of positive pulses can be followed by a pair of negative pulses. The time interval between the pulses can be of arbitrary length. The

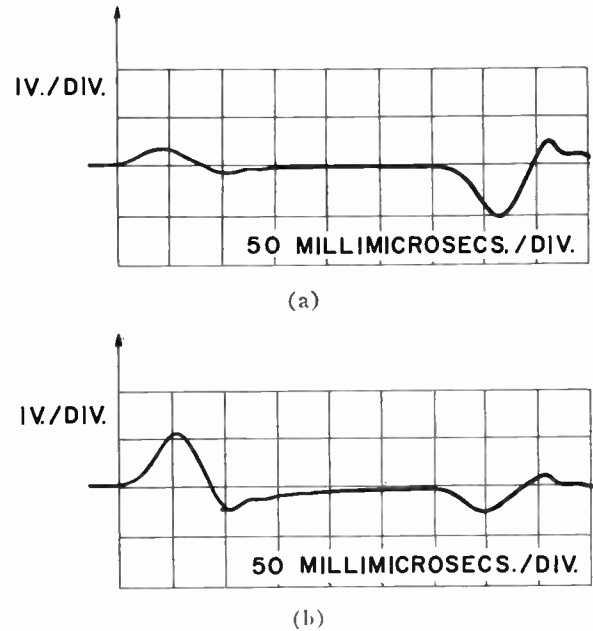


Fig. 3—Nondestructive read-out in $\frac{1}{8}$ -mil 4-79 Molybdenum Permalloy using symmetrical 0.1- μ sec half sine-wave pulses of 1.5-oersted peak amplitude. Core construction: as in Fig. 1. (a) Voltage signal across five-turn sense winding, core at positive remanence. (b) Voltage signal across five-turn sense winding, core at negative remanence.

permissible difference in amplitude is of the order of 7 per cent at 1.8 oersteds, and becomes larger as the pulses become smaller. Output voltage waveforms resulting from the alternate application of positive and negative pulses to a core are shown in Fig. 3, with the core at positive and negative remanence.

The technique of current amplitude coincidence for core selection in conventional memories employs the core coercivity as a threshold mechanism. The switching speed of cores selected in this fashion is limited because the total switching field applied cannot be made greater than twice the coercivity. The results described above make it possible to use amplitude coincidence for core selection using much larger fields than the coercivity and consequently attaining much higher switching speeds.

Some numerical results for switching with 0.1- μ sec pulses are summarized in Table I. It is interesting to compare the flux change associated with complete

TABLE I
REVERSIBLE AND IRREVERSIBLE SWITCHING IN $\frac{1}{8}$ -MIL GRAIN-ORIENTED 4-79 MOLYBDENUM PERMALLOY USING 0.1-MICROSECOND HALF SINE-WAVE PULSES

Mode of Operation	Driving Pulse	“I” Output Voltage Pulse	“O” Output Voltage Pulse	Peak Flux Change
Destructive switching	2.9 oersteds*	0.30 volt/turn	0.07 volt/turn	19 μ sec volts/turn
Nondestructive read-out using pulses of one polarity	0.63 oersted†	0.050 volt/turn	0.016 volt/turn	2.4 μ sec volts/turn‡
Nondestructive read-out using symmetrical pulse excitation	1.8 oersted	0.20 volt/turn	0.07 volt/turn	9.1 μ sec volts/turn‡

* Minimum excitation for complete switching.

† Peak excitation which can be used in this mode.

‡ This represents the total flux change which occurs during the application of a pulse tending to reverse the magnetization.

switching—19-volt millimicroseconds/turn with the completely reversible 2.4-volt millimicroseconds/turn which occurs during nondestructive read-out with pulses in one direction.

The flux change which occurs during the application of a sensing pulse of 1.8 oersteds is shown to be 9.1-volt μsec /turn. Numerical integration of the waveforms of Fig. 3 shows that approximately 43 per cent of this flux change is elastic, *i.e.*, reversible, and exists only during the application of the sensing pulse. The other 57 per cent is inelastic and remains after the termination of the sense pulse. This inelastic flux change can be cancelled out by a pulse which is within 7 per cent of the initial pulse in peak amplitude but in the opposite direction. The fact that the net flux excursion over a whole cycle is zero is proved by the fact that the nondestructive read-out effect is maintained even when positive and negative pulses are applied billions of times.

Physical Mechanisms

The effects which have been described can be explained at least qualitatively in terms of existing domain theory. The viscosity of domain wall movement appears to account satisfactorily for the elastic switching effects for short pulses. The large elastic flux change may be partly associated with the onset of domain rotation, a mechanism which has been used to account for the magnetization reversal effects in small particle magnets¹ and thin films.²

Elastic Switching: It has been reported above that it is possible to apply an indefinitely large number of very short magnetizing pulses considerably exceeding the coercive force to 1/8-mil or 1/4-mil grain-oriented Molybdenum Permalloy tape without causing a cumulative change of the state of magnetization. This can be explained in terms of the domain wall surface tension and the viscosity of the wall motion.

The fact that elastic switching occurs indicates that any existing domain walls are moved over such a relatively small distance during the application of the nondestructive read-out pulse that they fall back to their original position after the cessation of the pulse. It is known that the movement of domain walls over small enough distances is not accompanied by irreversible magnetization changes. This is proved by the well-known fact that the application of fields which are much weaker than the coercivity and which are of arbitrary duration to conventional magnetic materials will not result in irreversible magnetization changes. This is true even in portions of the hysteresis loop near the coercive point where most of the magnetization change takes place by means of Barkhausen jumps executed by the domain walls.

¹ E. C. Stoner and E. P. Wohlfarth, "A mechanism of magnetic hysteresis in heterogeneous alloys," *Phil. Trans.*, vol. A240, pp. 599-642; May, 1948.

² R. L. Conger, "High Frequency Effects in Magnetic Films," AIEE Conf. on Magnetism and Magnetic Materials, Boston, Mass.; October, 1956.

It is calculated in Appendix I that the distance moved by a domain wall under the influence of the maximum 0.1- μsec pulse of 0.63 oersted which gives nondestructive read-out in the case of 1/8-mil Permalloy is approximately three times its own thickness. This result indicates that the mechanism assumed for the nondestructive read-out effect is plausible since studies of the Barkhausen effect in related materials indicate that irreversible changes only become important as a domain wall moves through a distance which is between one and 10 times its own thickness.³

The nondestructive read-out signal from 1/8-mil material shown in Fig. 1(a) shows a slight exponential "tail." This feature is accentuated in 1/4-mil material and is probably associated with eddy currents. The calculated decay time constant of the eddy current field is calculated in Appendix II and agrees to within an order of magnitude with the experimentally observed values. The value of permeability used in this calculation is 4000, a value which is appropriate for a case where magnetization is mainly by rotation rather than wall movement.

Size Anomaly of the Elastic Flux Change: It has just been suggested that nondestructive read-out using short pulses is possible because the domain walls move over a relatively short distance. It was pointed out that purely reversible magnetization changes can also be brought about by the application of very weak fields where domain wall motion is limited by field amplitude rather than field duration. In the case of nondestructive read-out by means of very weak fields, the magnetization changes are a very small fraction of the change associated with an irreversible transition from positive to negative remanence. Reference to Table I shows that the reversible changes accompanying the application of pulses of 0.63 oersted are, however, as large as 12 per cent of the major loop magnetization change. Moreover, the application of nondestructive read-out pulses of 1.8 oersteds gives rise to purely reversible magnetization changes of 40 per cent of 9.1, *i.e.*, of 3.6- μsec volts/turn. This is 19 per cent of the flux change associated with complete switching. These results suggest that the magnitude of the reversible magnetization changes associated with nondestructive read-out may not be accounted for on the basis of domain wall movement alone.

A second process which may contribute to the reversible magnetization changes during nondestructive read-out by short pulses is that of spin rotation, *i.e.*, the coherent rotation over a small angle of the magnetization of a whole domain. This process is known to occur in particles whose diameter is comparable to that of a domain wall.¹ Conger's work on thin films of 80-20 nickel-iron shows that magnetization reversal takes place by rotation as well as wall movement for applied fields

³ R. S. Tebble, I. C. Skidmore, and W. D. Corner, "The Barkhausen effect," *Proc. Phys. Soc. A*, vol. 63, pp. 739-761; July, 1950.

larger than a few oersteds.³ It is difficult to calculate the critical field for irreversible spin rotation because the value of the magnetic anisotropy for Molybdenum Permalloy is very uncertain. The critical field, however, has been measured directly for a 1000 Å film of 80-20 permalloy by Smith⁴ who obtains a value of approximately 2 oersteds.

This result suggests that reversible spin rotation processes may be responsible for a part of the magnetization changes due to pulses of the order of 1 oersted and above.

A third process which may contribute to the elastic flux change is that of the nucleation of reversal domains around imperfections in the material such as grain boundaries. The fact that the flux change is elastic indicates that any domains which were nucleated during a nondestructive read-out pulse must be reabsorbed after the pulse. If a nucleated domain has not reached a size greater than a critical value by the end of the nucleating pulse, then the surface tension of the domain boundary would lead to its reabsorption.⁵

Elastic Switching with Symmetric Excitation: It was pointed out above that nondestructive read-out is possible with pulses as large as half the amplitude required to switch the core completely, provided that each positive pulse or pair of pulses is followed at an arbitrarily long time interval by an equal number of negative ones. In this case, the application of the first pulse tending to switch the material results in a degree of nonelastic wall movement. It is clear that the reabsorption pulse moves the domain walls to a position sufficiently close to their remanence location for no cumulative changes to occur under the influence of repeated pairs of pulses.

The results of the above section can be summarized as follows.

The phenomenon of nondestructive read-out associated with the application of very short intense magnetizing pulses is attributed to the fact that existing domain walls are moved over distances within their "elastic limit." Any domains created during a nondestructive read-out pulse are reabsorbed after its termination.

The reversible magnetization change occurring during the nondestructive read-out is ascribed to the reversible movement of existing domain walls. Temporary coherent rotation of the direction of magnetization in areas large compared to the wall thickness may also play a part as may the creation of temporary reversal domains around imperfections in the material.

Review of Related Work: Many nondestructive read-out techniques have been described which involve the

use of cores with special geometries.⁶⁻¹⁰ A nondestructive read-out technique which uses cores having a conventional geometry has been described by Widrow.¹¹ This makes use of the sense of the curvature of the hysteresis loop near remanence. The output obtained is relatively small in amplitude.

Haynes¹² showed several years ago that the application of microsecond pulses larger than the coercivity to metal tape cores having a switching time of the order of milliseconds produces a reversible flux change whose duration is dependent on the state of remanence. The switching of the cores investigated was subject to heavy eddy current damping and the nondestructive read-out phenomena observed were interpreted in this light.

Eddy current damping does not play an important part in the materials reported on in the present paper. This makes it possible to demonstrate and utilize the dynamic properties of the domain walls and spins to a greater extent than would otherwise be possible.

APPLICATIONS

Some of the possible data-handling applications of the two types of nondestructive read-out will now be described.

Magnetic Indicator

The order of magnitude of the nondestructive read-out obtainable with the high excitation possible when symmetrical drive is used is demonstrated by the device shown in Fig. 4. In this deliberately simple circuit, the nondestructive read-out signals from a conventional tape core are rectified and used to operate a forward biased neon bulb. The status of the neon indicator shows whether the core being sensed is in a state of positive or negative remanence. In a practical case the discrimination of the output signal could be increased by the use of a bucking core. Alternatively, the diode could be replaced with a transistor used as a combined rectifier and amplifier.

Magnetic Switch

Nondestructive read-out has been applied to a channel-selecting magnetic switch which embodies the

⁶ J. A. Rajchman and A. W. Lo, "The transfluxor—a magnetic gate with stored variable setting," *RCA Rev.*, vol. 16, pp. 303-311; June, 1955.

⁷ R. L. Snyder, "Magnistor circuits," *Electronic Design*, vol. 3, pp. 24-27; August, 1955.

⁸ D. A. Buck and W. I. Frank, "Nondestructive sensing of magnetic cores," *Commun. and Electronics*, no. 10, pp. 822-830; January, 1954.

⁹ R. Thorensen and W. R. Arsenault, "A new non-destructive read for magnetic cores," *Proc. Western Joint Computer Conf.*, pp. 111-116; March, 1955.

¹⁰ A. Papoulis, "The nondestructive read-out of magnetic cores," *Proc. IRE*, vol. 42, pp. 1283-1288; August, 1954.

¹¹ B. Widrow, "A radio frequency nondestructive readout for magnetic core memories," *IRE TRANS.*, vol. EC-3, pp. 12-15; December, 1954.

¹² M. K. Haynes, "Magnetic Cores as Elements of Digital Computing Systems," Ph.D. dissertation, Univ. of Illinois, Urbana, Ill.; August, 1950.

⁴ D. O. Smith, "Magnetic Relaxation in Thin Films," AIEE Conf. on Magnetism and Magnetic Materials, Boston, Mass.; October, 1956.

⁵ D. S. Rodbell and C. P. Bean, "Influence of pulsed magnetic fields on the reversal of magnetization in square loop metallic tape," *J. Appl. Phys.*, vol. 26, pp. 1318-1323; November, 1955.

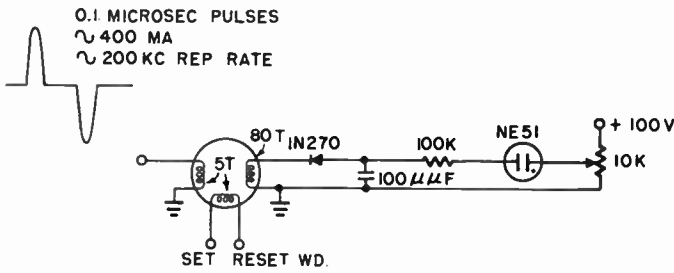


Fig. 4—Nondestructive read-out used to operate neon indicator. Core construction: 30 wraps of $\frac{1}{8}$ -mil, 4-79 Molybdenum Permalloy, $\frac{1}{8}$ inch wide, $\frac{3}{8}$ -inch diameter.

current steering technique proposed by Karnaugh.¹³ The principle of the circuit is illustrated in Fig. 5. Each core is provided with set and reset windings which ensure that only one core is set at a time. There are not shown in Fig. 5.

Nondestructive read-out current pulses are applied through $R1$ in such a direction as to tend to reset the cores. The output windings of the unselected cores produce voltage pulses similar to those shown in Fig. 1(a). The selected core produces a voltage output similar to that shown in Fig. 1(b). The initial output pulse from this core serves to bias off the diodes associated with the unselected cores and "steers" the clock pulse through its own output winding into the selected load. In the circuit shown the clock pulse is produced by delaying and compressing the read-out pulse. Following the termination of the drive pulse, the selected core recovers to its "set" state in a fraction of a microsecond. A further read-out pulse can then be applied.

The arrangement of the diodes ensures that no current can flow through any of the loads in the absence of a clock pulse, *i.e.*, during the set and reset of the cores or during their recovery from read-out. Each load can be equipped with a separate filter if required. In this circuit the provision of bucking cores in series with each switch core is not required since the operation of the switch ensures that all the sensing current is diverted through the output winding exhibiting the largest voltage pulse. Delay line effects must however be carefully controlled in the design.

Shift Register With Permanent Output Indication

A one-core-per-bit shift register¹⁴ which is well suited to nondestructive read-out operation is shown in Fig. 6. Point P is normally held at a positive potential. The application of a current pulse through the shift winding resets all the cores which were previously set, and in doing so, charges the associated intermediate storage capacitors positive. Immediately after the termination of the shift pulse, point P is pulsed negative, thus discharging any of the intermediate storage capacitors

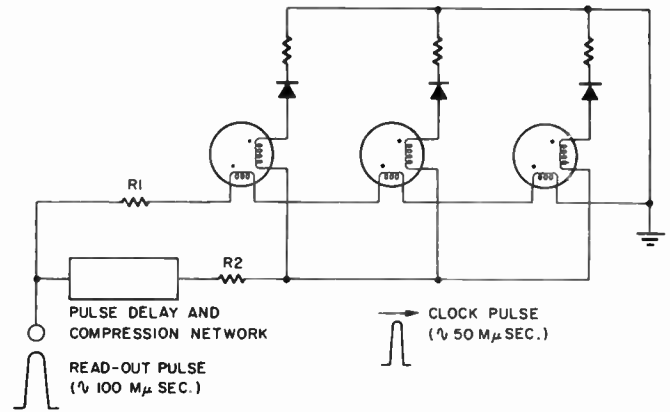


Fig. 5—Application of nondestructive read-out to current steering switch using cores of $\frac{1}{8}$ -mil grain-oriented tape.

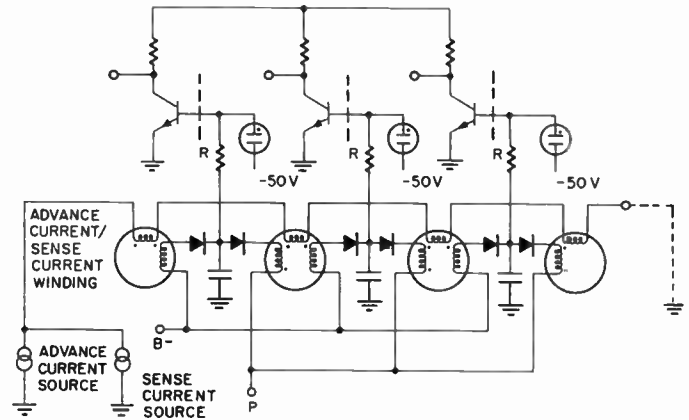


Fig. 6—One-core-per-bit shift register using nondestructive read-out to provide permanent output.

which were charged positive in the previous part of the cycle. In discharging a particular capacitor, the subsequent core is set to a state of positive remanence. In Fig. 6 the shift register has been modified to provide a permanent indication of its contents. A sensing current source has been attached to the shift winding as shown and each intermediate storage capacitor is connected to a neon indicator through a large resistor R . The other end of the neon indicators are taken to a negative potential so as to minimize the inverse voltage required across the diodes of the circuit.

Between the application of shift pulses the sense pulses which can remain "on" continuously, charge the capacitors which follow cores set to a positive state of remanence, and excite the associated neon. A continuous indication of the contents of the shift register is thereby provided. If the neon indicators are replaced by transistor or vacuum-tube amplifiers as indicated in the diagram, other computing or indicating devices can be driven.

It is noteworthy that the conversion of the shift register proposed above to provide a continuous indication of its content is achieved with a minimum of added components—one resistor and neon indicator per stage, one current source of pulses, and an extra bias supply

¹³ M. Karnaugh, "Pulse switching circuits using magnetic cores," Proc. IRE, vol. 43, pp. 570-584; May, 1955.

¹⁴ V. L. Newhouse and N. S. Prywes, "High speed shift registers using one core per bit," IRE TRANS., vol. EC-5, pp. 114-120; September, 1956.

for the neon indicators. In particular, no extra windings are required.

Random Access Memories

Perhaps the most important applications of the time dependent effects lie in the field of data storage.

The use of nondestructive read-out for random access memories of the conventional type is illustrated schematically in Fig. 7. A parallel memory is represented where all the digits of a particular word are read in and sensed simultaneously. The read-in process can take place by means of coincident current techniques. A word line corresponding to a particular address is selected by means of the word line selector switch. This switch may utilize vacuum tubes and diodes, transistors, etc. To enter a particular word into the store, the selected word line is pulsed and those digit selection lines corresponding to "ones" in the word are pulsed simultaneously in the well-known manner. To clear a given address, the corresponding word line is pulsed with an opposite polarity current in such a way as to reset all the cores in that line.

To sense a given address in a nondestructive manner, the corresponding address line is selected by the word selection switch and is pulsed with a limited amplitude pulse of very short duration. Each of the cores on the pulsed line will emit a voltage pulse on the corresponding digit selection line whose amplitude will be a function of its remanent state. These pulses are then sensed by the amplifiers. It should be noted that this well-known configuration has the advantage that the digit selection lines are used for sensing also, and even more important, that each sensing line only passes through one activated core during the sensing operation. This means that the sensing line passing through each core being sensed does not have other half-activated cores in series with it, producing disturbing signals. The signal-noise ratio of the nondestructive sensing effect does not therefore have to be very high.

The advantages of using nondestructive read-out in a random access memory are as follows:

- 1) Regeneration is unnecessary. This simplifies the logic circuitry required.
- 2) The fact that a memory interrogation does not have to be followed by a regeneration cycle decreases the effective access time of the memory by a factor whose value depends on the proportion of memory interrogation to memory entries. In the extreme case where all the memory references are interrogations, the minimum time between interrogations need be no longer than the sum of the length of the interrogation pulse and the time required to refer to a new address in the memory.

To enter information into a memory by means of time dependent inertia effects, several modes of operation are possible. One of the most interesting has been named the pulse interlace method and operates as follows:

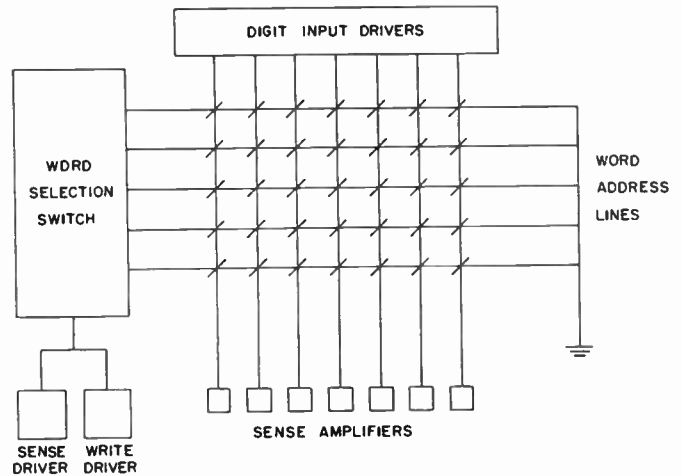


Fig. 7—Parallel digit memory suited for non-destructive read-out.

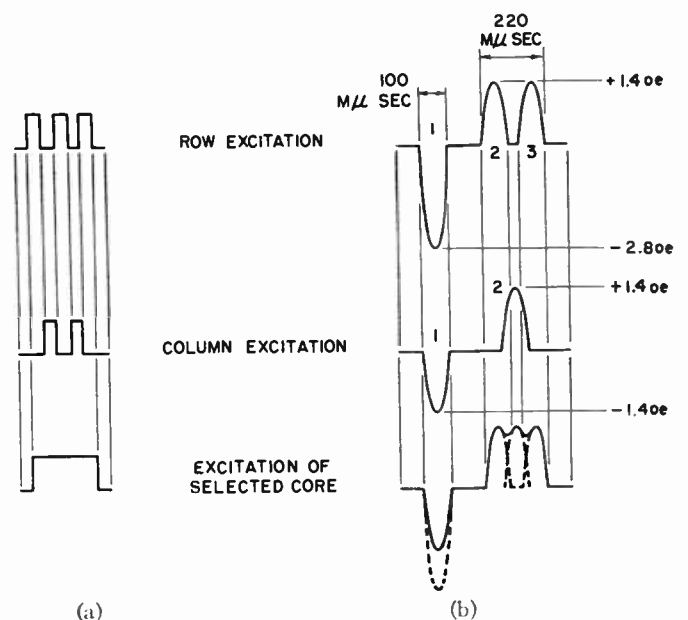


Fig. 8—Pulse interlace waveforms for writing into two-dimensional core arrays. (a) For use in serial digit arrays (e.g., Fig. 9). (b) For use in parallel digit arrays (e.g., Fig. 7).

To switch a particular core in a two-dimensional matrix without disturbing any of the others, anti-coincident current pulse trains are sent along the appropriate row and column as shown in Fig. 8(a). The length and amplitude of each pulse and the number of pulses in each train depend on the material used for the storage elements. In the case of the cores described above, the pulse trains shown in Fig. 8(b) using 1.4-oersted pulses 0.1 μ sec in length are sufficient.

These waveforms are for use in a parallel digit memory of the type shown in Fig. 7. Pulse no. 1 of the row pulse train is used to clear the selected address and is made large enough to perform this purpose even in the absence of column pulse no. 1. Column pulse no. 1 is applied only to those column wires passing through cores which are to be "set" during the read-in portion of the cycle. Its purpose is merely to prevent column pulse no. 2 from

initiating cumulative magnetization changes in cores on unaddressed rows.

The application of row excitation pulses nos. 2 and 3 to a row of reset cores results in a small amount of undesired magnetization change in those cores which have not been switched by the application of a column excitation pulse in the time interval between the two row pulses. This feature is of no consequence in this type of memory structure since every pair of row set pulses is always preceded by a "clear" pulse.

In the pulse interlace method the selected core is excited continuously, whereas the nonselected cores are excited discontinuously or not at all. The process of magnetization reversal in the selected core must therefore take place by domain wall movement.

A method of reversing the magnetization by means of spin rotation makes use of the second threshold effect. To switch a core in a two-dimensional matrix in this way, conventional amplitude coincidence techniques may be used provided that each positive pulse on any one line passing through cores which are not to be switched is followed or preceded by a negative pulse and vice versa. (These pulses are of half the switching amplitude.) Such a cycle is used in the experimental memory described below.

By making use of the second threshold effect, relatively high speeds of operation are possible. Using the type of core described above, it is possible to write into any one core of a matrix by means of two-time coincident 1.4-oersted $0.1\text{-}\mu\text{sec}$ pulses preceded by two identical coincident "pre-disturb" pulses of opposite polarity. The total writing time is approximately one tenth the duration of the switching time required for the same material using conventional coincident current techniques. The nondestructive read-out procedure which can be used in memories of this type takes $0.1\text{ }\mu\text{sec}$ or less, and is thus at least one twentieth the duration of the conventional destructive read-out procedure if this has to be followed by re-entry of sensed information.

An Experimental Memory

A very small transistorized random access memory has been built to investigate the use of the time dependent effects for entry of information and non-destructive sensing.

The cores described in connection with Fig. 1 were used as the storage element and were arranged in a two dimensional matrix. The associated control logic is shown in Fig. 9, and enabled the memory locations to be addressed individually for writing, or in sequence for nondestructive read-out.

The core matrix line selection circuits use base-driven, grounded-emitter transistor switches whose collectors are connected in series with the matrix lines through diodes (not shown in Fig. 9). Before pulsing a specific line the emitter-base junction of the corresponding switch transistor is forward biased. The application

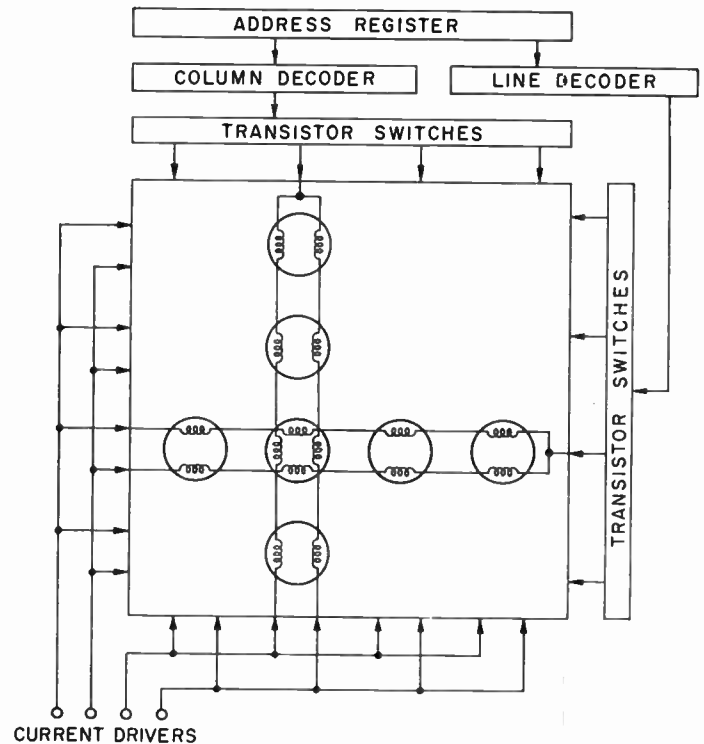


Fig. 9—Two-dimensional memory.

of the matrix drive pulse thus finds this transistor in a "presaturated" state. This configuration has two advantages.

- 1) The transistor is not required to undergo a change of state during the application of the drive pulse.
- 2) The collector base dissipation is a minimum. (Most of the dissipation occurs in the emitter base junction.)

In this way, conventional rf transistors (2N140) are able to switch millimicrosecond pulses of several hundred milliamps at high repetition rates. In the present instance, these pulses were generated from commercial vacuum tube equipment.

Writing a "one" into an individual core is accomplished by passing a 220-ma $0.1\text{-}\mu\text{sec}$ pulse along one of the pair of vertical lines, passing through that core as selected by the corresponding transistor switch. Simultaneously, an identical pulse is passed through one of the pair of horizontal lines intersecting the selected core. These coincident pulses have the effect of entering a "zero" into the selected core and of applying a disturb action in the "zero" direction to the other cores on the selected vertical and horizontal lines. To complete the entry of a "one" into the selected core, current pulses are sent along the two previously unexcited lines. This switches the selected core into the "one" state and cancels out the disturbance applied to the other cores on the selected vertical and horizontal lines. The whole process requires a minimum period of $0.2\text{ }\mu\text{sec}$. To enter a "zero" into an individual location, the order of exciting the selected lines is simply reversed.

By setting the address counter and making use of the single-cycle facilities of the control equipment, it was verified that a "one" or a "zero" could be entered into any memory location in a single cycle. It was also established that the continuous entry of "ones" or "zeros" into any position of the memory did not disturb the information in other positions. The contents of the memory could be observed on the column lines by cycling the address counters continuously, while applying nondestructive current pulses corresponding to 0.4 oersted to the rows of the matrix.

It is of interest to compare this memory with the evaporated film memory described by Pohm and Rubens.¹⁵ In that memory the elements are switched by the application of two time coincident field pulses with the resultant field directed at an angle to the easy direction of magnetization. This produces the effect of a transverse as well as of an antiparallel field on the elements being switched. The switching times reported for the evaporated film memory are of the order of 0.5 μ sec. Destructive read-out is used and the sense signals are of the order of 4 millivolts. Since the magnetization in the partially selected elements undergoes reversible rotation, it would appear that nondestructive read-out techniques can be used in a film memory with a corresponding sacrifice in signal strength.

CONCLUSION

The emphasis in the work done to date has been on the applications of the time dependent effects rather than on a very detailed examination of the effects themselves. An experimental and theoretical study of the wall viscosity, however, should lead to results of importance to the theory of switching at high fields and may reveal further applications. For example, the use of tape-wound toroids, where the easy axis of the tape makes an angle with the plane of the toroid, should lead to greater speeds of switching for given applied fields at the expense of loss in the effective squareness of the hysteresis loop.

Wall viscosity effects have been looked for in ferroelectric materials but have not yet been demonstrated in the samples available. Further investigation may reveal their presence.

The construction of memories of large size will necessitate the investigation of techniques for applying the time dependent effects to three-dimensional core structures or alternatively to two-dimensional memory arrays driven by magnetic switches.

The work described has been concerned with the use of the effects in digital devices only. It seems likely however that applications will reveal themselves in allied fields such as that of analog computation.

¹⁵ A. V. Pohm and S. V. Rubens, "A compact coincident current memory," *Proc. Eastern Joint Computer Conf.*, pp. 120-123; December, 1956.

APPENDIX I

The movement of a domain wall can be represented by an equation of the form.¹⁶

$$\frac{1}{2}m(\dot{r}^2/r + \ddot{r}) + \beta\dot{r} = 2(\hat{H} - \hat{H}_0) \cdot \hat{I}_s \quad (1)$$

H_0 is the threshold field for which $\dot{r}=0$, approximately equal to the coercivity, and I_s is the saturation magnetization. The mass per unit area of the wall is $m = \epsilon / (8\pi\gamma^{*2}A)$ and has been estimated¹⁶ as 10^{-10} gm/cm^2 for Molybdenum Permalloy. ϵ is the wall surface energy density per cm^2 . A is the energy exchange parameter defined below and γ^{*2} is defined in terms of the gyromagnetic ratio in (5). β is the viscous damping parameter and has been shown experimentally¹⁷ to lie in the range 0.1-1.0.

It can be shown that the acceleration of the wall described by (2) under the influence of an external field will take place in a period not longer than $10m/\beta \sim 10^{-9}$ sec since $\beta \ll 0.1$.

The inertia term in the equation of wall motion can therefore be neglected in the consideration of switching phenomena in Moly Permalloy taking place in periods of 10 μ sec or longer.

Since acceleration can be neglected, the distance d traveled by a domain wall under the influence of an external field can be given as

$$d = \int_0^t v dt \quad (2)$$

where

$$v = 2I_s(H - H_0)/\beta, \quad (3)$$

Kittel¹⁸ has shown that

$$\beta = 2\Lambda(K/A)^{1/2}/\gamma^* \quad (4)$$

Where

$$\gamma^* = \gamma^2 + 2\Lambda^2/I_s^2, \quad (5)$$

γ is the gyromagnetic ratio and Λ is the intrinsic spin relaxation frequency derived from the phenomenological equation of motion.¹⁹

$$\frac{dI}{dt} = \gamma(I \times \hat{H}) + \Lambda(I \times \hat{H} \times I)/I^2.$$

The anisotropy and strain energy is represented by²⁰

¹⁶ N. M. Menyuk and J. B. Goodenough, "Magnetic materials for digital computer components 1," *J. Appl. Phys.*, vol. 26, pp. 8-18; January, 1955.

¹⁷ J. K. Galt, J. Andrus, and H. G. Hopper, "Motion of domain walls in ferrite crystals," *Rev. Modern Phys.*, vol. 25, pp. 93-97; January, 1953.

¹⁸ C. Kittel, "Note on the inertia and damping constant of ferromagnetic domain boundaries," *Phys. Rev.*, vol. 80, p. 918; December 1, 1950.

¹⁹ L. Landau and E. Lifshitz, "Theory of dispersion of magnetic permeability in ferromagnetic bodies," *Physik. Z. Sowjetunion*, vol. 8, pp. 153-169; 1935.

²⁰ R. M. Bozorth, "Ferromagnetism," D. Van Nostrand Co., Inc., New York, N. Y., p. 816; 1951.

$$K = (K_0 + 3\lambda_s\sigma/2)^{1/2}$$

where K_0 is the anisotropy constant, λ_s the saturation magnetostriction, and σ the tension.

In (4):

$$A = k\theta/a.$$

k is Boltzman's constant, θ the Curie temperature, and a the interatomic distance.

The term β can be expressed in terms of the domain wall thickness δ which is given by Bozorth²⁰ for a 180° wall parallel to a (100) plane in a material of the iron type as

$$\delta = 12(A/K)^{1/2}. \quad (6)$$

From (2) through (6), the distance of the wall motion d in terms of the wall thickness is obtained as

$$d/\delta = \frac{I_s\gamma^*}{12\Lambda} \int_0^t (H - H_0) dt. \quad (7)$$

For a half sine-wave pulse of width τ and peak height H_p , (7) becomes

$$d/\delta = \frac{I_s\gamma^*}{12\Lambda} \tau \left(\frac{2}{\pi} H_p - H_0 \right). \quad (8)$$

γ is a constant independent of the material equal to $1.76 \cdot 10^7$. The value of Λ can be assumed to be close to the corresponding value for Supermalloy which can be deduced from the width of the ferromagnetic resonance line for that material as equal to approximately 200 mc.

For Molybdenum Permalloy $H_c \sim 0.07$ oersted and $I_s = 690$ emu. Table I shows the peak field for nondestructive read-out as $H_p = 0.63$ oersted for a 0.1- μ sec half sine-wave pulse. Substituting these figures in (7) gives $d/\delta \sim 2.9$.

APPENDIX II

McColl²¹ has shown that the effect of eddy currents in delaying the change in flux in an infinite sheet resulting from a stepwise change of applied field is

$$\frac{B(t)}{\mu H} = 1 - \frac{8}{\pi^2} \sum_{n=1}^{\infty} \frac{\sin^2(n\pi/2)}{n^2} e^{-n^2 t/\tau}$$

or in series form

$$\frac{B(t)}{\mu H} = 1 - \frac{8}{\pi^2} \left(e^{-t/\tau} + \frac{1}{9} e^{-9t/\tau} \dots \right), \quad (9)$$

where

$$\tau = \frac{4\sigma\mu d^2}{\pi}$$

d is the thickness of the sheet, σ the conductivity, and μ is the permeability which is assumed constant.

In the case under consideration here, the movement of domain walls makes a minor contribution to the magnetization change compared to the spin rotation. The relevant value of the permeability to be used in (9) is that for spin rotation rather than wall movement, *i.e.*, approximately 4000 emu. The resistivity of Molybdenum Permalloy is 55 micro ohm-cm and this gives the time constant of $\frac{1}{8}$ -mil Molybdenum Permalloy as $\tau \sim 10 \mu$ sec.

This indicates that any eddy currents induced at the start of a 100- μ sec pulse will have decayed long before the end of the pulse, and therefore, will not contribute appreciably to the reset of the magnetization which occurs in the case of nondestructive read-out.

ACKNOWLEDGMENT

The author would like to acknowledge the contributions of W. L. McMillan who played an important part in the work described in this paper and in the design and construction of the two-dimensional memory.

²¹ *Ibid.*, p. 784.

CORRECTION

C. G. Peattie and J. R. Macdonald, authors of the Correspondence item, "Prediction of Semiconductor Surface Response to Ambients by Use of Lewis Acid-Base Theory," which appeared on page 1292 of the September, 1957 issue of these PROCEEDINGS, would like to point out that the last sentence of the second paragraph should read:

"The extent to which these mechanisms are obscured by the onset of ionic-like surface currents has yet to be determined."

As printed, "are observed" was used instead of the correct verb "are obscured."

IRE Standards on Reference Designations for Electrical and Electronic Equipment, 1957*

(57 IRE 21. S2)

COMMITTEE PERSONNEL

Joint ASA-IRE Task Group on Reference Designations

H. R. TERHUNE, *Chairman*

L. Bonosevich
E. W. Borden
D. C. Bowen
M. C. Cisler
C. J. Eiuwen

W. J. Everts
W. A. Ford
F. G. Gerrold
R. T. Haviland
I. L. Marin
C. D. Mitchell

M. P. Robinson
R. M. Stern
R. E. Thiemer
H. J. Turpin
H. P. Westman

Symbols Committee

1956-1957

H. R. TERHUNE, *Chairman*

R. T. HAVILAND, *Vice-Chairman*

H. W. Becker
E. W. Borden
D. C. Bowen
M. C. Cisler
W. A. Ford

I. L. Marin
C. D. Mitchell
E. W. Olcott
M. B. Reed

H. P. WESTMAN, *Secretary*

C. F. Rehberg
R. V. Rice
M. P. Robinson
M. S. Smith
R. M. Stern

Standards Committee

1957-1958

M. W. BALDWIN, JR., *Chairman*

C. H. PAGE, *Vice-Chairman*

J. Avins
W. R. Bennett
J. G. Brainerd
D. R. Brown
T. J. Carroll
P. S. Carter
A. G. Clavier
G. A. Deschamps
S. Doba, Jr.
J. E. Eiselein
D. Frezzolini
E. A. Gerber

A. B. Glenn
H. Goldberg
V. M. Graham
R. A. Hackbusch
H. C. Hardy
D. E. Harnett
A. G. Jensen
I. M. Kerney
J. G. Kreer, Jr.
W. A. Lynch
A. A. Macdonald
Wayne Mason
D. E. Maxwell

R. F. SHEA, *Vice-Chairman*

L. G. CUMMING, *Vice-Chairman*

H. R. Mimno
G. A. Morton
J. H. Mulligan, Jr.
W. Palmer
R. L. Pritchard
P. A. Redhead
R. Serrell
H. R. Terhune
W. E. Tolles
J. E. Ward
E. Weber
W. T. Wintringham

FOREWORD

In 1949, the Institute of Radio Engineers issued the first formal Standard on reference designations, 49 IRE 21.S1. This Standard was adopted by the Munitions Board Standards Agency and issued as MIL-STD-16 with full recognition of the pioneering work of the Insti-

tute. As the growing complexity of electronic equipment revealed the inadequacy of MIL-STD-16 with regard to its application, the Standard went through several revisions and was approved in 1956 by the Office of the Assistant Secretary of Defense as MIL-STD-16B.

* Approved by the IRE Standards Committee, July 11, 1957. Reprints of this Standard, 57 IRE 21. S2, may be purchased while available from the Institute of Radio Engineers, 1 East 79th Street, New York, N. Y., at \$0.70 per copy. A 20 per cent discount will be allowed for 100 or more copies mailed to one address.

This IRE Standard was prepared by a Joint Task Group composed of members of the IRE Symbols Committee and the ASA Y32.2 Committee on Graphical Symbols. It is based upon, and is compatible with, MIL-STD-16B and avoids the need for two systems of reference designations where both commercial and military work may be performed in the same organization.

1.0 INTRODUCTION

1.1 Scope

This Standard establishes principles governing the formation and application of electrical and electronic reference designations. It also provides a list of designating letters for parts and assemblies or subassemblies shown on diagrams (wiring, schematic, etc.) for electrical and electronic equipment.

1.2 Purpose

The purpose of this Standard is to establish two reference designation methods for use in marking part locations in equipment and on diagrams of electrical and electronic circuits for correlating graphical symbols shown thereon with parts lists and descriptions of and instructions concerning the circuits.

2.0 USE

Reference designations, as defined in Section 3 of this Standard, are for use in equipment, on diagrams, drawings and associated parts lists, in manuals, and in similar publications. Reference designations are not intended to replace drawing, part, type, or stock numbers. Device designations for separate power switch-gear and power control systems are not covered by this Standard. This Standard does not preclude the use of other than reference designations. In cases where other designations are used, it is preferable that the reference designations be used in addition.

3.0 DEFINITIONS

For the purpose of this Standard, the following definitions shall apply.

3.1 Part

One piece, or two or more pieces joined together which are not normally subject to disassembly without destruction of designed use. (Examples: electron tube, resistor, relay, power transformer, bracket.)

3.2 Subassembly

Two or more parts which form a portion of an assembly or a unit replaceable as a whole, but having a part or parts which are individually replaceable. (Examples: filter network, resistor-capacitor board.)

3.3 Assembly

A number of parts or subassemblies or any combina-

tion thereof joined together to perform a specific function. (Examples: electric generator, audio-frequency amplifier, power supply.)

Note: The distinction between an assembly and a subassembly is not always exact—an assembly in one instance may be a subassembly in another where it forms a portion of an assembly.

3.4 Unit

An assembly or any combination of parts, subassemblies, and assemblies mounted together, normally capable of independent operation in a variety of situations. (Examples: receiver, transmitter, power supply, indicator.)

Note: The size of an item may determine whether it is regarded as a unit or a part. For instance, a small electric motor may be considered as a part if it is not normally subject to disassembly.

3.5 Set

A unit or units and necessary assemblies, subassemblies, and parts connected or associated together to perform an operational function. (Examples: search radar set, radio transmitting set.)

3.6 Reference Designations

Reference designations are combinations of letters and numbers which identify parts, subassemblies, assemblies, and units of a set on equipment diagrams, drawings, parts list, technical manuals, etc. The letters in a reference designation show the class of parts such as a resistor, coil, electron tube, etc., or identify a subassembly. The number differentiates between parts or subassemblies of the same class. A reference designation is not necessarily an abbreviation for the name of an item.

Note: For applying reference designations, subassemblies and assemblies shall be treated as being equivalent.

4.0 FORMATION OF REFERENCE DESIGNATIONS

4.1 Letters

4.1.1: The letter or letters of the reference designation shall be as indicated in Section 6.

4.1.2: Where no confusion will result, the letter *E*, in the case of terminals, may be omitted from drawings and need not be stamped on equipment for such parts as transformers, panels, sockets, etc.

4.2 Numbers

The number of the reference designation follows the letter or letters without a hyphen (except as indicated in 5.2.2) and shall be of the same size and on the same line. For example C1, S14, and MG5. The assignment of numbers should preferably start with the lowest number in the upper left-hand corner of the schematic drawing of the assembly or subassembly and proceed in

a logical manner from left to right and from top to bottom as in reading a page of text. However, it is not required that the series of numbers be necessarily consecutive or complete. For instance, in the case of successive improvements of a piece of equipment, some of the parts may be eliminated. Here it is unnecessary to redesignate the remaining parts merely to keep the number series consecutive. The parts list will usually show which numbers are missing. Reference designations applying to eliminated parts or subassemblies should not be reassigned.

5.0 APPLICATION

5.1 General

Either of two methods of assigning reference designations shall be used as outlined in 5.2 or 5.3. Only one method shall be used to identify parts of a given unit. Insofar as practicable, the same method shall be used throughout a set, except for units that have been previously supplied. Normally, the unit numbering method (5.3) is used on sets or units which contain plug-in assemblies which will be removed, repaired, and stocked as single items and the block numbering method (5.2) is used on sets or units which do not contain multiple plug-in assemblies.

5.2 Block Numbering Method

5.2.1 Parts: Reference designations shall consist of a letter(s) which identifies the class to which a part belongs (see Section 6) and a number identifying the specific part within that class (see Fig. 1). Parts in the first unit shall be numbered consecutively from 1 to 199, and parts in the second unit from 201 to 299, etc. If there are more than 99 parts of a single class in a unit, or more than 199 in the first unit, two or more consecutive blocks of numbers should be assigned. When additional numbers are required after the blocks have been assigned, a block which is not consecutive with the assigned numbers may be used, provided a note explaining the combination of blocks is included on the drawing and in the parts list. However, every effort shall be made to assign blocks of numbers of sufficient range to avoid the assignment of nonconsecutive blocks for the same unit.

5.2.2 Subassemblies: Reference designations may be assigned to nonduplicated subassemblies for convenience in correlating description with diagrams but must be assigned for duplicated assemblies and units. (See 5.2.2.1 and 5.2.2.2.) However, the assignment of a reference designation to a subassembly does not preclude the necessity of assigning designations to each of its individual parts.

5.2.2.1 Reference Designation for Identical Subassemblies: Identical subassemblies that are duplicated within a unit or used in other units of the same or different sets shall be assigned reference designations. Parts with-

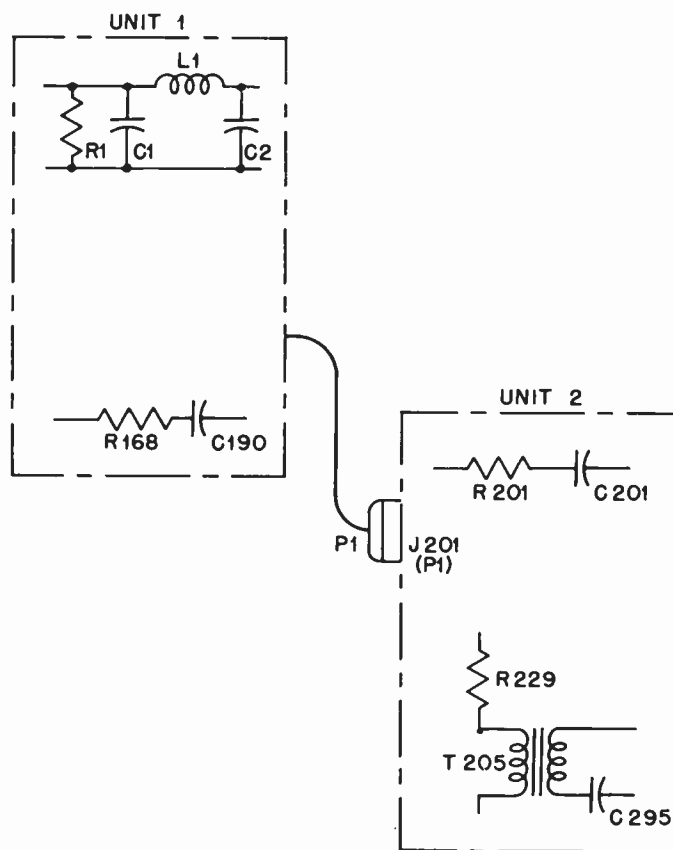


Fig. 1—Application of reference designations using the block numbering method.

in such subassemblies shall be assigned basic (incomplete or abbreviated) reference designations. The letter portions shall be as specified in Section 6. The number portion shall start with the number 1 and run consecutively. Examples: R1, C1, T1, T2, K3. The complete identification of the parts in these subassemblies shall be made by prefixing the basic designation by the subassembly reference designation. Examples: A1R1, A201R1, A202R1. On the diagrams and drawings where the incomplete reference designations are used, a note shall be included substantially as follows:

“Reference designations are incomplete. For complete identification, prefix the part designation with the subassembly designation.”

Where incomplete designations are used on only a portion of a diagram, the note shall specify the portion of the diagram to which it applies.

5.2.2.2. Identical units: If a set includes two or more identical units, the reference designation of the parts in each unit shall be identical.

5.3 Unit Numbering Method

5.3.1 Identification of Units: An identifying number shall be assigned to each unit. This number shall start with one and run consecutively for all units of the set.

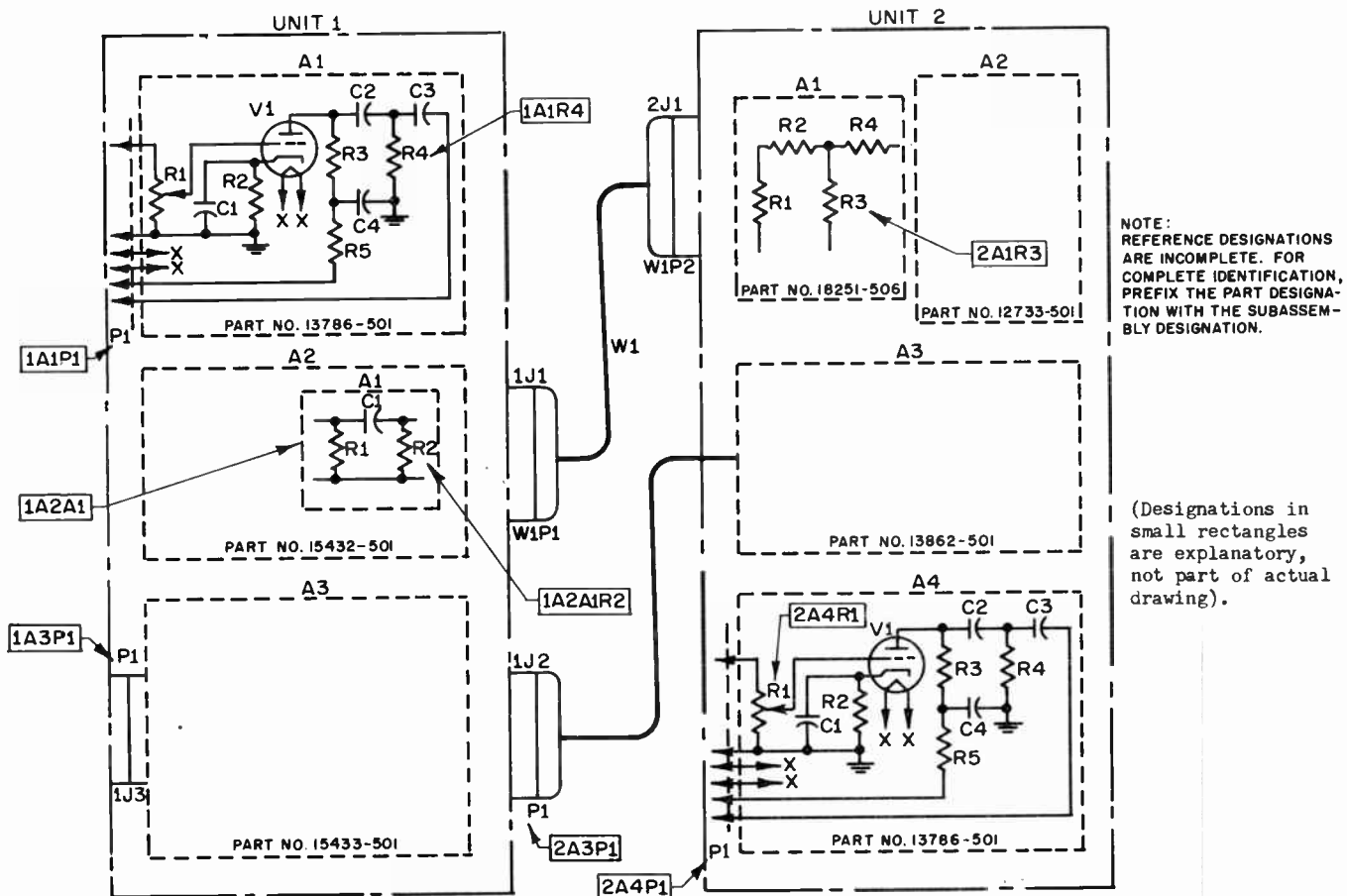
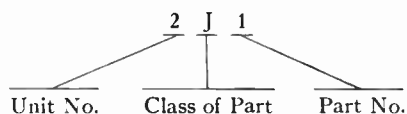


Fig. 2—Application of reference designations using the unit numbering method.

This number is the equivalent of a reference designation of the unit. An exception is made for units which are enclosed within the same cabinet, mounted in a common rack or otherwise similarly joined together with other units, subassemblies, etc. In this case the units shall be treated as subassemblies.

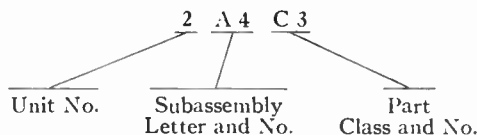
5.3.2 Subassemblies and Parts not Integral with Subassemblies: The complete reference designation of a part which is not an integral part of a subassembly, consists of the unit number identifying the specific unit, a letter(s) identifying the class to which the part belongs (Section 6), and a number identifying the specific part within that group. Numbers within each class of parts shall start with one and run consecutively. Subassemblies shall be identified in the same manner as parts that are not integral with a subassembly. Examples:



- 1C2 Second (2) capacitor (C)* of first (1) unit.
- 4R11 Eleventh (11) resistor (R)* of fourth (4) unit.
- 5T6 Sixth (6) transformer (T)* of fifth (5) unit.
- 8V9 Ninth (9) electron tube (V)* of eighth (8) unit.
- 3A2 Second (2) subassembly (A) of third (3) unit.

* Parts not integral with subassembly.

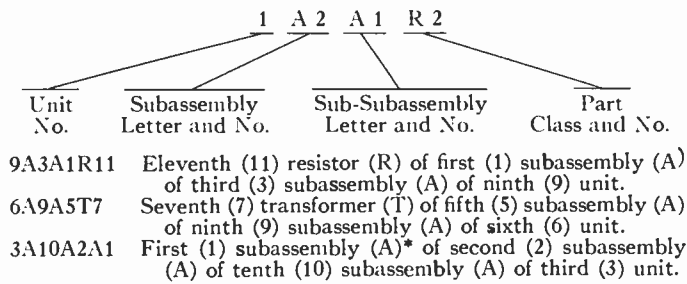
5.3.3 Parts of Subassemblies (or Subassemblies of Subassemblies): The complete reference designation of a part of a subassembly consists of the unit number identifying the specific unit; the letter "A" identifying a subassembly, a number identifying the specific subassembly; a letter(s) identifying the class of items to which the part belongs, and a number identifying the specific part. Numbers within each class shall start with one and run consecutively. Subassemblies of subassemblies are identified in the same manner as parts of subassemblies. Examples (see Fig. 2):



- 1A3R4 Fourth (4) resistor (R) of third (3) subassembly (A) of first (1) unit.
- 2A4C1 First (1) capacitor (C) of fourth (4) subassembly (A) of second (2) unit.
- 6A1T10 Tenth (10) transformer (T) of first (1) subassembly (A) of sixth (6) unit.
- 11A2A3 Third (3) subassembly (A) of second (2) subassembly (A) of eleventh (11) unit.

5.3.4 Expansion of Method: The unit numbering method can be expanded as much as is necessary (in the manner described in 5.3.3) to permit identification of items resulting from any degree of subdivision required

for fabricating or stocking purposes. However, every effort should be made to keep application of the method as simple as possible. Examples of extension of the system are:



* Such as an IF transformer.

5.3.5 Subassemblies and Parts not Integral with Units: Subassemblies and parts not associated with units (such as interconnecting cables) may be identified if desired. If designations are assigned, the subassemblies and parts shall be identified in the same manner as those associated with units, except for the omission of the unit number.

5.3.6 Abbreviated reference designations: Abbreviated reference designations may be used on diagrams, drawings, and units when the appropriate unit and subassemblies are evident. For these applications, the reference designation may be limited to the class letter(s) and the number identifying the subassembly or part. For example: C6, L12, A2, etc. (See Fig. 2.)

Where parts comprising a subassembly are scattered throughout a drawing, a sufficient portion of the complete reference designation shall be included to permit positive identification. Examples: A3C2—for the second capacitor in subassembly three, where the unit number is evident and has been omitted. On diagrams, drawings, and units, either the complete reference designation shall be used or, where abbreviated reference designations are used, a note shall be included substantially as follows:

“Reference designations are incomplete. For complete identification, prefix the designations with unit number or assembly designation or both.”

5.3.7 Identical Units: Different unit numbers shall be used to identify identical units of a set. However, except for the unit number, the reference designations of all subassemblies and parts shall be the same as for corresponding items of identical units. For example: If units 3 and 9 are identical, and a particular resistor of unit 3 is designated 3R10, the corresponding resistor in unit 9 will be 9R10.

5.3.8 Identical Assemblies: Different reference designations shall be used to identify identical assemblies of a unit. However, the reference designations assigned to all the subassemblies and parts of the assembly shall be the same as of other identical assemblies. For example:

If the third assembly of unit 6 (6A3) and the fourth assembly of unit 8 (8A4) are identical, and a particular capacitor in 6A3 is designated 6A3C11, the corresponding capacitor in 8A4 will be 8A4C11.

5.4 Suffix Letters

Parts having multiple characteristics or all portions of such parts as relays, capacitors, that for drawing simplicity are shown separated from one another on schematics, shall be identified by adding a suffix letter to the reference designation of the composite item. The suffix letters shall start with A and run consecutively. For example: C2A, C2B, and C2C identify each portion of triple capacitor C2, and V2A and V2B identify each portion of electron tube V2.

5.5 Marking

The reference designations shall be located adjacent to each subassembly and part and shall be marked on the chassis, back of the front panel, on partitions, on insulator strips, etc. Reference designations shall not be marked on parts and subassemblies which are subject to replacement (this does not preclude marking of parts within such subassemblies). The reference designations shall be marked in such a position as to physically locate the parts and yet be readily visible for purposes of maintenance without removal of other parts. The primary intent of this requirement is that removal of a part or subassembly shall not result in loss of identification of the physical location of that part or subassembly. Reference designations marked on an identical subassembly as defined in 5.2.4, or on any subassembly thereof, shall be abbreviated as necessary to permit subassemblies to be used in multiple applications. If space limitations preclude such marking, as an alternate, a diagram showing the location of parts or subassemblies shall be placed on the subassembly or unit, respectively, where the diagram is visible when the parts or subassemblies are viewed. The requirements in this paragraph for marking do not apply to consumer products where it is not customary to mark reference designations on the equipment.

5.5.1 Enclosed Parts: Reference designations for parts enclosed in separate and removable shields or compartments may be marked on the shields or supporting structures for such parts, provided that the replacement of such parts does not require destruction of the original shields or supporting structures and provided that such shields or supporting structures are not interchangeable with other shields or supporting structures within the unit. Reference designations shall not appear on electron tube shields.

5.5.2 Plug-In Parts and Sockets: Reference designations of such parts as electron tubes shall be marked next to the socket of the part on the insertion side of the chassis or supporting structure. Reference designations of sockets shall be marked next to the socket on the

Coil, induction, loading, relay operating, re- tardation, tuning	L	Heating lamp	HR
Coil, induction (telephone usage), repeating (telephone usage)	T	Hybrid coil or junction	HY
Coil, repeating	T	Hydraulic part	U
Computer	A	Indicator	DS
Connector, receptacle, electrical (with male, female, or male and female contacts and de- signed to be mounted on a bulkhead, wall, chassis or panel)	J	Inductor	L
Connector, plug, electrical (with male, female, or male and female contacts, constructed to be affixed to the end of a cable, conduit, co- axial line, cord or wire)	J	Instrument	M
Contact, electrical		Insulator	E
Contact (electrically operated)		Interlock, mechanical	MP
Contact (mechanically or thermally oper- ated)		Interlock, safety, electrical	S
Counter (indicating device)	M	Jack—see Connector, receptacle, electrical	
Counterpoise	E	Junction, hybrid	HY
Coupler, directional	DC	Junction (tee or wye), coaxial or waveguide	CP
Coupling (aperture, loop or probe)	CP	Key switch	S
Crystal detector	CR	Key, telegraph	S
Crystal diode	CR	Lamp, ballast	RT
Crystal, piezoelectric	Y	Lamp, heating	HR
Crystal unit	CR	Lamp, illuminating	DS
Cutout, thermal	S	Lamp, pilot	DS
Delay line	DL	Lamp, resistance	RT
Detector, crystal	CR	Lamp, signal	DS
Device, indicating (except meter or thermome- ter)	DS	Lampholder	X
Dial (circuit interrupter)	S	Line, artificial	Z
Diaphragm	DP	Line, delay	DL
Dipole antenna	E	Loop antenna	E
Disconnecting device	S	Loudspeaker	LS
Discontinuity	Z	Magnet	E
Drop	DS	Magneto	G
Dynamotor	D	Mechanical part	MP
Electron tube	V	Meter	M
Equalizer	EQ	Microphone	MK
Exciter	G	Mode suppressor	Z
Fan	B	Mode transducer	MT
Filter	FL	Modulator	A
Flasher	DS	Motor	B
Fuse	F	Motor-generator	MG
Fuseholder (see 5.6.1)	X	Mounting (not in electrical circuit and not a socket)	MP
Gap	E	Nameplate	N
Gauge	M	Network, general (where specific letters do not fit, when considered as a part)	Z
Generator	G	Oscillator (excluding electron tube used in oscillator), magnetostriction oscillator	Y
Governor switch	S	Oscillograph	M
Gyroscope	MP	Oscilloscope	M
Handset	HS	Pad	AT
Hardware; bolts; nuts; screws	H	Part, miscellaneous electrical	E
Head, erasing, recording, reproducing	PU	Part, hydraulic	U
Headset	HT	Part (miscellaneous mechanical); bearing; coupling; gear; shaft	MP
Hearing aid	HT	Part, structural	MP
Heater (element for thermostat, oven, etc.)	HR	Path, guided transmission	W
		Pickup; erasing head; recording head; repro- ducing head	PU
		Phototube	V
		Plug—see Connector, plug, electrical	
		Potentiometer	R
		Power supply; source of power	A

Prime mover	B	Transistor	Q
Protector (carbon-block or gap)	E	Transmission path	W
Receiver, telephone (not part of handset)	HT	Transmitter, telephone	MK
Receptacle (connector, fixed)	J	Tube, electron	V
Rectifier, crystal or metallic	CR	Tuned cavity	Z
Regulator, voltage (except an electron tube)	VR	Tuned circuit	Z
Recorder, elapsed time	M	Varistor, asymmetrical	CR
Recorder, sound	A	Varistor, symmetrical	RV
Reed, vibrating	MP	Vibrator, indicating	DS
Register, message	M	Vibrator, interrupting	G
Relay (electrically operated contactor or switch)	K	Visual signaling device	DS
Repeater (telephone usage)	RP	Voltage regulator (except an electron tube)	VR
Reproducer, sound	A	Waveguide	W
Resistive termination	AT	Winding	L
Resistor	R	Wire	W
Resistor, current regulating	RT	<i>6.4 Alphabetically by Letters</i>	
Resistor, variable	R	*A	Assembly; subassembly
Resolver	B	AT	Attenuator; pad; resistive termination
Resonator	E	*B	Blower; fan; motor; prime mover; resolver; synchro
Rheostat	R	BT	Battery
Ringer, telephone set	DS	C	Capacitor; capacitance bushing
Selenium cell	CR	CB	Circuit breaker
Sensor	A	CP	Coupling (aperture, loop, or probe), coaxial or waveguide junction (tee or wye); adapter, connector
Shield, electrical	E	CR	Crystal detector; crystal diode; crystal unit; crystal, contact or metallic rectifier; selenium cell; varistor, asymmetrical
Short	E	D	Dynamotor; converter; inverter
Shunt	R	DC	Directional coupler
Slip-ring	E	DL	Delay line
Socket (see 5.6.1)	X	DP	Diaphragm
Solenoid	L	*DS	Indicator; miscellaneous illuminating or indicating device (except meter or thermometer) such as: alarm; annunciator; audible or visual signalling device; bell; buzzer; drop; flasher; pilot, illuminating or signal lamp; telegraph sounder; telephone set ringer; vibrator (indicating)
Sounder, telegraph	DS	*E	Miscellaneous electrical part such as: aerial; aluminum or electrolytic cell; antenna; bi-metallic strip; binding post; brush; carbon block; cord tip; counterpoise; dipole antenna; electrical shield; electric contact; gap; individual terminal; insulator; lightning arrester; loop antenna; magnet; protector; resonator; short; slip ring
Speaker; loudspeaker	LS	EQ	Equalizer
Speed regulator	S	F	Fuse
Strip, terminal	TB	FL	Filter
Structural part	MP	G	Exciter; generator; magneto; rotating amplifier; vibrator (interrupting)
Subassembly	A	*H	Hardware; bolts; nuts; screws; etc.
Switch (mechanically or thermally operated)	S		
Synchro	B		
Taper, coaxial or waveguide	T		
Telephone station	A		
Teletypewriter	A		
Teletypewriter	A		
Terminal, individual	E		
Terminal board or strip	TB		
Termination, resistive	AT		
Test block	TB		
†Test point	†TP		
Thermistor	RT		
Thermocouple	TC		
Thermometer	M		
Thermostat	S		
Timer	M		
Transducer	MT		
Transducer, mode	MT		
Transformer	T		

† Not a reference designation, but included in this listing to permit usage in connection with reference designations where required.

* See 6.2.

HR	Heater (element for thermostats, oven, etc.), heating lamp	RP	Repeater
HS	Handset	RT	Current regulating resistor; ballast lamp; resistance lamp; thermistor
HT	Headset; hearing aid; telephone receiver	RV	Symmetrical varistor
HY	Hybrid coil: hybrid junction	S	Switch (mechanically or thermally operated); contactor; disconnecting device; dial (circuit interrupter); electrical safety interlock; governor switch; interlock; speed regulator; telegraph key; thermal cutout; thermostat
J	Connector, receptacle, electrical (with male, female, or male and female contacts and designed to be mounted on a bulkhead, wall, chassis, or panel); jack; receptacle	T	Transformer; autotransformer; IF transformer; repeating coil (telephone usage); transformer, waveguide or coaxial taper; induction coil (telephone usage)
K	Relay (electrically operated contactor or switch)	TB	Terminal board; connecting block; group of individual terminals on its own mounting; terminal strip; test block
L	Choke; inductor; loading coil; relay operating coil; retardation coil; solenoid; tuning coil; winding	TC	Thermocouple
LS	Loudspeaker; speaker	†TP	Test point
*M	Meter; clock; counter (indicating device); elapsed time recorder; gauge; instrument; message register; oscillograph; oscilloscope; thermometer; timer	*U	Hydraulic part
MG	Motor-generator	V	Electron tube; barrier photocell; blocking layer cell; light-sensitive cell; photoemissive cell; photoconductive cell; phototube
MK	Microphone; telephone transmitter	VR	Voltage regulator (except an electron tube)
*MP	Miscellaneous mechanical part such as: bearing; coupling; gear; mechanical interlock; shaft; vibrator reed; gyroscope; structural part; mounting (not in electrical circuit and not a socket)	*W	Cable; coaxial cable; guided transmission path; waveguide; wire
MT	Mode transducer	X	Socket; fuseholder; lampholder (see para. 5.6.1)
N	Plate, identification chart; nameplate; etc.	Y	Oscillator (excluding electron tube used as an oscillator); piezoelectric crystal; magnetostriction oscillator
P	Connector, plug, electrical (with male, female, or male and female contacts, constructed to be affixed to the end of a cable, conduit, coaxial line, cord or wire); plug	Z	Artificial line; discontinuity; tuned cavity; tuned circuit; network
PU	Pickup; erasing head; recording head; reproducing head		
Q	Transistor		
R	Resistor; shunt; resistor, variable; potentiometer; rheostat		

† Not a reference designation, but included in this listing to permit usage in connection with reference designations where required.
* See 6.2.



Design of Transistor Regulated Power Supplies*

R. D. MIDDLEBROOK†, MEMBER, IRE

Summary—A new form of transistor series regulated power supply is presented which permits unusually good performance characteristics to be realized with simple and economical circuitry. Expressions are given for the open-circuit output voltage and the output resistance in terms of the supply voltages and the circuit parameters. Application of the new circuit to two practical laboratory regulated power supplies is described, the specifications of which are: 0.5 ampere at 18 to 22 volts, and 1 a at 5 to 25 v. The output resistance is of the order of 0.01 ohm for both supplies; for sudden change of load current between minimum and maximum the transient in output voltage is 80 mv or less, and decays in 40 μ sec or less. At full load, ripple in the output voltage is less than 5 mv and line voltage variations of ± 10 per cent produce output variations of less than 5 mv. Each supply uses only one line transformer.

I. INTRODUCTION

THE DESIGN of vacuum tube regulated power supplies is well-established. Such supplies are suited for powering equipment in which relatively low currents at high voltages are required. However, for high-current low-voltage applications, vacuum tube supplies become bulky and inefficient, and the design is conveniently implemented with transistors instead of with tubes. Although various types of transistor regulated power supplies have been described¹⁻⁵, most of these possess comparatively low current ratings and poor transient response unless rather complex circuitry is used.

This paper presents a new form of transistor series regulated power supply which permits unusually good performance characteristics to be realized with simple and economical circuitry. Expressions are given for the regulated output voltage and the output resistance in terms of the supply voltages and circuit parameters.

Practical circuits for two laboratory regulated power supplies are presented. The input in each case is 110 v 60 cps and the other specifications are as follows:

Supply No. 1: 0.5 a at 18 to 22 v, output resistance 0.03 ohm.

Supply No. 2: 1 a at 5 to 25 v, output resistance <0.01 ohm.

* Original manuscript received by the IRE, February 4, 1957; revised manuscript received, July 15, 1957. The work described in this paper was performed for ElectroData Corp., Div. of Burroughs, Pasadena, Calif., and is reported by kind permission of ElectroData Corp.

† Elec. Eng. Dept., Calif. Inst. Tech., Pasadena, Calif.

¹ S. Sherr and P. M. Levy, "Design consideration for semiconductor regulated power supplies," *Electronic Design*, vol. 4, pp. 22-25; July 15, 1956.

² F. H. Chase, "Power regulation by semiconductors," *Elec. Eng.*, vol. 75, pp. 818-822; September, 1956.

³ J. W. Keller, "Regulated transistor power supply design," *Electronics*, vol. 29, pp. 168-171; November, 1956.

⁴ M. Lillienstein, "Transistorized regulated power supply," *Electronics*, vol. 29, pp. 169-171; December, 1956.

⁵ L. P. Hunter, "Handbook of Semiconductor Electronics," McGraw-Hill Book Company, Inc., New York, N. Y., pp. 13.26-13.28; 1956.

The transient response of each supply is excellent: sudden increase of load current from zero to maximum produces a transient in output voltage of less than 80 mv with a recovery time of about 10 μ sec; sudden decrease of load current from maximum to zero produces a transient in output voltage of less than 40 mv with a recovery time of about 40 μ sec. At full load, ripple in the output voltage is less than 5 mv and line voltage variations of ± 10 per cent produce output voltage variations of less than 5 mv. Each supply uses only one line transformer.

II. QUALITATIVE DEVELOPMENT OF THE NEW SERIES REGULATOR CIRCUIT

A simple form of standard series regulated power supply using *p-n-p* transistors is shown in Fig. 1. The voltage E is the regulated output and E_p is the unregulated "raw" input voltage with internal resistance R_p . It is required that the voltage E should be as constant as possible with respect to load current I for both steady-state and transient conditions, and should be as independent as possible of input voltage and circuit parameter variations.

If in Fig. 1, the base current of the transistor T_4 is neglected compared to the current through the potential divider, and if the base current of transistor T_1 is neglected compared to the collector current of T_4 , an equation for the output voltage may be simply derived as follows. In the steady state the output voltage E is given by

$$E = n(e + v) \quad (1)$$

where

e = the reference voltage developed across the zener diode D_1 ,

v = the emitter-to-base dc voltage of T_4 (approximately a tenth of a volt), and

n = ratio of the potential divider as defined in Fig. 1.

At any given load current I , there will be a voltage drop between the emitter and base of T_1 which is approximately $R_e I$, where R_e is the effective emitter-to-base resistance of T_1 . The voltage v at the input of T_4 adjusts itself so that the collector current of T_1 produces a voltage drop V across resistance R so that

$$V = E_p - R_p I - E - R_e I \quad (2)$$

Combining (1) and (2) gives

$$E = \left(ne + \frac{E_p}{G} \right) - \left(\frac{R_p + R_e}{G} \right) I \quad (3)$$

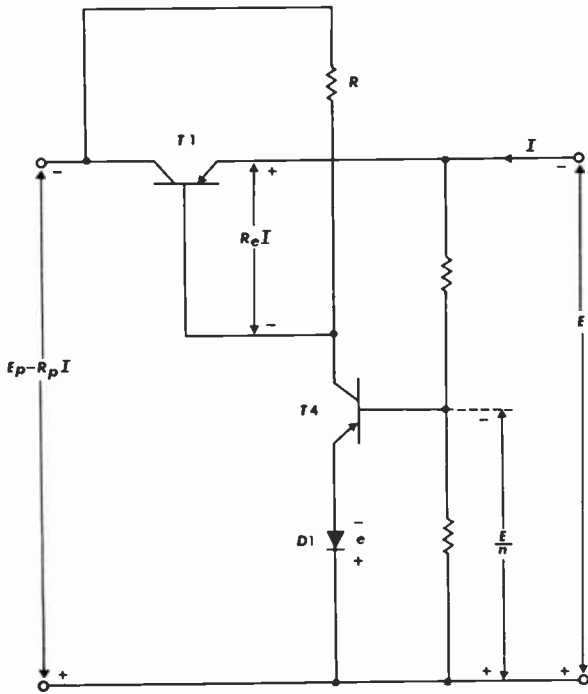


Fig. 1—Simple series regulator circuit, in which E is the regulated output voltage, and the supply voltage is E_p with internal resistance R_p . The output resistance is approximately $(R_e + R_p)/G$.

where $G = V/nv$, and is the dc gain of $T4$ and the potential divider. It is assumed that $G \gg 1$ in the derivation of (3).

In an ideal regulator $E = ne$, and thus (3) indicates the extent to which the circuit of Fig. 1 fails to be ideal. The undesired terms in (3) show that a practical regulator exhibits a finite output resistance and that the open-circuit output voltage is partially dependent on the raw supply voltage. In a typical case, suppose that the power supply is to provide zero to 1 a at 20 v and let $e = 5$ v, $R_e = 1$ ohm, $R_p = 9$ ohm, and $G = 10$. At maximum load of 1 a, 9 v will be dropped in the internal resistance R_p of the raw supply, so in order to maintain at least 1 v reverse bias between the base and collector of $T1$, the supply voltage E_p must be at least 30 v. To provide $E = 20$ v with $e = 5$ v requires $n = 4$ if the regulator approaches ideal performance. Substitution of the given figures into the undesired terms of (2) shows that $E_p/G = 3$ v, $(R_p + R_e)/G = 1$ v at 1 a load current. Thus if there is any variation in E_p (such as change in supply voltage or ripple) the variation in the output voltage E is 3/20 of the variation in E_p . The factor $(R_p + R_e)/G = 1$ ohm is the output resistance R_0 of the regulated supply, which is an improvement by about a factor of 10 over the output resistance R_p of the raw supply.

However, an output resistance of 1 ohm is still too high for many applications. A circuit modification which will further reduce the output resistance presents itself after a qualitative examination of how the circuit of Fig. 1 operates when the load current I is changed.

In the circuit of Fig. 1, an increase in load current I tends to cause a drop in output voltage E not only be-

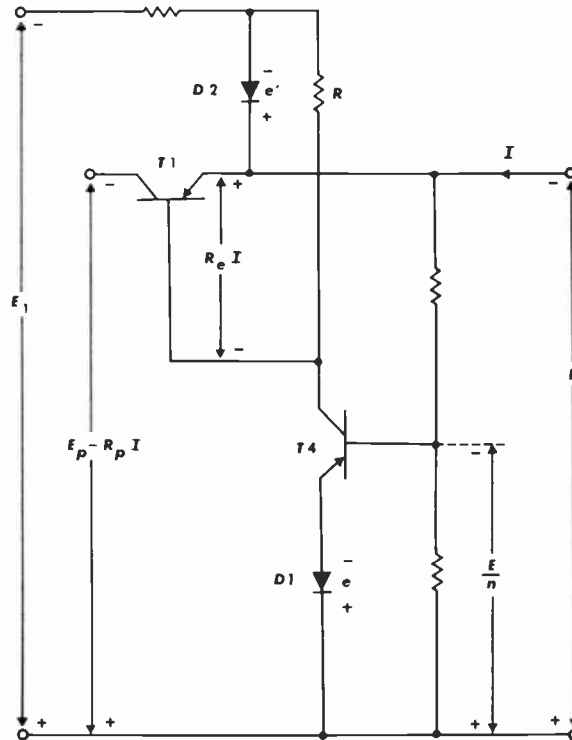


Fig. 2—Principle of the new series regulator circuit, in which the output resistance is reduced approximately to R_e/G .

cause of the larger drop $R_e I$ in $T1$, but also because of the larger drop $R_p I$ in the internal resistance of the raw supply E_p which is connected to the output via the resistor R and transistor $T1$. Thus the amplifier $T4$ is required to compensate for both these drops, and hence the factor $(R_p + R_e)$ occurs in (3). Obviously, if some means could be found to maintain the voltage at the top end of R constant with respect to changes in load, the output resistance would be equal to R_e/G instead of to $(R_p + R_e)/G$, or 0.1 ohm instead of 1 ohm for the above numerical values. This may be accomplished by the circuit of Fig. 2, in which the top end of R is connected to a voltage more negative than the output voltage by a fixed amount. The presence of the zener diode $D2$ insures that the voltage at the top end of R is always essentially constant for all load currents, and thus the above conditions for lower output resistance are realized.

An expression for the output voltage E in the circuit of Fig. 2 is easily obtained by substituting $E + e'$ for $E_p - R_p I$ in (3), which leads to

$$E = ne + \frac{e'}{G} - \frac{R_e}{G} I. \tag{4}$$

It is seen that the output resistance R_0 is indeed R_e/G , or 0.1 ohm for the figures given previously. Further, the output voltage is independent of E_p and the auxiliary supply E_1 , and thus E will be independent of supply voltage variations or ripple.

It is apparent that the circuit of Fig. 2 provides a marked improvement over that of Fig. 1, and yet re-

quires only two more components and an extra (low-current) supply voltage. The simple semiquantitative discussion above is sufficient to explain the principle of the modified regulated supply circuit of Fig. 2, but in practical circuits several additional factors must be taken into account. The most important of these are that the zener reference diodes $D1$ and $D2$ possess finite dynamic resistance (thus the voltages e and e' are not quite constant for different currents), and that for maximum load currents in excess of a few milliamperes the base current of $T1$ will certainly not be negligible compared to the collector current of $T4$. All these factors affect the gain G of $T4$, and also cause the output voltage not to be completely independent of the supply voltage. A more detailed analysis of this new circuit follows in the next section.

III. ANALYSIS OF THE REGULATOR CIRCUIT

A practical embodiment of the principle described in the previous section is shown in Fig. 3. The most important change is the addition of two more transistors $T2$ and $T3$, connected as emitter followers, to provide current amplification so that load currents of several amperes may be drawn, and yet to keep the base current of $T3$ small enough to be comparable with or smaller than the collector current of $T4$. A base current in $T3$, which is not negligible compared to the collector current of $T4$, means that the input resistance of $T3$ shunts appreciably the resistance R . The three transistors $T1$, $T2$, and $T3$ will usually be adequate for load currents up to 1 a. An ammeter will normally be required to monitor the load current, and must be inserted inside the feedback loop; otherwise, the output resistance of the supply will be increased by the resistance of the meter.

If the dc current through the transistor $T4$ is insufficient to maintain the reference diode $D1$ in the breakdown region, the auxiliary supply E_2 may be necessary to provide extra current. It is desirable that E_2 be obtained from the same line transformer that supplies the external load current, in which case E_2 will contain a ripple component and will vary with load current I owing to the imperfect regulation of the raw supply. This effect may be accounted for by supposing the supply E_2 to contain a "transfer internal resistance" R_2 , which may be of the order of 10 ohms. The other auxiliary supply E_1 will possess in a similar way a transfer internal resistance R_1 .

The resistance R_f is very small, of the order of a fraction of an ohm, and is inserted to provide positive feedback proportional to the load current so that the output resistance of the regulated supply can be made zero or slightly negative. The feedback resistance may not always be necessary, but will be included in the analysis so that its effect can be evaluated.

Analysis of the circuit of Fig. 3 requires finding the equation corresponding to (4) for the regulated output voltage, and is conveniently broken down into two

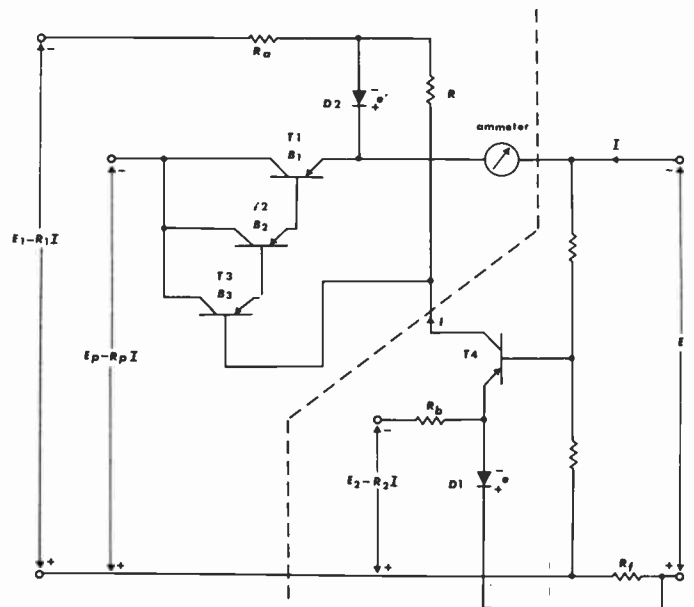


Fig. 3—Practical embodiment of the circuit principle of Fig. 2.

parts. First, an expression for the collector current i of transistor $T2$ is found in terms of the output voltage E by consideration of the voltage amplifier part of the circuit to the right of the dashed line in Fig. 3. Second, an expression for E in terms of i is obtained by consideration of the current amplifier part of the circuit to the left of the dashed line in Fig. 3. Elimination of i from the two resulting equations leads to the desired expression for the output voltage E :

$$E = \left[ne + \frac{r}{R_b} nE_2 + \frac{r'}{R_a} \frac{1}{G} E_1 + \frac{1}{G} e' \right] - I \left[\frac{(R_{e1} + R_{e2} + R_{e3}) + R/B_1B_2B_3}{G} + \frac{R_1 + R_m}{(R_a/r')G} + \frac{r}{R_b} nR_2 - \frac{1+n}{n} R_f \right] \quad (5)$$

where

- e, r = the reference voltage, dynamic resistance of zener diode $D1$,
- e', r' = the corresponding quantities of zener diode $D2$,
- R_m = the resistance of the ammeter,
- B_1, B_2, B_3 = the common-emitter dc current gains of $T1, T2, T3$,
- R_{e1}, R_{e2}, R_{e3} = effective emitter-base resistances of $T1, T2, T3$ (defined in each case as the ratio: change in emitter-base voltage/change in load current I),
- n = the ratio of the potential divider, defined as in Fig. 1,
- G = is the dc gain of the potential divider and the amplifier $T4$,

and the other quantities are as shown in Fig. 3. The gain G corresponds to the quantity V/nv previously:

mentioned, and is given by

$$G = R/n[r_e + r + (r_p + r_b)/B_4] \quad (6)$$

where r_p is the resistance of the two potential divider resistors in parallel, and r_e , r_b , and B_4 are the emitter resistance, base resistance, and common-emitter dc current gain of T_4 .

In the derivation of (5), the following good approximations are made:

$$B \gg 1 \text{ for all transistors} \quad (7)$$

$$R_b \gg r \quad (8)$$

$$R_a \gg r' \quad (9)$$

$$R \gg r' \quad (10)$$

$$(R_a/r')G \gg 1. \quad (11)$$

It is further assumed that the load current I is considerably larger than the current drain through the potential divider, and is also considerably larger than the current through the diode D_2 .

Eq. (5) may be written

$$E = E_0 - R_0 I \quad (12)$$

where E_0 is the open-circuit output voltage and R_0 is the effective output resistance of the regulated supply. The criteria of a satisfactory design are that E_0 should be as independent as possible of the raw supply voltages E_p , E_1 , and E_2 , and the output resistance should be as small as possible (less than 1 ohm). Eq. (5) shows the relative effects of the raw supply voltages and the various internal resistances which cause the output voltage to deviate from the ideal value $E = ne$. A discussion of the implications of (5) is desirable, and is given in the next section.

IV. DISCUSSION OF THE ANALYTICAL RESULTS

Consider first the effects of the raw supply voltages on the open-circuit output voltage E_0 , where, from (5) and (12),

$$E_0 = ne + \frac{r}{R_b} nE_2 + \frac{r'}{R_a} \frac{1}{G} E_1 + \frac{1}{G} e'. \quad (13)$$

In an ideal regulator $E_0 = ne$, and thus the other terms in (13) are undesirable and should be minimized in a good design. In order to obtain a high value of the ratio R_a/r' , the supply E_1 should be at least twice the output voltage E . Let typical figures again be taken of $e = 5$ v, $n = 4$; then E_0 will be equal to 20 v plus correction terms. The supply E_1 should be at least 40 v, and for $G = 10$ and $R_a/r' = 100$ the term in E_1 is equal to 0.04 v, or 0.2 per cent of the output voltage. Thus E_0 is almost completely independent of E_1 , and practically none of any ripple on E_1 will get through to the output.

In some cases the supply E_2 will not be required at all, since sufficient dc current to break down the reference diode D_1 may be available through transistor T_4 . In this case, of course, the terms in E_2 will not appear in the

equation for E_0 . However, if extra current is required for the diode D_1 , it may be obtained from the supply E_p in which case $E_2 = E_p$. For $E_p = 30$ v, the ratio R_b/r may be about 100, and so the term in E_2 in (13) will be equal to 1.2 v. This represents 6 per cent of the output voltage E_0 , a figure which is undesirably high since variations in line voltage and ripple will thus be transmitted to the regulated output with appreciable magnitude. A way to overcome this problem is to make E_2 equal not to E_p but to E ; that is, to derive the extra current for D_2 from the regulated output instead of from the raw input. Putting $E_2 = E$ in (5) leads to

$$E_0 = \frac{1}{1 - nr/R_b} \left(ne + \frac{r'}{R_a} \frac{1}{G} E_1 + \frac{1}{G} e' \right) \quad (14)$$

and the result is essentially the same as when $E_2 = 0$ except that the no-load output voltage is increased by the factor $1/(1 - nr/R_b)$ which, however, is close to unity.

The remaining term to consider in (5) is that in e' . If $e' = 5$ v, this term amounts to 2 per cent of the output voltage and is not detrimental since e' is itself a reference voltage.

To summarize the above discussion of the open-circuit output voltage, the typical numerical values obtained above are shown below in a form in which the terms correspond to those in (14), where $E_2 = E$:

$$E_0 = \frac{1}{1 - 0.04} (20 + 0.04 + 0.5) \quad (15)$$

$$E_0 = 21.36 \text{ v.} \quad (16)$$

Consider next the effects of the various internal resistances on the output resistance R_0 . From (5) and (12),

$$R_0 = \frac{(R_{e1} + R_{e2} + R_{e3}) + R/B_1B_2B_3}{G} + \frac{R_1 + R_m}{(R_a/r')G} + \frac{r}{R_b} nR_2 - \frac{1+n}{n} R_f. \quad (17)$$

In an ideal regulator R_0 should be as small as possible, and hence all the terms in (17) should be minimized in a good design. Each term which contributes to the output resistance R_0 can be identified with an independent process occurring in the circuit of Fig. 3.

The quantity $(R_{e1} + R_{e2} + R_{e3})$ is the total effective internal resistance of the current-amplifying transistors T_1 , T_2 , and T_3 and corresponds to the internal resistance R_e of the single transistor shown in the circuit of Fig. 2. As predicted by the simple analysis given in connection with Fig. 2, the internal resistance of the current-amplifying transistor contributes a term $(R_{e1} + R_{e2} + R_{e3})/G$ to the output resistance of the supply. However, in the simple analysis it was assumed that the base current of the current-amplifying transistor was negligible compared to the current through R , that is, the resistance looking into the base of the current-amplifying transistor was much larger than the resistance R . In the

more accurate analysis given above this assumption was not made, and the presence of this shunting effect is represented by the term in R in (17).

Some typical figures again will help to give a feeling for the relative magnitudes of the terms in (17) for the output resistance. Suppose that $G=10$, $R=6000$ ohms, $B_1, B_2, B_3=30, 40, 50$, and $R_{e1}, R_{e2}, R_{e3}=0.70, 0.15, 0.15$ ohms respectively. The total effective internal resistance R_e of transistors $T1, T2$, and $T3$ is then 1 ohm, and the additional resistance contributed by the term in R is 0.1 ohm. Hence, the component of output resistance arising from these two sources is $(1+0.1)/10=0.11$ ohm, which may be compared with the result of 0.10 ohm which would be calculated by neglecting the shunting effect.

From (17) it is seen that an additional component of output resistance arises from the presence of the ammeter resistance R_m , and of the auxiliary supply transfer internal resistance R_1 . Typical values are $R_m=1$ ohm, $R_1=10$ ohm. However, it is seen that the resulting component of output resistance is the sum of the two resistances divided not by G alone, but by $(R_a/r')G$. For the above typical figures, this component of output resistance is 0.011 ohm, and is only 10 per cent of the component due to R_e and R .

A third component of output resistance is introduced by the transfer internal resistance R_2 of the auxiliary supply E_2 . As described in connection with the open-circuit output voltage E_0 , the supply E_2 will not be required in some cases, and so $R_2=0$. However, if E_2 is taken from the main supply voltage E_p , $R_2=R_p$ and may be about 10 ohm. For $R_b/r=100$, $n=4$ as before, the component of output resistance due to R_2 will be 0.4 ohm and is undesirably large. This problem may be resolved by again deriving the extra current supply for diode $D1$ from the output voltage E instead of from E_p . In this case $R_2=0$, and putting $E_2=E$ in (5) gives

$$R_0 = \frac{1}{1 - nr/R_b} \left[\frac{(R_{e1} + R_{e2} + R_{e3}) + R/B_1B_2B_3}{G} + \frac{R_1 + R_m}{(R_a/r')G} - \frac{1+n}{n} R_f \right] \quad (18)$$

and the result is essentially the same as when E_2 and R_2 are zero, except that the output resistance is increased by the factor $1/(1 - nr/R_b)$ which, however, is close to unity.

The remaining term to consider in (17) is that due to the feedback resistance R_f . As described in Section III, R_f introduces positive current feedback whose magnitude can be adjusted to make R_0 zero or even negative. From (18) the value of R_f which would be required to make $R_0=0$ for the above typical figures, and where $E_2=E_p$ and $R_2=R_p$, is given by

$$0 = 0.11 + 0.011 + 0.4 - (5/4)R_f \quad (19)$$

or

$$R_f = 0.417 \text{ ohm.} \quad (20)$$

A resistance of this small magnitude is furnished by a few inches of wire, and, in practice, the best way to obtain the desired value of R_f is to adjust the length of a piece of wire in the appropriate place in the completed regulated supply circuit until the output resistance is zero. This method of reducing the output resistance is not particularly satisfactory, however, since the adjustment is awkward to make and in any case will only be correct for a particular value of n . Thus, if a variable output voltage E is required (which is obtained by varying the potential divider ratio n), the output resistance R_0 may vary considerably over the range of output voltage. Therefore, it is preferable to design for a low inherent output resistance by making G as large as possible.

To summarize the above discussion of the output resistance, the typical numerical values obtained above are shown below in a form in which the terms correspond to those of (18), in which $E_2=E_1$, $R_2=0$, and where $R_f=0$:

$$R_0 = \frac{1}{1 - 0.04} (0.11 + 0.011) \quad (21)$$

$$= 0.126 \text{ ohm.} \quad (22)$$

V. A FURTHER CIRCUIT MODIFICATION

There is yet another beneficial modification which may be made in the regulated power supply circuit, and which is suggested by (15) for the output voltage.

It may be noted that in (15) there is a component of output resistance due to the total effective internal resistance $R_e=(R_{e1}+R_{e2}+R_{e3})$ of the current-amplifying transistors $T1, T2$, and $T3$, and another component due to the resistance R_m of the ammeter. The former component is equal to R_e divided by G , but the latter component is R_m divided by $(R_a/r')G$ where R_a/r' is at least 100. Examination of Fig. 3 suggests that if the diode $D2$ were connected not to the emitter of transistor $T1$ but to the emitter of $T2$, then the two above components of output resistance might be equal to $(R_{e2}+R_{e3})/G$ and $(R_m+R_{e1})/(R_a/r')G$, respectively, and the sum of the components and hence the output resistance R_0 would be reduced.

If the above modification is introduced, analysis corresponding to that for Fig. 3 leads to

$$E = \left[ne + \frac{r}{R_b} nE_2 + \frac{r'}{R_a} \frac{1}{G} E_1 + \frac{1}{G} e' \right] - I \left[\frac{(R_{e2} + R_{e3}) + R/B_1B_2B_3}{G} + \frac{R_1 + R_m + R_{e1}}{(R_a/r')G} + \frac{r}{R_b} nR_2 - \frac{1+n}{n} R_f \right]. \quad (23)$$

The result of (23) shows that the expectation described above is justified: the open-circuit output voltage E_0 is the same as before, but in the output resistance R_0 , the resistance R_{e1} is now divided by $(R_a/r')G$ instead of by

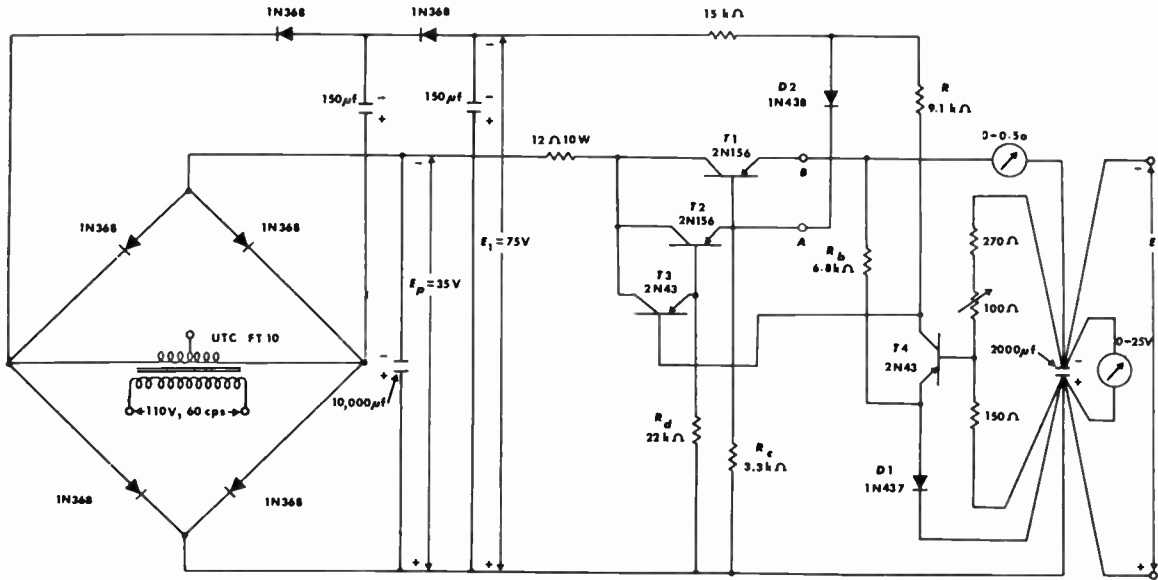


Fig. 4—Circuit of regulated supply to provide 0.5 a at 18 to 22 v. The output resistance is 0.007 ohm.

G alone. The same typical figures assumed before will show the improvement introduced by the circuit modification. If $G = 10$, $R = 6000$ ohm, $B_1, B_2, B_3 = 30, 40, 50$, and $R_{e1}, R_{e2}, R_{e3} = 0.70, 0.15, 0.15$ ohm, respectively, then

$$\frac{(R_{e2} + R_{e3}) + R/B_1B_2B_3}{G} = \frac{0.3 + 0.1}{10} \tag{24}$$

$$= 0.04 \text{ ohm} \tag{25}$$

and

$$\frac{R_1 + R_m + R_{e1}}{(R_a/r')G} = \frac{10 + 1 + 0.7}{100 \times 10} \tag{26}$$

$$= 0.0117 \text{ ohm.} \tag{27}$$

and if $E_2, R_2,$ and R_f are all zero the output resistance R_0 is

$$R_0 = 0.04 + 0.0117 \tag{28}$$

$$\approx 0.052 \text{ ohm} \tag{29}$$

which may be compared with $R_0 = 0.121$ ohm obtained with the circuit of Fig. 3.

Obviously, whether or not the circuit modification introduces a significant reduction in R_0 depends on the actual numerical values in the circuit. For example, the improvement will not be significant if there is appreciable shunting of R , that is, if $R/B_1B_2B_3$ is comparable to $(R_{e1} + R_{e2} + R_{e3})$, or if R_{e1} is comparable with or smaller than $(R_{e2} + R_{e3})$. This latter condition may occur if two transistors are used in parallel in place of the single transistor $T1$ in order to obtain larger maximum load current I .

The discussion of the preceding two sections has presented the analysis and interpretation of the results to be expected from a new form of series-regulated power supply circuit. Although the treatment has been in

terms of a fixed output voltage E , there is nothing in the principle which prevents extension to variable-voltage supplies. However, certain practical problems do arise if the output voltage is required to be varied by more than about ± 10 per cent. In the following sections two practical power supplies embodying the above principle are described, one having an output voltage variable by ± 10 per cent, and one having an output voltage variable over a wider range.

VI. PRACTICAL SUPPLY NO. 1: 0.5 A AT 18 TO 22 V

The schematic diagram of a regulated power supply to provide up to 0.5 a at 18 to 22 v is shown in Fig. 4. The input power source is 110 v 60 cps.

The raw supply voltage E_p is obtained from a bridge rectifier circuit, and the auxiliary supply voltage E_1 is obtained from a voltage-doubler from the same line transformer. The auxiliary supply E_2 is not required; instead, extra bias current for the zener diode $D2$ is obtained from the output voltage through resistor R_b , as described in Section IV.

The two resistors R_c and R_d are introduced so that the transistors $T2$ and $T3$, respectively, will not be cut off when the load current is small. The transient response is also improved because the current-amplifying transistors are working in a linear region over a greater part of their range. The presence of the resistors R_c and R_d modifies the details of the analysis presented in the previous sections, but the principle remains the same.

The 2000- μ f capacitor connected across the regulated output is added to improve the transient response. The wiring layout indicated in Fig. 4 is particularly important: all leads should be returned directly to the capacitor terminals as shown. The reason is that the load current must not be allowed to develop undesired voltages which find their way to the amplifier input. As described in Section IV, the presence of a feedback re-

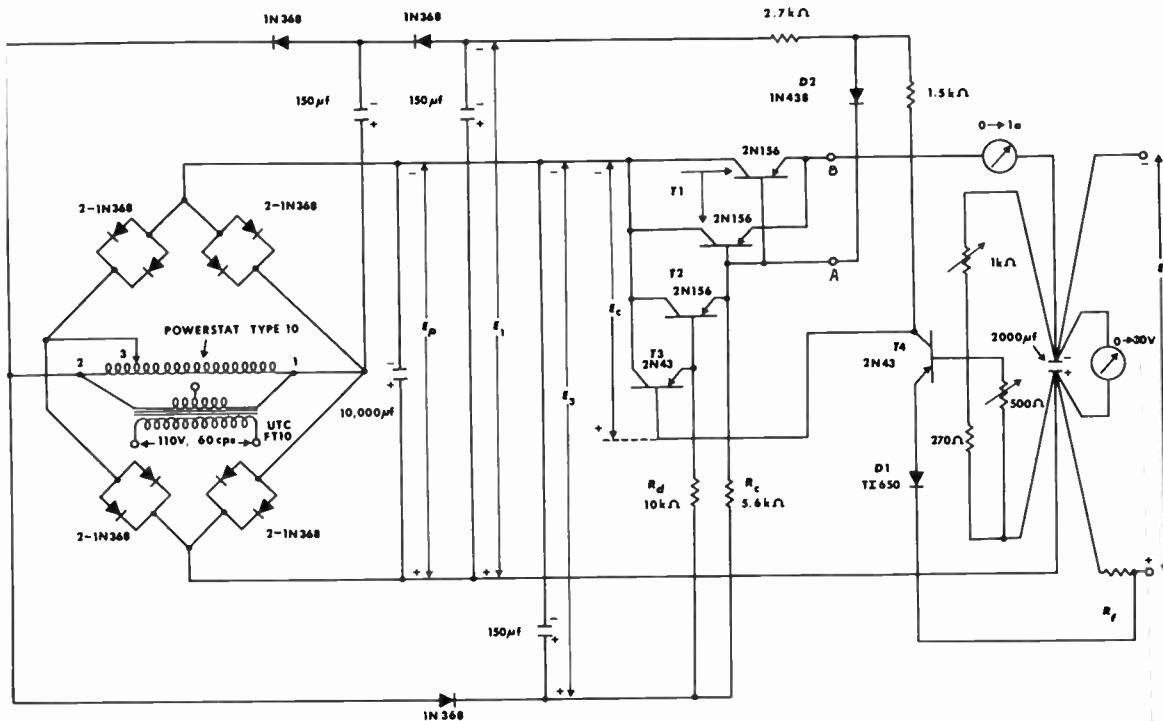


Fig. 5—Circuit of regulated supply to provide 1 a at 5 to 25 v. The output resistance can be made zero at the maximum output voltage.

sistance R_f of only a fraction of an ohm in the right place can cause an appreciable change in output resistance.

The presence of the resistors R_e and R_d , the difficulty in measuring the dynamic resistances of the reference diodes, and the difficulty in predicting the gain of the voltage amplifier make it rather impracticable to calculate the value of the output resistance to be expected. Experimental measurements indicate the following performance characteristics: for a suddenly applied load of 0.5 a, the output voltage drops 40 mv and recovers in about 10 μ sec; for a suddenly removed load of 0.5 a the output voltage rises 20 mv and recovers in about 40 μ sec. Ripple and noise in the output are less than 5 mv at full load, and the output voltage changes by less than 5 mv for line voltage changes of ± 10 per cent.

With the diode $D2$ connected to point B instead of to point A, the steady-state output resistance is 0.03 ohm. With the diode connected to point A the output resistance is 0.007 ohm, showing that significant improvement is obtained by the circuit modification described in Section V.

VII. PRACTICAL SUPPLY NO. 2: 1 A AT 5 TO 25 V

The design of a regulated power supply to provide an output voltage variable over a wide range poses several problems in addition to those already discussed for small-range supplies. The most important problem is that at low output voltage settings the power dissipation in the current-amplifying transistor becomes excessive. This can, of course, be alleviated by putting more transistors in parallel, but this is a wasteful and expensive procedure. A more attractive solution is to reduce

the raw dc supply voltage E_p by means of a Powerstat, at the same time that the output voltage E is reduced, and then the power dissipation in the series transistors remains small.

The schematic of a regulated power supply to provide up to 1 a at any voltage between 5 and 25 v is shown in Fig. 5. The input power source is 110 v 60 cps. The Powerstat is ganged to the 1-kilohm rheostat which sets the output voltage. The regulator part of the circuit is similar in principle to the corresponding part of the 20-v supply described in the previous section. However, the raw dc supplies in Fig. 5 are of special interest.

Three input voltages are provided: the heavy-current supply E_p , obtained from a bridge rectifier; the auxiliary supply E_1 to bias the zener diode $D2$, obtained from a voltage doubler; and another auxiliary supply E_3 to provide current through the resistors R_e and R_d , obtained from a half-wave rectifier. Fig. 6 shows the variation of the open-circuit characteristics of these three input voltages with Powerstat setting. The purpose of arranging the inputs in this way is to maintain all the diodes and transistors at the same operating point, and the same currents in resistors R_e and R_d , at all settings of the output voltage.

An additional problem encountered in a power supply to provide a wide range of output voltages is that extra current for biasing zener diode $D1$ cannot be obtained from the output voltage E as was done in the 20-v supply described previously. The reason is that since the output voltage may vary over a wide range, the extra current would vary likewise and in fact would fall to zero at the lowest output voltage. An alternative is

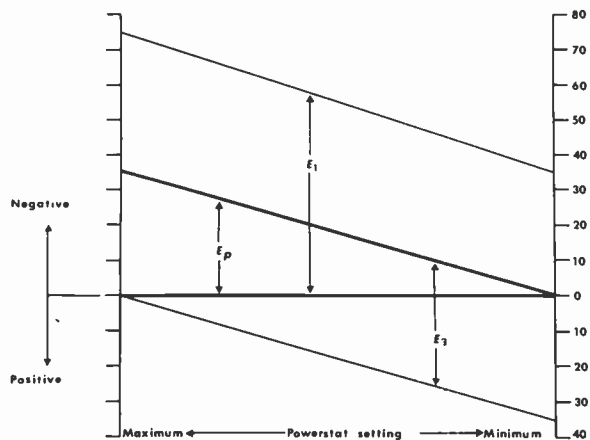


Fig. 6—Variation of the raw supply voltages, E_p , E_1 , and E_2 with Powerstat setting, in the circuit of Fig. 5.

to derive the extra current from another auxiliary supply E_2 (as described in Section III) which does not vary with the output voltage setting. However, this is unsatisfactory because of the unavoidably large transfer internal resistance R_2 of the supply E_2 , and because of the ripple introduced into the output. The only remaining possibility (short of using a second line transformer and well-filtered rectified output) is to allow sufficient current through the voltage-amplifying transistor to bias the diode $D1$ adequately without the necessity for extra current. In the circuit of Fig. 5, the resistance R is therefore made small in order to pass about 5 ma through the voltage-amplifying transistor. Consequently, the gain of this stage is considerably less than in the supply described previously.

In the absence of the resistance R_f in the circuit of Fig. 5, the output resistance is about 0.25 ohm at the maximum output voltage of 25 v, irrespective of whether the diode $D2$ is connected to point A or to point B. This rather large value of output resistance is principally due to the low gain of the voltage amplifier (because of the low value of R) and also to the high value of n (the potential divider ratio). However, the introduction of positive current feedback as described in Section III can be usefully employed to reduce the output resistance. The circuit must be carefully wired as indicated in Fig. 5, and the resistance R_f consists of about 30 inches of No. 22 tinned copper wire. The required length is best found by trial and error, and is chosen so that the output resistance is zero or slightly positive at maximum output voltage setting. At lower output voltages, the output resistance will then be almost zero or slightly negative. The transient response is comparable with that of the 20-v supply described in the previous section, the actual magnitudes involved being dependent on the output voltage setting.

VIII. CONCLUSION

A new form of transistor series regulated power supply circuit has been introduced and analyzed. Application of this new circuit to two practical regulated supplies has been described, one variable over a small range and one variable over a wide range of voltage. Each supply is simple and economical and requires only one line transformer. Independence of line voltage variations, output voltage ripple, output resistance, and transient response are unusually good.

CORRECTION

W. Guggenbuehl and M. J. O. Strutt, authors of "Theory and Experiments on Shot Noise in Semiconductor Junction Diodes and Transistors," which appeared on pages 839–854 of the June, 1957, issue of these PROCEEDINGS, have brought the following corrections to the attention of the editors.

P. 841, (5), should read: $\overline{i_{ntot}^2}$.

P. 843, (12), should read: $\overline{i_{nth}^2}$.

P. 843, three lines below (12), should read: $\overline{i_{ne}^2} = 2eI_c\Delta f$.

P. 843, first column, second line from bottom, should read: $\overline{i_{nc}^2}$.

P. 843, (13), Y Index should read: Y_L .

P. 845, first column, sixth line from top, should read:

$$|Y_{11}| \gg |Y_{12}|, |Y_{21}| \gg |Y_{22}|.$$

P. 846, first column, thirteenth line from top, should read: $\overline{i_{ne}^2}$.

P. 846, first column, fourteenth line from top, should read: $\overline{i_{nc}^2}$.

P. 846, second column, tenth line from bottom, should read: $\overline{u_{nh}^2}$.

P. 846, second column, ninth line from bottom, should read: $\overline{i_{nh}^2}$.

P. 847, first column, third line from bottom, should read:

$$\overline{(i_{n1}^* + i_{n2}^*)(i_{n1} + i_{n3} + i_{np})}.$$

P. 854, Acknowledgment, second line from top, should read to the firms Brown, Boveri at Baden and Hasler at Berne, Switzerland.

A New Technique in Ferrite Phase Shifting for Beam Scanning of Microwave Antennas*

F. REGGIA†, ASSOCIATE, IRE, AND E. G. SPENCER‡, SENIOR, IRE

Summary—A reciprocal ferrite phase shifter for 3-cm wavelength has been developed which makes use of a new design technique for obtaining large phase changes per unit length by electrical means. The device consists essentially of a longitudinal magnetic field applied to a ferrite rod centrally located inside a rectangular waveguide excited in the TE₁₀ mode. With a proper choice of rod diameter and impedance matching elements, phase shifts of greater than 250° per inch and variations in transmitted power of less than ±0.2 db have been obtained with external control fields as low as 60 oersteds. Zero-field insertion loss of less than 0.1 db per inch has been measured. These characteristics, along with its geometrical configuration and small size, make this electrically controlled ferrite device useful in the design of rapid-scanning antennas or any similar microwave system requiring phase modulation.

INTRODUCTION

MANY investigators¹⁻³ have attempted to develop a small electrically controlled ferrite phase shifter for 3-cm wavelength which would give large reciprocal phase changes per unit length with small dc control fields. Such a device has been developed which makes use of a relatively large ferrite rod (ferrod) centrally located inside a standard rectangular waveguide and a longitudinally applied magnetic field to produce the necessary phase shift.

When a longitudinal magnetic field is applied to a ferrite rod inside an axially symmetrical waveguide system excited with a linear wave, a rotation of the plane of polarization⁴ of the microwave energy occurs. If, however, the ferrite rod is placed inside a nonsymmetrical waveguide system (one of its dimensions at cutoff) and providing the diameter of the rod is not too large, this rotational effect is suppressed and a large phase change of the microwave energy occurs.

Such is the case for the reciprocal ferrite phase shifter to be described. When a small diameter ferrite rod, less than 0.20 inch, is placed inside a standard rectangular waveguide used at X band and a longitudinal magnetic field is applied, small phase shifts of the microwave energy occur. If, however, the rod diameter is increased above this value, large phase changes with applied dc

field begin to occur with relatively small changes in transmitted power. This increase in phase change is consistent with a larger percentage of microwave energy concentrated in the rod⁵ and since the rectangular waveguide boundary is still sufficient to suppress the rotational effect of the ferrite, only small changes in transmitted power occur. When the diameter of the ferrod exceeds 0.30 inch, a maximum phase change per unit length is reached and relatively large variations of transmitted power with applied magnetic field begin to occur. It is now believed that the rectangular waveguide boundary no longer plays a significant part in suppressing the rotation of polarization of the microwave energy and since it cannot transmit such variations beyond the rod relatively large reflections occur as indicated by the large impedance changes observed at the input of the device.

Phase shifts in excess of 300° per inch with relatively small applied fields have been obtained with a typical MgMn ferrite for X-band frequencies. Variations of transmitted power no greater than ±0.2 db and zero-field insertion losses less than 0.1 db per inch have been measured. Reversing the direction of the external applied field and/or direction of propagation gives a phase delay of the microwave energy, resulting in a reciprocal electrically controlled ferrite phase shifter.

Impedance matching⁶ is accomplished by attaching short dielectric tips to both ends of the ferrite rod or by tapering the ends of the rod. This impedance matching along with the use of a low-loss ferrite inside a traveling-wave transmission system accounts for the small insertion loss of the ferrite phase shifter. The redistribution of the microwave field and the variation of the guide wavelength (λ_g) as a function of the diameter of the ferrod are discussed in a later section. Application of the new phase shifting technique to the antenna beam scanning problem and the results obtained are also given in a later section.

A theoretical analysis of the field configuration and energy distribution inside a ferrite-loaded circular waveguide has been made by J. E. Tompkins of the Diamond Ordnance Fuze Laboratories. Some results of this analysis are of interest in the present case because of the similarity between the electrical characteristics obtained

* Original manuscript received by the IRE, June 11, 1957; revised manuscript received, August 13, 1957.

† Diamond Ordnance Fuze Labs., Washington, D. C.

¹ B. Lax, K. J. Button, and L. M. Roth, "Ferrite phase shifters in rectangular waveguide," *J. Appl. Phys.*, vol. 25, pp. 1413-1421; November, 1954.

² H. Scharfman, "Three new ferrite phase shifters," *Proc. IRE*, vol. 44, pp. 1456-1459; October, 1956.

³ F. Reggia, E. G. Spencer, R. D. Hatcher, and J. E. Tompkins, "Ferrod radiator systems," 1956 IRE CONVENTION RECORD, pt. 1, pp. 213-224.

⁴ A. G. Fox, S. E. Miller, and M. T. Weiss, "Behavior and applications of ferrites in the microwave region," *Bell Sys. Tech. J.*, vol. 34, pp. 5-103; January, 1955.

⁵ J. L. Melchor, W. P. Ayres, and P. H. Vartanian, "Energy concentration effects in ferrite loaded waveguides," *J. Appl. Phys.*, vol. 27, pp. 72-77; January, 1956.

⁶ R. F. Sullivan and R. C. LeCraw, "A Broadband Ferrite Microwave Switch," DOFL Tech. Rep. No. TR-59; March, 1954.

with the above phase shifter and those obtained with a ferrite-loaded circular waveguide propagating a negative rotating mode. These results will be published later.

RECIPROCAL FERRITE PHASE SHIFTER

A simplified sketch of the reciprocal phase shifter for 3-cm wavelength is shown in Fig. 1. It consists of a ferrite rod, dielectric impedance matching elements, a low current solenoid, and a section of standard rectangular waveguide having outside dimensions of $\frac{1}{2} \times 1$ inch. The length of the entire system is approximately 5 inches.

The ferrite rod used as the phase shifting element consists of a commercially available low-loss MgMn ferrite⁷ and its useful range of diameters is from 0.20 to 0.30 inch. It is centrally located inside the rectangular waveguide section by a teflon or polyfoam support. The demagnetizing factor of the ferrid, when used with a longitudinal magnetic field, is very small. The electric and magnetic properties of the ferrite at the operating frequencies used are given in LeCraw and Spencer⁸ and Spencer, *et al.*⁹

The solenoid supplying the longitudinal magnetic field consists of approximately 3000 turns of no. 28 wire wound around the rectangular waveguide section. Magnetic field strengths up to 200 oersteds have been measured at the center of the windings through a small hole in the top of the waveguide.

The impedance matching elements shown at the input and output ends are short lengths of a dielectric material¹⁰ having the same diameter as the ferrite rod. Their lengths range from 0.30 to 0.50 inch, depending upon the length and diameter of the ferrite rod used. Tapered ferrite ends and polyfoam supports were used in later models of the phase shifter to obtain better bandwidth characteristics and smaller variations in transmitted power with applied magnetic field.

The electrical characteristics of the reciprocal phase shifter at 9100 mc vs applied magnetic field are shown in Fig. 2. Phase shift, power variation, and input vswr are given for the device using a ferrite rod 4.0 inches long, and 0.30 inch in diameter. This was found to be the maximum diameter rod that could be used in the phase shifter and still maintain reasonably low variations in the transmitted power. A phase shift of 300° per inch and a variation in transmitted power with applied magnetic field no greater than ± 0.7 db were obtained. It is interesting to note that most of the phase

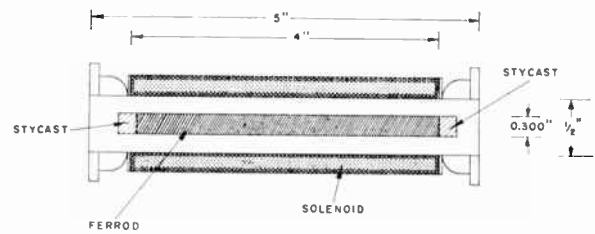


Fig. 1—Cross-sectional view of the reciprocal phase shifter showing the ferrite rod centrally located inside a rectangular waveguide section and the solenoid used for obtaining a longitudinal magnetic field.

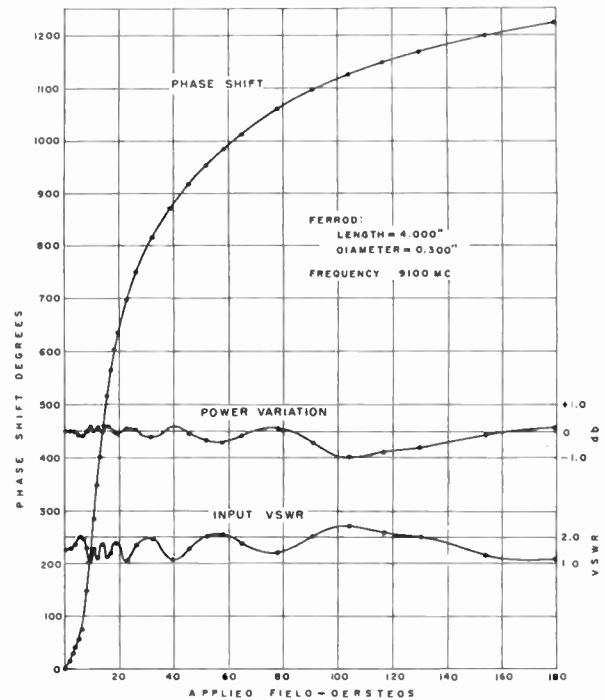


Fig. 2—Phase shift, variation in transmitted power, and input vswr vs applied dc magnetic field for a 0.30-inch diameter ferrite rod at 9100 mc.

shift obtained occurred for magnetic fields less than 100 oersteds. A 0.30-inch length of Styrcast #5 dielectric¹⁰ having the same diameter as the ferrite rod was used at both ends to obtain a reasonably good impedance match. The zero-field insertion loss of this phase shifter was approximately 0.5 db and a dc power of 5 watts was required to obtain a field strength of 100 oersteds.

A simplified circuit arrangement used for the above measurements is shown in Fig. 3. A square-wave amplitude-modulated klystron, well isolated from the phase measuring circuit, was used as the microwave power source. Its frequency and power output were constantly monitored during the measurements. A null type of phase detector (magic tee) was used in the measuring circuit because of its sensitivity to small changes in phase and power incident upon it. Minimum probe coupling of the standing-wave machine was used to minimize errors when monitoring the input impedance of the phase shifter under test. Matched phase shifters

⁷ All data reported in this paper were taken for the Ferramic R-1 ferrite at 9100 mc.

⁸ R. C. LeCraw and E. G. Spencer, "Tensor permeabilities of ferrites below magnetic saturation," 1956 IRE CONVENTION RECORD, pt. 5, pp. 66-74.

⁹ E. G. Spencer, R. C. LeCraw, and F. Reggia, "Measurements of microwave dielectric constants and tensor permeabilities of ferrite spheres," PROC. IRE, vol. 44, pp. 790-800; June, 1956.

¹⁰ Styrcast No. 5 Hi-K Dielectric, loss factor less than 0.001 and dielectric constant of 5.

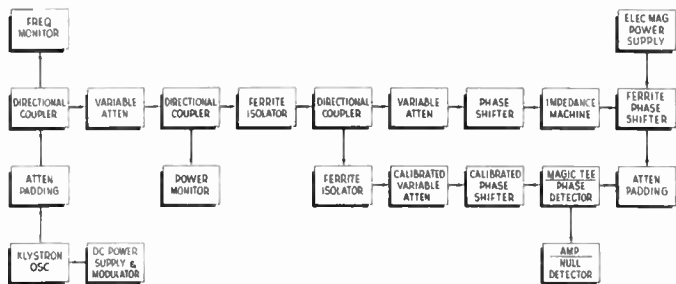


Fig. 3—Block diagram of the equipment used for determining the microwave characteristics of the ferrite phase shifter.

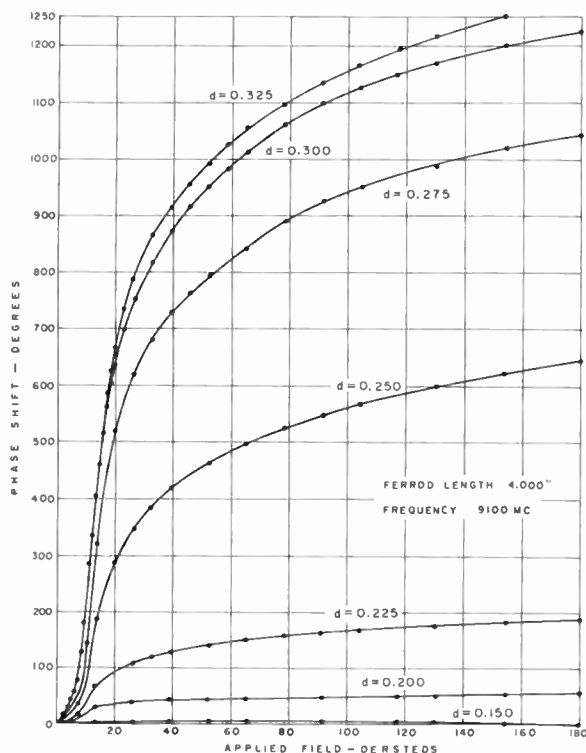


Fig. 4—Measured phase shift as a function of the applied magnetic field for ferrite rods of different diameters. Data were taken for the Ferric R-1 at 9100 mc.

and calibrated precision attenuators were used throughout the measurements.

The phase shifting characteristics at 9100 mc vs applied dc field and diameter of ferrite rod used in the phase shifter are shown in Fig. 4. These rods were all 4.0 inches long and taken from the same batch of material. It can be seen that small phase changes are obtained for rod diameters less than 0.225 inch. Increasing the rod diameter above this value results in large phase changes, most of which occur for fields less than 60 oersteds. As seen from the curves, phase shifts greater than 300° per inch are possible for rod diameters approximately 0.30 inch. For diameters greater than 0.30 inch, little increase in phase shift is obtained and large changes in the transmitted power (not shown in the figure) begin to occur.

A photograph of the seven ferrite rods used to obtain the above data is shown in Fig. 5. The dielectric impe-

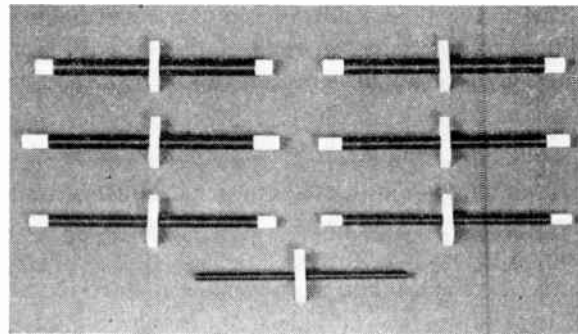


Fig. 5—The seven ferrite rods used in the reciprocal phase shifter to obtain the data in the preceding figure.

dance matching tips and teflon supports are clearly seen in the figure. In more recent phase shifters, impedance matching is accomplished by tapering the input and output ends of the rod and a polyfoam support is used to center the ferrite rod inside the rectangular waveguide section.

A series of curves showing the electrical characteristics of the phase shifter at 9100 mc as a function of length of the ferrite rod and applied dc field are shown in Fig. 6. The lengths of rods used varied from $\frac{7}{8}$ inch to $5\frac{1}{2}$ inches and were taken from the same batch of material. A maximum phase shift of 200° per inch was obtained from these 0.270-inch diameter rods. It is interesting to note that, at least for this and smaller diameter rods, the variation in transmitted power over the range of dc fields used was almost entirely due to the impedance mismatch seen at the input of the phase shifter. It can also be seen that for the maximum values of applied magnetic field, the magnitude of phase shift increased almost linearly with the length of the ferrite rod.

A conservative power rating for the ferrite rods used in the reciprocal phase shifter is 25 watts of average power. This maximum rating depends upon the rf losses in the ferrite and can be increased when better microwave ferrites become available. With presently available ferrites, it is believed that this power handling capability can be extended to 50 watts.

The cross-sectional views of an improved X-band phase shifter which resulted in better bandwidth characteristics and smaller variations in transmitted power with applied field are shown in Fig. 7. Tapered ferrite ends ($1\frac{1}{2}$ inches long) were used for impedance matching and a $\frac{13}{16}$ -inch polyfoam support was used to centrally locate either a round or square rod inside the rectangular waveguide section (0.40×0.90 inch id). The maximum useful cross section of the square rod was found to be 0.275 inch and that for the round rod was 0.300 inch, both giving approximately the same electrical characteristics. The longitudinally applied magnetic field was supplied by a low current solenoid wound around the waveguide section as previously described. End views of the phase shifter using either a round or square ferrite rod are shown at the right of the figure.

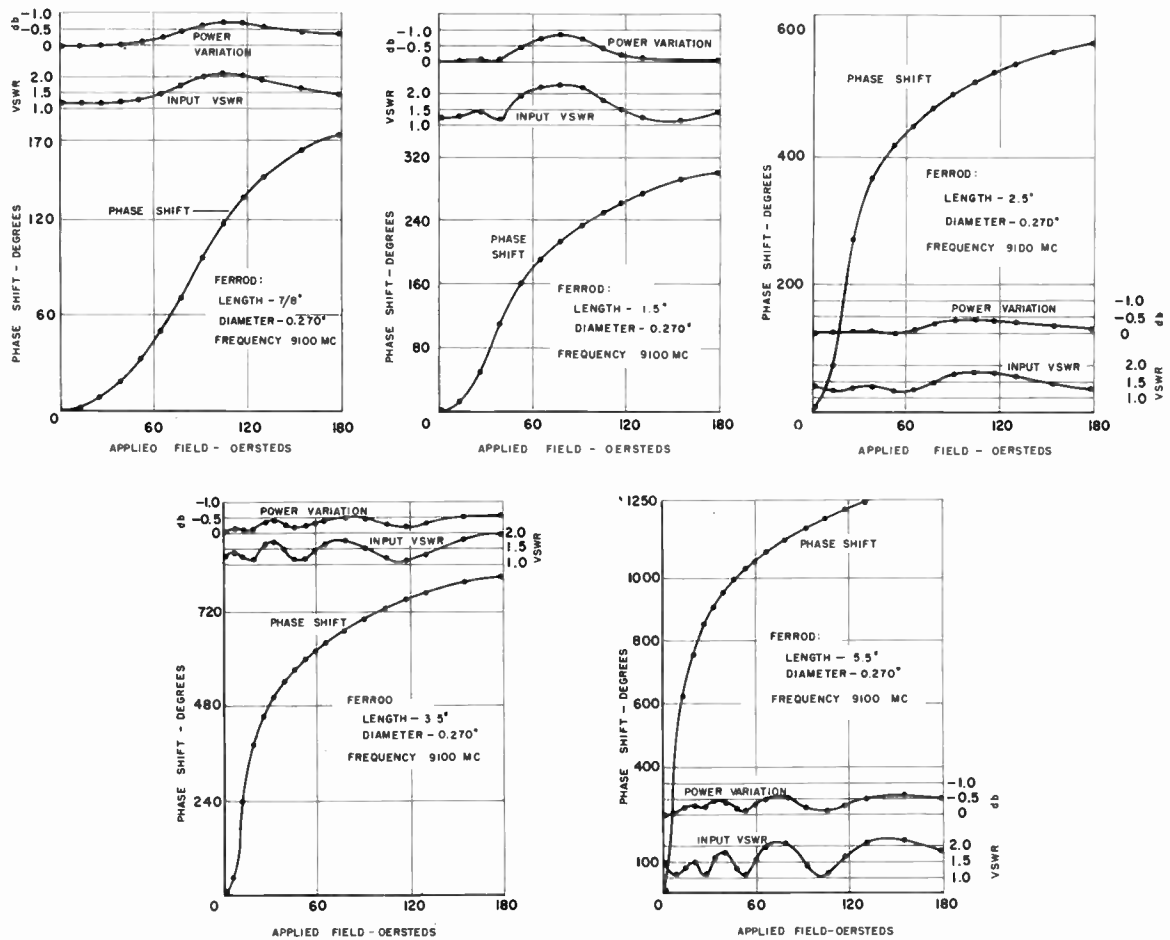


Fig. 6—Phase shifts, power variations, and changes in input vswr for several lengths of ferrite rods (0.27-inch diameter) vs applied dc magnetic field.

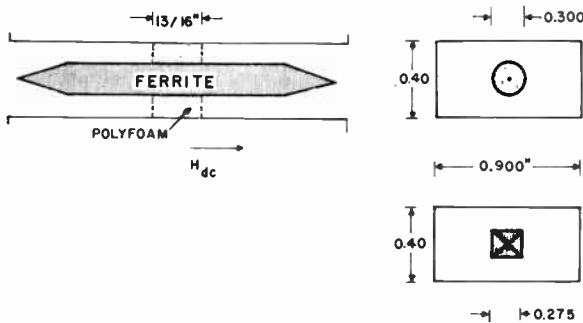


Fig. 7—Simplified sketch of an improved X-band phase shifter using tapered ferrite rods with circular and square cross sections.

The bandwidth characteristics for the improved phase shifter of the preceding figure are shown in Fig. 8. Phase shift and input vswr as a function of the applied magnetic field are given for three frequencies within a 500-mc bandwidth. Data taken at 9000 mc (not included) gave similar results to that shown in the figure. The round ferrite rod which was used to obtain the data had a diameter of 0.300 inch and the length of its tapered ends was 1 1/2 inches. The length of the untapered section at the center of the rod was 4 7/8 inches. Phase changes greater than 1200° with an applied field of approxi-

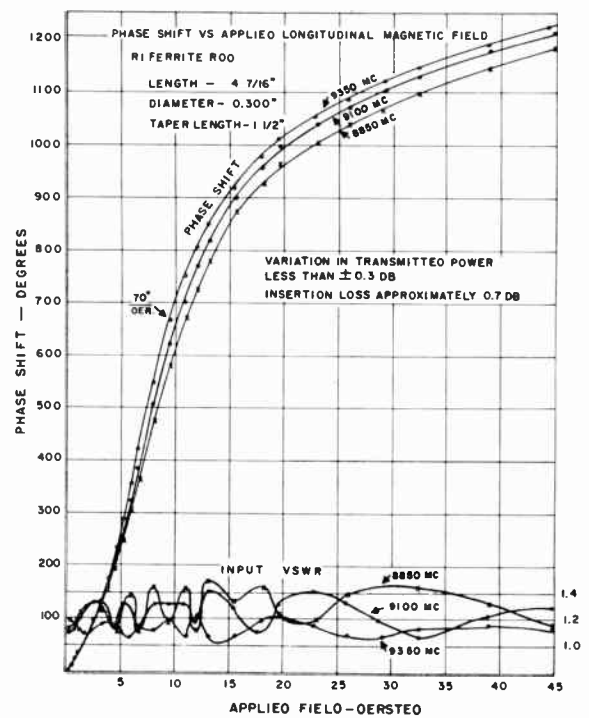


Fig. 8—Bandwidth characteristics of the improved ferrite phase shifter as a function of the applied magnetic field.

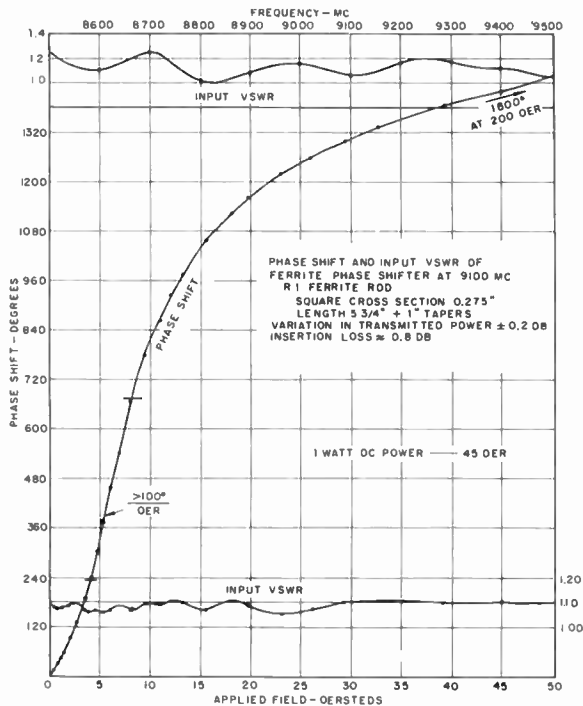


Fig. 9—Electrical characteristics of the reciprocal phase shifter using a square ferrite rod with a 0.275-inch cross section.

mately 45 oersteds and an input vswr of less than 1.5 were obtained over the bandwidth shown. The zero-field insertion loss for this rod was from 0.7 db to 0.8 db and the variations in transmitted power superimposed on this value was no greater than ±0.3 db. A reduction in the zero field insertion loss is possible when better ferrite materials become available. A slight increase in phase shift with frequency can also be seen from the curves. A dc power of one watt was required to obtain the 45-oersted field shown in the figure.

The electrical characteristics of the reciprocal phase shifter using a square ferrite rod with a 0.275-inch cross section and tapered ends one inch long are shown in Fig. 9. The length of the untapered section of this square rod was 5 3/4 inches long. The two lower curves show the input vswr and phase shift at 9100 mc as a function of the applied magnetic field. Phase changes greater than 1400° and an almost constant input vswr of 1.1 were obtained for this square rod with applied fields up to 50 oersteds. A sensitivity of greater than 100° per oersted was obtained in the region indicated by the figure. The upper curve shows the input vswr vs operating frequency with zero applied magnetic field to be no greater than 1.4. The zero-field insertion loss for the square rod was approximately 0.8 db and the variation in transmitted power with applied magnetic field was no greater than ±0.2 db. A dc power of one watt was required to obtain a field of 45 oersteds.

Another compact arrangement for obtaining a longitudinal magnetic field in the ferrite phase shifting element is shown in Fig. 10. This design is useful in conjunction with a linear array of radiators coupled from

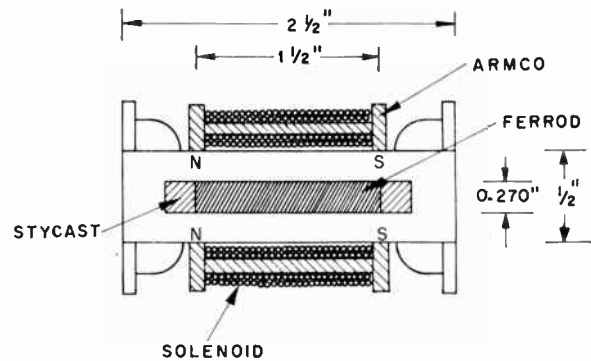


Fig. 10—Cross-sectional view of the ferrite phase shifter showing another arrangement for obtaining a longitudinal magnetic field in the ferrite rod.

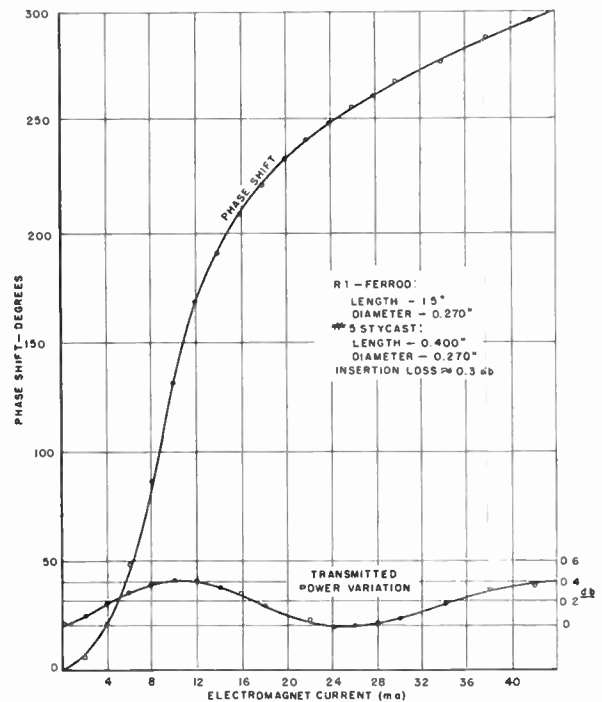


Fig. 11—Phase shift and variation in transmitted power at 9100 mc vs coil current (in milliamperes) of the small phase shifter shown in the preceding figure.

the narrow side of rectangular waveguide. Two commercially available low current solenoids,¹¹ 1 1/2 inches long, are used to supply the dc field. The directions of the dc field were such as to give opposing fields across the narrow side of the waveguide and adding fields parallel to the length of the rod. This type of construction is preferable for applications requiring a small phase modulator to operate from a low current source (0–50 ma). The total length of the system was 2 1/2 inches.

Curves showing the phase shift and transmitted power variations for the above device vs the dc control current (in milliamperes) at 9100 mc are shown in Fig. 11. The 1 1/2-inch long ferrite phase shifting element had a diameter of 0.270 inch. Phase changes greater than 200°

¹¹ Sensitive plate circuit relay coils, Type LM-11, resistance of each winding is 2500 ohms.

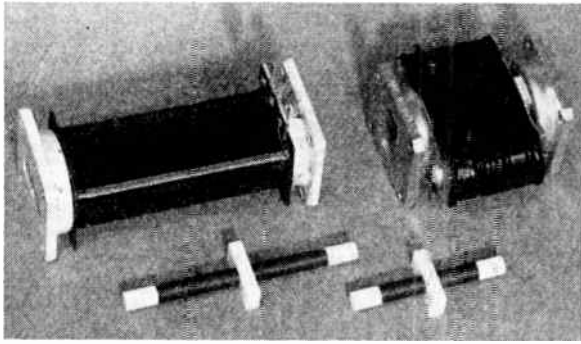


Fig. 12—Photograph showing the component parts of the two reciprocal phase shifters described in the preceding sections.

per inch were obtained, most of which occurred for control currents less than 25 ma. The transmitted power variations with applied magnetic field did not exceed 0.4 db over the range shown. The dimensions of the impedance matching elements are shown in the figure, along with the measured zero-field insertion loss of the phase shifter. These electrical characteristics make the device suitable in microwave systems requiring a physically small phase shifter for electrical switching, beam scanning, or changing the radiation pattern. Modulation frequencies in the kilocycle range have been used with the phase shifting system described above.

A photograph of the two reciprocal phase shifters described in Figs. 1 and 10 as well as their ferrite rods, teflon supports, and impedance matching tips is shown in Fig. 12. The phase shifter on the left has approximately 3000 turns of no. 28 wire wound around a 5-inch section of standard rectangular waveguide used at X band. The one on the right is $2\frac{1}{2}$ inches long and uses two low current (0–50 ma) solenoids for supplying the longitudinal magnetic field in the ferrite as shown diagrammatically in Fig. 10. The outside dimensions of the rectangular waveguide sections are $\frac{1}{2} \times 1$ inch.

REDISTRIBUTION OF MICROWAVE FIELD INSIDE WAVEGUIDE

In designing microwave devices such as rapid-scanning antennas, making use of the longitudinal-field phase shifting technique described above, it is necessary to evaluate the microwave field distribution inside the ferrite-loaded waveguide in order to determine its effect on the feed-point impedance of the radiating elements.

When a ferrite rod is centrally located inside a rectangular waveguide, an increase in the energy concentration occurs in this region.⁵ Although this redistribution of microwave energy is difficult to determine experimentally, some data have been obtained which indicate that it has shifted toward the center of the waveguide.

A curve showing the change of guide wavelength (λ_g) at 9100 mc vs the diameter of the ferrite rod used in the phase shifter with no applied magnetic field is shown in Fig. 13. This information was obtained by placing

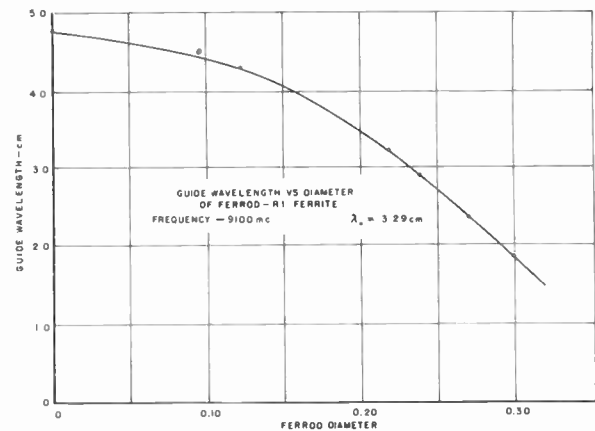


Fig. 13—Guide wavelength at 9100 mc as a function of the diameter of the ferrite rod centrally located inside a rectangular waveguide excited in its fundamental TE_{10} mode.

a polyfoam supported ferrite rod inside a rectangular waveguide slotted line terminated in a short circuit. The distance between two nodal positions was measured to determine the guide wavelength. Starting with λ_g equal to 4.75 cm for the empty waveguide, it is seen that little change in guide wavelength occurs for rod diameters up to approximately 0.15 inch. However, for diameters greater than this, a rapid decrease in λ_g occurs reaching a value of 1.86 cm for a rod diameter of 0.30 inch. These facts are important in designing long linear arrays making use of the phase shifting technique described above.

Sampling the rf power through a small hole in the narrow side of the ferrite-loaded waveguide has resulted in the data shown at the top of Fig. 14. Here it is seen that as the diameter of the ferrod inside the waveguide is increased above 0.20 inch, the rf power coupled from this wall begins to decrease rapidly. This redistribution of the microwave energy toward the center of the waveguide must be considered in the designing of beam scanning antennas with radiating elements excited from the narrow side of the waveguide.

Further data which give an indication of the increased rf energy concentration at the center of the ferrite-loaded waveguide and the physical arrangement used for the measurement are shown in the lower part of Fig. 14. A matched ferrite rod having a diameter of 0.275 inch and length of 4 inches was supported by a polyfoam dielectric and placed inside a long slotted waveguide which was terminated with a matched load (ml). A tuned rf probe was inserted at the top center of the waveguide and an indication of the electric field distribution along the length of the waveguide was obtained. An increase of electric field strength in the region of the rod is clearly shown.

Other data, not shown because it has not been fully evaluated, indicate that the field strength at the top center of the waveguide begins to increase as the diameter of the ferrod is increased to about 0.25 inch and then begins to decrease again as the rod diameter becomes greater than this value. This information was obtained

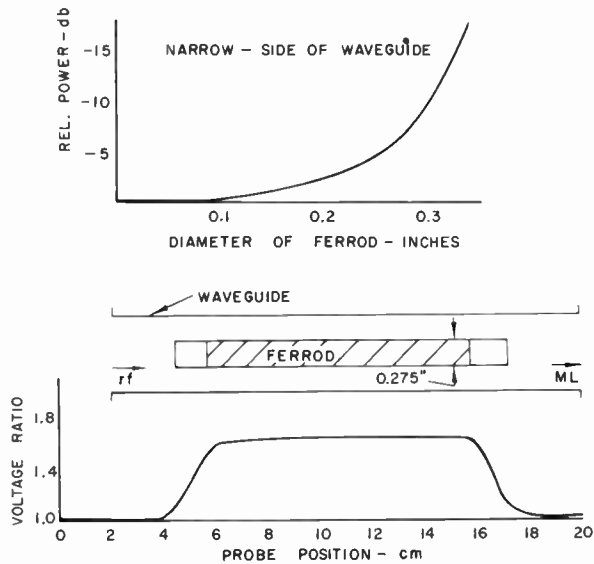


Fig. 14—Experimental data at 9100 mc indicating a redistribution of the microwave energy toward the center of the ferrite-loaded rectangular waveguide used as the reciprocal phase shifter.

by using a very short transverse slot at the top center of the waveguide.

ANTENNA BEAM SCANNING

The design of a relatively small antenna system for beam scanning microwave energy by electrical means has been the goal of microwave system engineers for many years.^{12,13} Numerous attempts^{14,15} have been made to use transverse magnetic fields with various configurations of ferrites in rectangular waveguides making up antenna arrays. However, because of the large magnetic fields required to obtain the necessary phase shifting per unit length, no practical systems have been reported. Small variations in transmitted power during the phase shifting and low insertion losses are also important in the beam scanning antenna design.

Using the longitudinal-field phase shifting technique described in the preceding sections, several types of radiating structures have been designed for antenna beam scanning. One arrangement made use of two open-end rectangular waveguide sections as radiating elements, their centers placed 2 inches apart, and the phase shifter of Figs. 10 and 12 was used in one arm to provide the necessary phase shift of the microwave energy. Although the side lobe amplitudes obtained with this arrangement were large, a beam scan of 22° and a deterioration of the main beam amplitude no

¹² H. N. Chait and N. G. Sakiotis, "Ferrites at Microwaves," *Proc. Fourth Symposium on Scanning Antennas*, NRL Rep. 4000, pp. 123-131; April, 1952.

¹³ F. Reggia, E. G. Spencer, R. D. Hatcher, and J. E. Tompkins, "Ferrod radiator systems," *PROC. IRE*, vol. 45, pp. 344-352; March, 1957.

¹⁴ D. J. Angelakos and M. M. Korman, "Radiation from ferrite-filled apertures," *PROC. IRE*, vol. 44, pp. 1463-1468; October, 1956.

¹⁵ M. S. Wheeler, "Non-mechanical beam steering by scattering from ferrites," presented at Symposium on Microwave Ferrites and Devices and Applications, New York, N. Y.; May, 1957.

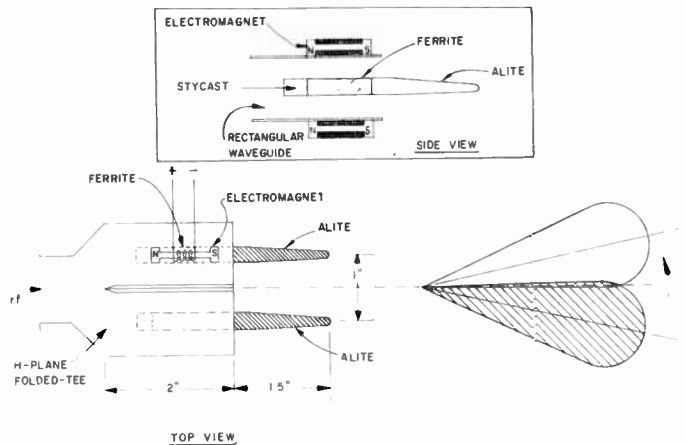


Fig. 15—Schematic diagram of a simple beam scanning antenna system making use of the new phase shifting technique described in the preceding sections.

greater than ± 0.5 db were obtained. A dc control current of less than 15 ma was used to obtain this beam scanning angle. The electrical characteristics of the phase shifter used for these measurements at 9100 mc are shown in Fig. 11.

Another arrangement made use of two open-end rectangular waveguide sections, centers one inch apart, and a one-inch length of ferrite rod (0.270-inch diameter) in one arm to obtain the necessary phase shift. The longitudinal magnetic field applied to the ferrite was supplied by two series-connected low current solenoids¹⁶ used in a manner similar to that shown in Fig. 10. As much as 20° beam scanning was obtained with this arrangement with relatively constant power (± 0.2 db) radiated in the main beam. Larger scan angles of 30° and 40° have been obtained with variations in main beam amplitude no greater than ± 1 db and ± 2 db, respectively.

The same technique described above but with short dielectric radiators coupled from the open ends of a broad-band *H*-plane folded tee was used and reasonably good results were obtained. A simplified sketch of this beam scanning antenna system is shown in Fig. 15. Two tapered dielectric radiators,¹⁷ spaced one inch apart, were used to reduce the side-lobe amplitudes and to give a somewhat narrower beam than that obtained from the open-end waveguide sections. The beam width of a single element was approximately 55° and that of the two rods together was 32°. A ferrite rod, one inch long and 0.270-inch diameter, preceded one of the radiators to provide the phase shifting necessary for beam scanning. The two series connected low current solenoids were used to provide the longitudinal magnetic field as shown in the figure.

With no dc field applied to the ferrite phase shifting element, the coupling length of one radiator was ad-

¹⁶ Plate circuit relay coils, Type LP-5, resistance of each winding is 5000 ohms.

¹⁷ Alite No. AE-212, dielectric constant of 8.5 and loss tangent of 0.0008 at 10,000 mc.

justed to give maximum radiation of the main beam off to the right as shown. Application of the longitudinal control field to the ferrite causes a delay in the microwave energy in this arm which in turn causes the main beam to move to the left. A beam scan of 22° with relatively constant power radiated in the main beam was obtained with control currents no greater than 30 ma. The side-lobe amplitude remained at least 10 db below that of the main beam throughout the scanning range.

A simplified diagram showing an extension of the phase shifting technique described above to beam scanning of long linear arrays excited from a rectangular waveguide section is shown in Fig. 16. Polyfoam dielectric or its equivalent is used to locate centrally the ferrite phase shifting elements, both of which are made up in convenient lengths and joined together with little discontinuity. The radiating elements can be either narrow slots or dielectric rods and the impedance matching element is similar to that previously described. The direction of maximum radiation of the fan-shaped beam depends upon the guide wavelength (λ_g) which decreases when a longitudinal magnetic field is applied to the ferrite phase shifting element. This change in the ferrite magnetization produces a phase shift which introduces a progressive delay in the wavefront down the waveguide, thus causing the radiated wavefront to sweep over the scanning sector.

Several methods have been tried in order to obtain a uniform longitudinal magnetic field over the path length

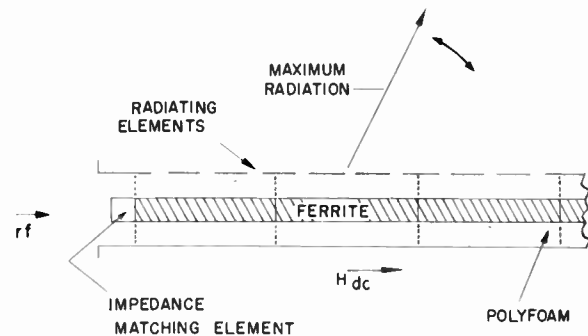


Fig. 16—Cross-sectional view of a long linear array excited from a rectangular waveguide and making use of the new phase shifting technique.

required for long linear arrays. Various types of radiating structures were also designed for scanning narrow fan-shaped beams. These devices, the results obtained, and the optimum configuration of the ferrite phase shifting element that can be used in long linear arrays will be reported at a later date.

ACKNOWLEDGMENT

The authors wish to thank R. D. Hatcher, R. C. LeCraw, and J. E. Tompkins for their helpful suggestions and discussions, and J. M. DeLawter of the DOFL Development Shop for preparation of various components of the phase shifter and antenna beam scanning systems.

Slalom Focusing*

J. S. COOK†, ASSOCIATE MEMBER, IRE, R. KOMPFFNER‡, FELLOW, IRE,
AND W. H. YOCOM‡, ASSOCIATE MEMBER, IRE

Summary—In the search for a scheme of electron focusing which would permit a beam to weave in and out through an rf structure, it was discovered that a linear array of line charges in free space produces two equipotential surfaces which contain exact electron trajectories. The field about such an array may be nearly duplicated by an array of positive wires sandwiched between two negative plates. It has been found that such a structure will effectively focus a ribbon type electron beam of surprisingly high perveance.

A backward-wave oscillator was built which utilized this "slalom" type focusing.¹ Although this tube was of the rough, experimental variety, oscillations were obtained throughout the range of 3.3 to 4.3 mc.

* Original manuscript received by the IRE, July 11, 1957; revised manuscript received, August 30, 1957.

† Bell Telephone Labs., Inc., Murray Hill, N. J.

‡ Varian Associates, Palo Alto, Calif. Formerly with Bell Telephone Labs., Inc., Murray Hill, N. J.

¹ The term "slalom" is borrowed from the Norwegian downhill ski race known by that name.

A beam tester was constructed which has a beam-focusing structure just ten times the size of that of the oscillator's. Ninety-seven per cent transmission through 27 wires of a beam of perveance (2×10^{-6}) has been achieved with this tester.

Slalom focusing may also find application in the field of switching.

INTRODUCTION

MANY structures, used as circuits in traveling-wave and backward-wave tubes, consist of arrays of conductors to which the rf wave is so tightly bound that only the fringe of the rf field is accessible for interaction with the usual straight electron beam. Since this field diminishes exponentially with distance from the circuit, the beam must be placed as close to the structure as possible. On the other hand, the boundary of an electron beam is inevitably some-

what diffuse so that if the beam is placed too close to the circuit some of it will be intercepted. There is a minimum practical spacing, then, between the useful beam and its adjacent circuit. The necessarily small separation between beam and circuit poses a serious problem at higher frequencies.

In addition, there is the problem of providing high current density within interaction distance of the circuit. There are several disadvantages in using high voltages; at limited voltage, high current flowing through a small cross section implies large space charge forces, which, in turn, call for strong focusing forces. Means for providing a strong magnetic focusing field add weight, sometimes a great deal, to the tube or its mount. Previous proposed types of electrostatic focusing, on the other hand, have not been entirely satisfactory, mainly because they called for high electric fields between adjacent electrodes.

These facts have led the authors to consider a new electrostatic focusing scheme in which a sheet electron beam is made to weave sinusoidally through an array of positive rods or wires placed midway between two negative plates, as shown in Fig. 1. These wires also may constitute a slow wave rf transmission line. Thus, one might hope to hold together a dense stream of electrons against the action of space charge forces, and at the same time have the electrons actually interlacing the slow wave circuit in a region where the rf field is very strong.

Consider a linear array of positive line charges in free space which are assumed to be of infinite extent normal to the page. Such an array, with the appropriate equipotential surfaces, is shown in Fig. 2. In particular, notice the two equipotential surfaces which intersect at the midpoint between the wires. It can be shown that if an electron has just the right velocity and disposition it will exactly follow one of these equipotential surfaces, winding a sinuous path in and out among the line charges.

For the array in Fig. 2 the potential at any point (x, y) may be expressed as

$$V(x, y) = V_0 \left[1 - \frac{1}{2} \ln \frac{1}{2} \left(\cosh \frac{2\pi y}{a} - \cos \frac{2\pi x}{a} \right) \right] \quad (1)$$

where V_0 is the potential at the "crossover" point midway between the line charges, and "a" is the distance between line charges. The "crossover equipotential," is defined as the locus of points where $V(x, y) = V_0$, which requires that

$$\cosh \frac{2\pi y}{a} - \cos \frac{2\pi x}{a} = 2$$

or

$$\cos \frac{\pi x}{a} = \sinh \frac{\pi y}{a} \quad (2)$$

The electrostatic force on an electron moving along the crossover equipotential is

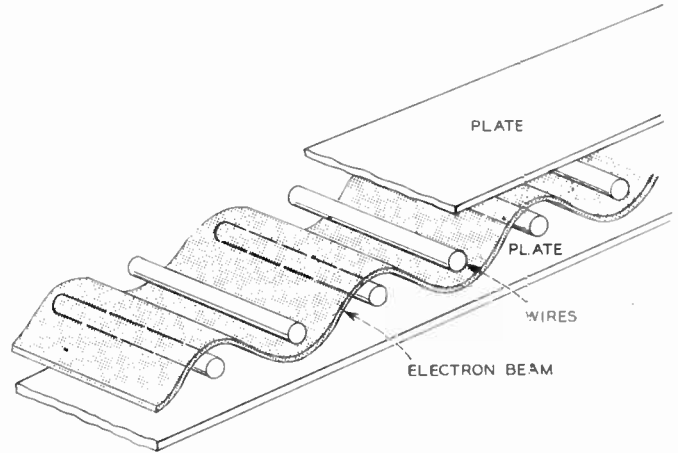


Fig. 1—Slalom structure showing sinuous sheet electron beam.

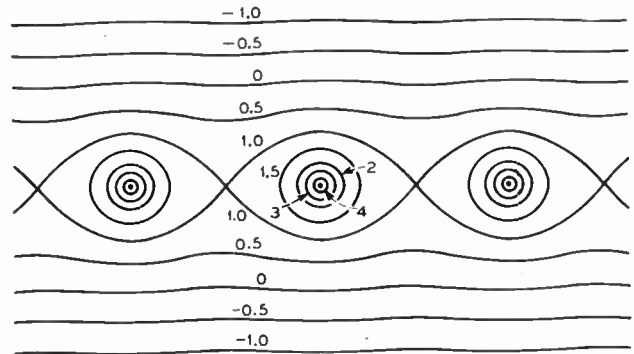


Fig. 2—Equipotentials about an infinite linear array of infinite line charges.

$$eE(x, y) = \mp e \left[\left(\frac{\partial V}{\partial x} \right)^2 + \left(\frac{\partial V}{\partial y} \right)^2 \right]^{1/2}$$

which with (1) and (2) becomes

$$eE(x, y) = \frac{\mp \pi \sqrt{2}}{a} eV_0 \cos \frac{\pi x}{a} \quad (3)$$

The centrifugal force on an electron following the same equipotential is

$$\frac{mv^2}{\rho} = \frac{mv^2 \left(\pm \frac{d^2y}{dx^2} \right)}{\left[1 + \left(\frac{dy}{dx} \right)^2 \right]^{3/2}}$$

where ρ is the radius of curvature of the trajectory. From (2) this becomes

$$\frac{mv^2}{\rho} = \pm mv^2 \cdot \frac{\pi}{\sqrt{2}a} \cos \frac{\pi x}{a} \quad (4)$$

If the crossover equipotential is to be an electron trajectory, the centrifugal and electrostatic forces must be equal in magnitude, and oppositely directed. Equating (3) and (4) this condition is satisfied when

* K. R. Spangenberg, "Vacuum Tubes," McGraw-Hill Book Co., Inc., New York, N. Y., p. 126; 1948.

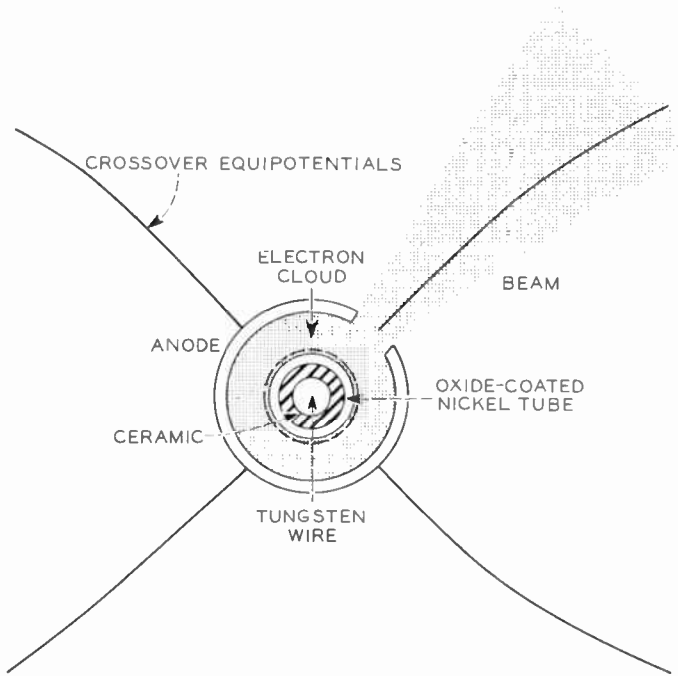


Fig. 3—Internal injection gun used in early experiments.

$$v^2 = 2 \frac{e}{m} V_0. \tag{5}$$

This means that if an electron is injected along the path determined by (2) with a velocity given by (5), it will continue along that path indefinitely.

Observe Fig. 2. Notice that the crossover equipotentials, in effect, cross each other at an angle of 90°. The field strength at these crossover points is zero, and in the immediate vicinity the field strength is very small. Hence, an extra electrode placed there with an applied potential equal to that of the crossover potential will create little disturbance.

Note also, that the equipotentials in the region of the line charges rapidly become circular as their potentials increase. Therefore, replacing the line charges with small circular cylinders, or wires, will cause little change in the field distribution. Furthermore, the equipotentials flatten out as they get farther away from the wire array, and placing perfectly flat plates at the position of the (-0.5 V₀) equipotential should create very little disturbance in the assumed field distribution.

Altogether, it is indeed surprising that a field distribution describable by simple analytic functions, that can be easily generated using only round wires and flat plates includes singular sinuous equipotentials which are also exact electron trajectories.

LAUNCHING THE BEAM

There are several methods by which an electron beam might be launched along the crossover equipotential in such a "slalom" structure. These methods can be divided into two classes; internal and external. Internal injection shall be defined as any scheme where the

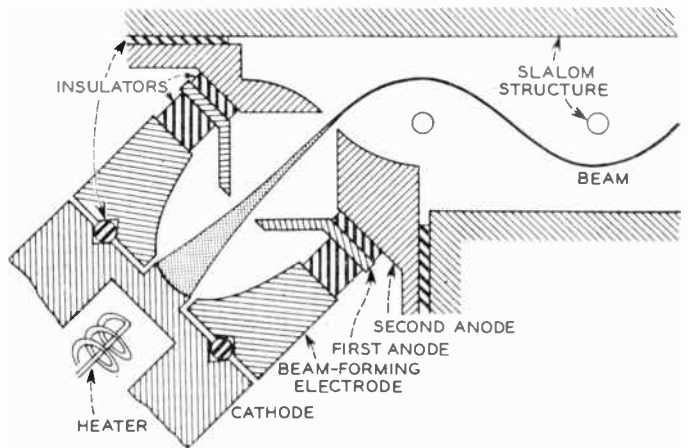


Fig. 4—Improved internal injection gun.

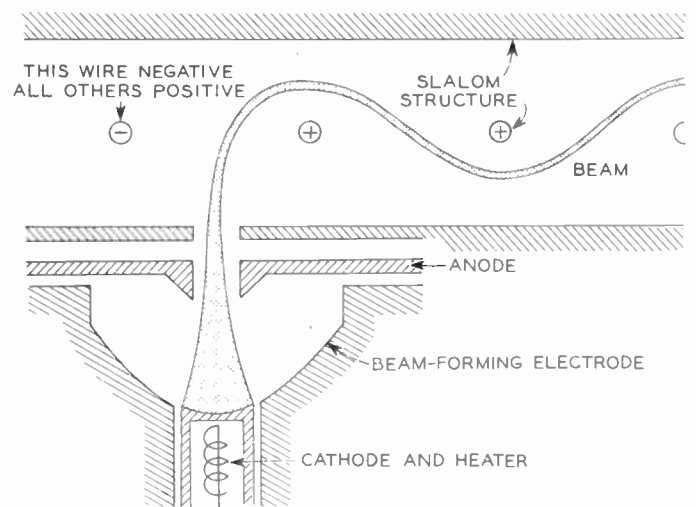


Fig. 5—A simple external injection gun.

beam originates between the planes of the plates.

The first slalom experiments used the internal injection method shown in Fig. 3.

This type of gun has several shortcomings, however, due to the fact that it is confined within a small cylinder. A search for something better led to the configuration shown in Fig. 4. In this gun, the anode surface follows the surface of the crossover equipotential so that the slalom field is not distorted as long as the anode is operated at crossover potential. This provides a means for internal injection where the electron gun is no longer confined. One can use a "Pierce" type or any other type gun of any perveance or dimensions desired. It is this configuration that was used in the first slalom oscillator and in most of the later beam testers.

A third configuration, which is an external injection scheme, is shown in Fig. 5. A possible advantage of such a gun is the simpler anode structure which lends itself to scaling down more readily than the internal gun. The removal of the gun from the region of the rf circuit is a further advantage. One disadvantage is that it must be designed and positioned in an empirical manner since the beam is not launched along the regular slalom path and

the fields about the point of injection are anything but simple. In addition, the beam must pass through the plates, which must operate at a low positive if not negative potential with respect to the cathode; thus an optical problem is introduced. Nevertheless, such a gun can be made to work, as has been shown experimentally.

SLALOM OSCILLATOR

Though early beam testers did not prove that the beam was stable, they did show that a certain amount of current could be made to slalom through several wires to a collector. On the assumption that a slalom beam could be stable, and in order to test the compatibility of slalom-focusing and rf interaction, a backward-wave oscillator using this new focusing principle was built. The helix, rather than an interdigital or folded line, was chosen as the wave retarding circuit because it appeared to give the greatest spacing between wires for the fundamental phase velocity; promised of a simple input and output match; and presented the best hope of calculating the impedance. Because of the measuring equipment available, 4000 mc was chosen as the operating frequency.

The helix was flattened into an oval cross section, and so wound that all the "skew" part of the winding was on one side, the turns on the other being normal to the helix axis. The latter were used as the slalom structure (Fig. 6).

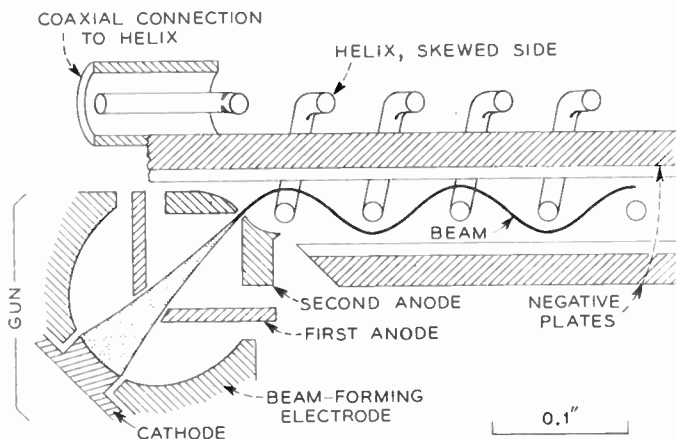


Fig. 6—Section of gun end of experimental slalom oscillator.

The actual helix had an effective

$$ka = \left(\frac{\text{helix turn length}}{\lambda_0} \right) = 0.4,$$

the wire diameter was 0.020 inch and the pitch was 0.080 inch. At 4 kmc this results in a fundamental phase velocity of $c/15$ and a backward harmonic phase velocity ($n = -1$) of $c/-22.5$. These are the values in the axial direction and they must be multiplied by 1.18 to account for the fact that the slalom path is not straight. This gives a 1560-volt beam for fundamental operation, and a 700-volt beam for backward-wave interaction.

The gun was of the internal injection type and pro-

jected a beam into the circuit at an angle of 45° with the axis. It was designed to give 21 ma at 700 volts. Inasmuch as the electrons would be in a region of appreciable rf field only about one-half the time, and because of the angle of 45° between the beam and the field, the impedance of the helix was estimated to be about one-fourth its free space value of $30/k\bar{a}$, or about 19 ohms. Thus, Pierce's coupling factor C is 0.04; and, since CN should be about 1.5 for reasonable output and efficiency, this gives $N_{-1} = 37.5$, and an active length of five inches. The tube was made approximately seven inches long for safety.

At first, flattened coupling helices were considered for input and output, but simple coaxial connections were finally used and proved to be adequate, although a fairly poor match. After various mechanical difficulties were overcome it was possible to get a maximum of 1.5 ma out of about 10 ma through the circuit to the collector. Under these circumstances backward-wave oscillations were observed in the range from 3.3 to 4.3 kmc, and were voltage-tunable throughout the range. Oscillations could not be sustained for any great period of time due to the large amount of current being intercepted on the first two or three wires. The hot wires buckled and intercepted increasing amounts of current until the beam was cut off.

In spite of poor transmission and the relatively poor rf results, the experiment was valuable in showing that rf interaction can be obtained between a slalom beam and its focusing structure.

LARGE SLALOM TESTER

The amount of transmitted current in the slalom oscillator was disappointing. Since reasonable care had been taken in the physical design and construction of the tube it was felt that structural errors could not entirely account for the focusing difficulty. It was evident that at least part of the trouble lay somewhere in the beam injection conditions. The small size of the oscillator, and the fact that it was sealed off, seriously limited the possibility of making controlled experiments with it; so a demountable version of the slalom structure and gun was constructed ten times as large. The gun was arranged so that the angle at which the beam was launched could be mechanically adjusted through several degrees.

From this tester it was found that the optimum angle for launching the beam was not 45° from the plane of the line charges, as originally anticipated, but more nearly 35° . Moreover, better than 97 per cent transmission of the beam was obtained over the tester length of 27 wires.

The maximum current density, or perveance, obtained was surprisingly large. The perveance for slalom tubes may be defined as

$$p = \frac{I_c}{V_0^{3/2}} \quad (6)$$

where I_c is the collector, or transmitted, current in amperes and V_0 is the crossover potential in volts. In the transmission tests reported here the wires were maintained at 600 volts to provide a crossover potential of about 265 volts. Maximum transmission could be obtained for a collector current as high as 8.7 ma or

$$p = \frac{8.7 \times 10^{-3}}{(265)^{3/2}} = 2 \times 10^{-6}.$$

At 18 ma collector current the transmission was about 92 per cent and perveance about 4.2×10^{-6} . The highest perveance obtained (with a wire potential of 150 volts) was 12.7×10^{-6} with a little less than 48 per cent transmission. Since scaling does not affect the perveance, if $V_0 = 700$ volts, a current of about 40 ma could have been passed through the slalom oscillator with less than 1.5 ma interception on the wires;—provided the structure had been perfectly aligned and the gun properly designed.

It was also learned from the tester that turning down the edges of the side plates to form "edge-hats" as shown in Fig. 7 is a very effective way to contain a slalom beam of finite width.

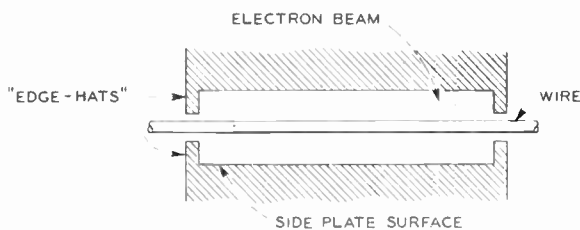


Fig. 7—Cross section of slalom structure illustrating the use of "edge-hats" to prevent the beam from spreading sideways.

It should be added here that computations have shown that stable slalom trajectories do exist, although the crossover equipotential trajectory is "astable," *i.e.* on the limit of stability, hence, not stable. The optimum launching conditions and maximum perveance for a stable slalom beam have been computed in some detail, and checked experimentally.³

EXTERNAL INJECTION

The external method of beam injection was shown in Fig. 5. In the only case of external injection studied, the gun was mechanically over-simple. A flat strip cathode, beam forming electrode, and anode were mounted outside one side plate in which a slit had been cut to allow entry of the beam. The beam entered the slalom structure approximately at the midpoint between the first and second wires, and was deflected down the structure by operating the first wire at some appropriate negative potential.

By operating the beam forming electrode negative

³ A paper on this subject by J. S. Cook, W. H. Louisell, and W. H. Yocom, has been submitted for publication in *J. Appl. Phys.*

with respect to the cathode it was possible to get 0.55 ma to the collector out of 0.57 ma total current passing through the anode slit, or 96 per cent transmission, at a beam voltage of about 400 volts. The slalom electrode voltages under the above conditions were within a few per cent of what one would calculate from the geometry of the structure.

When the tube was dismantled the ceramic supports had a sinuous brown stain winding in and out between the holes which had mounted the rods. The stain line crossed the axis of symmetry at an angle of about 35° instead of 45° as had been anticipated. This stain (the result of organic deposits on the charged portions of the ceramic) further corroborates what is now known about the nature of the stable electron paths. Fig. 8 is a photograph of the ceramic support.

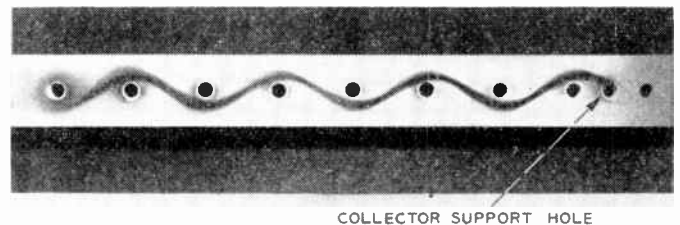


Fig. 8—Ceramic slalom wire support stained where electrons caused surface charge during external injection experiment.

DISCUSSION

The basic soundness of the principle of slalom focusing has been demonstrated:

- 1) A slalom backward-wave oscillator has been made to operate over a 20 per cent bandwidth, thus demonstrating the ability of the beam to interact with its focusing circuit.
- 2) Computer calculations for the launching conditions required to produce a stable slalom beam have been substantiated by experiments with an actual slalom electron beam.

There is, of course, a great deal yet to be learned; but some insight as to the character and possibilities of slalom focusing has already been gained. At first it was hoped that a slalom arrangement might lead to greatly increased interaction between the electron beam and rf circuit. Closer inspection has dampened this hope. Rough calculation indicates that the effective longitudinal coupling between a circuit and a slalom beam is actually somewhat less than that using a straight grazing beam. What effect any transverse field interaction may have on a slalom beam is still a matter of speculation. Thus, the over-all gain per unit length of a slalom amplifier may be no better and no worse than that of a comparable traveling-wave tube using the more usual straight beam.

Perhaps the most persuasive argument in favor of slalom focusing is its ability to focus very high perveance beams electrostatically, as demonstrated in the large

slalom tester. This perveance compares with the best periodic magnetic focusing schemes.

There are several varieties of slow wave circuit that lend themselves to slalom focusing. Of primary interest are the squashed helix, serpentine or zigzag line,⁴ and the various modified easitron type circuits.^{5,6}

How high a frequency one can obtain using slalom focusing is still a question. If one considers employing only the fundamental mode of propagation the slalom circuit is already very small at *x*-band. This difficulty can be overcome partially by using oversize circuits and allowing the beam to interact with higher order modes or space harmonics. Although their use cuts down the gain per unit length available, the simplicity of the electrostatic focusing readily permits the building of tubes indefinitely long.

This paper has discussed only one general aspect of slalom focusing; namely, its possibilities in connection with traveling-wave tubes. Slalom beams may also find application in the field of switching. If anyone of the center wires in the linear array is driven negative the beam will not go past it as usual, but will shoot off toward one of the side plates instead. Where along the

⁴ A. Leblond, and G. Mourier, "Étude des lignes à barreaux à structure périodique," *Ann. Radioléc.*, vol. 9, pp. 311-328; October, 1954.

⁵ J. R. Pierce, "Traveling-Wave Tubes," D. Van Nostrand Co., Inc., New York, N. Y., p. 90; 1950.

⁶ A. Karp, "Traveling-wave tube experiments at millimeter wavelengths with a new space harmonic circuit," *Proc. IRE*, vol. 43, pp. 41-46; January, 1955.

array the beam will shoot off will be determined simply by which wire is made negative. Thus, a high-perveance, well-focused beam may be switched by changing the potential of an electrode which draws very little current.

Yet another possible application of slalom focusing, takes the form of a short interval storage device. It has been observed that, if one of the wires in an array is made negative enough, a slalom beam may actually be made to double back along the circuit, following the alternate stable path. If at a given instant a train of electron bunches is traveling along the circuit and one wire somewhere ahead of it and one somewhere behind it are driven to the proper negative potential, the train of bunches will slalom back and forth between these negative wires until they are released in one direction or the other by allowing the negative wires to assume, once more, their proper positive potential. The possible storage time would be limited, of course, by collisions between the electrons and the residual gas molecules, and possibly by effects due to their own space charge.

ACKNOWLEDGMENT

The authors wish to thank Dr. W. H. Louisell for his mathematical assistance, and G. E. Helmke, E. J. Flannery and D. O. Williams, for their able assistance in designing and building the oscillators and testers for the project.

Biperiodic Electrostatic Focusing for High-Density Electron Beams*

KERN K. N. CHANG†

Summary—A focusing scheme employing two counteracting periodic fields without the use of any magnet is shown to be superior to schemes which involve only one periodic focusing field. The potential valley formed by the combination of these two counteracting fields is steeper than all previous focusing systems and thus is capable of maintaining a very stable beam flow. The combined field also gives rise to proper cancellation of the space charge field. This field cancellation not only results in an ideal focusing for high-density beam but also compensates for the potential depression inside the beam.

With a periodic voltage variation of 5 per cent on the beam, it is theoretically possible to focus with an ideal gun, an electron beam of perveance in the order of 10^{-6} amp/volt^{3/2}. With a nonoptimized gun, a beam of perveance 2×10^{-6} amp/volt^{3/2} has been focused to a 97 per cent current transmission. A 10-db rf gain was observed at a frequency of 2950 mc.

* Original manuscript received by the IRE, May 23, 1957; revised manuscript received, July 3, 1957.

† RCA Laboratories, Princeton, N. J.

INTRODUCTION

THE development¹⁻³ of beam focusing by periodic electrostatic fields has offered the possibility of a light-weight focusing system that may result in a major simplification of traveling-wave tubes. From the point of view of stability in the beam flow, periodic electrostatic fields of very short periods³ also give a

¹ P. K. Tien, "Focusing of a long cylindrical electron stream by means of periodic electrostatic fields," *J. Appl. Phys.*, vol. 25, pp. 1281-1288; October, 1954.

² R. Adler, O. M. Kromhout, and P. A. Clavier, "Resonant behavior of electron beams in periodically focused tubes for transverse signal fields," *Proc. IRE*, vol. 43, pp. 339-341; March, 1955. Also, "Transverse-field traveling-wave tubes with periodic electrostatic focusing," *Proc. IRE*, vol. 44, pp. 82-89; January, 1956.

³ K. K. N. Chang, "Confined electron flow in periodic electrostatic fields of very long short periods" *Proc. IRE*, vol. 45, pp. 66-73; January, 1957.

focusing superior to those of comparatively long periods. While promising results³ have been obtained in such focusing systems with thin electron beams of low perveance, no attempts have been made with those focusing systems on thick beams of high perveance. The reason is that, because of the initial thermal velocity, the space charge force which is to be balanced by the focusing force becomes more complicated and uncontrollable as the current density in the beam becomes larger. If the focusing system is of the "confined-flow" type, where the space charge force is relatively small compared with the external focusing force, a tremendous applied balancing force is required for high-density beams. The attainment of this balancing force will complicate the focusing scheme, and sometimes is not practical. Above all, the most serious drawback of the previous focusing systems in using short-period electrostatic fields is the limitation on the beam size to very thin dimensions. For thick electron beams, special provisions such as a specified nonuniform space charge distribution¹ must be made in order to maintain a proper force balance in the beam. These provisions usually offset the simplicity of using the periodic electrostatic field as the focusing means.

The following presentation will discuss a new focusing method which, while retaining the feature of simplicity possessed by electrostatically focused tubes, offers an additional merit of focusing a thick beam of high current density without any special provision. The method essentially adopts a periodic scheme formed by two non-coplanar periodic structures which are characterized by extremely short periods. Between these two structures, an exponential field is formed that varies in an opposite sense around a "null" or zero-field plane. The variation of this exponential field, which happens to be opposed to that of the space charge field, can be approximated to balance the same space charge field within the beam.

A similar biperiodic field of very long period was used on transverse-field tubes.² The periodic focusing scheme on those particular tubes, however, has its use limited to very thin beams with long-period fields. Since a periodic field of long periods yields a slowly varying force function instead of an exponential one, this particular biperiodic focusing scheme results in a poor stability in the beam flow and thus rules out its use on high-density electron beams.

FOCUSING MODEL

The focusing model to be investigated is shown in Fig. 1. For analysis, a model of cylindrical geometry (r, z) has been chosen with two coaxial periodic ring structures of radii r_1 and r_2 and of periods L_1 and L_2 . Suppose a potential difference $2V_1$ is applied to each adjacent pair of rings on the inner structure with an average potential V_0 ; and a potential difference $2V_2$, on the outer structure with the same average potential V_0 . The potential $V(r, z)$ between the two structures can be

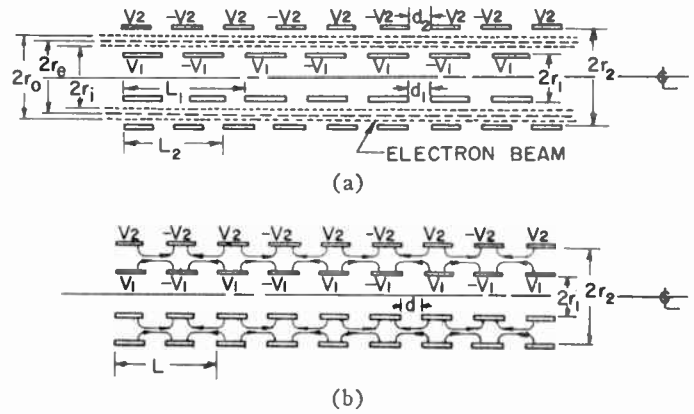


Fig. 1—(a) Biperiodic structures of unequal periods. (b) Biperiodic structure of equal periods.

approximately expressed as follows:^{4,5}

$$V(r, z) \cong V_0 + \hat{V}_1(r) \cos\left(\frac{2\pi}{L_1} z\right) + \hat{V}_2(r) \cos\left(\frac{2\pi}{L_2} z\right)$$

$$V_0 \gg \hat{V}_1(r), V_0 \gg \hat{V}_2(r) \quad (1)$$

$$\hat{V}_1(r) = 4V_1 \frac{\sin \sigma_1 \pi}{\sigma_1 \pi^2}$$

$$\frac{I_0\left(\frac{2\pi}{L_1} r\right) K_0\left(\frac{2\pi}{L_1} r_2\right) - I_0\left(\frac{2\pi}{L_1} r_2\right) K_0\left(\frac{2\pi}{L_1} r\right)}{I_0\left(\frac{2\pi}{L_1} r_1\right) K_0\left(\frac{2\pi}{L_1} r_2\right) - I_0\left(\frac{2\pi}{L_1} r_2\right) K_0\left(\frac{2\pi}{L_1} r_1\right)} \quad (2)$$

$$\hat{V}_2(r) = 4V_2 \frac{\sin \sigma_2 \pi}{\sigma_2 \pi^2}$$

$$\frac{I_0\left(\frac{2\pi}{L_2} r\right) K_0\left(\frac{2\pi}{L_2} r_1\right) - I_0\left(\frac{2\pi}{L_2} r_1\right) K_0\left(\frac{2\pi}{L_2} r\right)}{I_0\left(\frac{2\pi}{L_2} r_2\right) K_0\left(\frac{2\pi}{L_2} r_1\right) - I_0\left(\frac{2\pi}{L_2} r_1\right) K_0\left(\frac{2\pi}{L_2} r_2\right)} \quad (3)$$

$$\sigma_1 = \frac{d_1}{L_1} \quad (4)$$

$$\sigma_2 = \frac{d_2}{L_2} \quad (5)$$

I_0 and K_0 are the modified Bessel functions. A ring-type cylindrical beam of radii r_0 and r_i constrained between the two structures is illustrated in the model being investigated. The electron motions in the electrostatic field produced by the periodic structures follow the equations³

$$\ddot{r} - \eta \frac{\partial V}{\partial r} = \frac{\eta^2}{4} B_0^2 \frac{r_0^2}{r} \quad (6)$$

$$\ddot{z} = \eta \frac{\partial V}{\partial z} \quad (7)$$

⁴ E. Weber, "Electromagnetic Fields," John Wiley and Sons, Inc., New York, N. Y., vol. 1, pp. 458-461; 1950.

⁵ K. K. N. Chang, "Optimum design of periodic magnet structures for electron beam focusing," *RCA Rev.*, vol. 16, pp. 65-81; March, 1955.

Here dots denote the derivatives with respect to time, η is the ratio of electron charge to mass, and B_b is the equivalent Brillouin field which represents the space charge field at an outer radius r with an outer beam current I_0 which is, as defined in the Appendix, the part of the beam current outside the "null" field radius where the space charge field is zero.

In mks units

$$B_b^2 = 0.69 \times 10^{-6} \frac{I_0}{V^{1/2} r_0^2} \frac{r^2 - r_e^2}{r_0^2 - r_e^2}. \quad (8)$$

The equations of electron motion (6) and (7) can be solved approximately by assuming that the beam radius r is sinusoidally perturbed to a very small amount around the equilibrium radius r_e , that is,

$$r = r_e + \hat{r}_1 \cos\left(\frac{2\pi}{L_1} z\right) + \hat{r}_2 \cos\left(\frac{2\pi}{L_2} z\right) \quad (9)$$

where \hat{r}_1 is the perturbed peak value radius due to its periodic field of period L_1 ; and \hat{r}_2 , due to the periodic field of period L_2 . By differentiating (9) with respect to time, one obtains

$$\begin{aligned} \dot{r} = & -\hat{r}_1 \left(\frac{2\pi}{L_1}\right) \dot{z} \sin\left(\frac{2\pi}{L_1} z\right) \\ & - \hat{r}_2 \left(\frac{2\pi}{L_2}\right) \dot{z} \sin\left(\frac{2\pi}{L_2} z\right) \end{aligned} \quad (10)$$

where the axial velocity \dot{z} is

$$\begin{aligned} \dot{z} = & \sqrt{2\eta V} \cong \sqrt{2\eta V_0} \left[1 + \frac{\hat{V}_1}{2V_0} \cos\left(\frac{2\pi}{L_1} z\right) \right. \\ & \left. + \frac{\hat{V}_2}{2V_0} \cos\left(\frac{2\pi}{L_2} z\right) \right]. \end{aligned} \quad (11)$$

Expand $\hat{V}_1(r)$, $\hat{V}_2(r)$, $\hat{V}_1'(r)$ and $\hat{V}_2'(r)$, and drop high-order terms, where primes indicate derivatives with respect to r ,

$$\begin{aligned} \hat{V}_1(r) \cong & \hat{V}_1(r_e) \\ & + \hat{V}_1'(r_e) \left[\hat{r}_1 \cos\left(\frac{2\pi}{L_1} z\right) + \hat{r}_2 \cos\left(\frac{2\pi}{L_2} z\right) \right] \end{aligned} \quad (12)$$

$$\begin{aligned} \hat{V}_2(r) \cong & \hat{V}_2(r_e) \\ & + \hat{V}_2'(r_e) \left[\hat{r}_1 \cos\left(\frac{2\pi}{L_1} z\right) + \hat{r}_2 \cos\left(\frac{2\pi}{L_2} z\right) \right] \end{aligned} \quad (13)$$

$$\begin{aligned} \hat{V}_1'(r) \cong & V_1'(r_e) \\ & + \hat{V}_1''(r_e) \left[\hat{r}_1 \cos\left(\frac{2\pi}{L_1} z\right) + \hat{r}_2 \cos\left(\frac{2\pi}{L_2} z\right) \right] \end{aligned} \quad (14)$$

$$\begin{aligned} \hat{V}_2'(r) \cong & V_2'(r_e) \\ & + \hat{V}_2''(r_e) \left[\hat{r}_1 \cos\left(\frac{2\pi}{L_1} z\right) + \hat{r}_2 \cos\left(\frac{2\pi}{L_2} z\right) \right]. \end{aligned} \quad (15)$$

Using the relation

$$\ddot{r} = \frac{d^2 r}{dz^2} \dot{z} + \ddot{z} \frac{dr}{dz}, \quad (16)$$

substituting (7) and (9)–(15) in (6), equating the constant terms and the coefficients of the cosine terms of (6), and remembering that \hat{r}_1 and \hat{r}_2 are small compared to r_e , we have

$$\begin{aligned} & \frac{\hat{V}_1'(r_e)}{V_0} \left[\left(\frac{L_1}{2\pi}\right)^2 \hat{V}_1''(r_e) + \hat{V}_1(r_e) \right] \\ & = - \frac{\hat{V}_2'(r_e)}{V_0} \left[\left(\frac{L_2}{2\pi}\right)^2 \hat{V}_2''(r_e) + \hat{V}_2(r_e) \right] + \eta B_b^2 \frac{r_0^2}{r_e} \end{aligned} \quad (17)$$

$$\hat{r}_1 = - \frac{\hat{V}_1'(r_e)}{2V_0} \left(\frac{L_1}{2\pi}\right)^2, \quad \hat{r}_2 = - \frac{\hat{V}_2'(r_e)}{2V_0} \left(\frac{L_2}{2\pi}\right)^2. \quad (18)$$

Eq. (17) gives the force balance on the electron beam. The term on the left-hand side represents the focusing force contributed by the periodic fields originating from the ring structure of the radius r_1 . The restoring forces which are on the right-hand side consist of the balancing force due to the periodic field produced by the ring structure of radius r_2 , and the space charge force. The balancing force can be made large enough, in some instances, so that the space charge force may well be neglected. This corresponds to a "confined" electron flow, where the focusing and balancing forces are very strong compared to the space charge effect. It will be shown in a later section that the type of flow resulting from the force balance in (17) will form a more stable focusing system than all previous ones.

EXAMPLE

For direct application of the above focusing model to helix-type traveling-wave tubes, a bifilar helix is used as the periodic structure. Suppose, for convenience, as a special case, both the inner and the outer bifilar helices are wound with the same turns per unit length and thus are applied with a periodic field of the same period L [Fig. 1(b)]. A modified equation of (17) for force balance in this case is³

$$\begin{aligned} & \left[\left(\frac{L}{2\pi}\right)^2 \hat{V}_1''(r_e) + \hat{V}_1(r_e) + \left(\frac{L}{2\pi r_e}\right)^2 \hat{V}_1(r_e) \right] \frac{\hat{V}_1'(r_e)}{V_0} \\ & = - \left[\left(\frac{L}{2\pi}\right)^2 \hat{V}_2''(r_e) + \hat{V}_2(r_e) + \left(\frac{L}{2\pi r_e}\right)^2 \hat{V}_2(r_e) \right] \frac{\hat{V}_2'(r_e)}{V_0} \\ & \quad + \eta B_b^2 \frac{r_0^2}{r_e} \end{aligned} \quad (19)$$

where

$$\hat{V}_1(r_e) = \frac{4 \sin \sigma \pi}{\sigma \pi^2} \frac{V_1 K_1\left(\frac{2\pi}{L} r_2\right) - V_2 K_1\left(\frac{2\pi}{L} r_1\right)}{I_1\left(\frac{2\pi}{L} r_1\right) K_1\left(\frac{2\pi}{L} r_2\right) - I_1\left(\frac{2\pi}{L} r_2\right) K_1\left(\frac{2\pi}{L} r_1\right)} I_1\left(\frac{2\pi}{L} r_e\right) \tag{20}$$

$$\hat{V}_2(r_e) = \frac{4 \sin \sigma \pi}{\sigma \pi^2} \frac{V_2 I_1\left(\frac{2\pi}{L} r_1\right) - V_1 I_1\left(\frac{2\pi}{L} r_2\right)}{I_1\left(\frac{2\pi}{L} r_1\right) K_1\left(\frac{2\pi}{L} r_2\right) - I_1\left(\frac{2\pi}{L} r_2\right) K_1\left(\frac{2\pi}{L} r_1\right)} K_1\left(\frac{2\pi}{L} r_e\right). \tag{21}$$

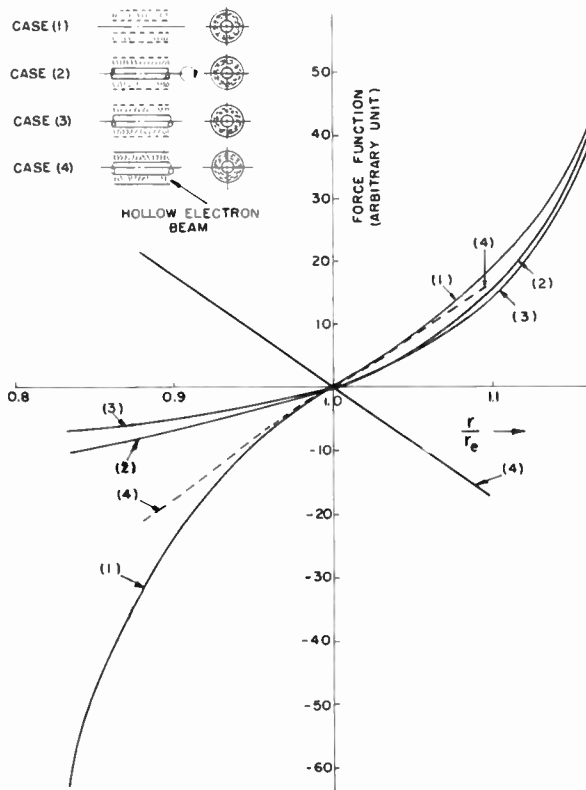


Fig. 2—Force functions near the equilibrium radius.

The terms $(L/2nr_e)^2 \hat{V}_1$ and $(L/2nr_e)^2 \hat{V}_2$, which are missing in (17), represent the focusing and balancing forces due to the angular field resulting from the winding pitch of the helix. For very small periods, these forces are very small and can be ignored.

To study the focusing performance of our doubly periodic electrostatic fields, let us plot (19) as so. Assume that a hollow beam is focused in a confined flow condition at an equilibrium radius r_e by these two periodic electrostatic fields alone. The resultant force function vs beam radius in the neighborhood of r_e is plotted as curve 1 in Fig. 2. For comparison, resultant forces in confined flows of previous focusing schemes using a single periodic electrostatic field are also shown with the same potential difference on the periodic structures of the same geometry. Curve 2 indicates the case in which a centrifugal force³ is employed as a bal-

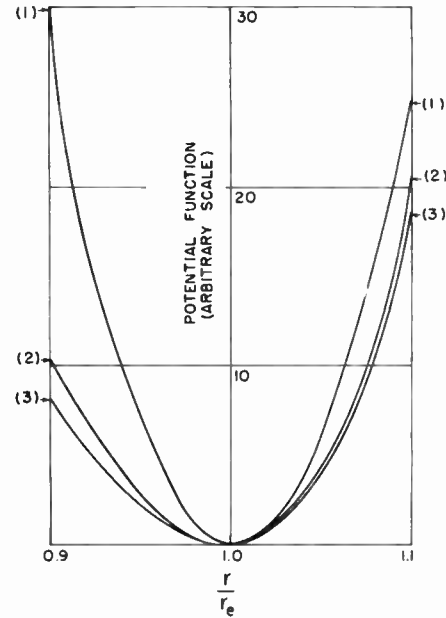


Fig. 3—Potential valley near the equilibrium radius.

ancing force in such a single periodic focusing scheme. The case in which a radial electric force⁶ is used as a restoring force instead is shown by curve 3. The corresponding potential functions of the three cases are plotted in Fig. 3. The space charge force inside a hollow beam which has a ratio of the outer radius to the inner one equal to 1.25 in the coaxial structure of Fig. 1 is derived in the Appendix and is plotted as curve 4 in Fig. 2. Space charge force is assumed to have a zero field at r_e , and an equal but opposite field to curve 1 at $r = 1.05 r_e$. The dotted curve which is the negative of the space charge force, is drawn here for the purpose of comparing the degree of compensation for the space charge inside the beam by the three indicated focusing systems.

It is interesting to note from Fig. 2 and Fig. 3 that the doubly periodic fields not only give the steepest potential valley of all but also offer the approximate cancellation to the space charge force everywhere inside a thick hollow beam. This is extremely important for

⁶ O. Sauseng, "Investigations on electrostatic focusing of electron beams," Ph.D. dissertation, Technische Hochschule Vienna, Vienna, Austria; 1956.

focusing a thick beam of very high current density. The single periodic electrostatic field, as shown by curves 2 and 3 in Fig. 2, deviates very much in magnitude from the space charge field, and thus limits its use to the focusing of very thin electron beams near the equilibrium radius.

In this numerical example, with a periodic voltage variation of 5 per cent³ on the beam, it is possible to focus an electron beam of perveance in the order of 10^{-8} amp/volt^{3/2}.

EXPERIMENTAL RESULTS

An experimental tube for testing the focusing performance was built and is shown in Fig. 4. The tube uses an inner bifilar-helix and an outer bifilar-helix as shown. The dimensions are as follows:

- Hollow cathode: od = 0.305 inch
 id = 0.275 inch
 Outer bifilar helices: tpi = 10
 od = 0.400 inch
 id = 0.360 inch
 Inner bifilar helices: tpi = 10
 od = 0.220 inch
 id = 0.180 inch
 Helix length: = 6 inches.

With a potential difference of 200 v between the two inner helices and 200 v between the two outer helices and with an average beam potential of 180 v (which is equivalent to a periodic voltage variation of 100 per cent on the helices but only 5 per cent on the beam) a current transmission of 97 per cent at a beam current of 4 ma was obtained. The current transmission would have been even better and would have operated equally well at a much higher beam perveance if a better electron gun had been used. The electron gun used in the particular tube is a Pierce type annular gun which was not optimized in dimensions. The current interception in the gun is in the order of 25 per cent of the total beam current.

The tube was also put on rf tests. The outer bifilar-helix was used as the rf interacting helix. To eliminate all possible undesirable rf interaction on the inner helix, the inner helix was wound with resistive wire in the same sense as the outer helix. Using coupled helices, a net power gain of 10 db was observed at a power level of 100 mw at a frequency of 2950 mc. The observed gain was found to be in good agreement with the calculated value.

CONCLUSION

The focusing scheme employing two counteracting periodic fields of very short periods is shown to be superior to that which involves only one focusing periodic field. The potential valley formed by the combination of these two counteracting periodic fields is steeper than all previous focusing systems, and thus is capable of maintaining a very stable beam flow.

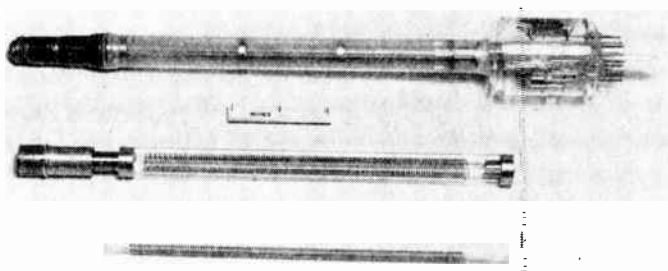


Fig. 4—An experimental electrostatically focused tube.

The most outstanding feature of the new focusing system is the proper cancellation between the focusing field and the space charge field. This field cancellation not only results in an ideal focusing for the beam but also compensates for the potential depression inside the beam so that all electrons in the beam travel with the same average velocity. This has never been true in previous periodic focusing systems of short periods unless special provisions have been made.

Eq. (19) reveals that the force balance on the beam in the confined-flow condition is independent of the average potential. This may extend the application of the new focusing scheme to the accelerating region where the average electron velocity varies with distance. In the drift region where electrons interact with rf delay line, if the beam focusing is not dependent upon the dc velocity of electrons, defocusing caused by rf interaction may be avoided.

Promising experimental results have been obtained on an experimental tube especially built for focusing test. A 97 per cent current transmission has been reached even with a beam launched from a nonoptimized gun. RF gain has also been observed, indicating that a traveling-wave tube can operate without using *any* magnet.

APPENDIX

Suppose the electron beam shown by Fig. 1(a) has been focused to hollow cylindrical ring with radii r_0 and r_i with a uniform space charge density ρ . Then the Poisson's equation for the space charge is

$$\frac{1}{r} \frac{d}{dr} \left(r \frac{dV}{dr} \right) = - \frac{\rho}{\epsilon_0} \quad (22)$$

Integration of (22) yields

$$\frac{dV}{dr} = - \frac{\rho r}{2\epsilon_0} + \frac{1}{r} C_1 \quad (23)$$

where C_1 is an arbitrary constant determined by the boundary conditions at $r=r_0$ and $r=r_i$. In the space-charge free region, the electric fields are:

$$\frac{dV}{dr} = \frac{\phi_0 - \phi_2}{r \ln \frac{r_2}{r_0}} \quad \text{for } r_2 > r > r_0 \quad (24)$$

and

$$\frac{dV}{dr} = \frac{\phi_1 - \phi_i}{r \ln \frac{r_i}{r_1}} \quad \text{for } r_1 < r < r_i \quad (25)$$

where ϕ_i is the potential at $r=r_i$; ϕ_1 at $r=r_1$, etc. To satisfy the boundary conditions, one obtains for the space charge field

$$\frac{dV}{dr} = -\frac{1}{r} \frac{\rho}{2\epsilon_0} \left[r^2 - \frac{1}{\ln \frac{r_2}{r_1}} \left\{ \left(r_0^2 \ln \frac{r_2}{r_0} + r_i^2 \ln \frac{r_i}{r_1} \right) + \frac{1}{2} (r_0^2 - r_i^2) + (\phi_2 - \phi_1) \frac{2\epsilon_0}{\rho} \right\} \right] = -\frac{1}{r} \frac{\zeta}{2\epsilon_0} [r^2 - r_e^2] \quad (26)$$

where r_e is the equilibrium radius at which the space charge field is zero. According to (26)

$$r_e^2 = \frac{1}{\ln \frac{r_2}{r_1}} \left[\left(r_0^2 \ln \frac{r_2}{r_0} + r_i^2 \ln \frac{r_i}{r_1} \right) + \frac{1}{2} (r_0^2 - r_i^2) + (\phi_2 - \phi_1) \frac{2\epsilon_0}{\rho} \right]. \quad (27)$$

If the beam current in the region between the radius r_e and r_0 is I_0 , then (26) becomes

$$\frac{dV}{dr} = \frac{\sqrt{2}I_0}{4\pi\epsilon_0\eta^{1/2}V_0^{1/2}} \frac{1}{r} \frac{r^2 - r_e^2}{r_0^2 - r_e^2}. \quad (28)$$

The Equalization of Base-Band Noise in Multichannel FM Radio Systems*

CHARLES A. PARRY†, SENIOR MEMBER, IRE

Summary—Pre-emphasis and de-emphasis networks are frequently incorporated in the radio equipment of multichannel systems in order to improve the distribution of noise among the channels. The pre-emphasis network has a rising frequency amplitude characteristic and this produces a redistribution of both signal power and nonlinear noise power over the working spectrum. The improvement in signal-to-noise ratio in any channel which the technique of equalization affords is dependent not only on this effect, but also on the contribution of the multiplex equipment to the total channel noise.

This is discussed for typical networks having a maximum slope of attenuation of 6 db per octave and the general case when second-order distortion is predominant. Under practical conditions, the maximum possible improvement is almost entirely obtained when the mean power of the multichannel signal is unchanged by the presence of the networks; a convenient way of establishing this condition with sufficient accuracy is to maintain constant signal energy at a base-band frequency which is 55 per cent of the highest used. Practical considerations usually dictate that the networks do not have a maximum insertion loss exceeding 26 db. With this value and with the multiplex contributing 25 per cent of the total channel noise, an improvement of 3.6 db in the signal-to-noise ratio of the top channel can be expected; provided this loss is not exceeded, the relative noise power, in general, will still be greatest in the top channel.

LIST OF PRINCIPAL SYMBOLS

f = any frequency in the base band.
 f_0 = value of f when $f = 0$.
 f_m = maximum frequency used in the base band.

* Original manuscript received by the IRE, March 19, 1957; revised manuscript received, July 23, 1957.

† Page Communications Engineers, Inc., Washington 5, D. C.

This corresponds with the top channel of the associated frequency division multiplex equipment.

f_h = frequency at which the insertion loss of the equalizing network is half maximum (measured in db).

f_z = reference frequency used by Starr and Walker in the design of certain equalizing networks.

$X = f/f_h$.

$a = f_m/f_h$.

$\phi = f_z/f_m$.

ψ = normalized noise power which falls in a narrow band in the base band. Subscripts are described in the section entitled "The Improvement in Top Channel Signal-to-Noise Ratio and the Over-all Distribution." Primes have been used to indicate that the defined terms apply at a frequency f with equalization applied.

y = a distribution factor for nonlinear noise power. It depends on the relative channel position and the order of distortion producing the noise. y_1, y_2 are those factors which pertain with and without equalization applied, respectively.

$k = y_1/y_2$. k_f is the value applying when y_1 is measured at the frequency f and y_2 is measured at the frequency f_m .

$k_{f_0}k_{f_m}$ = values of k at frequency f_0 and f_m , respectively.

β = order of distortion producing nonlinear noise.

In this instance $\beta = 2$.

K = ratio of the signal power which falls in a channel with equalization networks inserted to that without, K_f , value applying at frequency f .

p_1, p_2 = mean power of the multichannel signal with and without equalization, respectively, determined when the power at the reference frequency f_h is held constant.

$\alpha = p_1/p_2$.

L = maximum insertion loss of the equalizing networks in db, as defined in the text, is equal to $20 \log L$.

$b = \psi_{an}/\psi_{pn}$, where ψ_{an} is the component of nonlinear noise due to amplitude nonlinearities and ψ_{pn} is the component due to phase nonlinearities.

r = ratio of the noise power in a channel due to the multiplex equipment to the total noise power in the channel.

δ = factor by which the multiplex signal is reduced manually at the transmitting terminal, and increased at the receiving terminal.

ρ = factor by which the ratio of the signal-to-total noise in the top channel is increased due to the use of equalization.

INTRODUCTION

THE NOISE which falls in the base band of an fm radio system increases with the base-band frequency. Consequently, when the system is used in conjunction with typical frequency division multiplex equipment, the noise is greatest in the top channel, corresponding to the highest frequency in the base band.

In order to redistribute this noise more evenly among the channels, the practice has arisen to use a form of base-band equalization, in which the higher frequencies are emphasized in transmission and corrected on reception. This has been referred to as "hybrid modulation," and "pre-emphasized transmission." However, the term "base-band noise equalization" would seem to be a more appropriate one and will be used in the present text.

The amount of equalization, as indicated in the literature, varies from 6 to 14 db, but there is little indication as to the extent of the improvement in the signal-to-noise ratio which is obtained with the use of these networks.

It is the purpose of this paper to estimate this improvement under typical operating conditions.

THE TOTAL CHANNEL NOISE

The noise which falls in the channels of the multichannel system arises from two principal sources: 1) the multiplex equipment and 2) the radio equipment. The relative contributions of these equipments are subject to some discussion. For instance, it is generally considered that for high quality circuits, the multiplex

should contribute no more than 25 per cent of the total. On the other hand, when maximum economy is being employed, it may be expedient to use multiplex equipment which produces a considerably greater proportion than this. It is apparent that the net improvement in performance must take this into account, since reduction in the noise from the radio section will have less and less effect as the proportion of noise from the multiplex increases.

THE MULTIPLEX NOISE

Ideally, the base-band noise equalizing networks used in the radio equipment are complementary; that is, the input to output frequency response of the radio link is unaffected by their presence. Consequently, as far as the multiplex equipment is concerned, the radio link is "transparent," and noise from this source will not be affected by the presence or absence of the networks.

In the operating system, it can be expected that all the channels will be adjusted to the same transmission level and that there is a random selection of these channels. Therefore, it may be assumed that the multiplex noise is substantially flat over the signal spectrum.

THE RADIO NOISE

Noise arising in the radio equipment may be divided broadly into two categories:

- 1) Thermal noise, arising principally from the inputs to the receivers in the system. Cosmic and local noise may be grouped with this.
- 2) Nonlinear noise, which arises from the transmission of the multichannel signal through the nonlinear components of the system.

The distribution of thermal noise over the base band has been dealt with extensively in the literature¹ and will not be detailed here. In general, this noise has a triangular amplitude spectrum at the output of the receiver discriminator; the noise power at any frequency f relative to that at the highest base-band frequency f_m is given by $(f/f_m)^2$.

The manner in which the nonlinear noise is distributed over the useful frequency range was probably first worked out by Bennett.² Further investigations have been made by a number of authors.³⁻⁸

¹ W. R. Bennett, "Methods of solving noise problems," *Proc. IRE*, vol. 44, pp. 609-638; May, 1956.

² W. R. Bennett, "Cross modulation requirements on multichannel amplifiers below overload," *Bell Sys. Tech. J.*, vol. 19, pp. 587-610; October, 1940.

³ B. B. Jacobsen, "The effect of nonlinear distortion in multichannel amplifiers," *Electrical Commun.*, vol. 19, pp. 29-54; July, 1940.

⁴ R. A. Brockbank and C. A. A. Wass, "Nonlinear distortion in transmission systems," *J. IEE*, vol. 92, pt. III, pp. 45-56; March, 1945.

⁵ L. Lewin, "Interference in multichannel circuits," *Wireless Eng.*, vol. 27, pp. 291-303; December, 1950.

⁶ J. L. Slow, "Intermodulation noise in vhf multichannel telephone systems," *J. Brit. IRE*, vol. 15, pp. 67-83; February, 1955.

⁷ W. T. Brown, "Some factors in the engineering design of vhf multichannel telephone equipment," *J. Brit. IRE*, vol. 14, pp. 51-74; February, 1954.

⁸ A. T. Starr and T. H. Walker, "Microwave radio links," *Proc. IEE*, vol. 99, pt. III, pp. 241-255; September, 1952.

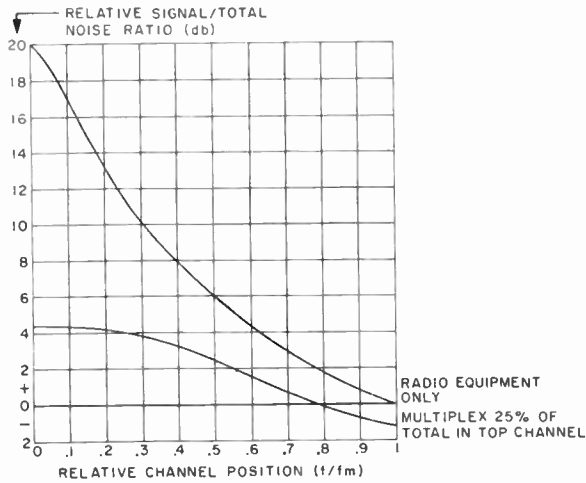


Fig. 1—Typical distributions for the signal-to-noise ratio among the channels of the fm system. The curve for the radio equipment only is drawn on the basis that the “flat” component of the noise is 20 db below the “triangular” component in the top channel. The total noise is the sum of the contributions from the radio and the multiplex equipments.

It can be shown that the nonlinear noise power ψ which falls in a band which is narrow compared with the base band can be given in the form $\psi = Ay p^\beta$ where A is a constant, p is the mean power of the multi-channel signal, y is a distribution factor, and β is the order of distortion which produces the noise. If S is the signal power in this narrow band, we can write the generalized equation

$$\frac{\text{signal/noise with base-band equalization}}{\text{signal/noise without base-band equalization}} = \alpha^{-\beta} k^{-1} K. \quad (1)$$

Where $\alpha = p_1/p_2$, $K = S_1/S_2$, $k = y_1/y_2$, and the subscripts 1 and 2 refer to the values with and without equalization respectively.

THE GENERAL DISTRIBUTION OF THE COMBINED NOISE

Nonlinear noise in the radio equipment is due to both phase and amplitude nonlinearities. The component due to the latter is evenly distributed over the base band. However, the distribution due to phase nonlinearities tends to follow the same $(f/f_m)^2$ law as thermal noise. Usually, at the highest base-band frequency, it can be expected that the phase component will be from 20 to 40 db greater than the amplitude component, so that only the former is significant in the top channels. When the multiplex equipment contributes as much as 25 per cent of the total noise in the worst channel, it is apparent that the noise in the lower channels is almost entirely from this source.

The signal energy is uniformly distributed over the spectrum so the noise power can be used as a measure of the signal-to-noise ratio in the channels. This has been shown in Fig. 1 for typical distributions of the various components of the total noise.

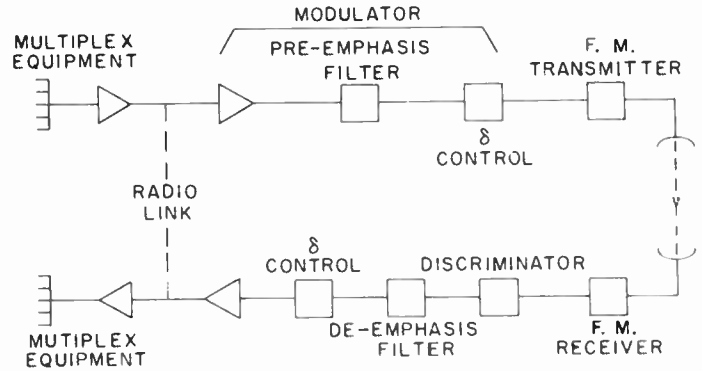


Fig. 2—General arrangement of the essential elements of the multi-channel fm radio system, shown for one direction of transmission only. This diagram is intended particularly to show the locations of the pre-emphasis and de-emphasis filters.

BASE-BAND NOISE EQUALIZATION

The Networks and the Change in Mean Power

The base-band noise equalization is accomplished by means of networks which have a rising amplitude-frequency characteristic in the transmitter and the inverse at the receiver. These are referred to as pre-emphasis and de-emphasis filters (or networks), respectively, and Fig. 2 shows the usual location of these in the fm radio equipment.

The simplest form of these networks is shown in Fig. 3. The maximum slope obtained is 6 db per octave and when this condition applies over the whole of the useful spectrum, the term “linear pre-emphasis” (and de-emphasis) is used.

A convenient reference frequency in the design of this type of network is the frequency at which the insertion loss is half the maximum. The maximum insertion loss is here defined as the difference between the insertion losses measured at zero and at infinite frequency.

In order that the over-all base-band frequency response be unaffected by these networks, it is necessary that they have complementary symmetry.

The principal design factors related to such networks are also shown in Fig. 3. Typical curves for the pre-emphasis network are given in Fig. 4. The half-loss frequency has been used as a reference point. The frequency response of this network can be expressed by normalizing the loss with respect to that at this half-loss frequency. We then have for R , the ratio of the signal amplitude at any frequency f to that at the frequency f_h ,

$$R = \left\{ \frac{1 + X^2 L}{L + X^2} \right\}^{1/2} \quad (2)$$

where $X = f/f_h$, f_h is the frequency corresponding to the half-loss point and the maximum insertion loss in db is $20 \log L$ (see Fig. 3).

The signal energy is uniformly distributed over the working spectrum, from zero frequency to the highest base-band frequency f_m . The ratio of the mean power in

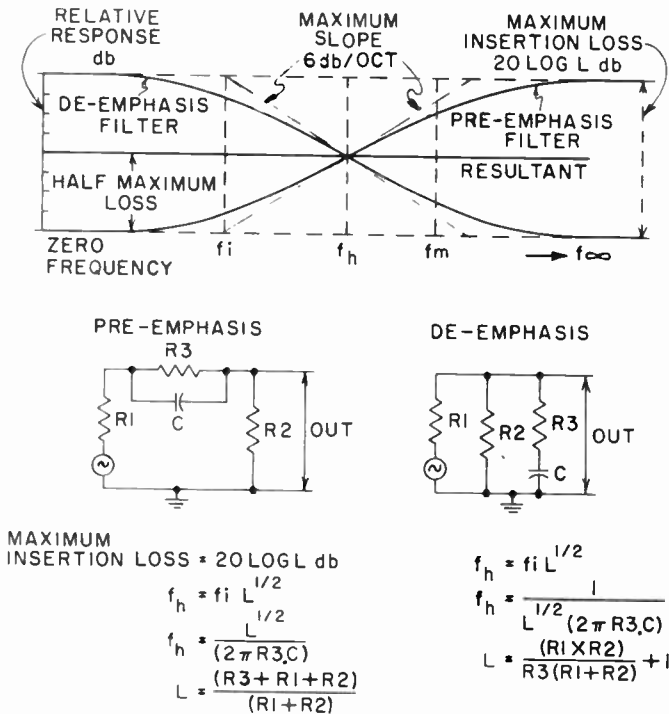


Fig. 3—Design factors for networks having complementary symmetry.

the multichannel signal with the pre-emphasis network in circuit, p_1 , to that without, p_2 , determined when the power at the reference f_h is held constant, will be given by

$$p_1/p_2 = \frac{1}{a \cdot f_h} \int_0^{a \cdot f_h} R^2 df$$

where $a = f_m/f_h$.

This yields

$$p_1/p_2 = \frac{(1 - L^2)}{aL^{1/2}} \tan^{-1}(a/L^{1/2}) + L. \quad (3)$$

This can be solved as a function of L using a as a parameter. When $a=1.8$, then $p_1/p_2 \approx 1$ provided $L \leq 20$, corresponding to 26-db insertion loss. This has been shown graphically in Fig. 5. When $a=1.8$, we obtain $f_h = 0.55 f_m$. This means that if the power at f_h is kept constant, the mean power of the multichannel signal is virtually unchanged by the presence of the network. The graphs of Fig. 4 have been drawn by making the frequency of half loss in the network design correspond to $0.55 f_m$. f_m is the highest frequency which is used in the base band. Under certain conditions of operation, of course, this may be much less than the highest frequency which the equipment is designed to handle.

In the case of linear pre-emphasis, the concept of half maximum loss has no meaning. In this case, the amplitude response is of the form f/f_h .

Then

$$p_1/p_2 = \frac{1}{a \cdot f_h} \int_0^{a \cdot f_h} (f/f_h)^2 df$$

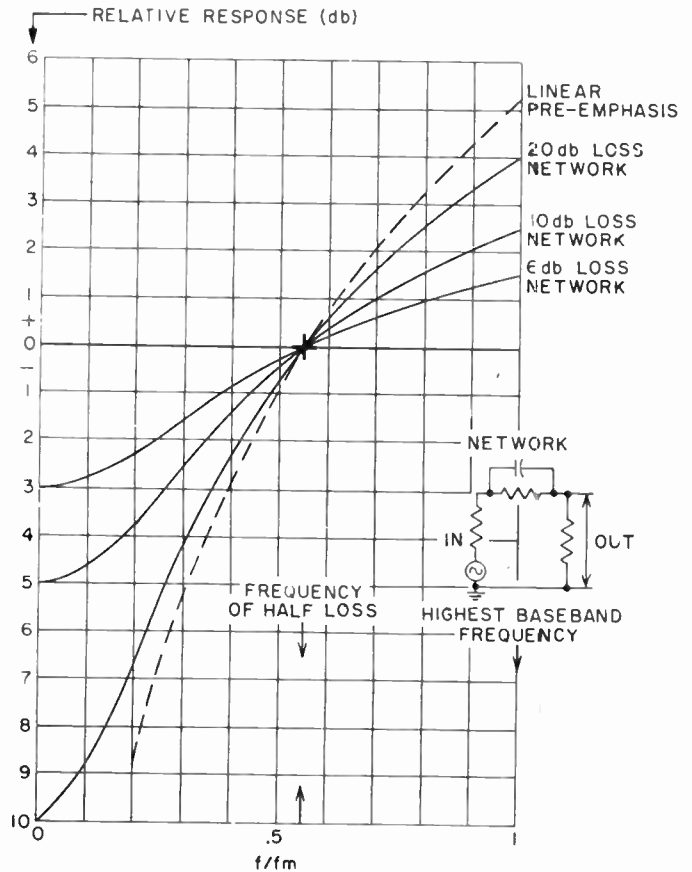


Fig. 4—Frequency response obtained for the pre-emphasis network. In this example the networks are designed so that the frequency of half-loss corresponds to the base-band frequency equal to $0.55 f_m$.

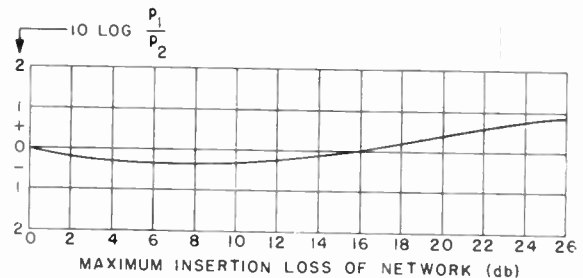


Fig. 5—The ratio p_1/p_2 plotted against maximum insertion loss for the case in which $a = 1.8$. This curve applies to (3).

and when $a = 1.8$, $p_1/p_2 = 1.09$, which is less than 0.5-db change in mean power. f_h in this case is simply a reference point.

The ratio p_1/p_2 of (3) corresponds, as far as the present treatment is concerned, to the factor α in (1). Since the amplitude at the reference frequency is held constant, we have from (2) $K_f = R^2$, where K_f is the value of K in (1) at the frequency f . Then from (3), when $f_h = 0.55 f_m$, $\alpha \approx 1$ and we have very closely,

$$\alpha/K_f = \frac{L + X^2}{1 + X^2 L}. \quad (4)$$

For the top channel in the system, $X=1.8$ and the value of α/K_f for this channel is given in Fig. 6. From

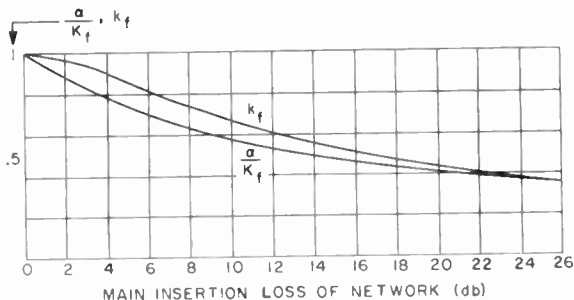


Fig. 6—The factors α/K_f and k_f vs the maximum insertion loss of the networks. Design details of these networks are given in Fig. 3. For these curves, $f=f_m$.

(4), when $L \rightarrow \infty$, $\alpha/K_{f_m} \rightarrow 0.306$. In the case of linear pre-emphasis, $f_m/f_h = 1.8$ and then $\alpha/K_{f_m} \rightarrow 0.334$, which differs by the factor 1.09 indicated above.

Nonlinear Noise Distribution

In typical radio links, it is not unusual for the second-order distortion to predominate, particularly when relatively long antenna feeders introduce echo effects. Starr and Walker⁸ have determined the distribution factor y for this case, using a pre-emphasis network with an amplitude frequency characteristic proportional to

$$(f + f_x)^{1/2} \tag{5}$$

where f_x is a suitable reference frequency. The basic expression is then

$$y = \frac{(\phi^4 + 2/3\phi^2 + 1/5) - f/f_m(\phi^4/2 + \phi^2 + 1/2) + (f/f_m)^2(\phi^2 + 1/3) - (f/f_m)^3\phi^2/3 - (f/f_m)^5/60}{(\phi^2 + 1/3)^2} \tag{6}$$

where $\phi = f_x/f_m$ and y gives the noise power relative to the mean power of the multichannel signal. The constant ϕ for the networks of Fig. 3 can be found by ascertaining the value which gives the same mean power as the networks studied by Starr and Walker. The ratio of the mean power with the network described by (5) to that without, when the amplitude at zero frequency is held constant, is given by

$$\frac{1}{f_m} \int_0^{f_m} [1 + f/f_x]^2 df = 1 + \frac{1}{3\phi^2}$$

The corresponding ratio for the network described by (2) is obtained with the aid of (3) when $a = 1.8$. Since this gives $p_1/p_2 \approx 1$, the ratio $\approx L$.

Thus we have

$$L = 1 + \frac{1}{3\phi^2}$$

so that

$$\phi = \left[\frac{1}{3(L - 1)} \right]^{1/2} \tag{7}$$

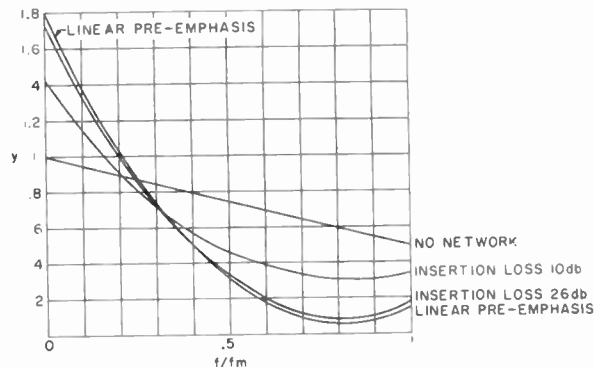


Fig. 7—The distribution factor y as a function of the base-band frequency f .

The distribution factor y has been plotted in Fig. 7 using this value of ϕ . It is useful to refer y to that value which pertains to the top channel when there is no pre-emphasis ($y = 0.5$). If k_f is this normalized value of y [corresponding to k of (1)], then $k_{f_m} = 2y$. For the top channel, $f = f_m$, so that we obtain

$$k_{f_m} = 2 \frac{(\phi^4/2 + \phi^2/3 + 0.016)}{(\phi^2 + 1/3)^2} \tag{8}$$

and from (7) and (8), when $L \gg 1$, $k_{f_m} \rightarrow 0.29$. The asymptotic value of k_{f_m} obtained for linear pre-emphasis, for which $\phi = 0$, is 0.3, which is in good agreement.

THE IMPROVEMENT IN TOP CHANNEL SIGNAL-TO-NOISE RATIO AND THE OVER-ALL DISTRIBUTION

It is convenient to normalize the noise power which falls in a channel with respect to the signal power in this channel. In this way the sum of the normalized noise powers from several separate sources may be used as a measure of the signal-to-noise ratio. It is also convenient to use as a reference the signal-to-noise ratio which pertains to the top channel prior to equalization.

Let

- ψ_n = normalized nonlinear noise power in the top channel prior to equalization.
- ψ_{an} = component of ψ_n due to amplitude nonlinearities.
- ψ_{pn} = component of ψ_n due to phase nonlinearities. The correction factor $(f/f_m)^2$ must be applied to this to find the power at the frequency f .

It will be assumed here that both ψ_{an} and ψ_{pn} are due to the same order of distortion.

$$b = \psi_{an}/\psi_{pn}$$

Then $\psi_n = \psi_{pn}(1 + b)$.

- ψ_L = normalized thermal noise power in the top channel prior to equalization.
- ψ_R = total normalized noise power due to the radio equipment.

$$\psi_R = \psi_n + \psi_L.$$

ψ_m = normalized multiplex noise appearing in a channel. This has the same value for all channels, with or without equalization.

ψ_τ = total normalized noise power appearing in the top channel prior to equalization. Then

$$\begin{aligned}\psi_\tau &= \psi_m + \psi_R. \\ r &= \psi_m/\psi_\tau.\end{aligned}$$

Then

$$\psi_R = \psi_m(1 - r)/r.$$

Relations Prior to Equalization

It can be shown that the maximum signal-to-noise ratio is obtained when $\psi_L = \psi_n(\beta - 1)$, where β is the order of distortion producing the nonlinear noise. Using this relation we have

$$\psi_R = \psi_n\beta = \psi_\tau\beta/(\beta - 1)$$

and, by definition,

$$\psi_\tau = \psi_m/r. \quad (9)$$

Relations Using Base-Band Noise Equalization

The pre-emphasis network will increase the mean power of the multichannel signal by the factor α , while the de-emphasis network will decrease the received signal by the same amount. Suppose now that by means of a manual adjustment, this signal is reduced at the transmitter and increased at the receiver by a factor δ . The physical location of these adjustments is shown in Fig. 2. It is apparent that the input to output frequency response of the radio link will be unchanged by the presence of these networks and the δ control. ψ_m is therefore unaffected.

The mean power of the (modulating) multichannel signal will now be increased by the factor α/δ and from (1) the nonlinear noise in a channel, measured at the input to the de-emphasis network, will be increased by the factor $(\alpha/\delta)^\beta k_f$. The signal power in the channel is increased by the factor K_f/δ where K_f has the significance given in (4). The de-emphasis network and δ control operate equally on signal and noise so that the normalizing factor for nonlinear noise power is $(\alpha/\delta)^\beta(\delta/K_f)k_f$.

The thermal noise is affected only by the de-emphasis network and δ control, so that the thermal noise power is reduced by the factor δ/K_f . Thus the normalizing factor for thermal noise in the channel is δ/K_f .

The total noise power in the channel corresponding to the frequency f in the base band will now be

$$\psi_\tau' = \psi_{an}' + \psi_{pn}' + \psi_L' + \psi_m$$

where the primes are used to indicate the powers as previously defined but refer to the frequency f and with base-band noise equalization applied.

We have

$$\begin{aligned}\psi_{an}' &= \psi_{anz}. \text{ (normalizing factor).} \\ \psi_{pn}' &= \psi_{pnz}. \text{ (normalizing factor)}x(f/f_m)^2. \\ \psi_L' &= \psi_{Lz}. \text{ (normalizing factor).}\end{aligned}$$

So, by definition,

$$\psi_{an}' + \psi_{pn}' = \frac{\psi_n}{1 + b} \{ (f/f_m)^2 + b \} (\alpha/\delta)^\beta (\delta/K_f) k_f;$$

also,

$$\psi_L' = \psi_L(f/f_m)^2(\delta/K_f).$$

Using (9) and the previous definitions, we now get for the total normalized noise power in a channel corresponding to the frequency f in the base band

$$\begin{aligned}\psi_\tau' &= \psi_m \left(\frac{\beta - 1}{\beta} \right) \left(\frac{1 - r}{r} \right) (f/f_m)^2 (\delta/K_f) \\ &+ \frac{\psi_m (1 - r)}{\beta} \left(\frac{1 - r}{r} \right) \left\{ \frac{(f/f_m)^2 + b}{1 + b} \right\} (\alpha/\delta)^\beta (\delta/K_f) k_f \\ &+ \psi_m.\end{aligned} \quad (10)$$

The use of equalization improves the signal-to-noise ratio in the top channel by a factor ρ which is obtained from (9) and (10). For this channel we have $f = f_m$, so that

$$\rho = \frac{1}{(1 - r) \left(\frac{\delta}{K_f \beta} \right) \left[\beta - 1 + \left(\frac{\alpha}{\delta} \right)^\beta k_f \right] + 1} \quad (11)$$

The maximum value of this ratio can be found in the usual way by differentiating the denominator with respect to δ and equating to zero. This gives $(\alpha/\delta)^\beta = 1/k_f$. Substituting back in (11) gives

$$\rho_{(\max)} = \frac{1}{(1 - r)(\alpha/K_f)(k_f)^{1/\beta} + r} \quad (12)$$

In practice, it is usually both convenient and preferable to arrange that the mean power of the multichannel signal does not change when the equalizing networks are introduced into the system. This avoids the possibility of overload, for instance. For this requirement we have $\alpha/\delta = 1$. Substituting this in (10) gives

$$\rho_{(\alpha=\delta)} = \frac{1}{\frac{(1 - r)\alpha}{\beta \cdot K_f} (\beta - 1 + k_f) + r} \quad (13)$$

We can now compare the improvement which is obtained for this condition to the maximum possible given by (12). We will call the ratio of these improvements ϵ^{-1} , and from (12) and (23) we obtain

$$\epsilon = \frac{(1-r) \cdot \alpha}{\beta \cdot K_f} (\beta - 1 + k_f) + r \div \frac{(1-r)(k_f)^{1/\beta} \cdot \alpha}{K_f} + r$$

This has a maximum for minimum α/K , corresponding to linear pre-emphasis. Substituting $\beta=2$ and the asymptotic values of α/K_f and k_f gives

$$\epsilon = \frac{0.215(1-r) + r}{0.183(1-r) + r}$$

again taking the limiting case in which the multiplex noise is negligible, we have $r=0$, and then $\epsilon=1.18$, or 0.7 db.

Consequently, if the system is adjusted so that the mean power in the multichannel signal is the same with and without the networks, the improvement in the signal-to-noise ratio obtained in the top channel will be virtually the maximum possible. As indicated by (3), this condition is achieved by maintaining constant signal power at the base-band frequency $f=0.55 f_m$.

Curves for the improvement factor ρ (in db) based on (13), with $\beta=2$, are given in Fig. 8.

Generally, it is not practical to use equalizers with more than about 26-db insertion loss. Fig. 8 shows that with this value and the recommended ratio of 25 per cent for r , the use of equalization will effect an improvement of 3.6 db.

It should be pointed out, perhaps, that the ratio r as used here applies before equalization. This implies that the ratio will be less after equalization, although the total noise is less. It is not felt that this decreased ratio would be considered a disadvantage under the circumstances. In the event that the ratio after equalization is important, it is a simple matter to devise an equation similar to (13) which is based on the final ratio permitted.

Before design equations can be based on the top channel noise, it is necessary to determine whether this will still be greater than that in any other channel, after equalization has been applied. Eq. (10) can be examined for this purpose.

Again assume that the mean signal power will be unchanged so that $\alpha=\delta$. Also, use (4) for α/K_f . Then

$$\frac{\psi_r'}{\psi_m} = \left[\frac{(1-r)}{r\beta} \left(\frac{L+X^2}{1+X^2L} \right) \left\{ \frac{k_f}{1+b} [b + (f/f_m)^2] + (\beta-1)(f/f_m)^2 \right\} + 1 \right]. \quad (14)$$

As before, $X=f/f_h=1.8f/f_m$.

This does not permit a simple algebraic solution and it is necessary to obtain a graph of ψ_r' to determine whether the noise has a maximum in the top channel.

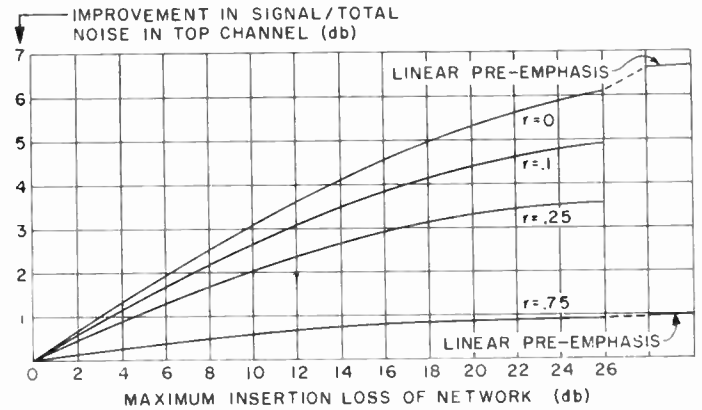


Fig. 8—The improvement in signal-to-total noise obtained in the top channel of the fm system when base-band noise equalization is used and second-order distortion is predominant. r =ratio of the multiplex noise to total channel noise prior to equalization. Design details of the networks are given in Fig. 3. The mean power of the multichannel signal is adjusted to be the same with or without equalization.

For typical values of L , ψ_r' increases as $f \rightarrow 0$. When $f=0$, $X=0$. With $\beta=2$, we then have

$$\psi_{r=f=0}' = \left[\left[\frac{(1-r)}{2r} \right] \left[\frac{L \cdot b \cdot k_{f_0}}{1+b} \right] + 1 \right] \psi_m.$$

While for the top channel,

$$\psi_{r=f_m}' = \left[\left[\frac{(1-r)}{2r} \right] \left[\frac{L+3 \cdot 2}{1+3 \cdot 2L} \right] \{ k_{f_m} + 1 \} + 1 \right] \psi_m.$$

In these equations, k_{f_m} is used to indicate k_f at $f=f_m$, and k_{f_0} indicates k_f at $f=0$.

In order that the noise in the top channel exceed that in the lowest, it is then necessary that

$$\frac{(1-r)(L \cdot b \cdot k_{f_0}) + 2r(1+b)}{\left[(1-r) \left(\frac{L+3 \cdot 2}{1+3 \cdot 2L} \right) (k_{f_m} + 1) + 2r \right] [1+b]} \leq 1$$

from which

$$\frac{b}{1+b} \leq \frac{(k_{f_m} + 1)(L + 3 \cdot 2)}{k_{f_0} \cdot L \cdot (1 + 3 \cdot 2L)}. \quad (15)$$

It is useful to observe that this requirement is independent of r . The maximum permissible value of b can be found by substituting values into (15). For instance, with a 26-db equalizer, $L=20$; from Fig. 6, $k_{f_m} 0.36$, and from (6), $k_{f_0}=3.5$. Substituting in (15) gives the requirement that $b \leq (1/144)$; that is, the component of the nonlinear noise due to amplitude nonlinearity must be at least 21.6 db below that due to phase nonlinearity, measured in the top channel. This is not an unreasonable value and is not particularly critical. For instance, consider that $r=25$ per cent. If $b=0$, the noise in the lowest channel will decrease by 2.5 db; if b increases by 3 db, the noise in the lowest channel will increase by 1.5 db.

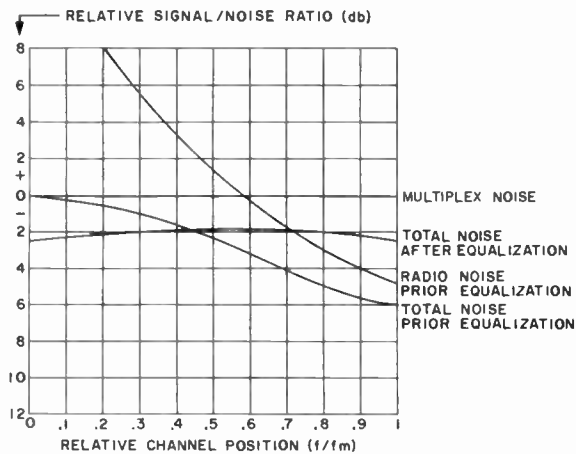


Fig. 9—Typical distribution of the signal-to-noise ratios obtained in the multichannel radio system when second-order distortion is predominant. These curves are based on the following relations. The proportion of multiplex noise to total noise prior to equalization is 25 per cent. The ratio of the component of nonlinear noise due to amplitude nonlinearity to the component due to phase nonlinearity is -21.6 db, measured in the top channel prior to equalization. The maximum insertion loss of the equalizers is 26 db. The improvement in the signal-to-noise ratio obtained in the top channel ($f=f_m$) is seen to be 3.6 db, which agrees with the value obtained from Fig. 8. [The curves for Fig. 9 are based on (14) and the following substitutions apply: $\beta=2$, $b=1/144$, $r=0.25$, $L=20$.]

Therefore, it would appear that in general, provided the maximum insertion loss of the equalizer does not exceed about 26 db, the noise will still be greatest in the top channel, and the system design can be based on this. The expected distribution of the various noise powers are shown for the values given above in Fig. 9.

As can be seen from Fig. 8, there is little improvement to be gained by increasing the equalizer loss beyond 26 db and from (15), it is apparent that to do so will only impose more severe requirements on the ratio b . This is one reason why there is generally little advantage to be gained by using larger equalizers and usually a maximum insertion loss from 14 to 20 db is adequate.

APPLYING EQUALIZATION

The following method may be used to adjust the system incorporating equalization.

- 1) The system is designed as an ordinary fm system.

The highest base-band frequency f_m will be determined by the number of channels and the bandwidth per channel. The equalizer networks to be used can then be designed on the basis that the frequency of half maximum loss will be equal to $0.55 f_m$.

- 2) The net improvement in the top channel signal-to-noise ratio can be obtained from Fig. 8.

- 3) The transmission level per channel is readily determined from a knowledge of equipment characteristics and required performance.⁹ The system is designed on this basis.

- 4) After the system is adjusted as a straight fm system, the equalizer networks are introduced into circuit. To readjust the system, the following procedure is used. A single-tone signal is injected into the equipment such that its frequency in the base band is $0.55 f_m$. The transmission level is measured at the receiver output. The pre-emphasis network is then inserted and the δ control in the modulator (Fig. 2) adjusted so that the received signal is the same as it was before the network was inserted. The same procedure is now used with the de-emphasis network and associated δ control.

This completes the system adjustment.

CONCLUSION

Simple networks may be used in the fm radio system to effect an improvement in the top channel signal-to-noise ratio. When the system is adjusted so that the mean power of the multichannel signal is unchanged by the presence of these networks, the improvement is virtually the maximum possible. A convenient indication for this condition is that the signal power at a frequency in the base band which is 55 per cent of the highest frequency used will remain constant.

The net improvement depends on the proportion of multiplex noise in the total channel noise. When this is 25 per cent, a 3.6-db improvement would be expected with an equalizer having a maximum insertion loss of 26 db. Provided the loss does not exceed this value, it can be expected that the noise will be greatest in the top channel even with equalization, so the system design may proceed on this premise.

⁹ C. A. Parry, "Design Factors for the Optimisation of Multi-channel Radio Systems," paper no. CP 57-60 presented at AIEE winter conference; January 22, 1957.



Theory of a Wide-Gap Emitter for Transistors*

HERBERT KROEMER†, MEMBER, IRE

Summary—In order to obtain a high current amplification factor, it is important in transistors that the ratio of the injected minority carrier current over the total emitter current, γ , be close to unity, or that the quantity $1-\gamma$, called the injection deficit, be as small as possible.

It is shown that the injection deficit of an emitter can be decreased by several orders of magnitude if the emitter has a higher band gap than the base region. This effect can be utilized either in addition to the commonly used high emitter doping in order to eliminate the alpha falloff with current, or to decrease the high emitter doping in order to obtain a lower emitter capacitance.

Decreasing the emitter capacitance in high-frequency transistors may be utilized either to extend their frequency range or to increase their power capabilities by increasing the area.

INTRODUCTION

AN important quantity characterizing the emitter of any transistor is the emitter efficiency, γ , defined as that fraction of the total emitter current that is minority-carrier injection current. Since the current amplification factor, α_{ce} , is proportional to γ , it is desirable that γ be high. Actually, it is very important that γ be close to unity. In the usual grounded-emitter operation the current amplification factor of the transistor is

$$\alpha_{cb} = \frac{\alpha_{ce}}{1 - \alpha_{ce}} \quad (1)$$

From this it follows that a change of γ such that α_{ce} increases from 0.98 to 0.99 (percentage-wise a very small change of about 1 per cent) increases α_{cb} from about 49 to about 99, that is, by a factor of two. It is therefore more appropriate to consider the "injection deficit" $1-\gamma \approx (1-\gamma)/\gamma$ rather than γ itself as a measure of the transistor performance. In a good transistor, the injection deficit ought to be small.

In a *p-n-p* transistor,

$$\gamma = \frac{j_p}{j_n + j_p} \quad (2)$$

$$\frac{1-\gamma}{\gamma} = \frac{j_n}{j_p} \quad (3)$$

where j_p and j_n are the densities of the hole and electron currents at the emitter junction. In order to obtain a low ratio of electron to hole current, it is necessary in a semiconductor with constant band gap to dope the *p* side of the junction much more heavily than the *n* side. There are practical limits, however, as to the magnitude of doping possible, and there are situations where a high

doping of the emitter is undesirable for other reasons. In all cases, an improvement could be obtained if the injection deficit could be decreased by other means instead of, or in addition to, the high doping.

The purpose of this paper is to point out that it is possible to lower the injection deficit by using an emitter material with a wider band gap than the base ma-

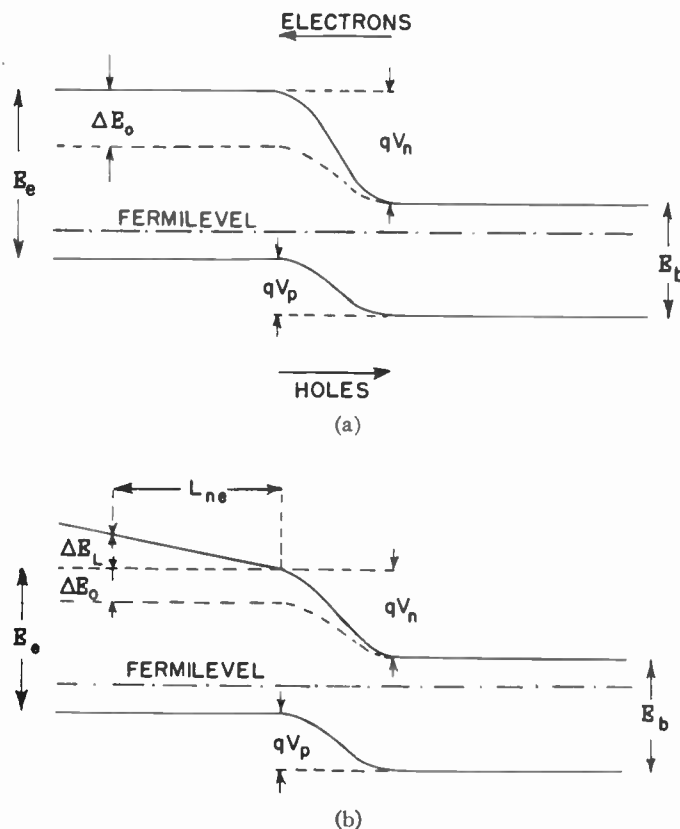


Fig. 1—Band structure of a wide-gap emitter junction. (a) With constant gap outside the depletion region and (b) with linear gap variation inside the emitter.

terial (Fig. 1).¹ The reason for this is that in such a case the activation energy (or contact potential) qV_n for electrons flowing from the base into the emitter is higher than the activation energy (or contact potential) qV_p for holes entering the base from the emitter (see Fig. 1). The difference in activation energies is the difference in bandwidth, ΔE . Since the activation energy enters exponentially into the current-flow equations, this means a decrease in the injection deficit by a fraction of $\exp(-\Delta E/kT)$, all other things being equal. This is shown quantitatively in the next section.

¹ It has been pointed out to the author that this principle was first suggested by W. Shockley in U. S. Patent No. 2,569,347, issued September 25, 1951.

* Original manuscript received by the IRE, April 12, 1957; revised manuscript received, July 29, 1957.

† RCA Labs., Princeton, N. J.

THE INJECTION DEFICIT IN A WIDE-NARROW JUNCTION

$$\left(\frac{m_{ne}^* m_{pe}^*}{m_{nb}^* m_{pb}^*}\right)^{3/2} \exp(-\Delta E_0/kT) \tag{9}$$

We introduce the following notation:

- j_n, j_p = electron and hole current densities at the junction.
- D_{ne}, D_{pb} = diffusion constants for electrons in the emitter and holes in the base, and
- L_{ne}, L_{pb} = corresponding diffusion lengths.
- n_{oe}, p_{ob} = equilibrium minority carrier densities in the emitter (electrons) and the base (holes) adjoining to the junction.
- V = applied bias.
- n_{ie}, n_{ib} = intrinsic carrier densities of the emitter and base semiconductors.
- P_e, N_b = net acceptor density in the emitter and net donor density in the base.
- $\left. \begin{matrix} m_{ne}^*, m_{pe}^* \\ m_{nb}^*, m_{pb}^* \end{matrix} \right\}$ = effective masses of the electrons and the holes in the emitter region and the base region.
- E_e, E_b = emitter band gap and base band gap.
- $\Delta E_0 = E_e - E_b$.

With this notation for a simple *p-n* junction,²

$$i_n = \frac{q D_{ne} n_{oe}}{L_{ne}} \left(e^{\frac{qV}{kT}} - 1 \right) \tag{4a}$$

$$j_p = \frac{q D_{pb} p_{ob}}{L_{pb}} \left(e^{\frac{qV}{kT}} - 1 \right) \tag{4b}$$

$$\frac{j_n}{i_p} = \frac{D_{pe}}{D_{pb}} \frac{L_{pb}}{L_{ne}} \frac{n_{oe}}{p_{ob}} \tag{5}$$

Now,

$$n_{oe} = \frac{n_{ie}^2}{P_e}, \quad p_{ob} = \frac{n_{ib}^2}{N_b} \tag{6a, b}$$

Furthermore,

$$\frac{n_{ie}^2}{n_{ib}^2} = \left(\frac{m_{ne}^* m_{pe}^*}{m_{nb}^* m_{pb}^*}\right)^{3/2} \exp(-\Delta E_0/kT) \tag{7}$$

Therefore,

$$\frac{j_n}{j_p} = \frac{D_{ne}}{D_{pb}} \frac{L_{pb}}{L_{ne}} \frac{N_b}{P_e} \left(\frac{m_{ne}^* m_{pe}^*}{m_{nb}^* m_{pb}^*}\right)^{3/2} \exp(-\Delta E_0/kT) \tag{8}$$

This expression differs from that for a junction between semiconductors of equal band gaps by the factor

² We treat the case of a simple *p-n* junction rather than a transistor to obtain more symmetrical notation. In a transistor with a base width $w_b \ll L_{pb}$, one has to replace L_{pb} by w and to omit the "minus one" behind the exponential factor. For the derivation of (4) see W. Shockley, "The theory of *p-n* junctions in semiconductors and *p-n* junction transistors," *Bell Sys. Tech. J.*, vol. 28, pp. 435-489; July, 1949.

of which the important part is the exponential factor. If, for example, ΔE is 0.2 *ev*, then at room temperature $kT = 0.025$ *ev* and $\Delta E/kT = 8$. Assuming the effective masses to be identical, the injection deficit is then decreased by a factor of $e^{-8} = 1:3000$.

If the band gap in the emitter region is not constant but increases linearly with increasing distance from the junctions [Fig. 1(b)], (8) still does not give a full account of the change in injection deficit. If the above ΔE_0 is the gap difference across the depletion layer and if ΔE_L is the gap variation along a diffusion length, L_{ne} , in the emitter, then it can be shown that the factor

$$f(\Delta E_L) = \sqrt{\left(\frac{\Delta E_L}{2kT}\right)^2 + 1} - \frac{\Delta E_L}{2kT} \tag{10a}$$

has to be added to (4a), (8), and (9). For $\Delta E_L \gg 2kT$

$$f(\Delta E_L) \rightarrow \frac{kT}{\Delta E_L} \ll 1. \tag{10b}$$

Therefore, a band-gap variation outside the depletion layer also reduces j_n/j_p . However, this is to a smaller degree, namely only linearly rather than exponentially.

Eq. (8) does not hold for arbitrarily large ΔE 's, however. This is because (4a) holds only so long as the density of electrons injected into the *p*-type region remains small compared to the electron density in the source, that is in the *n*-type region. The analogous statement holds for holes. Mathematically this means

$$V_n - V \gg kT \tag{11a}$$

$$V_p - V \gg kT. \tag{11b}$$

In a *p*-type wide-gap emitter $V_n > V_p$ and (11a) is fulfilled automatically if (11b) is. Consequently, (8) holds only for voltages that satisfy (11b). But, (11b) also implies that for a workable wide-gap emitter V_p must not

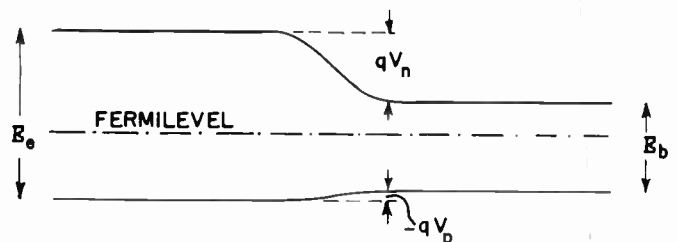


Fig. 2—Wide-narrow junction with negative V_p , due to a low doping ratio. Not suited as wide-gap emitter.

be negative. Therefore, a structure like in Fig. 2 would not be a good wide-gap emitter because the minority carrier density in the base is larger than the majority carrier density in the emitter.

ALPHA AND ALPHA FALLOFF

In order to estimate the influence of the decreased injection deficit upon α_{cb} in a transistor, one has to take the recombination losses into account. If ρ is the fraction of injected carriers that recombine on the way to the collector, then for $\rho \ll 1$, from (1) and (2)

$$\frac{1}{\alpha_{cb}} \approx \rho + (1 - \gamma) \approx \rho + \frac{j_n}{j_p} \quad (12)$$

If j_n/j_p is small compared to ρ , α_{cb} is determined solely by the recombination losses. This is the case for many transistors at low injection currents. At high injection currents the injected hole density in the base becomes comparable to the donor density. To maintain electrical neutrality, the electrons in the base increase by the same number. This means that the electron current into the emitter is bigger than the value given by (4a) by the factor by which the electron density has increased. For increasing current, therefore, j_n/j_p is not constant but increases (linearly) with current. Eventually j_n/j_p becomes comparable with and larger than ρ , resulting in the well-known alpha falloff.³

If the emitter has a wide band gap, the ratio j_n/j_p increases with current by the same factor as for an ordinary emitter. Since on an absolute scale, however, j_n/j_p is lower by the factor (9), the alpha-falloff effect sets in at much higher current densities. Since j_n/j_p increases linearly with the total current, alpha falloff sets in at currents which are bigger by the reciprocal of (9), compared to an otherwise identical constant-gap transistor. In our numerical example of $\Delta E = 0.2 \text{ eV}$, the alpha falloff sets in at 3000 times the current. This means the alpha falloff is practically nonexistent.

CAPACITANCE

Another consequence of the exponential factor in (9) is the following:⁴ In many transistors for small-signal operation, it is of not primary importance to minimize the falloff effect to the point of vanishing. In these cases the exponential factor may be used to decrease the doping in the emitter by this same factor (9) and still have an unchanged falloff characteristic. It would then be possible to have a usable emitter efficiency with an emitter that has a considerably lower impurity density than the base region. This, however, would imply a reduced emitter transition capacitance.

In the case of audio-frequency large-signal transistors, the emitter transition capacitance is of no great importance while alpha falloff is a very serious effect. In this case one therefore should maintain the high doping

³ W. M. Webster, "On the variation of junction transistor current-amplification with emitter current," *Proc. IRE*, vol. 42, pp. 914-920; June, 1954.

⁴ H. Kroemer, "Zur theorie des diffusions und des driftransistors, part III," *Archiv der Elektrischen Übertragung*, vol. 8, pp. 499-504; November, 1954.

in the emitter. The situation is completely reversed, however, for very-high-frequency transistors, like the drift transistor or the *p-n-i-p* transistor. In these transistors the current amplification factor is, under usual operating conditions, not limited by the injection deficit but rather by transit time effects. The low-frequency alpha falloff therefore is not an important quantity in this case. However, since high-frequency transistors have a rather high impurity density in the base region, the emitter capacitance is rather high. As a result, the emitter capacitance often becomes the limiting factor for the over-all frequency behavior of the transistor. In such a case, a wide-gap emitter with a lower doping might improve the over-all frequency limit considerably.

Quantitatively, the capacitance of an abrupt junction is⁵ (per unit area)

$$C = \sqrt{\frac{q\epsilon}{8\pi} \frac{NP}{N+P} \frac{1}{V+V_c}} \quad (13a)$$

where V_c is the contact potential. If the two sides have a different dielectric constant,

$$C = \sqrt{\frac{q\epsilon_n N \cdot \epsilon_p P}{8\pi(\epsilon_n N + \epsilon_p P)} \frac{1}{V+V_c}} \quad (13b)$$

If $P \gg N$ this simplifies to

$$C = \sqrt{\frac{q\epsilon_n N}{8\pi(V+V_c)}} \quad (14a)$$

while for $P \ll N$

$$C = \sqrt{\frac{q\epsilon_p P}{8\pi(V+V_c)}} \quad (14b)$$

If, in a constant-gap transistor, a doping ratio $P:N = 30$ is assumed as an example, the introduction of a 0.2 eV wider emitter band gap allows a reduction of this ratio by 1/3000, namely to $P:N = 1:100$ without a change in γ . The capacitance, then, would be decreased to one tenth of the original value assuming identical dielectric constants.

A reduction of the emitter capacitance of this order could be utilized either to increase the frequency limit of the transistor or to increase the emitter (and collector) area. In the latter case, one would obtain a higher power capability for the same frequency response.

THE WIDE-GAP COLLECTOR

The use of a wide-gap semiconductor in the collector region would have an advantage only if the collector region at the same time had a lower impurity concentration than the base region.⁴ Then one would obtain the lower collector capacitance of a high-resistivity collector region without the increased saturation current that is associated with a higher resistivity collector region in the constant-gap transistor.

⁵ Shockley, *loc. cit.*

Shot Noise in Transistors*

G. H. HANSON†, MEMBER, IRE, AND A. VAN DER ZIEL‡, FELLOW, IRE

Summary—The shot noise generated in a transistor may be represented in an equivalent circuit by a current generator i_p across the collector junction and an emf e_s in series with the emitter junction.

The characteristics of i_p have been established by measurements of output equivalent saturated diode current made with the input open. The noise is independent of frequency up to approximately $f_\alpha \sqrt{1-\alpha_0}$, where f_α is the α -cutoff frequency of the transistor. It increases sharply in the neighborhood of f_α , but then levels off at higher frequencies. The collector saturated current shows full shot effect up to frequencies well beyond the α -cutoff frequency. Information about e_s and about the correlation between e_s and i_p has been obtained from measurements of the noise figure. At low frequencies ($f \ll f_\alpha$), e_s and i_p are partially correlated for some transistors, while in others there is little or no correlation. Except for very small values of the source resistance, the main contribution to the noise figure comes from i_p rather than from e_s .

The experimental results are interpreted in terms of a recent theory by van der Ziel. Good agreement has been obtained.

INTRODUCTION

AS TRANSISTOR technology advances, the frequency response is being increased steadily while excess noise or 1/f noise is gradually being reduced. The result is that over most of the frequency range of modern transistors, the limit of sensitivity is set by shot noise.

The shot noise in a $p-n-p$ junction transistor operated in the grounded base connection may be represented in the equivalent circuit of Fig. 1 by a noise voltage e_s in series with the emitter junction and a noise current generator i_p in parallel with the collector junction. The noise is completely specified, provided that the magnitude of e_s and of i_p and the correlation of e_s and i_p are known over the frequency range of interest. Recent work by van der Ziel¹ has provided theoretical expressions for these quantities. Some measurements made over a limited frequency range by Hanson² tended to support van der Ziel's theory. This paper will describe measurements of $\langle i_p^2 \rangle_{av}$ over a range of frequencies extending to as high as $10f_\alpha$, where f_α is the α -cutoff frequency. In addition, the results of measurements of $\langle e_s^2 \rangle_{av}$ and $\langle e_s i_p \rangle_{av}$ at frequencies much less than f_α will be given.

METHOD OF MEASUREMENT

In the measurements described here, the transistor under test was mounted in the grounded base connection

* Original manuscript received by the IRE, June 20, 1957; revised manuscript received, August 27, 1957. This work was supported by the U. S. Army Signal Corps.

† Bell Telephone Labs., Allentown, Pa. Formerly at Dept. of Elec. Eng., University of Minnesota, Minneapolis, Minn.

‡ Dept. of Elec. Eng., University of Minnesota, Minneapolis, Minn.

¹ A. van der Ziel, "Theory of shot noise in junction diodes and junction transistors," *PROC. IRE*, vol. 43, pp. 1639-1646; November, 1955. See also *PROC. IRE*, vol. 45, p. 1011; July, 1957.

² G. H. Hanson, "Shot noise in $p-n-p$ transistors," *J. Appl. Phys.*, vol. 26, pp. 1388-1389; November, 1955.

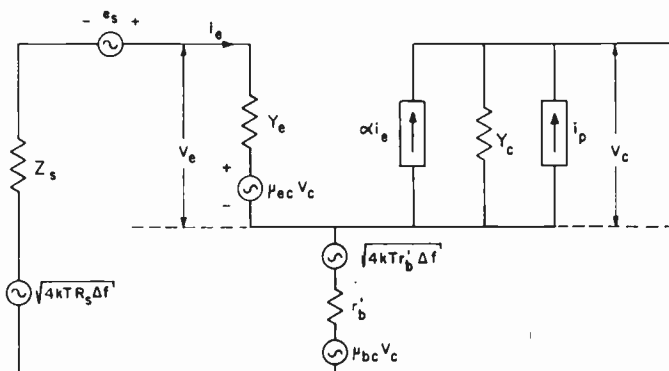


Fig. 1—Equivalent circuit for noise of a $p-n-p$ transistor operated in grounded base connection. The emf's $\mu_{ec}V_c$ and $\mu_{bc}V_c$ may be omitted since they do not influence the noise figure.

at the input of a preamplifier. A noise diode, Sylvania 5722, was used as a standard noise source. The equipment contained amplifiers tuned to 17 different frequencies spaced throughout the range from 1 kc to 60 mc. A common preamplifier was used for the channels below 1 mc. At the higher frequencies, several tuned preamplifiers are fed into common mixers and IF amplifiers. As a result of this arrangement the bandwidth of each amplifier was much smaller than that of the corresponding input circuits, a feature that is necessary for the accurate measurement of noise figures.

Linear detectors were used to rectify the outputs of each amplifier, which were then measured on microammeters. The measurements were made by comparing the rectified output due to noise from the transistor with that due to noise from the transistor plus the saturated diode.

The contribution of the noise generator e_s may be made negligible compared to that of i_p by the insertion of a large resistance in the emitter circuit of the transistor. The noise from i_p may then be measured directly in terms of output equivalent saturated diode current I_{eq} (defined by $\langle i_p^2 \rangle_{av} = 2eI_{eq}\Delta f$). For such measurements the noise diode is placed in the collector circuit of the transistor.

The magnitude of e_s and the correlation between e_s and i_p cannot be measured directly. However, measurements of the noise figure F may be used to determine these quantities indirectly in a manner that will be described later. In this work, the noise figures were measured by comparing noise from the transistor with that generated in a saturated diode in the emitter circuit of the transistor. If I_d is the diode plate current required to double the output noise power and if R_s is the source resistance, the noise figure is given by

$$F = 20I_dR_s. \tag{1}$$

MEASUREMENTS OF $\langle i_p^2 \rangle_{av}$ AND COMPARISON WITH THE THEORY

Van der Ziel's theory gives the following expression for the noise current generator i_p :

$$\begin{aligned} \langle i_p^2 \rangle_{av} &= 2eI_{eq}\Delta f \\ &= 2eI_c(\alpha_0 - |\alpha|^2)\Delta f + 2e(I_c)_{sat}\Delta f \end{aligned} \quad (2)$$

where the collector saturated current $(I_c)_{sat}$ is defined as the collector current for zero emitter current. We see that for zero emitter current

$$I_{eq} = (I_c)_{sat} \quad (2a)$$

at all frequencies.

Since $I_c = \alpha_0 I_e + (I_c)_{sat}$, (2) may be written

$$\langle i_p^2 \rangle_{av} = 2eI_c(1 - |\alpha|^2/\alpha_0)\Delta f + 2e(I_c)_{sat}(|\alpha|^2/\alpha_0)\Delta f. \quad (3)$$

Substituting

$$|\alpha|^2 = \alpha_0^2/[1 + (f/f_\alpha)^2] \quad (4)$$

where f_α is the α -cutoff frequency, we obtain, if $(I_c)_{sat} \ll I_c(1 - \alpha_0)$:

$$I_{eq} = I_c(1 - \alpha_0) \text{ for } f \ll f_\alpha, \quad (3a)$$

$$I_{eq} = 2I_c(1 - \alpha_0) \text{ for } f = f_\alpha\sqrt{1 - \alpha_0}, \quad (3b)$$

$$I_{eq} = I_c(1 - \frac{1}{2}\alpha_0) \text{ for } f = f_\alpha, \quad (3c)$$

$$I_{eq} = I_c \text{ for } f \gg f_\alpha. \quad (3d)$$

Eq. (3b) indicates that I_{eq} has risen to twice the low-frequency value at the frequency $f = f_\alpha\sqrt{1 - \alpha_0}$; for $\alpha_0 = 0.96$ this corresponds to the frequency $0.2f_\alpha$. Eq. (3c) indicates that the measurements of I_{eq} may be used to determine the α -cutoff frequency of the transistor. The value thus obtained is called the "apparent" α -cutoff frequency of the transistor in this paper; it agrees closely with the value of f_α obtained by other methods.

Results of measurements on different types of transistors are shown in Figs. 2 and 3. In Fig. 2, the noise spectra of a germanium junction transistor manufactured by the Telefunken Company of Ulm, Germany, are shown. This unit has an α -cutoff frequency of about 400 kc and α_0 is 0.98. At frequencies below 50 kc, 1f noise predominates. However, at higher frequencies, the shot noise steadily increases to a maximum at about 2 mc and then decreases somewhat. This behavior is the same as that reported earlier for similar transistors,² but the readings extend to much higher frequencies. A similar graph is shown in Fig. 3 for a germanium surface barrier transistor. This unit has an α -cutoff frequency of about 15 mc. In addition to excess noise, there is a shot noise component which is relatively small and constant up to about $0.2f_\alpha$ but which increases in the neighborhood of f_α to a value many times as great. It then levels off again. This behavior is in accord with van der Ziel's theory.

The noise of an RCA drift transistor was measured in a similar way, but in this case, the maximum frequency of measurement (60 mc) was too low for the complete

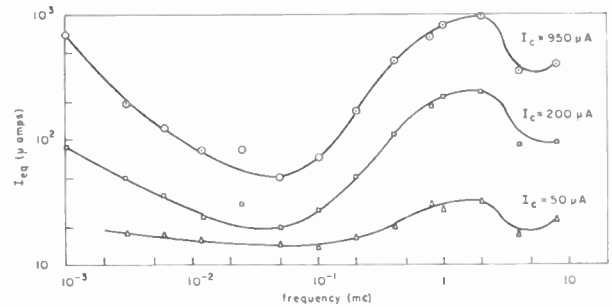


Fig. 2—Noise spectra of a low-frequency junction transistor. (The curves are not corrected for the thermal noise of the output circuit and for the induced grid noise of the first stage of the amplifier.)

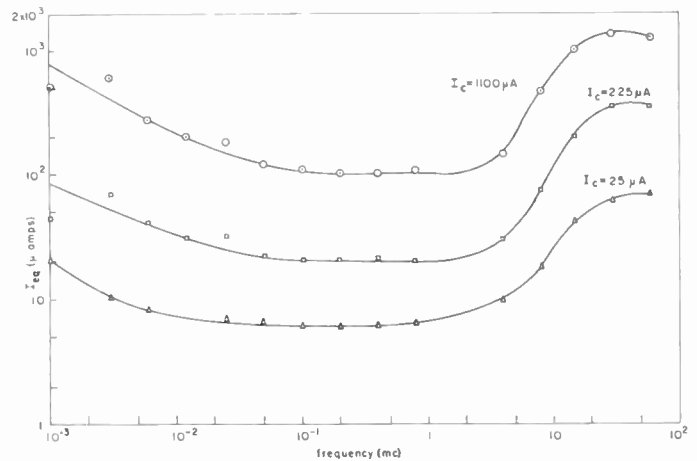


Fig. 3—Noise spectra of a surface barrier transistor. (The curves are not corrected for the thermal noise of the output circuit and for the induced grid noise of the first stage of the amplifier.)

spectrum to be obtained. There was reasonably good agreement with van der Ziel's theory at low frequencies, but it appears that for $f > f_\alpha$, the noise is increasing at a rate such that the theoretical values may be exceeded by a factor of two or so. It should be noted that (2) was obtained on the assumption that carrier motion in the base region of the transistor is due to diffusion only, whereas in this unit, the motion is partly due to drift.

A summary of the measurements and the corresponding theoretical values for several transistors is given in Table I. All of the measurements reported in this paper were taken with a collector voltage of 1 volt. The shot noise is not directly dependent on collector voltage. However, there is an indirect relation, based on the dependence of f_α , α_0 , and $(I_c)_{sat}$ on collector voltage.

In each case comparisons are made for $f \ll f_\alpha$ and for $f \gg f_\alpha$. In addition, the apparent values of f_α , as deduced from the noise measurements, are given. In almost all cases, the differences are less than the corresponding experimental errors. The agreement between I_{eq} and $I_c(1 - \alpha_0)$ is not very good for the first transistor, but here the condition $(I_c)_{sat} \ll I_c(1 - \alpha_0)$ was not satisfied. Making the necessary corrections gives reasonable agreement in this case too. As a result, there can be little doubt as to the correctness of the theory as it applies to the equivalent saturated diode current. It is important

TABLE I
COMPARISON OF SOME THEORETICAL AND EXPERIMENTAL QUANTITIES RELATING TO THE EQUIVALENT SATURATED DIODE CURRENT OF A TRANSISTOR. ALL CURRENTS ARE IN MICROAMPERES

Transistor Type	I_c	I_{eq} (hf)	α_0	$(1-\alpha_0)I_c$	$(I_c)_{sat}$	$I_{eq}(lf)$	f_α (Apparent)
Germanium junction	950	1000	0.976	23	5	40	500 kc
	200	240	0.978	4	5	18	450 kc
	50	35	0.978	1	5	10	400 kc
Silicon surface barrier	525	420	0.916	44	<0.001	42	6 mc
	35	30	0.871	4		7	7 mc
Germanium surface barrier	1100	1360	0.923	85	0.2	90	10 mc
	25	20	0.923	2		3	12 mc
Germanium surface barrier	740	700	0.720	205	0.5	195	30 mc
	35	30	0.680	11		9	20 mc
Germanium diffused base	1100	(2000)	0.98	22	—	11	30 mc

to note that the agreement exists for transistors whose α -cutoff frequencies differ by more than 100 to 1.

The data given in Table I are for shot noise only, the contributions of lf noise and of thermal noise generated in the biasing resistors having been subtracted. A further correction has been made at high frequencies to account for the fact that the thermal noise voltage developed between b' and b is not negligible in comparison with the noise voltage developed across the collector capacitance C_c . (See Fig. 1.) We then have for the open circuit noise voltage at the output, providing $1/\omega C_c \ll r_c$,

$$\langle e^2 \rangle_{av} = 4kTr_b \Delta f + (2eI_{eq} \Delta f) / \omega^2 C_c^2 = [r_b^2 + 1/\omega^2 C_c^2] 2eI_{eq}' \Delta f. \tag{5}$$

Here I_{eq} is the true equivalent saturated diode current of the noise current generator i_p , and I_{eq}' is the value measured. Solving (5) for I_{eq} yields

$$I_{eq} = I_{eq}'(1 + \omega^2 C_c^2 r_b^2) - (2kT/e)\omega^2 C_c^2 r_b. \tag{6}$$

This effect is at least partly responsible for the apparent decrease in noise at the high frequency end of the curves in Fig. 2.

Corrected experimental curves for a Philco silicon transistor are shown in Fig. 4, together with theoretical curves based on (2). The α -cutoff frequency assumed in obtaining the theoretical curves is that which gives the best fit to the experimental data. The close agreement between theory and experiment is evident from this graph.

Some measurements were made at zero emitter current to determine whether the collector current $(I_c)_{sat}$ shows full shot noise at all frequencies (except for the lf component, of course). For a silicon transistor, for which $(I_c)_{sat}$ is less than $0.01 \mu\text{amp}$, only noise corresponding to the thermal noise of the input and output circuits was found. However, for a germanium transistor with an $(I_c)_{sat}$ of $8 \mu\text{a}$, the measured values of I_{eq} were about $8 \mu\text{a}$ above the thermal noise level of the output stage for a frequency range extending well beyond f_α . Thus, it may be concluded that the collector saturated current shows full shot effect at all frequencies, in agreement with the theory.

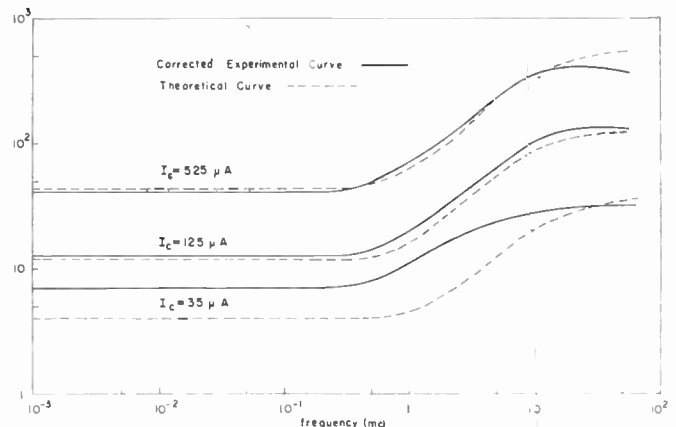


Fig. 4—Comparison of theoretical and experimental values of noise for a surface barrier silicon transistor. (Corrected for the thermal noise of output impedance, the induced grid noise of the first stage of the amplifier and for the influence of r_b .)

MEASUREMENT OF $\langle e_s^2 \rangle_{av}$ AND $\langle e_s^* i_p \rangle_{av}$ AND COMPARISON WITH THE THEORY

The magnitude of the noise generator e_s and the correlation between e_s and i_p cannot be measured directly. However, these quantities can be determined indirectly from measurements of noise figure. The method will be outlined here.

The noise figure of a transistor operated in the grounded base connection may be obtained by considering Fig. 1. The result is

$$F = 1 + \frac{r_b}{R_s} + \frac{|-e_s + i_p Z_{tot} / \alpha|^2}{4kTR_s \Delta f}, \tag{7}$$

where $Z_{tot} = Z_s + Z_b + r_b$.

Let e_s be split into a part e_s' that is completely correlated with i_p and a part e_s'' that is uncorrelated with i_p . That is,

$$e_s = e_s' + e_s''; \quad \overline{e_s'' i_p} = 0. \tag{8}$$

One may then introduce the quantities I_{eq} , R_{ns} , and Z_1 such that

TABLE II
NOISE PROPERTIES OF TRANSISTORS DEDUCED FROM MEASUREMENTS OF NOISE FIGURES AT LOW FREQUENCIES

Transistor Type	Frequency	$I_c(\mu\text{A})$	$I_{eq}(\mu\text{A})$	I_{eq} (Direct)	$R_{ns}(\Omega)$	$r_e/2(\Omega)$	$R_1(\Omega)$	c
Germanium surface barrier 1)	400 kc	20	4.6	3.0	510	600	115	0.052
		220	23	18	81	53	33	0.068
		1100	107	100	192	11	4	0.016
Germanium surface barrier 2)	400 kc	30	11.5	9	225	305	360	0.17
		65	22	20	125	150	180	0.23
		240	75	65	66	39	98	0.44
		700	204	200	9	13	16	0.16
Germanium-diffused base	800 kc	1050	29	30	23	12	30	0.13
Silicon surface barrier	400 kc	19	10	8	585	625	100	
		540	58	60	25	22	-100	

$$\langle i_p^2 \rangle_{av} = 2eI_{eq}\Delta f, \tag{9}$$

$$\langle e_s'^2 \rangle_{av} = 4kTR_{ns}\Delta f, \tag{10}$$

$$Z_1 = \alpha e_s' / i_p \tag{11}$$

Under the conditions $Z_e = R_e$, $Z_1 = R_1$ (low frequencies), substitution of (9), (10), and (11) into (7) yields,

$$F = 1 + 2 \left(\frac{e}{2kT} \right) \frac{I_{eq}}{|\alpha|^2} (R_e + r_{b'} - R_1) + \frac{e}{2kT} \frac{I_{eq}}{|\alpha|^2} R_s + \frac{(R_{ns} + r_{b'}) + \left(\frac{e}{2kT} \right) \frac{I_{eq}}{|\alpha|^2} (R_e + r_{b'} - R_1)^2}{R_s} \tag{12}$$

which may be written as

$$F = A + BR_s + C/R_s. \tag{13}$$

Thus, it is possible to measure F as a function of the source resistance R_s and to determine A , B , and C from the measurements. One may then calculate I_{eq} , R_{ns} and R_1 and from them $\langle e_s'^2 \rangle_{av}$ and $\langle e_s^* i_p \rangle_{av}$. Comparing (12) and (13) yields, for example:

$$I_{eq} = (2kT/e) |\alpha|^2 B, \\ R_e + r_{b'} - R_1 = \frac{1}{2}(A - 1)/B, \\ r_{b'} + R_{ns} = C - \frac{1}{2}(A - 1)^2/B. \tag{13a}$$

Expressions for R_{ns} and R_1 are given by van der Ziel where it is shown, for example, that $R_1 = 0$ and $R_{ns} \approx \frac{1}{2}r_e$ at low frequencies; here r_e is the resistance of the emitter junction.

A typical graph of F as a function of R_s is shown in Fig. 5 for a surface barrier transistor. A theoretical curve, based on (13), has been fitted to the experimental points and is shown as a dashed line. It is to be noted that the value of the source resistance corresponding to minimum noise figure is strongly dependent on collector current.

The results of noise figure measurements on several transistors are shown in Table II (above). The transistors are: 1) a Philco surface barrier transistor with

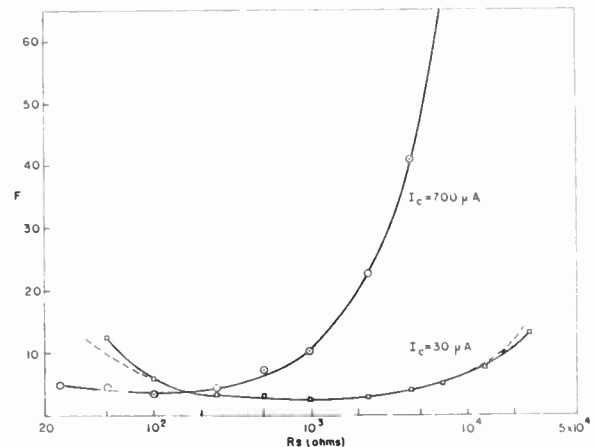


Fig. 5—Noise figure of a surface barrier transistor as a function of source resistance.

$\alpha_0 = 0.95$ and $f_\alpha = 15$ mc, 2) an experimental (1954) surface barrier transistor with $\alpha_0 = 0.70$ and $f_\alpha = 50$ mc, 3) a Philco silicon transistor with $\alpha_0 = 0.90$ and $f_\alpha = 6$ mc, and 4) an RCA drift transistor. In addition to the quantities I_{eq} , R_{ns} , and R_1 discussed above, three other quantities are tabulated for comparison. These are: the equivalent saturated diode current I_{eq} measured directly as described in the previous section, the correlation coefficient c , and $r_e/2$, r_e being the resistance of the forward biased emitter junction. The correlation coefficient c is defined by

$$c = \langle e_s^* i_p \rangle_{av} [\langle e_s'^2 \rangle_{av} \cdot \langle i_p^2 \rangle_{av}]^{-1/2} \tag{14}$$

and can be expressed in terms of I_{eq} , R_1 , R_{ns} .

Each of the quantities I_{eq} , R_{ns} , and c may be compared with their theoretical values. In the case of I_{eq} , it is better to compare the values obtained in the above manner with those obtained by direct measurement as described in the previous section. The agreement, as shown in Table II, is excellent at all operating points.

The agreement between R_{ns} and $\frac{1}{2}r_e$ is not so good, although the theoretical and experimental values differ by less than a factor of two. The reason for the rather large errors is that, in the calculation of R_{ns} in terms of the observed values of A , B , and C from (13a), the quantity $(r_{b'} + R_{ns})$ is expressed as a difference between

two terms of comparable size. It may be said that the agreement is as close as could be expected from the accuracy of the measurements.

The theory predicts that the correlation coefficient c should be nearly zero, except for small values of I_c comparable with $(I_c)_{\text{sat}}$. The values for c shown in the table were calculated from the experimental data; if one takes into account the large limit of experimental error (especially for the drift transistor), one may conclude that the agreement with theory is good. The only important exception is a high frequency surface barrier transistor with a low value of α_0 ; here the determination of c was much more accurate and the deviation between theory and experiment is far outside the limit of experimental error. Since this transistor has a rather low emitter efficiency, which is the main cause for the low value of α_0 , one might be tempted to attribute the discrepancy to this fact; unfortunately a more detailed theoretical investigation does not seem to support this view.

One may calculate the relative contributions of e_s and of i_p to F . For a surface barrier transistor, calculation shows that at high collector currents i_p is by far the more important quantity, even for low values of R_s . However, at low currents, e_s gives the greater contribution if R_s is small, but its contribution is still almost negligible if R_s is large.

The above calculations, together with data such as shown in Fig. 5 enable one to specify conditions under which transistors should be operated if a low noise figure is required. These conditions may be summarized as follows:

- 1) The collector current should be relatively small. This reduces the contribution of the noise current generator i_p . However, at extremely low currents, the noise generator e_s is important and, furthermore, the reduction in α prevents the quantity $(i_p Z_{\text{tot}})/\alpha$ from changing much.
- 2) The transistor should have a small collector saturated current $(I_c)_{\text{sat}}$.
- 3) The source resistance R_s should be that which yields minimum noise figure at the operating point in question. It is necessary to change R_s if I_c is changed.
- 4) The transistor should have α_0 very close to unity. This will reduce the contribution of the noise generator i_p .
- 5) The α -cutoff frequency of the transistor should be high enough so that the increase in noise near f_α does not degrade the average noise figure for the frequency range being used.

The above criteria relate to noise considerations only. The conditions for maximum gain may be quite different. When the frequency range is such that excess noise is important the above results may also be modified.

However, the condition of low collector current will very likely be desirable in those circumstances also.

After this paper was completed, articles by Guggenbuehl and Strutt³ and by Nielsen⁴ were published. Their results agree quite well with our data, and in some cases considerably extend them. Nielsen simplified the equivalent circuit by neglecting the correlation between e_s and i_p and found that the simplified circuit agreed quite well with the experimental data. Guggenbuehl and Strutt use equivalent but somewhat different formulas for the noise figure and also find good agreement between theory and experiment. At high frequencies and high-current levels they report deviations between theory and experiments.

Our results do not extend to sufficiently high currents to verify their results.

CONCLUSION

The measurements of equivalent saturated diode current at the output with open input have established the characteristics of the noise current generator i_p . The close agreement with an existing theory of transistor noise verifies the theory in a convincing manner. It has been found that the collector saturated current of a transistor shows full shot effect up to frequencies well above the α -cutoff frequency. This result is in agreement with the above theory.

The measurements of noise figure at low frequencies have yielded information about e_s . In addition, it has been found that there is some correlation between the two noise sources for some transistors, but that in others there is little or no correlation. These results give further support to the theory despite some disagreement regarding the correlation coefficient.

The measurements indicate that in order to design circuits with low-noise figures it is best to choose transistors with small $(I_c)_{\text{sat}}$ with α_0 near unity and f_α much higher than the maximum frequency of operation. The transistor should be operated at a relatively small collector current and the source resistance should be carefully chosen.

ACKNOWLEDGMENT

The transistors used in this investigation were provided by the following: Dr. W. H. Forster of the Philco Corporation; Dr. E. W. Mueller of RCA Laboratories; Dr. W. L. Leverton of the Raytheon Manufacturing Company, and Dr. H. Roth of Telefunken A. G., Ulm, Germany.

The authors are grateful to each of these individuals and organizations for their assistance.

³ W. Guggenbuehl and M. J. O. Strutt, "Theory and experiments on shot noise in semiconductor junction diodes and transistors," *Proc. IRE*, vol. 45, pp. 839-854; June, 1957.

⁴ E. Nielsen, "Behavior of noise figure in junction transistors," *Proc. IRE*, vol. 45, pp. 957-963; July, 1957.

Correspondence

Spectrum Analyzer for Whistlers*

I read with interest the paper by Grierson¹ in which he describes the need for a high-speed multiple-filter spectrum analyzer for audio frequencies and states that no instrument of this type is available because of filter tolerance requirements and necessity for a multiple display system.

Raytheon's Missile Systems Division has been selling for several years instruments similar to the one described in the paper. These analyzers have 420 narrow-band magnetostriction filters and a high-speed capacitance commutator for sampling the filter response voltages. A typical model analyzes 10.5 kc with resolution of 75 cps across the band and analysis rates of 60 or 100 scans per second.

Because of the high analysis rates, the only practical way to record analyzed data has been photography of *A*-scope or *Z*-axis oscilloscope presentations with single-frame, continuous strip, or motion picture cameras. Since Grierson's paper was written, an Alden high-speed helix recorder has been successfully used with the analyzer. This combination provides a 5-inch-wide permanent recording of frequency vs real time with amplitude indicated by the intensity or darkness of the recording. Graphs can be produced continuously without editing and with a resolution comparable to the analyzer itself.

RAYMOND R. NELSON
Raytheon Mfg. Co.
Bedford, Mass.

* Received by the IRE, June 25, 1957.

¹ J. K. Grierson, "A technique for the rapid analysis of whistlers," *Proc. IRE*, vol. 45, pp. 806-811; June, 1957.

Long Life Microwatt Batteries*

THE ZAMBONI CELL

In 1806, Behrens made voltaic cells with flints coated on one side with zinc and on the other, with copper. He also used disks of zinc, copper, and gilt paper [1].

In 1810, de Luc reported his experiments with dry cells—he called them "Electric Columns"—using zinc, silver, and writing paper [2]. In order to obtain good contact between the paper and the metals, he glued the paper to the metals, at first to both, but later to only one. He discovered that the flow of current was aided if the disk of paper was negative, and hindered if the paper was glued to the positive metallic disk.

* Received by the IRE, March 1, 1957.

These cells gave only the smallest of movements to a gold leaf electroscope, even when assembled in groups of twenty. When the paper disks were glued, the divergence of the gold leaves was five times as great.

De Luc made two cells consisting of 900 zinc, 700 tin, and 1600 gilt paper disks, with which he tried to keep a pendulum swinging, but without success until he fitted a small spring.

In 1812, Zamboni, professor of physics at Verona, improved on the de Luc arrangement by using ungunned silvered paper disks with a layer of manganese dioxide mixed with honey, on the nonmetallic side; he called the device a dry cell [3], [4].

Zamboni assembled 2000 disks tied together with silk threads and covered the outside with gum mastic. The container was a glass tube covered inside and out with sealing wax. Two of these cells were mounted vertically, five inches apart, on a brass base. Midway between the two cells he placed a movable needle, about two-thirds of the height of the cells, consisting of a fine glass tube with a small brass ring attached to the top end. The needle was pivoted and supported by a brass pedestal attached to the base. The lower end of the needle carried a crescent shaped counterweight.

The small brass ring was alternately attracted to large brass knobs mounted at the top of each cell. These knobs were connected to the top plates of the cells, one knob being positive and the other negative. Zamboni reported that the needle had been oscillating at about 30 cycles per minute for two years without interruption and that the rate of oscillation could be regulated, either by making the pendulum heavier or by moving the counterweight.

A paper published in 1814 was entitled, "An Explanation of the Zamboni Perpetual Electric Motor" [5].

In 1840, a Zamboni cell was constructed at the Clarendon Laboratory at Oxford University, where I saw it operating in 1923. Two columns containing 2000 elements of zinc, filter paper, and copper were installed under a bell jar to operate a bell. From all accounts the bell is still ringing [6].

THE ELCELL OR IMPROVED ZAMBONI CELL

All the foregoing was known well over a century ago. Today, many circuits in electronic and nucleonic work call for high potentials without any, or, at least, very small currents. Outstanding war time requirements were applications of the infrared converter tube, or "Snooper scope," the voltage requirements of which can be several thousand volts, with current requirements of the order of 0.01 to 0.04 microampere [7]-[9].

With many possible peace time applications, there may be a need for small power sources based on the Zamboni cell principle,

which offer light weight, long life, quick recovery after overload, high-short-circuit current, and possible other advantages. Light weight has been aided by the increase in voltage per disk from 0.6 v to 1.3 v.

By increasing the active area of the disks to 3, 9, 16, or 25 square inches, it is now possible to draw from 0.05 to 1 microampere continuously, and much more if the load is intermittent, as *e.g.*, pulse work. Much larger currents can be drawn if the area is increased by connecting a number of disks in parallel.

Containers must have high resistivity, or else the stacks of disks, with their high-internal resistance, may be shunted by a lower resistance path, which could gradually drain the cell.

The recovery rate after severe overload, or short-circuit conditions, is quite rapid and complete. One source of the overloading of cells with small areas may be due to reading of high voltages on a VTVM. For reading open-circuit voltages, the scale should be multiplied by placing a resistance of the order of 12,000 megohms in series with the VTVM, thus reducing the current to a small value. Alternately, electrostatic voltmeters may be used for the higher values.

Elcells have been used to construct a "decade" battery, by using ten "ones"; ten "tens," and ten "hundreds," connected to three-ceramic-type ten-position switches.

Single elements are remarkably stable over long periods, especially after stabilizing. Mass production methods can be used to produce reliable 500 and 1000 volt batteries, with taps at convenient intervals, which can be used singly or linked in series with a decade battery for voltage adjustment purposes. Cells can be trickle charged, if higher voltages are required temporarily.

As the continuous rating depends on the area of the coating, there is no limit to the current which may be drawn, with large increases in the short-circuit currents. For example, two 1-volt batteries, each with 540 square inches of active surface, have been used to operate continuously an oscillating circuit at af and uhf for long periods, using a transistor drawing 10 microamperes.

The short-circuit current of a 540 square inch (45 elements of 12 square inches in parallel) 1-volt battery is in the order of 24 milliamperes and one can draw intermittent currents of this magnitude for very short intervals. These large currents will rapidly diminish if drawn continuously, but when the load is relinquished the battery will rapidly recover due to the high recuperative properties of the battery.

Thousands of square inches can be simply made on a coating machine and will give 1 milliamperes and upwards, with correspondingly higher intermittent currents on low resistance loads.

As the power requirements of electronic equipment decreases with the incorporation

of solid-state active components, the use of these batteries becomes more feasible. Even now potential employment with transistors in the form of frequency (or time) references, warning systems, low-level signal sources, etc., is quite evident.

CYRIL F. ELWELL
Consulting Eng.
Hewlett-Packard Co.
Palo Alto, Calif.

BIBLIOGRAPHY

- [1] Behrens, G. B. "Das Merkwürdige aus Versuchen über Electricität," *Gilberts Ann. Phys.*, Vol. 23 (1806), pp. 1-27.
- [2] de Luc, J. A. "On the Electric Column and Atmospheric Electroscope," *Nicholson's J. Nat. Phil.*, Vol. 27 (May, 1810), pp. 81-99.
- [3] Gilbert L. W., De Luc, and Zamboni. "Historical Note on Their Dry Electric Cell," *Gilberts Ann. Phys.*, Vol. 49 (1815), pp. 35-61, 67-99, 100-128.
- [4] "Dissertation on the Electric Dry Pile," *Brugnatelli's Giornale di Fisica*, Vol. 5 (December, 1812), pp. 424-446; Vol. 6 (January, 1813), pp. 31-43.
- [5] Assalini. "An Explanation of the Perpetual Electric Motor," *Giornale dell'Adige* (1814).
- [6] *Corrosion*, (February, 1948), p. 5.
- [7] Morton, G. A., and Flory, L. E. *Electronics*, Vol. 19 (September, 1946), pp. 112-114.
- [8] Pratt, T. H. "The Infra-Red Converter Tube," *Electronic Eng.*, Vol. 20 (September, 1948), pp. 274-278.
- [9] Elliott, A. "The Dry Voltaic Pile," *Electric Eng.*, Vol. 20 (October, 1948), pp. 317-319.

Masers and Reactance Amplifiers—Basic Power Relations*

The general power relations for nonlinear reactance amplifiers were developed in a paper by Manley and Rowe.¹ These power relations are simple, but the analysis from which they were obtained is rather sophisticated. In a recent communication,² Weiss presented similar power relations for the related quantum-mechanical amplifiers designated generically as Masers. Weiss derived the latter relations in a simple and elegant way by using the principle of detailed balancing and the Planck energy relation $E = hf$. These power relations are fundamental not only to quantum-mechanical amplifiers such as the Maser and the Suhl magnetic amplifier,³ but also to the older "classical" counterparts known as the dielectric and magnetic amplifiers. For this reason, an alternative simple and nonquantum-mechanical derivation of the power relations given by Manley and Rowe is desirable. Such a derivation is presented here.

Consider a nonlinear capacitance modulator consisting of a lossless device, whose charge vs voltage characteristic is nonlinear, in series with two sources and a load circuit. For the latter elements assume the following: each of the source voltages is sinusoidal with characteristic frequencies f_1 and f_2 , respectively. To avoid the degenerate case for which the sum and difference frequencies

coalesce with the harmonic frequencies, f_1 and f_2 are assumed incommensurable. The internal source impedances are significant only at their respective source frequencies. The load circuit impedance is significant only at the combination frequency $f_3 = (mf_2 \pm nf_1)$, where m and n may be any of the integers 1, 2, 3, The load circuit voltage is thus also sinusoidal with characteristic frequency f_3 .

The voltage applied to the nonlinear capacitor is the sum of the load voltage and the two source voltages minus the corresponding internal source-impedance voltage drops. Since these voltages are all sinusoidal and since the charge vs voltage characteristic of the capacitor is nonlinear, the resultant charge is periodic and representable in general by a dc term and a series of sinusoidal terms in the fundamental and harmonics of f_1 and f_2 and in all possible sum and difference combinations of f_1 and f_2 . The amplitudes and phases of these terms are functions of the specific nonlinear device characteristic and of the amplitudes and phases of the three voltages, but not of the frequencies. These conclusions are reached directly if the nonlinear characteristic is represented, as it can be, by a power series in the voltage. The common steady-state current is the time derivative of the charge and therefore is representable by a similar series. The amplitudes of the terms in the current are proportional to the product of frequency and amplitude of the corresponding terms in the charge.

Since the nonlinear capacitor is lossless, conservation of energy requires that the sum of the load power, P_3 , and the external powers, P_1 and P_2 , supplied by the sources, be zero.

$$P_1 + P_2 + P_3 = 0. \quad (1)$$

Each term in (1) represents an average power, given by the dc term arising from the product of the appropriate voltage and the common current. The dc term in such products can only arise from the product of voltage and current of like frequency; the result is the familiar expression

$$P = (VI/2) \cos \phi \\ = f(\pi V^2 Q \cos \phi) = f\omega, \quad (2)$$

where V , I , and Q are the respective amplitudes of the voltage, current, and charge in the corresponding terms of frequency f , and ϕ is the phase angle between voltage and current or charge. The quantity ω is the energy per cycle; it is analogous to the quantity Nh in the Weiss paper.²

From (2) the expressions for the external energy per cycle supplied by each source and for the load are

$$\omega_1 = (\pi V_1 Q_1 \cos \phi_1) = P_1/f_1 \\ \omega_2 = (\pi V_2 Q_2 \cos \phi_2) = P_2/f_2 \\ \omega_3 = (\pi V_3 Q_3 \cos \phi_3) = P_3/f_3 \\ \epsilon_3 = mf_2 \pm nf_1. \quad (3)$$

The result of combining (1) and (3) is

$$f_1(\omega_1 \pm m\omega_3) + f_2(\omega_2 + m\omega_3) = 0. \quad (4)$$

As observed earlier, the amplitudes and phases of the charge components are functions only of the nonlinear device characteristic and of the amplitudes and phases of the

three voltages. However, the load voltage and current or charge are connected by the load circuit impedance, which is a function of f_3 . Therefore the charge amplitudes and phases in (3) are also functions of f_3 . Since f_3 is a linear combination of f_1 and f_2 and not a function of their ratio, the only admissible solution of (4) is the set

$$\omega_1 \pm m\omega_3 = 0 \\ \omega_2 + m\omega_3 = 0. \quad (5)$$

By using (3), (5) can be rewritten as

$$-P_3/(mf_2 \pm nf_1) = P_2/mf_2 = \pm P_1/nf_1. \quad (6)$$

Eq. (6) is the Manley-Rowe power relation for a load circuit responsive only to the sum or difference frequency $f_3 = (mf_2 \pm nf_1)$. The minus sign before P_3 indicates that the load absorbs power. If the load is responsive only to the sum frequency, both sources supply power to the load. When the load is arranged to absorb no power, $P_3 = P_2 = P_1 = 0$. Thus there can be no interchange of power between the sources unless an absorbing load is present. The ratio of the power absorbed by the load to the power supplied by source 1 is $-(P_3/P_1) = 1 + (mf_2/nf_1)$. This is the theoretical stable gain obtained by a lossless dielectric or magnetic amplifier. Such an amplifier consists of a signal source of frequency f_1 , an rf power source of frequency f_2 , and a sum-frequency load circuit whose output is subsequently demodulated.

If the load is responsive only to the difference frequency, both load and source 1 absorb power from source 2. This is the basis for the negative resistance type of amplifier exemplified by the multilevel Maser amplifiers and the Suhl magnetic amplifier. In these amplifiers source 2 is a "pumping" source of rf power whose frequency f_2 is equal to the sum of the signal frequency f_1 and the frequency $f_3 = (f_2 - f_1)$ of a built-in or "concealed" circuit. Power is transferred from source 2, whose frequency f_2 is the highest of the three frequencies f_1 , f_2 , f_3 to the signal source and to the "concealed" circuit. In the language of circuit theory, this process results in the presence of a negative resistance across the signal circuit. If the magnitude of this shunt negative resistance is greater than the effective shunt resistance of the signal circuit, the signal voltage is augmented; this represents an amplification of the signal. If the magnitude of the shunt negative resistance is less than the effective shunt resistance of the signal circuit, oscillation can occur.

If the load consists of two circuits in series, one responsive only to the sum frequency $f_+ = (mf_2 + nf_1)$ and the other responsive only to the difference frequency $f_- = (mf_2 - nf_1)$, (6) becomes

$$(P_1/nf_1) + (P_+/f_+) - (P_-/f_-) = 0 \\ (P_2/mf_2) + (P_+/f_+) + (P_-/f_-) = 0. \quad (7)$$

When $n = m = 1$, (7) becomes identical with the power relations developed by Weiss for the four-level Maser.

The general Manley-Rowe power relations can be obtained simply by considering the load as a series of circuits, each responsive only to a single combination frequency and including enough circuits to account for all possible sum and difference frequencies. For the case of two sources and 2 m load

* Received by the IRE, August 16, 1957.

¹ J. M. Manley and H. E. Rowe, "Some general properties of nonlinear elements—Part I. General energy relations," *Proc. IRE*, vol. 44, pp. 904-913; July, 1956.

² M. T. Weiss, "Quantum derivation of energy relations analogous to those for nonlinear reactances," *Proc. IRE*, vol. 45, pp. 1012-1013; July, 1957.

³ H. Suhl, "Proposal for a ferromagnetic amplifier in the microwave range," *Phys. Rev.*, vol. 106, pp. 384-385; April 15, 1957.

circuits, (4) remains the same except that the coefficients of f_1 and f_2 each contain $(2m+1)$ terms in the w 's. If there is only one source and m (harmonic) load circuits, (4) simplifies to the form $f_1 \cdot (w_1 + \text{sum of } w_m's) = 0$. Further extension to multiple sources and loads is straightforward.

Although the foregoing derivation was developed specifically for a lossless nonlinear capacitor, the method is equally valid for a lossless nonlinear inductor. The results in both cases are identical; the power relations involve only the source and load frequencies and are independent of the specific characteristics of the nonlinear device.

I am indebted to my colleagues, Dr. E. G. Fubini and E. W. Sard, for helpful discussion.

BERNARD SALZBERG
Airborne Instruments Laboratory, Inc.
Mineola, N. Y.

Very Narrow Base Diode*

The following comments are offered as a supplement to the above interesting paper.¹

It is perhaps worthwhile to point out that the current-voltage characteristics of a narrow base diode come readily from Shockley's² original solution for the characteristics of a $p-n-p$ transistor by letting the collector current density equal³ $-q p_n s [\exp qV_c/kT - 1]$, in which V_c represents the collector-base voltage.

It is also interesting to note that the small amplitude ac behavior of a narrow base diode with thickness w is like that of a transmission line with length w which has a characteristic admittance

$$Y_0 = \frac{Aq^2 p_n D}{kTL} (1 + j\omega\tau)^{1/2} \exp qV_j/kT \quad (1)$$

terminated by an admittance

$$Y_t = j\omega C_s + \frac{Aq^2 p_n s}{kT} \exp qV_j/kT \quad (2)$$

in which C_s represents the capacitance of the "ohmic" contact, which can be neglected with a sufficiently good ohmic contact. Therefore, the admittance may be written

$$Y = j\omega C_b + Y_0 \frac{1 + r \exp - 2w(1 + j\omega\tau)^{1/2} L^{-1}}{1 - r \exp - 2w(1 + j\omega\tau)^{1/2} L^{-1}} \quad (3)$$

in which r is the current reflection coefficient equal to $(Y_t - Y_0)/(Y_t + Y_0)$. Neglecting the capacitances C_s and C_b , (3) gives the same admittance as (11) of Rediker and Sawyer.

B. R. GOSICK
Motorola, Inc.
Phoenix, Ariz.

* Received by the IRE, July 26, 1957.
¹ R. H. Rediker and D. E. Sawyer, *Proc. IRE*, vol. 45, pp. 944-953; July, 1957.
² W. Shockley, "The theory of $p-n$ junctions in semi-conductors and junction transistors," *Bell Sys. Tech. J.*, vol. 28, pp. 435-490; July, 1949.
³ All symbols agree with those of Rediker and Sawyer, *loc. cit.*, except as noted.

The Use of Surface Weather Observations to Predict the Total Atmospheric Bending of Radio Rays at Small Elevation Angles*

Recent investigations of the atmospheric bending of radio rays have been based upon either a smoothed long term average refractive index profile¹ or refractive index profiles derived from "mandatory" standard pressure level data from radiosonde observations^{2,3} neither of which includes the effects of commonly observed marked departures of the actual refractive index profile from the smoothed profiles so obtained. It is the purpose of the present study to evaluate any possible effects of these departures by use of the radiosonde "significant" level data. Even with allowance for these departures from a smooth profile, it will be shown that the surface value of the refractivity alone may be used to predict the total bending with useful accuracy even for elevation angles of arrival or departure, θ_0 , as small as 10 milliradians. The analysis was extended to $\theta_0=0$ by substitution of profiles with strong ground based refractive layers for the ducting profile since it was found that the rays were trapped at $\theta_0 \leq 8.8$ milliradians.

The bending, $\tau_{1,2}$, of a radio ray passing between levels in the atmosphere at which the refractivities are N_1 and N_2 , can be expressed in radians by:

$$\tau_{1,2} = - \int_{N_1}^{N_2} \cot \theta dN \cdot 10^{-6} \quad (1)$$

where θ at any point along the ray path is the acute angle between the ray and the tangent to an imaginary sphere concentric with the earth and passing through this point of the ray path.

The refractivity, N , is given by,⁴

$$N = \frac{77.6}{T} \left(P + 4810 \frac{e_s RH}{T} \right) \quad (2)$$

where P is the station atmospheric pressure in millibars, RH is the per cent of the saturation vapor pressure, e_s , in millibars at the absolute temperature, T , in degrees Kelvin.

Since the refractivity data are available only along the particular paths of ascent of the radiosondes, the use of such data to calculate radio ray bending by (1) necessitates the assumption that the atmosphere is horizontally homogeneous; all the calculated values of τ given in this paper have been obtained on this assumption.

The total bending of a radio ray passing completely through the atmosphere from the earth's surface, where $N=N_s$, to the point where $N=0$ may be obtained by integrating (1) by parts:

$$\tau = - \int_{N_s}^0 \cot \theta dN \cdot 10^{-6} = N_s \cdot 10^{-6} \cot \theta_0 - \int_{(\cot \theta)_{N=0}}^{\cot \theta_0} N d(\cot \theta) \cdot 10^{-6} \quad (3)$$

The second term of (3) contributes less than 3.5 per cent of the total for $\theta_0=10^\circ$ and becomes negligibly small as θ_0 increases. Thus the first term of (3) asymptotically approaches τ with increasing θ_0 and therefore will be referred to as the asymptotic expression.

Following the method described by Schulkin,¹ (3) was evaluated using "significant" level data. The refractive index profiles used in the present study were derived from daily radiosonde observations taken at eleven selected United States Weather Bureau observatories plus those at Fairbanks, Alaska, and Truk, Caroline Islands. The selected United States stations (Bismarck, N. D., Columbia, Mo., Denver, Colo., Ely, Nev., Joliet, Ill., Miami, Fla., Portland, Maine, San Antonio, Tex., Santa Maria, Calif., Tatoosh, Wash., and Washington, D. C.) seemed to give adequate coverage of the climatic variations found within the country. The individual radiosonde observations taken during the years 1951-1952 were examined for each observing site and an example typical of each of the following four conditions was selected from each station: the profiles associated with the maximum and minimum of the surface value of the refractivity, a linear profile, and a profile with a ground-based duct. Also, if typical of the observation site, a fifth profile with an elevated duct was analyzed. Many times the linear and minimum surface value profiles were the same. The profiles, examples of which are shown in Fig. 1, were selected to obtain

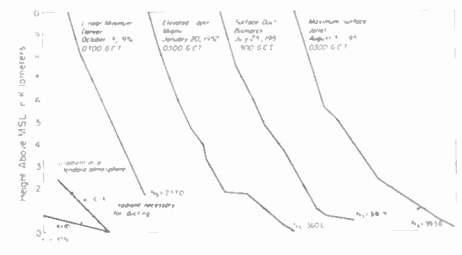


Fig. 1—Representative refractivity profiles.

a measure of the maximum variation of total bending as a function of both geographic and refractive index profile variations. The value of N_s is given with each of the profiles. The total bending was calculated for each of the selected profiles for values of θ_0 ranging from 0° to 15° . When this was done it was found that the ducting profiles trapped only those radio rays of $\theta_0 < 10$ mr. In fact, the average value of θ_0 for which the present selection of ducts trapped the radio rays was 5.1 mr with a maximum observed value of 8.8 mr. The total bending was obtained for $0 \leq \theta_0 \leq 10$ mr by substituting a profile with a strong ground-based refractive layer for the ducting profiles. By this is meant a ground-based layer with a gradient between 0.130 and 0.145 N units per meter instead of the ducting gradient of at least 0.157 N units per meter.

* Received by the IRE, June 24, 1957; revised manuscript received, July 19, 1957.

¹ M. Schulkin, "Average radio-ray refraction in the lower atmosphere," *Proc. IRE*, vol. 40, pp. 554-561; May, 1952.

² G. Reber, "Tropospheric refraction near Hawaii," *IRE TRANS.*, vol. AP-3, pp. 143-144; July, 1955.

³ B. M. Fannin and K. H. Jehn, "A study of radar elevation-angle errors due to atmospheric refraction," *IRE TRANS.*, vol. AP-5, pp. 71-77; January 1957.

⁴ E. K. Smith and S. Weintraub, "The constants in the equation for atmospheric refractive index at radio frequencies," *Proc. IRE*, vol. 41, pp. 1035-1037; August, 1953.

The radiosonde observations extended from the surface to at least 15 kilometers above the observing site. The small portion of total bending produced by the atmosphere above the radiosonde observation was evaluated by assuming an exponential decay of refractivity with height⁶ with no allowance for ionospheric refraction.

These total bendings were then examined by comparing all values at a common θ_0 . It was noted, for $\theta_0=15^\circ$, that the maximum total bending at each station was obtained from the profile having the maximum value of N_s . This was in contrast to $\theta_0=0.57^\circ$ (10 mr) where 8 of the 13 stations have the maximum value of total bending associated with a profile characterized by a surface-based duct. Thus, except for low angles, the total bending does not appear to be a sensitive function of the refractivity profile. Further, it was observed that the value of total bending obtained from a particular profile type from one particular observation site would be greater or less than the total bending obtained from a similar profile at another location, depending upon whether the value of N_s was greater or less at the first observation point. Thus, the conclusion that generally greater total bending is observed with the higher values of N_s regardless of geographic location or profile type led to the pooling of all the total bendings calculated at a common θ_0 . These data, given on Fig. 2 for $\theta=0^\circ, 1^\circ, 3^\circ$, and 15° , indicate

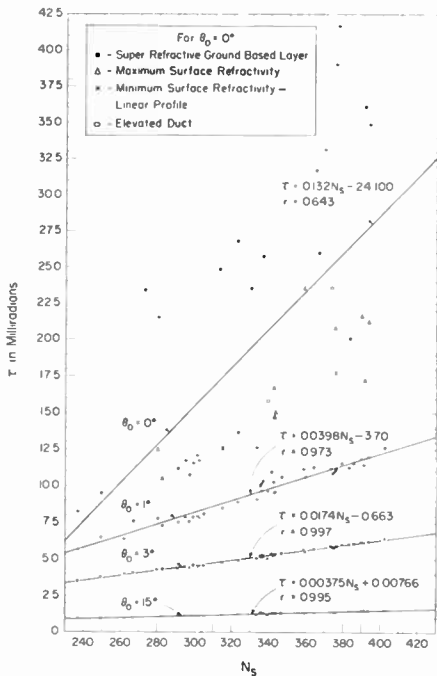


Fig. 2—Regression lines of total bending, τ , on the surface refractivity, N_s .

that τ appears to be a linear function of N_s . This suggests that the following regression relations might be employed to predict the total bending in terms of N_s , assuming that N_s is measured with negligible error:

⁶A. C. Stickland, "Refraction in the Lower Atmosphere and its Applications to the Propagation of Radio Waves," pp. 253-266, *Meteorological Factors in Radio-Wave Propagation*, Rep. of a conference held on April 8, 1956 at the Royal Inst. London, by The Phys., Soc. and The Royal Meteorological Soc.

TABLE I
Values of b and a in the regression equation $\tau = bN_s + a$, where: τ is the total bending in milliradians, N_s the value of the radio refractivity at the earth's surface, b the change in total bending expressed in milliradians per unit change in N_s and a is the zero intercept.

θ_0 (mr)	$\bar{\tau}$ (mr)	r	b	a (mr)	SE (mr)	s_τ	ρ
0.0	19.94	0.643	0.1318	-24.10	6.75	8.81	23.4 per cent
1.0	17.48	0.740	0.1030	-16.91	4.02	5.98	32.8 per cent
10.0	11.85	0.891	0.0537	-6.05	1.17	2.57	54.5 per cent
17.5	9.57	0.973	0.0398	-3.70	0.402	1.74	76.9 per cent
30.0	7.34	0.992	0.0275	-1.84	0.150	1.18	87.3 per cent
52.3	5.15	0.997	0.0174	-0.663	0.0553	0.746	92.6 per cent
261.5	1.26	0.995	0.00375	+0.00766	0.0161	0.161	89.9 per cent

r is the correlation coefficient.
SE is the standard error of prediction using the regression line.
 s_τ is the standard deviation of the calculated values of the total bending.

$$\tau = bN_s + a \quad (4)$$

Examples of such regression lines are given on Fig. 2 and statistics pertinent to all of them are given in Table I. (Note the relatively large correlation coefficients, r , even for $\theta_0 = 0$.)

In Table I, SE is the standard error of predicting the total bending from the regression line, while the final column, headed ρ , is the percentage reduction of the uncertainty of estimating τ by using these regression lines:

$$\rho = \left(1 - \frac{SE}{s_\tau}\right) 100 \text{ per cent.} \quad (5)$$

These percentage reductions assume that the atmosphere is horizontally homogeneous and do not consider the fact that the profile characteristics in one portion of the ray path might tend to counterbalance those for other portions of the ray path, with the result that the total bending could be expected to be nearer the value obtained by the regression line. For this reason, the standard errors of prediction given in Table I are perhaps too large.

It is observed that more of the uncertainty in estimating τ is removed by using the regression line as θ_0 increases. Even though this error is relatively large at $\theta_0 \leq 10$ mr, it appears that the best practical estimate of τ would be obtained from these regression lines since they depend only upon N_s , which is readily available, rather than detailed knowledge of the refractivity profile which is not generally available. The fact that ducts were omitted from this analysis at $\theta_0 < 10$ mr does not exclude this range of θ_0 from normal applications of the results since, as Cowan's analysis of radiosonde data has shown,⁸ the maximum monthly incidence of ground-based ducts in the United States is less than 25 per cent.

Interpolation for θ_0 may be done by reference to Fig. 3 where values of slope, b , and zero intercept, a , are given as a function of θ_0 . The values of the zero intercept are given as " $a+30$ " to facilitate graphical presentation. The asymptotic expression is used to estimate a and b for $\theta_0 > 15^\circ$. These values, shown on Fig. 3 as dashed curves, would not

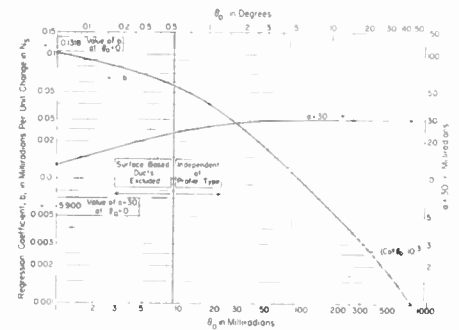


Fig. 3—Values of a and b in the expression $\tau = bN_s + a$ where b is the regression coefficient (milliradian change per unit change in N_s) and a is the value of τ when $N_s=0$.

be expected to differ from those of the regression line by more than the 0.02 mr observed at $\theta_0=15^\circ$.

The seasonal or geographic variation of the total bending may be conveniently estimated by reference to climatic variation of N_s .^{7,8}

The authors gratefully acknowledge the suggestions of K. A. Norton and the general assistance of Mrs. D. P. Gates.

B. R. BEAN
and B. A. CAHOON
National Bureau of Standards
Boulder, Colo.

⁷B. R. Bean, "Some meteorological effects on scattered radio waves," IRE TRANS., vol. CS-4, pp. 32-38; March, 1956.

⁸B. R. Bean, "Sur l'utilisation des observations météorologiques courantes en propagation radio-électrique," *Ondé Elect.*, no. 362, pp. 411-415; May, 1957.

Arc Prevention Using P-N Junction Reverse Transient*

The minority carrier storage phenomenon in p-n junctions will permit a transient reverse current to flow through a junction after the bias is switched from the forward to the back direction. The duration of the

⁸L. W. Cowan, "A radio climatology survey of the U.S.," *Proc. Conf. on Radio Meteorology*, Univ. of Texas, Austin, Texas, art. III-3; November 9-12, 1953.

* Received by the IRE, March 19, 1957; revised manuscript received, July 22, 1957.

reverse transient depends, in part, on the lifetimes of the minority carriers and the magnitudes of the forward and back biases. For typical commercially available junction diodes, the reverse resistance will vary by several orders of magnitude within a few microseconds after the bias is switched negative. This rapid variation in resistance has been used to provide a temporary low resistance shunt across a pair of relay contacts. This prevents the full load voltage from appearing across the relay contacts until they are well separated, thereby eliminating the usual arc, and also providing a faster over-all current breaking action.

The circuit of Fig. 1 represents a normal relay-controlled circuit if switch *S* is open.

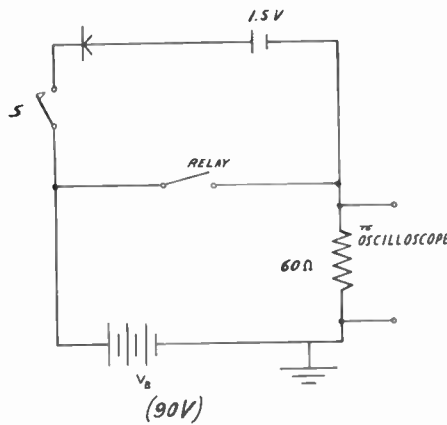


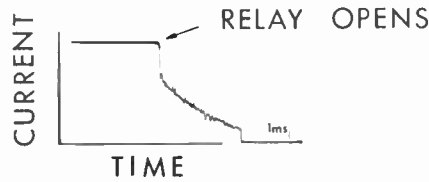
Fig. 1—Relay-controlled circuit with biased *p-n* junction across contacts.

Fig. 2(a) is an oscillogram of the current through the load at relay break, with *S* open. An arc is drawn for about 3 milliseconds. The oscillogram in Fig. 2(b) was obtained on relay make, with *S* open. The contact bounce is quite evident, and an arc is drawn on each bounce.

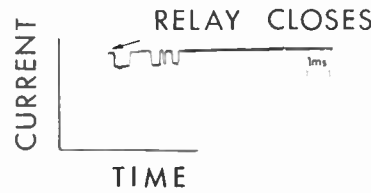
If the switch *S* is closed, the junction has a 1.5-volt forward bias whenever the relay contacts are closed. When the relay contacts are opened, the junction is biased negative and provides a low resistance shunt across the relay contacts for a few microseconds after the relay opens. Fig. 2(c) and 2(d) show the current through the load at relay break and relay make, with *S* closed. There is no discernible arcing.

The operation of the suppression circuit is further illustrated by Fig. 2(e) which was obtained with a double-beam oscilloscope. The upper trace shows the current through the load circuit dropping rapidly to zero at relay break. The lower trace shows the current through the diode and was obtained by placing a small resistor (0.5 ohm) in series with the diode and feeding the voltage across this resistor to the second input of the double-beam scope. The diode current runs forward when the relay contacts are closed, decreases as the relay contacts develop a resistance comparable to the diode forward resistance, reverses direction as the contact is broken, and returns to zero as the diode reverse resistance increases.

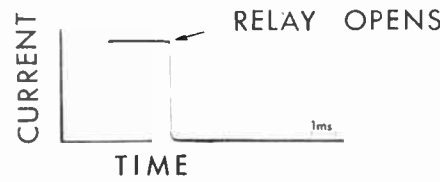
The author would like to thank C. Gadzi-ala for his assistance in carrying out the measurements.



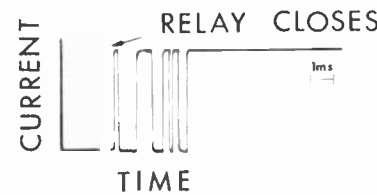
(a)



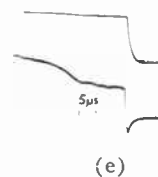
(b)



(c)



(d)



(e)

Fig. 2—Oscillograms obtained with circuit of Fig. 1. A double-beam oscilloscope was used in (e), with the second input connected so as to measure current through the diode.

WILLIAM MILLER
American Machine and Foundry Co.
Greenwich, Conn.

On Higher Order Approximations to the Solution of Nonuniform Transmission Lines*

From the familiar transmission line equations we can derive¹ the following differential equation for a nonuniform line:

* Received by the IRE, June 13, 1957.
¹ R. W. Klopfenstein, "A transmission line taper of improved design," *Proc. IRE*, vol. 44, pp. 31-35; January, 1956.

$$\frac{d\rho}{dx} - 2\gamma\rho + (1 - \rho^2)F(x) = 0 \quad (1)$$

where

$$\rho = \frac{V/I - Z_0(x)}{V/I + Z_0(x)} \quad (2)$$

$$F(x) = \frac{1}{2} \frac{d}{dx} [\ln Z_0(x)]$$

and

x = coordinate in the direction of propagation

V(*x*) = the voltage along the line

I(*x*) = the current along the line

*Z*₀(*x*) = the nominal characteristic impedance

$\gamma = \alpha + j\beta$ = the nominal propagation coefficient

α = the nominal attenuation coefficient

β = the nominal phase coefficient.

Bolinder² has shown that a good approximation to the solution of (1) can be obtained by neglecting the term $\rho^2(\rho^2 \ll 1)$. Our present aim is to find an approach leading to a solution, which can be made as accurate as desired. Thus, consider the differential equation

$$\frac{d\rho}{dx} - 2\gamma\rho + F(x) = 0 \quad (3)$$

satisfying the boundary condition $\rho(l) = 0$ (*l* is the length of the taper). Let $\rho_1(x)$ denote the solution of (3) and $\epsilon(x)$ the difference between $\rho_1(x)$ and the solution of the exact (1). The substitution of $\rho_1(x) + \epsilon(x)$ for ρ in (1) leads to

$$\frac{d\epsilon}{dx} - 2\gamma\epsilon - F(x) \cdot [\rho_1^2(x) + 2\epsilon\rho_1(x) + \epsilon^2] = 0. \quad (4)$$

The manner in which higher order approximations to the function ρ are obtained is as follows. $\rho_1(x)$ is the first-order approximation; the second-order approximation is given by $\rho_1(x) + \epsilon_1(x)$, where $\epsilon_1(x)$ is the solution of (4) with $2\epsilon\rho_1(x) + \epsilon^2$ neglected in comparison with $\rho_1^2(x)$; if only ϵ^2 is neglected, then third-order approximation is obtained.

The fourth-order approximation is obtained by substitution $\rho(x) = \rho_1(x) + \epsilon_2(x) + \mu(x)$ in (1), where $\rho_1(x) + \epsilon_2(x)$ is the third-order approximation, and so on for higher order approximations.

By proceeding in the manner indicated above, it can be shown that the second-order approximation to the $\rho(x)$ function is given by $\rho_1(x) + \epsilon_1(x)$, with

$$\epsilon_1(x) = \exp \left[2 \int_0^x \gamma d\xi \right] \int_0^x \rho_1^2(z) F(z) \cdot \exp \left[-2 \int_0^z \gamma d\xi \right] dz. \quad (5)$$

The quantity of primary interest is the input reflection coefficient $\rho(0)$, which to the first approximation is given by $\rho_1(0)$, and to the second order of quantities by $\rho_2(0)$

² E. F. Bolinder, "Fourier transforms in the theory of inhomogeneous transmission lines," *Proc. IRE*, vol. 38, p. 1354; November, 1950.

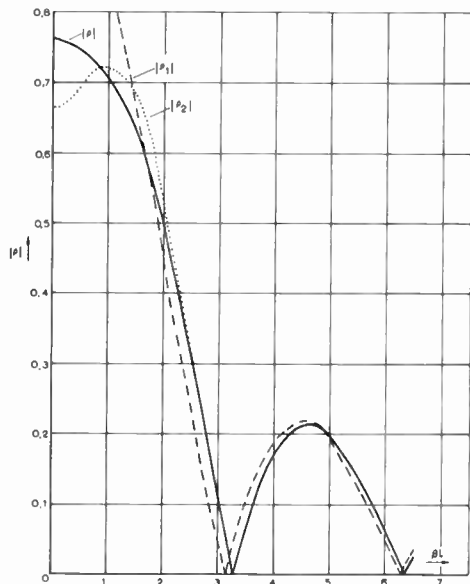


Fig. 1—Successive approximations to the reflection coefficient of the exponential taper. $|\rho|$ = the exact solution, $|\rho_1|$ = first-order approximation, $|\rho_2|$ = second-order approximation.

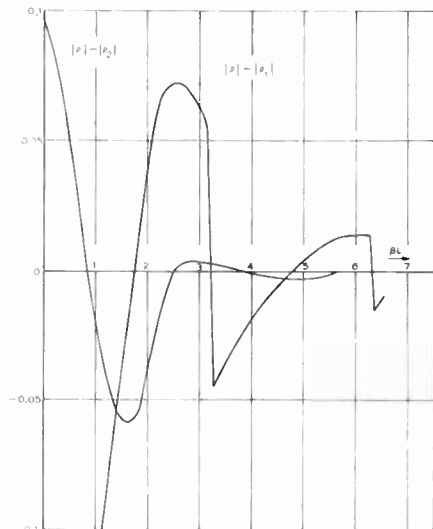


Fig. 2—The quantities $|\rho| - |\rho_2|$ and $|\rho| - |\rho_1|$ as a function of βl .

$= \rho_1(0) + \epsilon_1(0)$. These quantities are shown plotted in Fig. 1 as a function of βl and contrasted with the exact solution for the exponential taper. (β has been assumed independent of x .) Since the approximations are very good it is more instructive to plot the difference between the exact value and the approximate, as shown in Fig. 2. In this numerical example it has been assumed that $Z_2/Z_1 = e^2$.

It will be observed that, for values βl greater than about 2.5, the difference between the second-order approximation and the exact value is negligibly small. For small values of βl and particularly for $\beta l = 0$, the difference is significant. It transpires, however, that for this particular value ($\beta l = 0$) it is possible to derive expressions for the reflection coefficient in a closed form as follows. To the second order of quantities the reflection coefficient is given by

$$\rho_2(0) = \frac{1}{2} \ln \frac{Z_2}{Z_1} - \frac{1}{24} \left(\ln \frac{Z_2}{Z_1} \right)^3, \quad (6)$$

and to the third order of quantities the reflection coefficient is given by

$$\begin{aligned} \rho_3(0) &= \frac{1}{4} \ln \frac{Z_2}{Z_1} + \frac{1}{2} \exp \left[- \left(\frac{1}{2} \ln \frac{Z_2}{Z_1} \right)^2 \right] \\ &\quad \cdot \int_0^{1/2 \ln Z_2/Z_1} \exp v^2 dv \\ &= \frac{1}{2} \ln \frac{Z_2}{Z_1} - \frac{1}{24} \left(\ln \frac{Z_2}{Z_1} \right)^3 + \frac{1}{15.2^4} \left(\ln \frac{Z_2}{Z_1} \right)^5 \\ &\quad - \frac{1}{105.2^6} \left(\ln \frac{Z_2}{Z_1} \right)^7 + \dots \end{aligned} \quad (7)$$

However, it can be shown from the exact formulas that the reflection coefficient is given by

$$\begin{aligned} \frac{Z_2 - Z_1}{Z_2 + Z_1} &= 2 \sum_{k=1}^{\infty} \frac{(-1)^{k-1} (2k^2 - 1)}{(2k)!} B_k \left(\ln \frac{Z_2}{Z_1} \right)^{2k-1} \\ &= \frac{1}{2} \ln \frac{Z_2}{Z_1} - \frac{1}{24} \left(\ln \frac{Z_2}{Z_1} \right)^3 + \frac{1}{240} \left(\ln \frac{Z_2}{Z_1} \right)^5 \\ &\quad - \frac{17}{41320} \left(\ln \frac{Z_2}{Z_1} \right)^7 + \dots \end{aligned} \quad (8)$$

It will be observed from (6)–(8) that the third-order approximation is accurate up to and including the third member of the series and the fourth member is in error by a constant factor.

On a percentage basis, the reflection coefficient for $\beta l = 0$ is in error by 31.3 per cent for the first order, 12.5 per cent for the second, and 0.97 per cent for the third-order approximation, if $Z_2/Z_1 = e^2$.

LASZLO SOLYMAR
Standard Telecommunication
Labs., Ltd.
Enfield, Middlesex, England

Unilateralized Common Collector Transistor Amplifier*

A unilateralized transistor amplifier with very high input impedance, very low output impedance, and good transfer gain may be obtained with the circuit of Fig. 1. The input impedance may also be adjusted to a preset value in a wide range, thus permitting input matching. The circuit consists of a common collector amplifier where positive feedback is used to keep the input impedance constant, independent of the load. It may also be viewed as a common collector hook connection or hook p - n - p - n (or n - p - n - p transistor).

Letting Z_{sh} equal infinity at first, and assuming identical parameters for the two transistors, the input and the output imped-

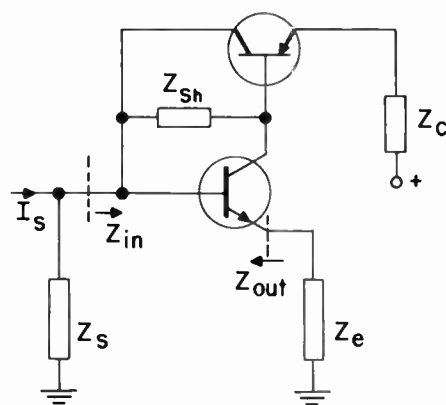


Fig. 1.

ances in the linear range of operation are approximately

$$\begin{aligned} Z_{in} &\approx \frac{Z_e [(1 - \alpha)z_c/2 + Z_c]}{Z_e + Z_c - (2\alpha - 1)z_c/2} \\ Z_{out} &\approx [Z_c - (2\alpha - 1)z_c/2] \\ &\quad \cdot \left[1 - \frac{1}{1 + Z_e/[Z_c + (1 - \alpha)z_c/2]} \right] \end{aligned} \quad (1)$$

In particular, if $Z_c = (2\alpha - 1)z_c/2$ the amplifier is unilateralized and (1) reduces to

$$Z_{in} \approx \alpha z_c/2, \quad Z_{out} \approx 0. \quad (2)$$

More accurately, $Z_{out} \approx r_e + r_b/2$. The upper limit of Z_{in} is $\alpha z_c/2$, the voltage gain is close to one, the current gain is inversely proportional to Z_c . If Z_{sh} is finite, the critical value of Z_c for unilateralization and the corresponding value of Z_{in} become smaller.

This amplifier, within its range and frequency limitations, may be considered as an example of synthesis of the so-called ideal amplifier, which has infinite-input impedance and zero-output impedance. It may be shown that the dual case (infinite-input admittance, zero-output admittance) may be approximated with a common base hook transistor using positive feedback.

LUCIO M. VALLESE
Dept. of Elec. Eng.
Polytechnic Inst. of Brooklyn
Brooklyn 1, N. Y.

Improvement of Impedance for Microwave Reflector Feed*

Dr. L. J. Chu has shown in U. S. Patent 2,646,506 how the impedance for the feed of a pill-box antenna can be improved by splitting the reflector into two parts and utilizing a split waveguide feed arrangement to excite them. The reflector halves are placed in a staggered relationship with respect to the direction of the beam, by a distance of a quarter wavelength. Each feed half is placed at the focus of its reflector, but there is a phase displacement of a quarter waveguide wavelength with respect to the common in-

* Received by the IRE, June 20, 1957

* Received by the IRE, July 22, 1957.

put which produces a common in-phase wave front for the energy from the reflectors. By this arrangement, the reflections back into the feed system from the reflector surfaces are minimized, but the radiating properties of the antenna as a whole are retained.

This same principle has been applied to the more commonly used simple-type paraboloid reflector antenna. The reflector was split into two parts in the *H* plane and rejoined with a quarter-wavelength step between them. The halves were separated by a neutral plane so that they could function independently as radiators. See Fig. 1. A hook-type waveguide feed was set into this neutral plane and split into two parts by this neutral plane, throughout the bend of the waveguide and the mouths of the feed proper. The proper phasing was secured by a variation of the forward position of the bends of the two waveguide paths. *E*-plane flaps were provided at each feed opening to

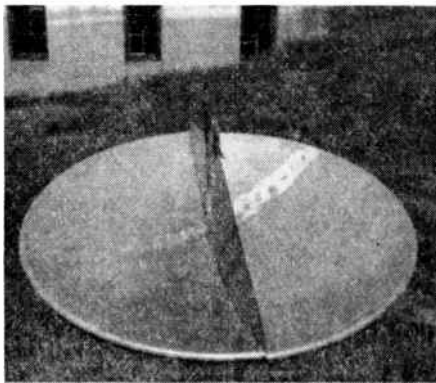


Fig. 1—Photograph of split-paraboloid antenna.

give the proper reflector illumination. Fig. 2 shows diagrammatically the feed and reflector relationships.

The standing-wave ratio achieved is indicated in Fig. 3. There is every reason to believe that this could be improved by more careful balancing of the halves of the system and more accurate adjustment of the phasing.

The comparisons of radiated patterns, with a simple reflector antenna, are indicated in Fig. 4. The side-lobe level refers to the amplitude of the highest side lobe (in some cases this side lobe was not the closest to

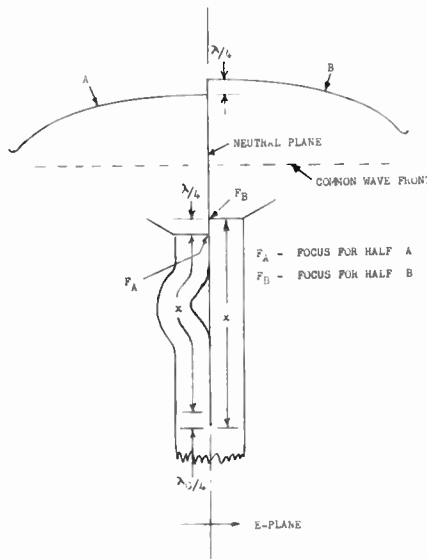


Fig. 2—Split-paraboloid principle.

the main beam). Theory indicates that the back-lobe structure should be improved when compared with the simple reflector antenna. This we were unable to verify experimentally.

M. W. SCHELDORF
Andrew Corp.
Chicago 19, Ill.

A Simplified Procedure for Finding Fourier Coefficients*

In correspondence on the above paper, Brenner and Fatechand¹ seem to imply they are extending Gibbons' work beyond that which has been accomplished to date here in the United States, and Klotter claims this procedure is well-known in Europe, but there seems to be only a single author here utilizing this method.

I would like to point out that Truxal, in his recent book,² describes in detail the method³ as applied to pulse-type waveforms.

JEAN A. DEVELET, JR.
Ramo-Wooldrige Corp.
Los Angeles 45, Calif.

* Received by the IRE, August 1, 1957. J. F. Gibbons, Proc. IRE, vol. 45, p. 243; February, 1957.
¹ E. Brenner, R. Fatechand, and K. Klotter, Proc. IRE, vol. 45, pp. 1022-1024; July, 1957.
² J. G. Truxal, "Control System Synthesis," McGraw-Hill Book Co., New York, N. Y.; 1955.
³ *Ibid.*, pp. 375-390.

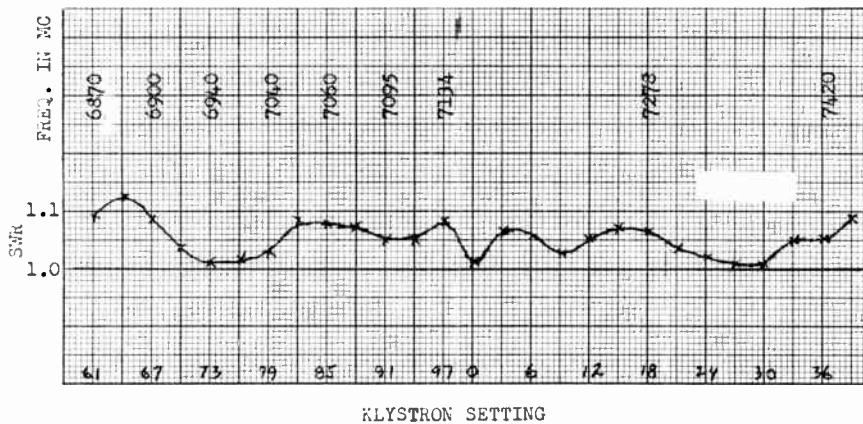


Fig. 3—Standing-wave ratio of split-paraboloid antenna.

On the Universal Standard of Time and the Velocity of Light*

Recently, many efforts have been directed toward a more accurate definition of the unit of time by exploring new and more reliable methods. The establishment of a standard with both high precision and ready reproducibility is still one of the most vehemently discussed problems of modern science.

The techniques that rely upon the application of atomic factors and their dependence on periodically recurring events within a statistical mean have emerged with the greatest promise for success. The intended combination of microphysical intervals with astronomical events appears to be satisfactory throughout a bandwidth of 20 orders of magnitude of the basic repetitive period.

The zero field resonance of a cesium atom resembles such events with an accuracy of one part in 9, 192, 631, 830 ± 10 or about one in 10⁹ per second. In this value, the second is defined as

$$(315, 569, 259, 747)^{-1} \approx 3 \times 10^{-1}$$

* Received by the IRE, July 19, 1957.

Frequency	Split-Paraboloid Antenna					Plain Antenna	
	6870	7040	7134	7278	7420	7134	
Beam Width Degrees	(E)	2.5	2.6	2.4	2.4	2.5	2.4
	(H)	2.4	2.5	2.5	2.4	2.4	2.6
Side Lobes db down	(E)	25.1	21.7	21.2	20.5	19.1	22.0
	(H)	25.9	28.1	27.7	27.3	29.2	27.7
Back Lobes db down	(E)	44.2	49.0	50.2	50.0	48.6	49.0
	(H)	51.7	52.1	52.7	52.9	53.2	52.7

Fig. 4—Pattern data.

of the tropical year of 1900.0,¹ which should be considered merely as a standard by definition. According to Essen, the probable uncertainty of this standard is about ± 1 in 2×10^9 for an interval of 10 years, or 1 in 2×10^8 for one year.²

Considering the total number of seconds per year ($\approx 3 \times 10^7$) and the accuracy of the defined time standard ($\approx 3 \times 10^{-12}$), one arrives at the conclusion that the basic element of the astronomically derived unit of time will last for about $3 \times 10^7 \times 3 \times 10^{-12} \approx 10^{-4}$ second. This is far too long for modern requirements in time determinations. Moreover, for a moderate length of a physical process or experiment, lasting about one week

$$\left(= \frac{7}{3650} \text{ of 10 years} \right),$$

the accuracy in astronomically defined time units (seconds) could never be expressed better than to about one part in

$$3.84 \times 10^6 \left(\approx 2 \times 10^9 \frac{7}{365 \times 10} \right).$$

It is obvious that a link must be established between the conservative astronomical definition and the recently introduced interval generators which utilize atomic processes. The result should be a reliable standard that is based upon as large a number of equal partitions as could be observed and compared with recurring macro-physical events. The cesium beam method provides such reproducibility, yet its calibration is a very delicate enterprise. Also, the comparison of results from various laboratories has not confirmed sufficient reliability for its intended use as a physical standard of time. Therefore, it appears worthwhile to consider another approach to the problem of defining such a standard.

According to the geometrical representation of the Lorentz transformation, the presently established unit of time acquires the very broad interval of an entire, and long elapsed, year in the negative region of the ct axis, i.e., the world vector.³ This vector is irreversible by definition and experience. Thus, the reproducibility of such a unit of time becomes impossible and renders the astronomical definition impracticable for all purposes of physics. A physicist, who is used to expressing his findings in terms of the C.G.S. system or its derivatives, that is, within the metric of the space-time-continuum, would wish to base the standard of time upon an omnipresent and easily accessible natural phenomenon as that which is furnished by the group velocity of electromagnetic radiation in vacuum.

Many methods have been developed to determine this universal constant to the utmost accuracy,⁴ but still more efforts are required to reach the perfection of expressing this value to at least one part in 10^{10} per second, or rather, to utilize this constant for the determination of the time interval

which will elapse while an electromagnetic signal propagates through a unit length. If a unit length has been established by comparing and associating it with the unidimensional extension of a system with known energy content, it will remain constant under selected laboratory conditions. Then, the unit of time will be based ultimately on a natural constant which is incorporated in the fundamental postulate of the relativistic conception of space and matter. This has proven to be correct at least throughout the dimensions of the solar system.⁵

Perturbations and deviations of any hypothetical "cosmic" value of the constant c , as Milne's theorems imply,⁶ should be still detectable. They will scarcely affect any physical phenomenon within the solar system. The Lorentz contraction will undeterminably correct for eventual accelerations of the unit length. Likewise, the Einstein formula $E=mc^2$ will preserve the energy invariance of this standard.⁷

While the astronomical determination of time remains necessary for comparison, a universal standard of time should not be based on the duration of astronomical events with their necessary corrections for influences from celestial bodies and terrestrial perturbations.⁸ An improvement and a redefinition of the standard of length is obligatory and efforts in this line appear of more urgency than a hasty introduction of a time standard. The velocity of light should regain its character as the fundamental reference which it deserves since the creation of modern physics. This constant demonstrates the most intimate union between space and time.⁹

The constituent subfactors s and t in the relation $c=s/t$, if separated, might never attain the expected ultimacy for which a standard is intended.¹⁰ But the search for a unit length with its easily comprehensible transfiguration into an extension of a mass in space promises to meet a higher degree of human intuitivity than the awe, inspired by the abstract concept of past and future aeons.

REINHOLD GERHARZ
Georgetown University Observatory
Washington, D. C.

- ¹ A. Einstein, *Ann. Phys.*, vol. 49, sec. 4; 1916.
² E. A. Milne, "Kinematic Relativity," Oxford University Press, London, England; 1948.
³ H. Weyl, "Raum-Zeit-Materie," Zurich, Switzerland, sec. 22; 1950.
⁴ E. C. Bullard, *Nature*, vol. 176, p. 282; 1956.
⁵ E. Schroedinger, "Expanding Universes," Cambridge University Press, Cambridge, England, 50 pp.; 1956.
⁶ A. March, "Quantum Mechanics of Particles and Wave Fields," John Wiley & Sons, Inc., New York, N. Y., ch. 10; 1951.

Propagation of a Pulse Across a Coast Line*

The pulse or the transient signal radiated from a lightning stroke is proving to be a powerful tool in studying propagation in the very low-frequency range (<100 kc). To interpret the waveform of the received

pulse, it is convenient to consider separately the ground wave and the higher-order sky wave signals. When the ground wave is propagating over an inhomogeneous soil, the character of the waveform can be radically changed. The purpose of this short communication is to discuss the transformation of the pulse shape of the ground wave as it crosses a coast line for a source over the sea. To simplify the discussion, the earth's curvature is neglected and the sea is assumed to be perfectly conducting.

The transmitter is a vertical electric dipole, located at a point A on a flat, perfectly conducting sea. A sharp coastline O is located at a distance d_2 from A (see Fig. 1).

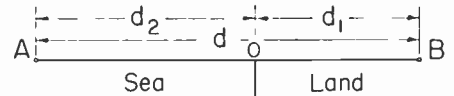


Fig. 1.

The receiving antenna which is also a vertical dipole is located at distance d_1 inland from the coast on a homogeneous flat ground of conductivity σ . The vertical electric field $E(\omega)$ at B , for a dipole of height h and average current $I(\omega)e^{i\omega t}$, can be written in the form

$$E(\omega)e^{i\omega t} = \frac{i\mu\omega I(\omega)e^{i\omega t}h}{2\pi d} e^{-(i\omega d/c)F'(d, \omega)} \quad (1)$$

where ω is the angular frequency, d is the distance between A and B , c is the velocity of light, and $F'(d, \omega)$ is some slowly varying attenuation function. Eq. (1), which is valid for d greater than a wavelength, is a special case of a more general result derived previously.¹ It was shown that

$$F'(d, \omega) = 1 - (i\omega) \left(\frac{\epsilon_0 d}{2\pi c \sigma} \right)^{1/2} \int_0^{d_1} \frac{F(\alpha, \omega)}{[\alpha(d-\alpha)]^{1/2}} d\alpha \quad (2)$$

where

$$F(\alpha, \omega) = 1 - i2\rho^{1/2}e^{-\rho} \int_{\rho}^{\infty} e^{-z^2} dz$$

with

$$\rho \approx \frac{\alpha\omega^2}{2\sigma\mu_0 c^3}, \quad \epsilon_0 = 8.854 \times 10^{-12}.$$

$F(\alpha, \omega)$ is the Sommerfeld-Norton attenuation function which occurs in the propagation over a homogeneous flat ground,² whereas $F'(d, \omega)$ is the modified form for a mixed land-sea path. As d_1 approaches d , it can be verified that $F'(d, \omega) \rightarrow F(d, \omega)$. In the above, it has been assumed that displacement currents in the ground are negligible, that is $\epsilon\omega/\sigma \ll 1$. This is valid for radio frequencies over moderately conducting soil.

Numerical results for $F'(\alpha, \omega)$ for various mixed paths were presented in a previous paper.¹ The task undertaken herein is to generalize the result to the case of a transient or pulsed source. As it turns out, the transient solution for the mixed land-sea path is simpler in form than its steady-state counterpart.

- ¹ J. R. Wait, "Mixed-path ground wave propagation," *J. Res. N.B.S.*, vol. 57, pp. 1-15; July, 1956.
² K. A. Norton, "Propagation of radio waves over the surface of the earth," *Proc. IRE*, vol. 25, p. 1203; September, 1937.

* Received by the IRE, June 13, 1957.

¹ G. Clemence, *Rev. Mod. Phys.*, vol. 29, p. 2; 1957.
² L. Essen and J. V. L. Parry, *Nature*, vol. 176, p. 669; 1955.
³ L. Essen, *Nature*, vol. 178, p. 34; 1956.
⁴ A. Sommerfeld, "Elektrodynamik," Wiesbaden, Germany, sec. 27; 1948.
⁵ *Ann. Franc. Chronometrie*, vol. 5, p. 167; 1951.

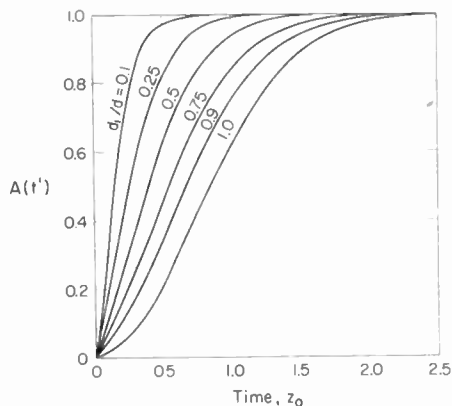


Fig. 2—Response for ramp current source.

As a starting point, the current $j(t)$ in the source dipole is taken to be a ramp function, that is

$$j(t) = \frac{I_0 t}{t_0} \text{ for } t > 0$$

$$= 0 \text{ for } t < 0. \quad (4)$$

The frequency spectrum of the source is then

$$I(\omega) = \int_0^{\infty} j(t)e^{-i\omega t} dt = \frac{I_0}{t_0(i\omega)^2}. \quad (5)$$

The electric field $e(t)$ at B can be expressed in terms of its spectrum $E(\omega)$ by

$$e(t) = \frac{1}{2\pi} \int_{-\infty}^{+\infty} E(\omega)e^{i\omega t} d\omega \quad (6)$$

where $E(\omega)$ is related to the source spectrum $I(\omega)$ by (1). It is not difficult to see that

$$e(t) = \frac{\mu I_0 h}{2\pi t_0 d} A(t')$$

where

$$A(t') = \frac{1}{2\pi} \int_{-\infty}^{+\infty} \frac{F'(d, \omega)}{(i\omega)} e^{i\omega t'} d\omega \text{ for } t' > 0 \quad (7)$$

with $t' = t - d/c$ and $A(t') = 0$ for $t' < 0$.

Using a previously derived result,³

$$\frac{1}{2\pi} \int_{-\infty}^{+\infty} F(d, \omega) e^{i\omega t'} d\omega = \frac{t'}{2\beta^2} e - \left(\frac{t'}{2\beta}\right)^2 \quad (8)$$

where

$$\beta^2 = \frac{\alpha^2}{2\sigma\mu c^3}$$

it follows that

$$A(t') = 1 - \left(\frac{\epsilon_0 d}{2\pi c \sigma}\right)^{1/2} (\sigma\mu c^3)^{1/2} t'$$

$$\int_0^{d_1} \frac{\exp\left[-\frac{\sigma\mu c^3 (t')^2}{2\alpha}\right] d\alpha}{\alpha^{3/2} (d - \alpha)^{1/2}} \quad (9)$$

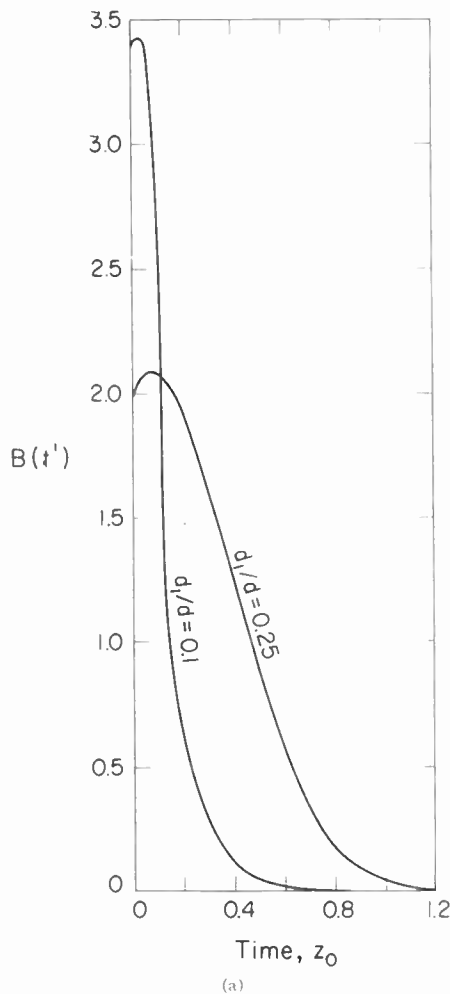
After a change of variable, this becomes

$$A(t') = 1 - \frac{2}{\sqrt{\pi}} \int_{z_1}^{\infty} \frac{e^{-z^2}}{(z^2 - z_0^2)^{1/2}} dz \quad (10)$$

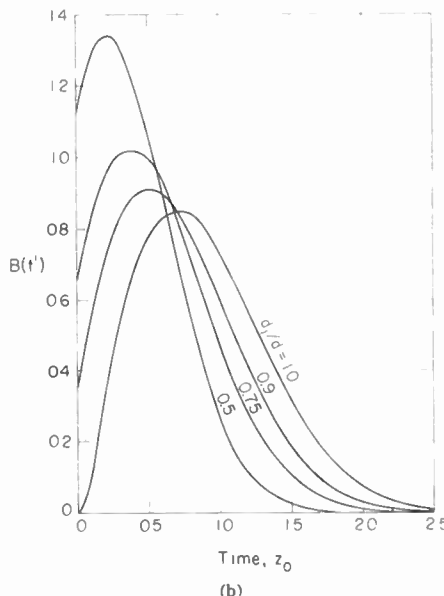
where $z_0^2 = \sigma\mu c^3 (t')^2 / (2d)$ and $z_1^2 = \sigma\mu c^3 (t')^2 / (2d_1)$. This can be written

$$A(t') = 1 - e^{-z_0^2} \operatorname{erfc} [(z_1^2 - z_0^2)^{1/2}] \quad (11)$$

in terms of the error function complement



(a)



(b)

Fig. 3—Response for step-current source.

$$\operatorname{erfc}(Z) = \frac{2}{\sqrt{\pi}} \int_Z^{\infty} e^{-z^2} dz. \quad (12)$$

In the case of an all sea path, $d_1 = 0$ or $z_1 = \infty$ and consequently $A(t') = 1$ which is a unit step at $t' = 0$ or $t = d/c$; whereas for an all land path, $d_1 = d$ or $z_1 = z_0$, and then

$$A(t') = 1 - e^{-z_0^2} \quad (13)$$

which agrees with a result derived previously.³

Using the preceding analysis, it is not difficult to extend the results to other source waveforms. For example, if the source current was a step-function, that is

$$j(t) = I_1 \text{ for } t > 0, = 0 \text{ for } t < 0$$

it is not difficult to show that

$$e(t) = \frac{\mu I_1 h}{2\pi d} \left(\frac{\sigma\mu c^3}{2d}\right)^{1/2} B(t')$$

where

$$B(t') = \frac{dA(t')}{dz_0}$$

$$= \frac{2}{\sqrt{\pi}} e^{-(d_1/d)z_0^2} \left(\frac{d}{d_1} - 1\right)^{1/2}$$

$$+ 2z_0 e^{-z_0^2} \operatorname{erfc} \left[\left(\frac{d}{d_1} - 1\right)^{1/2} z_0\right]$$

with $z_0 = (\sigma\mu c^3 / 2d)^{1/2} t' = 4.12 \cdot 10^9 \cdot t' \sqrt{\sigma/d}$ in mks units.

The responses $A(t')$ and $B(t')$ for a ramp and a step-function current source are shown in Figs. 2 and 3, respectively, for various values of d_1/d .

The abscissa is the "TIME" parameter z_0 which is proportional to t' . For negative values of t' or for $t < d/c$, the responses are zero. It can be readily seen that as d_1/d approaches zero, corresponding to an all sea path, the response $A(t')$ approaches a step-function, and the response $B(t')$ approaches an impulse function. On the other hand, as d_1/d approaches one, corresponding to an all land path between A and B , the pulses show considerable dispersion. To provide a more quantitative idea, the following example is quoted. For $d = 100$ km, and $\sigma \approx 6$ millhos/meter, the parameter z_0 is to read directly in microseconds. Since displacement currents in the ground have been neglected, the responses are only valid for $t' > \epsilon/\sigma$ where ϵ is the dielectric constant in the ground. In the above example $\epsilon/\sigma \approx 0.015$ μ secs for $\epsilon/\epsilon_0 \approx 10$.

JAMES R. WAIT
National Bureau of Standards
Boulder, Colo.

³ J. R. Wait, "Transient fields of a vertical dipole over a homogeneous curved ground," *Canad. J. Phys.*, vol. 34, pp. 27-35; January, 1956.

Yttrium Garnet UHF Isolator*

This letter describes an experimental low-frequency resonance absorption isolator utilizing yttrium garnet polycrystalline ceramic.

The geometry is shown in Fig. 1 and consists of a 12-inch section of a rolled dielectrically loaded ridge guide in 3½-inch coaxial line.

* Received by the IRE, July 24, 1957.

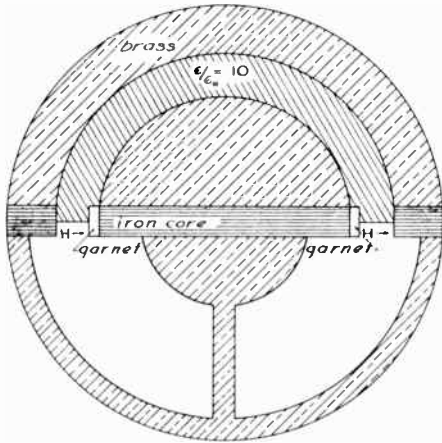


Fig. 1.

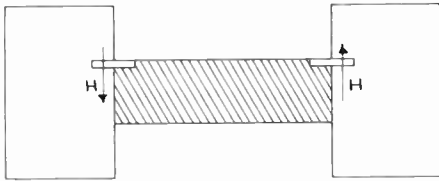


Fig. 2.

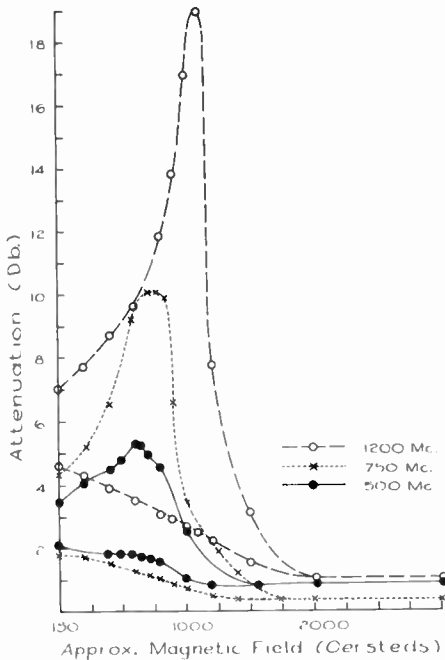


Fig. 3—Yttrium garnet uhf isolator forward and reverse attenuation vs applied field.

If the gap width is small, the cross section is approximately equivalent to that of Fig. 2.

The cutoff frequency for this geometry may be evaluated by transverse resonance techniques¹ and turns out to be approximately 200 mc, which agrees very well with the measured value.

Experimental curves of the forward and backward attenuation for several frequen-

¹ S. B. Cohn, "Properties of ridge waveguide," Proc. IRE, vol. 35, pp. 783-788; August, 1947.

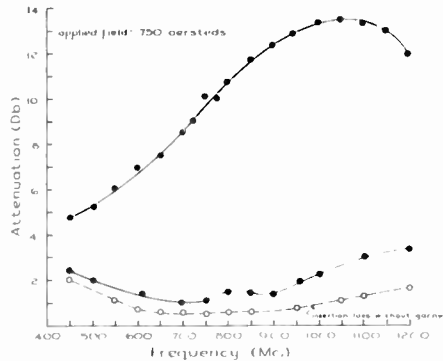


Fig. 4—Yttrium garnet uhf isolator forward and reverse attenuation vs frequency.

cies as a function of applied magnetic field are shown in Fig. 3. It may be noted that a significant gain over isolators employing ferrites at these frequencies has been achieved. The isolation could be improved still further by increasing the aspect ratio of the garnet slabs, which is presently 4 to 1.

The frequency characteristics of the isolator, biased to be resonant at 750 mc, is shown in Fig. 4.

All measurements were taken at low-power levels so that linear operation was assured.

The initial success of the isolator is due to the excellent yttrium garnet ceramic supplied by the Ferrite Laboratory at Harvard University through the cooperation of C. L. Hogan. This ceramic $3(Y_2O_3) \cdot 5(Fe_2O_3)$ has a Curie temperature of 280°C, a density 95 per cent of theoretical, and an X-band line width of 70 oersteds.

Additional measurements and the theoretical analysis of the geometry will be the subject of a future paper.

F. R. MORGENTHALE
AND D. L. FYE
Antenna Laboratory
Air Force Cambridge Research Center
Bedford, Mass.

Radio Observations of the Russian Earth Satellite*

Simple radio observations of signals from the Soviet satellite of October 4 were made by Lincoln Laboratory beginning on the evening of October 5, 1957. Plots of received frequency vs time, one of which is shown in Fig. 1, were made by analyzing the tape-recorded audio outputs of standard radio receivers which used beat frequency oscillators. By studying the shape of such curves it is possible to determine the slant range of the point of nearest passage of the satellite to the observing point. This distance will be referred to as the miss distance, r_0 . This quantity is given by

* Received by the IRE, October 14, 1957. The research in this document was supported jointly by the Army, Navy, and Air Force under contract with the Mass. Inst. Tech.

$$r_0 = \frac{f_0 v^2}{c \dot{f}_{\max}}$$

where f_0 = carrier frequency (20.005 or 40.002 mc),
 v = speed of satellite,
and \dot{f}_{\max} = steepest derivative of the Doppler frequency curve.

Data of this type taken at Ipswich, Mass., on the satellite passage of 0335 GMT, October 7, showed an unexpectedly low r_0 of about 137 nautical miles from records made simultaneously at 20.005 mc and 40.002 mc. The close agreement between results at the two frequencies appeared to rule out large errors due to distortion of the path by the ionosphere.

A more intensive program was then initiated employing additional radio receivers at various points in eastern Massachusetts. During the succeeding days a number of passages of the satellite were recorded at these locations on both 20 and 40 mc for night-time and day-time passages.

It was clear from early reports that late each night and in the middle of each morning several transits could be observed occurring once per 96-minute period, with each transit some 1000 to 1500 miles to the westward of its immediate predecessor. Attention was focused on those transits that occurred nightly at about 0335 GMT. It was known that these were shifting slowly westward on successive nights. Therefore, an attempt was made to fit together the miss distances r_0 calculated from the radio data of the nights of October 5, 6, and 7, so as to predict the value of r_0 to be expected on October 8.

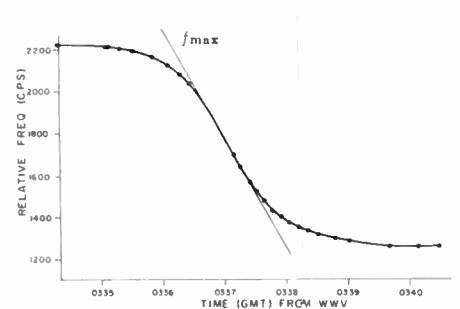


Fig. 1—Round Hill 0335 GMT, October 7, 1957—20 mc.

A few remarks will outline the nature of the calculation. In preparing the prediction of the fourth transit, it was assumed that corresponding tracks on successive nights differed in longitude by a constant amount and had the same altitude above the earth. A value of speed v was first computed using an approximate knowledge of the period and an arbitrarily assumed value of altitude h . This value of v enabled the values of r_0 for the three nights to be computed using the above formula. The three measurements of r_0 were then used to solve for a better value of h which was reinserted in the calculation for v . One such iteration proved to be sufficient to fix v and h and provide the r_0 prediction for the fourth track.

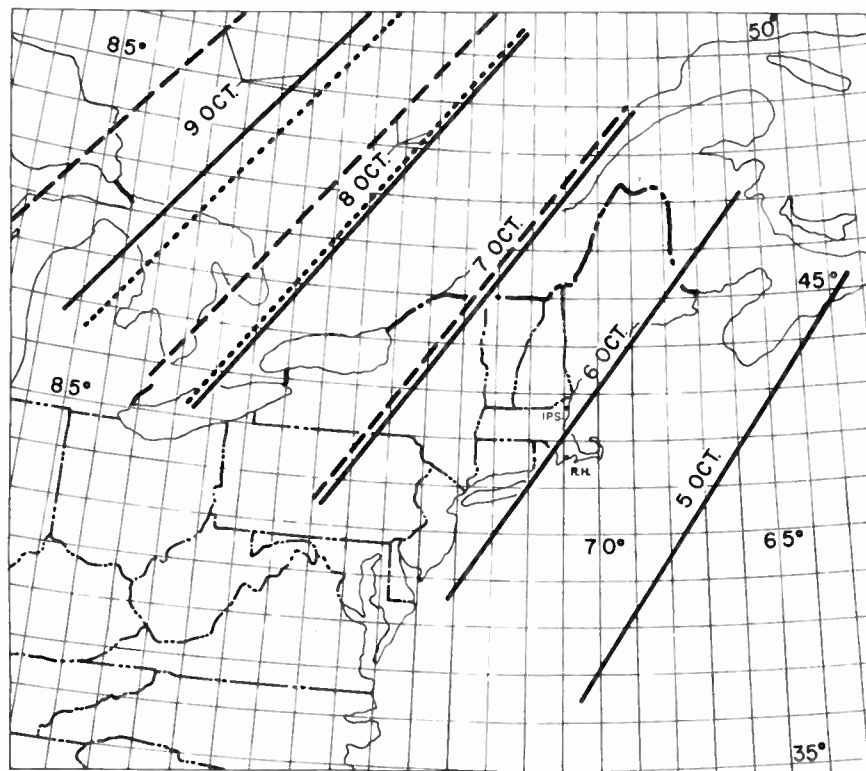


Fig. 2.

Three of the heavy lines of Fig. 2 show ground projections of the tracks of October 5, 6, and 7 fixed according to the above calculation. The fourth and fifth heavy lines represent the predictions for October 8 and 9. The dotted lines indicate track position from r_0 values determined at Ipswich. The dashed lines show data obtained at Round Hill. A general consistency is to be noted between predicted and observed values. The azimuthal angle of the evening track was taken as 35° True at latitude 42° North, based on the publicized angle of launching.

As mentioned above, the calculation from radio Doppler data also provides altitude and velocity of the satellite at time of passage. These quantities were computed to be 137 nautical miles and 4.26 nautical miles per second, respectively, for the night-time observations (both with an accuracy of ± 8 per cent). The same calculations for morning observations gave an altitude of 339 nautical miles and a velocity of 4.06 nautical miles per second with the same tolerance. The two heights permitted a preliminary calculation of 0.0455 for the eccentricity. A computation of the period based on observed times of passage gave a value of 96.05 minutes as averaged through October 9.

The work described here is continuing and will be reported fully later.

R. R. BROWN
P. E. GREEN, JR.
B. HOWLAND
R. M. LERNER
R. MANASSE
G. PETTEGILL
Lincoln Laboratory,
Mass. Inst. Tech.
Lexington, Mass.

Radio and Radar Tracking of the Russian Earth Satellite*

With the announcement of the successful launching of the Russian earth satellite on October 4, 1957, it appeared urgent to obtain all possible scientific information which could be learned from the satellite's flight. As a result, hastily organized observing programs were placed into operation in many parts of the United States. Spontaneity of action seems to have been the keynote, and the enthusiasm for the job to be done has seldom been matched in scientific research efforts. Although progress was hampered by lack of preparation for radio studies at the frequencies employed in the satellite, it now appears that much information of scientific value will be learned from the flight of this first earth satellite.

The Stanford Research Institute (S.R.I.) is but one among many research groups which have participated in this work. This letter is an account of the techniques employed at S.R.I. and the results obtained to date. Since early prediction of the times of passage of the satellite near Stanford were unreliable, a considerable effort was made to obtain information on the position and motion of the satellite. This information is required if successful interpretation of the recorded signals is to be obtained by detailed data analysis at a later date. In addition to the monitoring of the radio transmission from the satellite on 20.005 mc and 40.002 mc, attempts to obtain radar echoes from the satellite or associated parts of the launch vehicle were planned.

Of those characteristics of the satellite

radio signals which can be measured, the two which have proven most valuable at S.R.I. have been bearing angle and rate of change of frequency (Doppler shift). Accurate rate of change of frequency measurements permit the determination of minimum slant range to the satellite in accordance with the following relationship

$$R_0 \approx \frac{v^2}{\lambda \left(\frac{df}{dt} \right)_{\max}}$$

where

v = velocity of the satellite,
 λ = wavelength of radio transmission,
 df/dt = rate of change of frequency.

In addition, the time of passing minimum range can be measured accurately using this method. Using direction finding techniques and plotting bearing angle vs time it is possible to obtain the distance along the earth's surface from the observing point to the projection on the earth's surface of the track of the satellite. Rate of change of frequency measurements were made at frequencies of 20.005 and 40.002 mc while direction finding measurements were undertaken only on 40.002 mc. The Doppler data are more precise and hence more useful for most purposes than the direction finder data but the latter serve as a check on validity of the results.

Fig. 1 (p. 1554) shows a block diagram of the Doppler recording equipment and Fig. 2 shows a block diagram of the signal recording equipment and direction finder which have been used at S.R.I. Fig. 3 shows an example of the simultaneous Doppler measurements at Stanford, Calif. and Bozeman, Mont., together with the direction finder data at Stanford. The minimum slant ranges measured from the Doppler curves are 1080 km for Stanford and 810 km for Bozeman. The direction finding data indicate that the passage of the satellite was to the east of Stanford and to the west of Bozeman. Fig. 4 (p. 1554) shows two rates of change of frequency plots for passage of the satellite at different distances from Stanford.

The direction finder and Doppler data were used as the basis for estimating position and time of passage information, in attempts to obtain radar echoes from the satellite and associated parts of the launch vehicle. The radar used was one designed at S.R.I. for the study of radar reflections from the moon, meteor ionization trails, and the aurora. This radar uses a 61-foot steerable parabolic reflector (Fig. 5, p. 1555) and is equipped with cross-polarized feeds to allow for possible polarization changes in the received signal. Radar echoes have been obtained for those passages of the satellite in which the prediction of its location was sufficiently accurate that the antenna orientation allowed the satellite to pass through the beam. The sensitivity of the radar was such that echoes were detected only when the range to the satellite was in the order of 700 km or less. The radar characteristics are shown in Table I (p. 1555).

Echoes were detected on the morning of October 9 from two objects believed to be parts of the launch vehicle. On the morning of October 10 one echo was obtained which

* Received by the IRE, October 15, 1957.

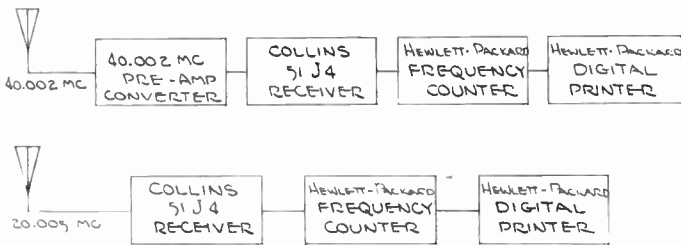


Fig. 1—Block diagram of Doppler measuring equipment.

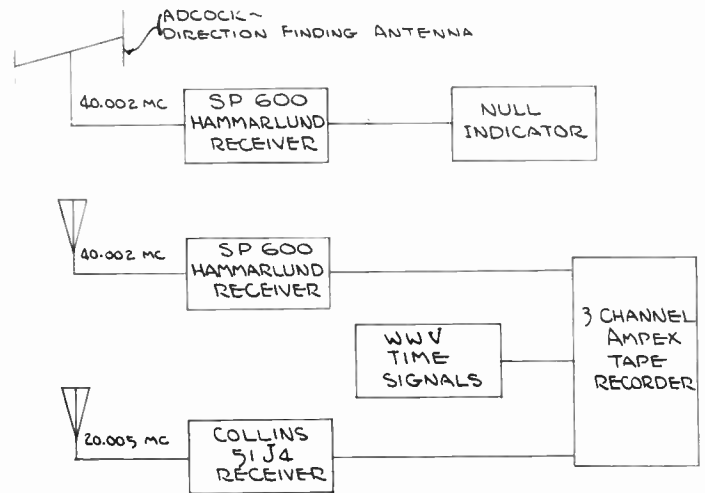
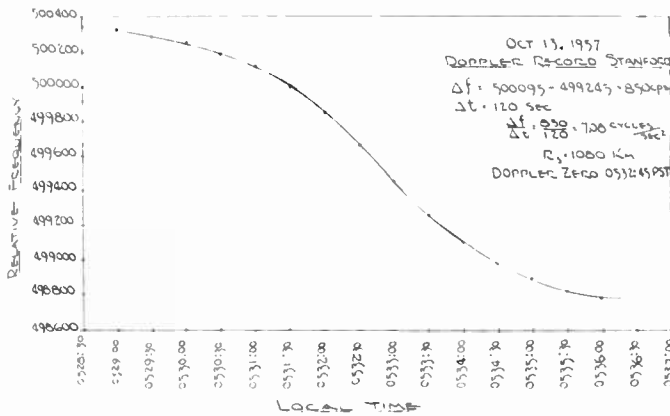
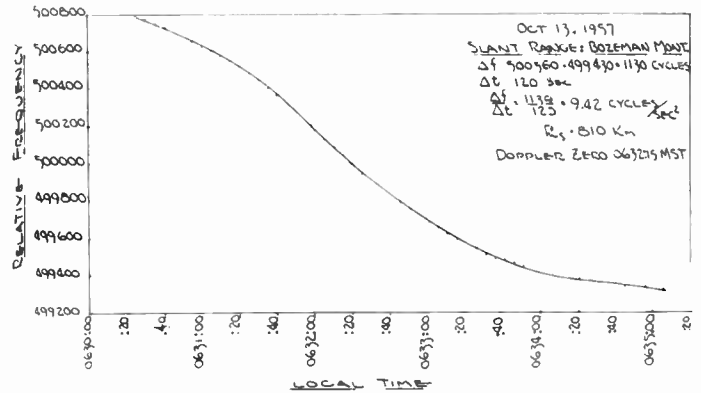


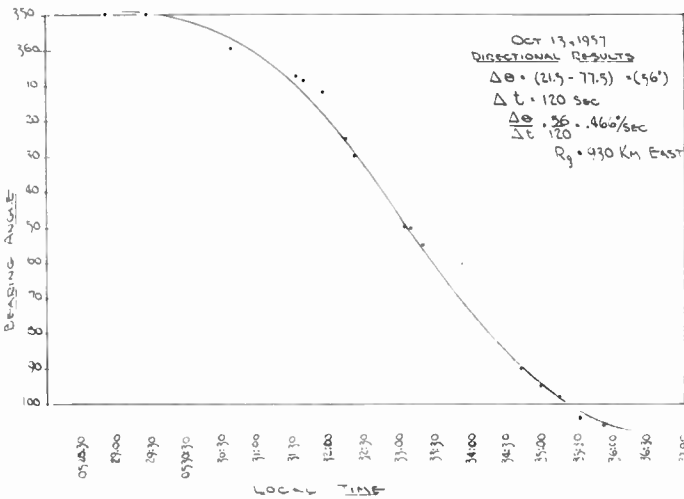
Fig. 2—Block diagram of data recording and direction finding equipment.



3(a)



3(b)



3(c)

Fig. 3—(a) Doppler record from Stanford for the 0532 PST, October 13, 1957, satellite passage. (b) Doppler record from Bozeman, Mont. for the 0532 PST, October 13 satellite passage. (c) Direction finding record from Palo Alto for the 0532 PST, October 13 satellite passage.

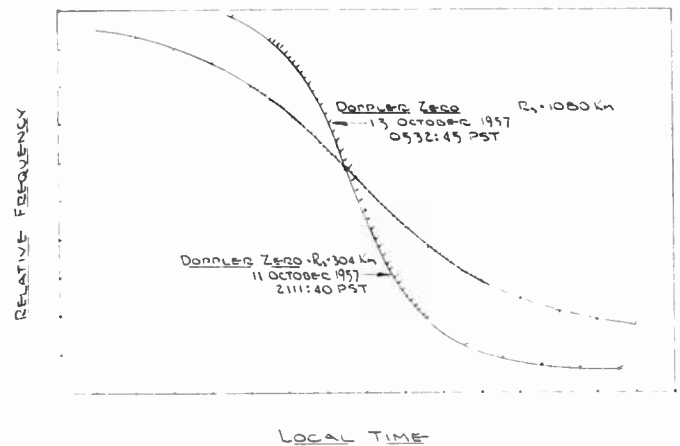


Fig. 4—Two Doppler records showing difference in slopes of the Doppler curves for different passage ranges of the satellite.

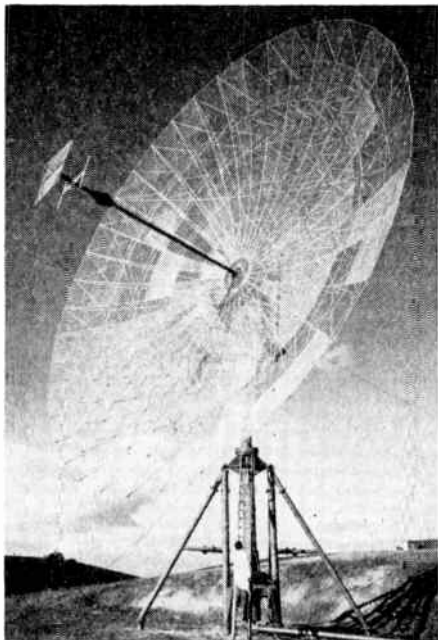


Fig. 5.

is believed to have resulted from reflection from the satellite itself.

The signals transmitted from the satellite on 20.005 mc and 40.002 mc were recorded along with timing information on a three-channel magnetic tape recorder during those times when it could be heard. These recordings will later be studied to obtain information which may be contained on propagation through the ionosphere and the physics of the upper atmosphere.

The equipment used during these experiments has been hastily assembled, and many ways to improve it have come to mind. However, the measurements which have been taken since October 4 appear to be of sufficient accuracy to permit valuable scientific data to be obtained.

The work reported here was carried on in

cooperation with the Rome Air Development Center, Air Research and Development Command. The work was made possible by the help of the many volunteers of the S.R.I. Engineering Division who manned the equipment.

Acknowledgment is made to Professor Cunningham at the University of California Astronomy Department for his help and exchange of data concerning the satellite orbit, and to Professor Weaver of the Montana State College, Bozeman, Mont. for his participation in the Doppler experiments.

The Staff, Special Techniques Group
By: A. M. PETERSON, Head
Stanford Research Institute
Menlo Park, Calif.

TABLE I

106.1 MC RADAR CHARACTERISTICS

Peak power = 50 kw.
Pulse length = 1 ms.
PRF = 75 cps and 150 cps.
Antenna
61-foot steerable parabolic reflector
12° beamwidth between $\frac{1}{2}$ power points
24-db gain above an isotropic radiator.
Receiver noise figure = 2.5 db.
Minimum detectable echo power = 10^{-14} watts.
Minimum detectable radar cross section at 500-km range = 0.1 m ² .
Receiver bandwidth = 6 kc.

Contributors

Kern K. N. Chang was born in Shanghai, China, on September 9, 1919. He received the B.S. degree from National Central University, Nanking, China, in 1940, the M.S. degree in electrical engineering from the University of Michigan in 1948, and the D.E.E. degree in 1954 from the Polytechnic Institute of Brooklyn.

From 1940 to 1945, he was associated with the Central Radio Manufacturing Works, Kunming, China, working on radio receivers, and from 1945 to 1947, he was a radio instructor in the Office of Strategic Service, U. S. Army, China Theatre. Since 1948, he has been a member of the technical staff at RCA Laboratories, Princeton, N. J., where he is presently engaged in research on microwave tubes.

Dr. Chang is a member of Sigma Xi.



K. K. N. CHANG

J. S. Cook (S'52-A'53) was born on May 30, 1927, in Flint, Mich. He served with the United States Navy from 1945 to 1947. In 1952, he received the B.E.E. degree and the M.S. degree from Ohio State University, Columbus, Ohio. From 1950 to 1952, he was associated with the Ohio State University Research Foundation.

Since 1952, he has been engaged in electronics research with Bell Telephone Laboratories, Murray Hill, N. J.

Mr. Cook is a member of Eta Kappa Nu and Tau Beta Pi.



J. S. COOK

Gordon H. Hanson (S'56-M'57) was born in Vancouver, B. C., Canada on August 28, 1926. He received the B.A. and M.A. de-

grees in physics from the University of British Columbia, Vancouver, B. C., in 1949 and 1951 respectively, and the Ph.D. degree in electrical engineering from the University of Minnesota in 1957.

From September, 1951 to September, 1953, Mr. Hanson was employed at the Radio Physics Laboratory of the Defense Research Board, Ottawa, Canada, where he was engaged in the study of ionospheric phenomena. Since February, 1957, he has been with the Bell Telephone Laboratories in Allentown, Pa., where he is working on the development of diffused base transistors.



G. H. HANSON

Edward W. Herold (A'30-M'38-SM'43-F'48) was born in 1907 in New York, N. Y. He received the B.S. degree in physics from

the University of Virginia in 1930, and the M.S. degree, also in physics, from the Polytechnic Institute of Brooklyn in 1942. From



E. W. HEROLD

1924 to 1926 he was associated with the Bell Telephone Laboratories, and from 1927 to 1929, with E. T. Cunningham, Inc. Since 1930 he has been with the Radio Corporation of America, first at Harrison, N. J., and, since 1942, at RCA Laboratories, Princeton, N. J., where he is presently Director, Electronic Research Laboratory. Mr. Herold has been engaged in research and development and has specialized in electron tubes and semiconductor devices.

He is a member of Phi Beta Kappa and Sigma Xi and is a Director of the IRE.



Rudolf Kompfner (F'50) was born in Vienna, Austria, on May 16, 1909. He attended the Realschule and Technische Hochschule in Vienna, and was graduated from the faculty of architecture in 1933. In 1934, he went to England to continue his studies in architecture privately, and became the director of a building firm in 1937. He has devoted much of his spare time to the study of television, radio, and physics.



R. KOMPFNER

Mr. Kompfner entered the Admiralty Service in 1941 as temporary experimental officer, beginning in the physics department at Birmingham University. In 1944, he became associated with the Clarendon Laboratory at Oxford University, England and received the degree of D.Phil. in 1951. Since 1952, he has been at the Bell Telephone Laboratories, Murray Hill, N. J., working on microwave tubes.



Herbert Kroemer (M'56) was born on August 25, 1928, in Weimar, Germany. He received the degree of a Dr.rer.nat. from the University of Goettingen, Germany, in 1952.



H. KROEMER

From 1952 to 1954, he worked at the semiconductor laboratory of the German Post Office, where his main interest was the theory and development of high-frequency transistors. In 1954 he joined RCA Laboratories in Princeton, N. J., where he continued working in the semiconductor and transistor field.

Dr. Kroemer is a member of the American Physical Society and Sigma Xi.



Conrad Lanza was born in New York, N. Y., on June 19, 1918. He received the bachelor's degree in electrical engineering at the Polytechnic Institute of Brooklyn, N. Y. in 1947. In 1956, he was awarded the M. S. E. E. degree at Northeastern University, Boston, Mass.



C. LANZA

Upon graduation from Polytechnic Institute, Mr. Lanza joined the Hazeltine Electronics Corp. where he worked on the development of radio-aids-to-navigation systems. In 1953, he joined the communications section at Raytheon Manufacturing Co. and worked on transistor circuit design. In 1956, Mr. Lanza transferred to Raytheon's research division to work on the development of semiconductor devices.



R. D. Middlebrook (S'55-M'56) was born in England in 1929. Before entering Cambridge University, he was a senior technical instructor and a member of the trade testing board in the Royal Air Force. Later he worked for a short time on sound recording at the British Broadcasting Corporation.



R. D. MIDDLEBROOK

He received the B.A. and M.A. degrees from Cambridge, and then went to Stanford University, Stanford, Calif., where he completed graduate work in electrical engineering and received the M.S. and Ph.D. degrees. He was a research assistant at the Stanford Electronics Research Laboratory and was the first member of the transistor group.

Since 1955, Dr. Middlebrook has been assistant professor of electrical engineering at the California Institute of Technology, where he teaches transistor electronics and conducts a transistor research program.

His publications include "An Introduction to Junction Transistor Theory." He is a member of the American Physical Society, the American Institute for the Advancement of Science, and Sigma Xi.



Vernon L. Newhouse (M'55) was born on January 30, 1928. He received the B.Sc. degree in physics in 1949 and the Ph.D. degree in 1952, both from the University of Leeds, England. His postgraduate work was con-

cerned with the theoretical and experimental study of the Barkhausen effect in single ferromagnetic crystals.



V. L. NEWHOUSE

In 1951, he joined the computer department of Messrs. Ferranti of Manchester, England, where he carried out the initial development of the coincident current memory used in the Ferranti Mark II computer. In 1954, after some months at the David Sarnoff Research Laboratories, Princeton, N. J., he joined the Bizmac Engineering Section of RCA as project engineer of the circuit design and development group. Since then, he has been associated with the development of a real time computer and is presently project engineer in charge of advanced magnetic development.

Dr. Newhouse is a graduate member of the IRE.



Charles A. Parry (SM'53) was born in Cairns, Australia, on January 25, 1916. He is a graduate of the University of Queensland, Australia.



C. A. PARRY

During World War II, while with Communications Engineering, Ltd., Mr. Parry designed transcontinental multichannel carrier equipment for the Australian Government. For several years after the war, he was engaged in the development of equipments for mobile and ground air communications. Later, he joined the Plessey Company in London to work on fsk equipment for transoceanic circuits.

In 1953, he joined RCA in Montreal, Canada and was responsible for the initial phases of the Doppler radar network and associated communications for the Canadian Air Force. Later, as a representative of RCA International in Clark, N. J., he negotiated with Pakistan, India, and Iran for the establishment of international multichannel vhf networks.

Now with Page Communications Engineers, Inc., of Washington, D. C., Mr. Parry is consultant to the director of engineering and technical advisor on overseas projects.

He was a member of the examination and editorial boards of the IRE in Australia and acted on the RETMA Committee for communication standards while in Canada. In addition to his Australian IRE membership, Mr. Parry is affiliated with the British IRE and the Television Society of Great Britain.



For a photograph and biography of R. A. Pucel see page 369, March, 1957 issue of the PROCEEDINGS.

For a photograph and biography of Frank Reggia, see page 369 of the March issue of PROCEEDINGS.



John D. Ryder (A'29-SM'45-F'52) was born on May 8, 1907, in Columbus, Ohio. He received the B.E.E. degree in 1928 and the



J. D. RYDER

M.S. degree in 1929 from Ohio State University. In 1944 he was awarded the Ph.D. degree in electrical engineering by Iowa State College.

From 1929 to 1931, he was affiliated with the General Electric Company, working on vacuum tube development. In 1931, he joined the Bailey

Meter Company, Cleveland, Ohio, as supervisor of the electrical and electronic section of the Research Laboratory. He holds 24 patents on this work covering temperature-recording and automatic control applications of electronics. In 1941, he was appointed assistant professor of electrical engineering at Iowa State College, was made professor in 1944, and in 1947 assumed the position of assistant director of the Iowa Engineering Experiment Station. In September, 1949, he became head of the Department of Electrical Engineering at the University of Illinois, and in July, 1954, was named Dean of the College of Engineering at Michigan State University, East Lansing, Mich.

He is the author of four textbooks, "Electronic Engineering Principles," "Networks, Lines, and Fields," "Electronic Fundamentals and Applications," and "Engineering Electronics with Industrial Applications and Control," in addition to technical papers.

He has been active in the development and construction of two electronic-type 10,000-cycle network analyzers for power transmission studies, one at Iowa State College and the other at the University of Illinois.

Dr. Ryder was President of the IRE in 1955, and has served as a Director of the IRE since 1952. He was President of Eta Kappa Nu, the electrical engineering honorary society in 1956-1957, and President of the National Electronics Conference for 1953. He is a Fellow of the American Institute of Electrical Engineers, and of the American Association for the Advancement of Science, as well as a member of Tau Beta Pi, Eta Kappa Nu, Sigma Xi, Phi Kappa Phi, and Pi Mu Epsilon. He has been a member and chairman of various AIEE and IRE committees in the fields of education, electronics, and research.



For a photograph and biography of Edward G. Spencer, see page 369 of the March issue of PROCEEDINGS. Mr. Spencer is now a senior member of the IRE.



For a photograph and biography of H. Stutz see page 370, March, 1957 issue of the PROCEEDINGS.



A. van der Ziel (SM'49-F'56) was born in Zandweer, The Netherlands, on December 12, 1910. From 1928 to 1934 he studied physics at the University of Groningen, The Netherlands, where he received the Ph.D. degree in 1934.

He was a member of the research staff of the Physics Laboratory of N. V. Philips' Gloeilampenfabrieken, Eindhoven, The Netherlands, from 1934 to 1947. At that time he became an associate professor at the University of British Columbia, Vancouver, Canada, and has been professor of electrical engineering at the University of Minnesota since 1950.

A. VAN DER ZIEL

Society and Sigma Xi.

Dr. van der Ziel is a member of the American Physical



W. H. Yocom was born in Oberlin, Ohio, on May 15, 1919. He attended Oberlin College receiving the B.A. degree in physics in



W. H. YOCOM

1940. He received the B.S. degree in electrical engineering from the Massachusetts Institute of Technology in 1942. In 1950 he received the M.S. degree in electrical engineering from Stevens Institute of Technology, Hoboken, N. J. Since 1942 Mr. Yocom has been employed by Bell Telephone Laboratories, Murray Hill, N. J. Mr. Yocom is concerned with the various aspects of carrier and microwave system development, including the design of testing equipment. Since 1952 he has been engaged in research in the field of microwave electronics. Mr. Yocom is now with Varian Associates, Palo Alto, Calif.



IRE News and Radio Notes

Calendar of Coming Events and Authors' Deadlines

- Annual Symp. on Aero Commun., Hotel Utica, Utica, N. Y., Nov. 6-8
- Radio Fall Meeting, King Edward Hotel, Toronto, Can., Nov. 11-13
- PGI Conference, Atlanta-Biltmore Hotel, Atlanta, Ga., Nov. 11-13
- Mid-America Electronics Convention, Kan. City Mun. Audit., Kan. City, Mo., Nov. 13-14
- New England Radio Eng. Mtg., Mechanics Bldg., Boston, Mass., Nov. 15-16
- Conf. on Magnetism, Sheraton-Park Hotel, Wash., D. C., Nov. 18-21
- Elec. Computer Exhibition, Olympia, London, England, Nov. 28-Dec. 4
- Human Factors in Systems Eng., Penn-Sherwood Hotel, Phila., Pa., Dec. 3-4
- PGVS Conf., Hotel Statler, Wash., D. C., Dec. 4-5
- Eastern Joint Computer Conf., Park-Sheraton Hotel, Wash., D. C., Dec. 9-13
- EIA Conf. on Maintainability of Elec. Equip., U.S.C., Los Angeles, Calif., Dec. 18-19
- Nat'l Symp. on Reliability & Quality Control, Statler Hotel, Wash., D. C., Jan. 6-8, 1958
- Scintillation Counter Symp., Shoreham Hotel, Wash., D. C., Jan. 27-28
- Transistor-Solid State Circuits Conf., Phil., Pa., Feb. 20-21
- Nuclear Eng. and Science Congress, Palmer House, Chicago, Ill., Mar. 16-21
- IRE Nat'l Convention, N. Y. Coliseum and Waldorf-Astoria Hotel, New York City, Mar. 24-27 (DL*: Nov. 1, G. L. Haller, IRE Headquarters, New York City)
- Instruments & Regulators Conf., Univ. of Del., Newark, Del., March 31-Apr. 2
- SW Regional Conf. & Show, Mun. Audit., San Antonio, Tex., Apr. 10-12
- Conf. on Automatic Techniques, Statler Hotel, Detroit, Mich., Apr. 14-16
- Elec. Components Symp., Ambassador Hotel, Los Angeles, Calif., Apr. 22-24 (DL*: Nov. 15, E. E. Brewer, Convaire, Pomona, Calif.)
- Seventh Region Conf. & Show, Sacramento, Calif., Apr. 30-May 2
- PGMTT Symp., Stanford Univ., Stanford, Calif., May 5-7 (DL*: Jan. 15, K. Tomiyasu, G. E. Microwave Lab., 601 California Ave., Palo Alto, Calif.)
- Western Joint Computer Conf., Ambassador Hotel, Los Angeles, Calif., May 6-8
- Nat'l Aero & Nav. Elec. Conf., Dayton, Ohio, May 12-14
- IEE Convention on Microwave Valves, Savoy Place, London, England, May 19-23
- PGPT Symp. Hotel New Yorker, New York City, June 5-6
- PGMIL Convention, Wash., D. C., June 15-18
- * DL = Deadline for submitting abstracts

1958 IRE AWARDS ANNOUNCED

A. W. Hull, consultant to the General Electric Research Laboratory, Schenectady, N. Y., was named to receive the Medal of Honor, the highest technical award in the radio-electronics field, "for outstanding scientific achievement and pioneering inventions and development in the field of electron tubes." Dr. Hull is credited with creating a greater number of new types of electron tubes than any other man.

The Founders' Award, bestowed only on special occasions to outstanding leaders in communications and electronics, will be given to W. R. G. Baker (A'19-F'28) "for outstanding contributions to the radio engineering profession through wise and courageous leadership in the planning and administration of technical developments which have greatly increased the impact of electronics on the public welfare."

The Morris Liebmann Memorial Prize will go to E. L. Ginzton (S'39-A'40-SM'46-F'51), professor of applied physics and electrical engineering, Stanford University, "for his creative contribution to the generation and useful application of high energy at microwave frequencies." The award is given annually to a member of the IRE for a recent important contribution to the radio art.

E. W. Allen, Jr. (M'44-F'53), Chief Engineer of the Federal Communications Commission, was named to receive the Harry Diamond Memorial Award "for his technical and administrative contributions in the field of radio spectrum utilization." The award is presented annually to outstanding engineers in government service.

The Vladimir K. Zworykin Television Prize will go to C. P. Ginsburg (A'48-M'55), Ampex Corp., Redwood City, Calif. "for pioneering contributions to the development of video magnetic recording." The award is given annually to a member of the IRE for important contributions to television.

The awards will be presented at the IRE National Convention banquet next March in New York City.

MARS NOVEMBER SCHEDULE SET

The Air Force MARS Eastern Technical Net which broadcasts over the air every Sunday afternoon at 2 P.M. (EST) on 3295, 7540 and 15,715 kc announces the following program for November: Nov. 3 and 10—Nuclear Science. Nov. 17 and 24—Transistor theory and applications. Speakers have not yet been announced as we go to press.

Alois W. Graf (A'26-M'44-SM'45-F'55), IRE Director and partner in the patent law firm of Graf, Nierman and Burmeister, died recently.



A. W. GRAF

For more than a decade Mr. Graf had been a leading figure in IRE sectional, regional, Professional Group, and national activities. From 1944 to 1947, he had served the Chicago IRE Section as its secretary, vice-chairman, and chairman in consecutive terms, and in the years that followed he remained one of the Section's most active members and ardent supporters. Elected to the IRE Board of Directors during 1952-1953, he represented Region Five, and this year he held an appointment to the Board for a one-year term. In addition, he had held important posts on a dozen national committees and represented the IRE on the board of directors of the National Electronics Conference.

As chairman of the IRE Constitution and Laws Committee since 1954 he had devoted a great deal of personal time and effort to studying the IRE constitution and bylaws, New York state laws of incorporation, and trade-mark laws affecting the IRE name, emblem and publication titles. His contributions to the welfare of the IRE in this area alone were monumental.

Mr. Graf was born March 20, 1901, at Mankato, Minn. He obtained a bachelor's degree in electrical engineering from the University of Minnesota in 1926, and a bachelor's of law degree from the National Law University in 1931.

He was first employed as an examiner in the U. S. Patent Office. He subsequently was employed by a patent lawyer to work on validity and infringement searches and resulting prosecutions. The next eight years, from 1930 to 1938, saw him associated with the patent department of the General Electric Company for which he standardized patent procedures and formulated manufacturing policies for vacuum tube devices. He became a patent lawyer for Productive Inventions, Inc., Gary, Ind. In 1940 he began his own private patent law practice, and subsequently became associated with a number of patent law firms, among which were Sheridan, Davis and Cargill; Davis, Lindsey, Smith and Shonts; and Loftus, Moore, Olson and Trexler. He again opened his own law practice in 1949, and in May, 1956, announced the formation of a new patent law firm with L. G. Nierman and M. A. Burmeister. This firm specializes in patent, trade-mark, and copyright law in the radio communications and electronics field.

Mr. Graf had been a member of the bar in the District of Columbia, Indiana and Illinois. He also held membership in American Bar Association, Illinois Society of Professional Engineers, and National Society of Professional Engineers.

MID-AMERICA CONVENTION REVEALS TOPICS AND PAPERS

The Kansas City IRE Section is sponsoring, for the ninth year, the IRE Mid-America Electronics Convention. Headquarters will be at the Municipal Auditorium and Hotel Muehlebach. There will be a hundred exhibits on display, and ten technical sessions during which thirty papers will be presented. Pre-registration information can be obtained from I. H. Rubaii, 425 Volker Blvd., Kansas City 10, Mo.

The keynote speaker at the opening session of the convention will be J. T. Henderson, IRE President. The speaker at the annual banquet will be Simon Ramo, Ramo-Wooldridge Corp.

Session topics and some of the papers to be presented are as follows: *Central Simulation Council*—Simulation of Hydraulic Systems, H. F. Harrington, McDonnell Aircraft; Problems in Simulation of Airplane Spin, M. S. Fineberg, McDonnell Aircraft; *Medical Electronics*—Further Progress in Electronic Control of Artificial Respiration, L. H. Montgomery, Vanderbilt Univ.; Electronics for Medicine, R. G. Stranix, Elec. Ind. & Tele-Tech; Recent Development in Medical Aids at the Univ. of Kansas Medical Center, M. R. Klein, Kansas Univ. Medical Center; *Engineering Management*—Engineering Basis for Modern Management, Richard Mather, Mather Associates; Engineering Management Development, G. W. Jernstedt, Westinghouse Electric; Scientific Basis for Management Planning, Ernest Koenigsberg, Midwest Research Inst.; *Airborne Electronics*—Cooling Airborne Electronic Equipment, David Carlson, Rotron, Inc.; Systems Development in Airborne Communications, Bob Van Zant, Wilcox Electric; Printed Wiring for Airborne Electronic Equipment—Friend or Foe, J. J. Staller, American Bosch Arma Corp.; *Microwaves*—The Reflection Coefficient Method of Measuring Feed Horn Efficiency, R. R. Jenness, Northwestern Univ.; A Miniature Microstrip Directional Coupler, D. J. Nigg, Bendix Aviation; *Automation*—Electrical Connections for Electronics Industry, D. R. Bonwit, Burndy Co.; Automatic Testing, F. A. Spies and L. A. Robinson, Bendix Aviation; *Electronics and Nucleonics*—On Designing Nuclear Tests for Saving Manpower, Merle Jones, Sandia Corp.; The Investigation of G. M. Counter Discharge by the Use of a Short Duration Pulse of High Velocity Electrons, D. H. LeCroissette, Southampton Univ.; *IGY*—Microlock, A Minimum Weight Radio Instrumentation System for a Satellite, Henry Richter, Jet Propulsion Lab. of California Inst. of Technology; *Components*—Ferrite Materials, J. D. Moynihan, Ferroxcube Corp. of America; Higher Voltage, Higher Microfarad Tantalum Capacitors, J. P. Holloway, General Electric Co.

IGY BEGINS MOONBEAM PROJECT DURING IGY

The IGY Committee of the National Academy of Sciences announces the MOONBEAM program to organize and provide technical assistance to amateur radio groups for the operation of simplified tracking sys-

tems during the International Geophysical Year. These systems, Minitrack Mark II and Microlock, will enable volunteers to locate the IGY satellite in its flight and to receive scientific data transmitted from it.

The Naval Research Laboratory has been named to head the MOONBEAM project, with the assistance of the Jet Propulsion Laboratory of the California Institute of Technology. The American Radio Relay League will give active support to the program.

The IGY Committee expects that the cost of these systems will be within the reach of interested amateurs. Of particular importance will be the role of MOONBEAM volunteers in detecting small deviations in the satellite's orbit due to local irregularities in gravity and in recording scientific data which might be telemetered from the satel-

lite coincident with a solar flare.

MOONBEAM teams may be able to make other important contributions to the IGY program by providing supplemental acquisition data (in initially locating the satellite), providing additional data on the effects of the ionosphere, the electrically charged layers of the upper atmosphere, on radio signals, providing time and position checks for the primary recording of data from certain satellite experiments, and providing data upon the occasion of serious damage to the satellite, should this occur.

Requests for technical information and consulting assistance on equipping, establishing, and operating stations in the MOONBEAM volunteer radio network should be directed to the Satellite Office, IGY Committee, National Academy of Sciences, Washington, D. C.

NEREM SESSIONS WILL FEATURE PANEL DISCUSSIONS AND MOVIES

The Northeast Electronics, Research and Engineering Meeting will be held at Mechanics' Hall, Boston, Mass., November 15-16. Over 125 exhibitors will display their wares on the first floor of Mechanics' Hall at this meeting. The four technical sessions will be held on the second floor of the same building accompanied by concurrent showings of films.

Registration arrangements can be made at the door. Admission is free to IRE members, but non-members will be charged \$1.00. During the afternoon of November 15, a cocktail party will be held, for which tickets at \$2.50 may be obtained. Further information regarding the NEREM meeting can be had from the IRE Boston Section, 73 Tremont St., Rm. 1006, Boston 8, Mass.

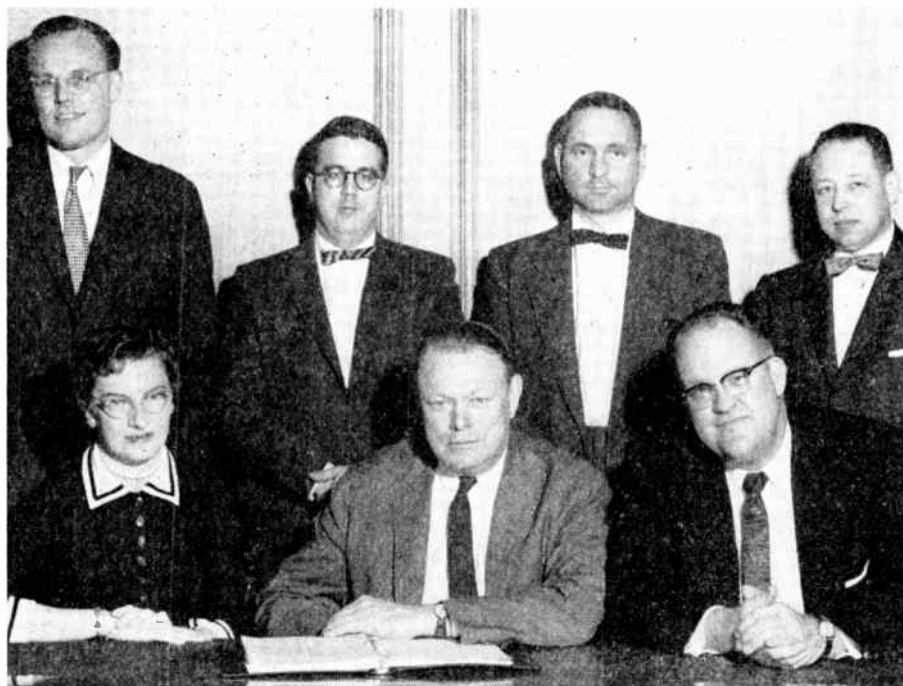
Doors will open 9 A.M. Friday, November 15. During the first session, scheduled

for 10 A.M. to 12:30 P.M., a panel consisting of E. W. Engstrom, RCA; I. J. Getting, Raytheon Mfg. Co.; and a third person yet to be announced will discuss "Electronics in Industry."

The afternoon session on the same day, from 2-4 P.M., will present a panel consisting of James Davis, Vertrol Aircraft Corp.; Maj. Gen. A. L. Pachynski, USAF; and Charles Stec, Bureau of Ships, USN. They will elaborate on the subject of "Electronics in National Defense."

The following morning, Robert Seamans, Jr., RCA; W. W. Finke, Datamatic Corp.; and Vernon Westcott, Trans-Sonics, will discuss "Problems in Establishing a New Engineering Company."

Saturday afternoon, there will be a discussion of "Magnetic Domains, Masers and Transistors," led by T. O. Paine, General Electric Co.; H. E. D. Scovil and J. M. Early, Bell Tel. Labs.; and C. L. Hogan, Harvard Univ.



1957 NEREM Committee—Seated (left to right): S. M. Whitcher, recording secretary; K. C. Black, general chairman; P. G. Yewell, vice-chairman and arrangements. Standing (left to right): Frank Hobbs, treasurer; D. S. Randall, publicity; Leo Rosen, program; S. B. Fishbein, registration. Absent: H. H. Dawes, exhibits.

TWO NEW SECTIONS ARE FORMED

On September 11, the IRE Board of Directors abolished the North Carolina-Virginia Section and the Piedmont Subsection. Two new Sections were formed from the territory of the abolished Section, the North Carolina Section and the Virginia Section.

The newly-formed North Carolina Section will absorb the Eastern North Carolina Subsection and the Western North Carolina Subsection. The newly-formed Virginia section will absorb the Hampton Roads Subsection.

GEORGE W. BAILEY IS NAMED ADVISOR TO STATE DEPARTMENT

G. W. Bailey (A'38-SM'46-F'56), IRE Executive Secretary, has been appointed advisor and consultant on telecommunications matters to Deputy Undersecretary of State C. Douglas Dillon in charge of economic affairs. The State Department stated that Mr. Bailey's services will be at the call of Mr. Dillon.

Mr. Bailey has served as general chairman of the IRE National Convention since 1948. He is a former president of the American Radio Relay League, International Amateur Radio Union, and Armed Forces Communications and Electronics Association.

PROFESSIONAL GROUP NEWS

The 1958 National Symposium of the Professional Group on **Microwave Theory and Techniques** to be held on May 5-7 at Stanford University, Stanford, Calif., has been announced by the General Chairman, A. L. Aden.

Authors should submit, *in triplicate*, prior to January 15, 1958, both: an 100-word abstract, title of paper, name and address; and a 500-word summary, title of paper, name and address.

Papers related to microwave physics and applications, microwave components, and

microwave techniques are considered appropriate.

Please submit papers to: Dr. Kiyo Tomiyasu, Chairman, Technical Program Committee, 601 California Ave., Palo Alto, Calif.

The Eighth National Conference of the IRE Professional Group on **Vehicular Communications** will take place at the Hotel Statler, Washington, D. C., Dec. 4-5.

The opening session on "Vehicular Communications Equipment Accessories" will include papers on *Transistorized Microphones for Vehicular Communications*, H. Johnson and L. Rosenman, Shure Bros.; *New-Type High-Gain Station Antenna*, M. W. Scheldorf, Andrew Corp.; *The End of the Line*, T. J. McMullin, Communications Engineering Co.; and *Sources of Interference Inherent in Vehicular Electrical Systems*, B. H. Short, Delco-Remy Div., General Motors Corp.

The second session, on "Trends in Mobile Equipment," will include the following papers: *A New Arm for Vehicular Communication*, J. R. Neubauer, RCA; *A Compact, Low-Cost 150 Mc Mobile Unit of Unusual Design*, M. A. Robbins, Canadian Marconi Co.; *Application of Single Sideband for Mobile Communications*, W. L. Firestone, Motorola, Inc.; and *Transistorized Frequency Reference and Control System for 920 Channel Military Vehicular UHF-FM Receiver-Transmitter*, Don Kammer and Frank Brauer, Avco Mfg. Corp.

The session on "Vehicular Systems Considerations" will consist of papers on *The Meat of the Backbone*, A. C. Giesselman, General Electric Co.; *Meeting the Demands for Vehicular Communications?* Curtis Plummer, the Federal Communications Commission; *Dial-Operated Mobile Radio Systems*, George Dodrill, the Rural Electrification Administration; *Dial Direct, Fully Automatic Radiotelephone System and Associated Equipment*, Ramsey McDonald, Richmond Radiotelephone, Inc.; and *Vehicular Transmissions*, John Egli, U. S. Army Signal Eng. Labs.

There will also be a panel discussion relating to mobile frequency allocation and assignment practices, moderated by E. M. Webster, former FCC Commissioner.

Papers presented at this conference will be published in the *TRANSACTIONS* of the PGVC as soon as possible after the conference's conclusion. Registration is \$3.

Members of the committee in charge of the conference details are: J. J. Renner, chairman of the Washington Chapter of PGVC; George Dodrill, chapter vice-chairman; G. J. Ikelman, chapter secretary; G. E. Woodside, program; R. L. Abel, exhibits; J. E. Keller, hospitality; G. J. Ikelman, registration; Merle Floegel, treasurer; and R. E. Tall, publicity.

TECHNICAL COMMITTEE NOTES

The following Technical Committees held meetings this past month:

- Aug. 13—Video Techniques Committee, S. Doba, Jr., Chairman, IRE Headquarters.
- Aug. 27—Nuclear Techniques Committee, G. A. Morton, Chairman, National Bureau of Standards, Washington, D. C.
- Sept. 10—Radio Frequency Interference Committee, A. B. Glenn, Chairman, IRE Headquarters.
- Sept. 12—Standards Committee, M. W. Baldwin, Jr., Chairman, IRE Headquarters.

The following IRE Standards have been approved recently by the IRE Standards Committee and will be published shortly in the *PROCEEDINGS*: IRE Standards on Graphical Symbols for Semiconductor Devices, 1957; IRE Standards on Letter Symbols and Mathematical Signs, 1948 (reprinted 1957); IRE Standards on Reference Designations for Electrical and Electronic Equipment, 1957; and IRE Standards on Television: Measurement of Luminance Signal Levels, 1957.

Professional Groups†

Aeronautical & Navigational Electronics—Joseph General, 6019 Highgate Dr., Baltimore 15, Md.

Antennas & Propagation—J. I. Bohnert, Code 5200, Naval Research Lab., Washington 25, D. C.

Audio—Dr. H. F. Olson, RCA Labs., Princeton, N. J.

Automatic Control—E. M. Grabbe, Ramo-Wooldridge Corp., Box 45067, Airport Station, Los Angeles 45, Calif.

Broadcast & Television Receivers—L. R. Fink, General Electric Co., X-Ray Dept., Milwaukee, Wis.

Broadband Transmission Systems—C. H. Owen, 7 W. 66th St., N. Y. 23, N. Y.

Circuit Theory—W. H. Huggins, 2813 St. Paul St., Baltimore 18, Md.

Communications Systems—J. W. Worthington, Jr., Dawn Dr., Mounted Route, Rome, N. Y.

Component Parts—R. M. Soria, American

Phenolic Corp., 1830 S. 54 Ave., Chicago 50, Ill.

Education—J. D. Ryder, Dept. of Elec. Eng., Mich. State Univ., E. Lansing, Mich.

Electron Devices—T. M. Liimatainen, 5415 Connecticut Ave., N.W., Washington, D. C.

Electronic Computers—Werner Buchholz, IBM Engineering Lab., Poughkeepsie, N. Y.

Engineering Management—C. R. Burrows, Ford Instrument Co., 31-10 Thomson Ave., Long Island City 1, N. Y.

Engineering Writing and Speech—D. J. McNamara, Sperry Gyroscope Co., Great Neck, L. I., N. Y.

Industrial Electronics—W. R. Thurston, General Radio Co., 285 Massachusetts Ave., Cambridge 39, Mass.

Information Theory—W. B. Davenport, Jr., Lincoln Lab., M.I.T., Cambridge, Mass.

Instrumentation—F. C. Smith, Jr., Southwestern Industrial Electronics Co., 2831

Post Oak Rd., Houston 19, Tex.

Medical Electronics—L. B. Lusted, M.D., Clinical Center, National Institute of Health, Bethesda 14, Md.

Microwave Theory and Techniques—W. L. Pritchard, Raytheon Mfg. Co., Newton, Mass.

Military Electronics—W. E. Cleaves, 3807 Fenchurch Rd., Baltimore 18, Md.

Nuclear Science—J. N. Grace, Westinghouse Atomic Power Div., Pittsburgh 34, Pa.

Production Techniques—E. R. Gamson, Autonetics, 395-91, 12214 Lakewood Blvd., Downey, Calif.

Reliability and Quality Control—Victor Wouk, Beta Electric Corp., 333 E. 103rd St., New York 29, N. Y.

Telemetry and Remote Control—C. H. Doersam, Jr., 24 Winthrop Rd., Port Washington, L. I., N. Y.

Ultrasonics Engineering—C. M. Harris, 425 Riverside Dr., New York, N. Y.

Vehicular Communications—C. M. Heiden, General Electric Co., Syracuse, N. Y.

† Names listed are Group Chairmen.

Sections*

- Akron (4)**—H. F. Lanier, 2220—27th St., Cuyahoga Falls, Ohio; Charles Morrill, 2248—16th St., Cuyahoga Falls, Ohio.
- Alamogordo-Holloman (6)**—V. J. Lynch, 1105 Maple Dr., Alamogordo, N. Mex.; R. B. Kleinman, Box 1054, Holloman AFB, N. Mex.
- Albuquerque-Los Alamos (7)**—B. L. Basore, 2405 Parsifal, N.E., Albuquerque, N. Mex.; John McLay, 3369—48 Loop, Sandia Base, Albuquerque, N. Mex.
- Atlanta (3)**—W. B. Miller, 1369 Holly Lane, N.E., Atlanta 6, Ga.; W. H. White, 1454 S. Gordon St., S.W., Atlanta 10, Ga.
- Baltimore (3)**—M. R. Briggs, Westinghouse Elec. Corp., Box 746, Baltimore 3, Md.; B. Wolfe, Director of Eng'g., Station WAAM-TV, 3725 Malden Ave., Baltimore 11, Md.
- Bay of Quinte (8)**—W. D. Ryan, Cavalry House, Royal Military College, Kingston, Ont., Canada; R. Williamson, R.R. 3, Belleville, Ont., Canada.
- Beaumont-Port Arthur (6)**—F. M. Crum, 1905 Prairie St., Beaumont, Tex.; H. K. Smith, 270 Canterbury Lane, Beaumont, Tex.
- Binghamton (1)**—Robert Nash, 12 Alice St., M.R. 97, Binghamton, N.Y.; Bruce Lockhart, R.D. 3, Binghamton, N. Y.
- Boston (1)**—C. J. Lahanas, 275 Massachusetts Ave., General Radio Co., Cambridge 39, Mass.; (secretary to be elected).
- Buenos Aires**—J. M. Onativia, Bustamante 1865, Buenos Aires, Argentina; L. F. Rocha, Caseros 3321, DTO. B., Buenos Aires, Argentina.
- Buffalo-Niagara (1)**—W. S. Holmes, Cornell Aeronautical Labs., 4455 Genesee St., Buffalo 21, N. Y.; R. B. Odden, 573 Allenhurst Rd., Buffalo, N. Y.
- Cedar Rapids (5)**—J. L. Dalton, 2900 E. Ave., N.E., Cedar Rapids, Iowa; S. M. Morrison, 2034 Fourth Ave., S.E., Cedar Rapids, Iowa.
- Central Florida (3)**—G. F. Anderson, Dynatronics, Inc., 717 W. Amelia Ave., Orlando, Fla.; J. W. Downs, 1020 Highland Ave., Eau Gallie, Fla.
- Central Pennsylvania (4)**—W. J. Leiss, 1173 S. Atherton St., State College, Pa.; P. J. Freed, Hallor, Raymond & Brown, State College, Pa.
- Chicago (5)**—D. G. Haines, 17 W. 121 Oak Lane, Bensenville, Ill.; S. F. Bushman, 1166 Oakwood Ave., Des Plaines, Ill.
- China Lake (7)**—C. F. Freeman, 100-B Halsey St., China Lake, Calif.; P. K. S. Kim, 200-A Byrnes St., China Lake, Calif.
- Cincinnati (4)**—F. L. Weidig, Jr., 3819 Davenport Ave., Cincinnati 13, Ohio; H. E. Hancock, R.R. 4, Branch Hill Box 52, Loveland, Ohio.
- Cleveland (4)**—J. F. Keithley, 22775 Douglas Rd., Shaker Heights 22, Ohio; C. F. Schunemann, 2021 Sagamore Dr., Euclid 17, Ohio.
- Columbus (4)**—T. E. Tice, 2214 Jarvis Rd., Columbus 21, Ohio; G. R. Jacoby, 78 N. James Rd., Columbus 13, Ohio.
- Connecticut Valley (1)**—B. R. Kamens, 94 Admiral Dr., New London, Conn.; J. D. Lebel, Benedict Hill Rd., New Canaan, Conn.
- Dallas (6)**—Frank Seay, Collins Radio Co., 1930 Hi-Line Dr., Dallas, Tex.; T. B. Moseley, 6114 Northwood Rd., Dallas 25, Tex.
- Dayton (4)**—N. A. Nelson, 101 Castle Dr., Dayton 9, Ohio; D. G. Clute, 2132 Merilene Ave., Dayton 10, Ohio.
- Denver (6)**—R. C. Webb, 2440 S. Dahlia St., Denver 22, Colo.; S. B. Peterson, 1295 S. Jackson, Denver 10, Colo.
- Detroit (4)**—E. C. Johnson, 4417 Crooks Rd., Royal Oak, Mich.; G. E. Ryan, 5296 Devonshire Rd., Detroit 24, Mich.
- Egypt**—H. M. Mahmoud, Faculty of Engineering, Fouad I University, Giza, Cairo, Egypt; El Garhi I El Kashlan, Egyptian Broadcasting, 4, Shari Sherifein, Cairo, Egypt.
- Elmira-Corning (1)**—R. G. Larson, 220 Lynhurst Ave., Windsor Gardens, Horseheads, N. Y.; D. F. Aldrich, 1030 Hoffman St., Elmira, N. Y.
- El Paso (6)**—J. Crosson, 1100 Honeysuckle Drive, El Paso, Tex.; H. Markowitz, 700 E. Paisano Dr., El Paso, Tex.
- Emporium (4)**—H. S. Hench, Jr., Sylvan Heights, Emporium, Pa.; H. J. Fromell, Sylvania Elec. Prod. Inc., Emporium, Pa.
- Evansville-Owensboro (5)**—A. K. Miegler, 904 Kelsey Ave., Evansville, Ind.; M. Casler, Evansville College, Evansville, Ind.
- Florida West Coast (3)**—L. J. Link, 3216 Ninth St., North, St. Petersburg, Fla.; R. Murphy, 12112 N. Edison Ave., Tampa 4, Fla.
- Fort Huachuca (7)**—J. K. Oliver, Box 656, Ft. Huachuca, Ariz.; W. C. Shelton, Box 2919, Fort Huachuca, Ariz.
- Fort Wayne (5)**—T. L. Slater, 1916 Eileen Dr., Waynedale, Ind.; F. P. Smith, Windsor Rd., R.R. 15, Fort Wayne, Ind.
- Fort Worth (6)**—C. W. Macune, 3132 Forest Park Blvd., Fort Worth, Tex.; G. H. Robertson, 5749 Tracyne Drive, Fort Worth 14, Tex.
- Hamilton (8)**—C. N. Chapman, 40 Dundas St., Waterdown, Ont., Canada; C. J. Smith, Gilbert Ave., Dancaster Courts, Sub. Serv. 2, Ancaster, Ont., Canada.
- Hawaii (7)**—Vaughn Kelly, 99-1215 Aiea Hgts. Dr., Aiea, Hawaii; D. L. Grubb, 236 Paiko Dr., Honolulu, Hawaii.
- Houston (6)**—M. A. Arthur, Humble Oil & Refining Co., P.O. Box 2180, Houston 1, Tex.; C. G. Turner, Communications Engineering Co., P.O. Box 12325, Houston 17, Tex.
- Huntsville (3)**—W. O. Frost, P.O. Box 694, Huntsville, Ala.; J. E. Douma, 804 Carmelian, S.E., Huntsville, Ala.
- Indianapolis (5)**—B. V. K. French, 4480 Marcy Lane, Apt. 62, Indianapolis 5, Ind.; N. G. Drilling, 3002 Ashland Ave., Indianapolis 26, Ind.
- Israel**—E. H. Frei, Weizman Inst. of Science, Rehovoth, Israel; Moshe Tkatch, P.O.B. 1, Kiryat Motzkin, Haifa, Israel.
- Ithaca (1)**—H. S. McGaughan, Dept. of Elec. Eng., Cornell Univ., Ithaca, N. Y.; W. H. Murray, General Electric Co., Ithaca, N. Y.
- Kansas City (6)**—P. C. Constant, Jr., 3014 E. Meyer Blvd., Kansas City 30, Mo.; N. E. Vilander, 2509 W. 83rd St., Kansas City 15, Mo.
- Little Rock (6)**—J. D. Reid, 2210 Summit, Little Rock, Ark.; J. P. McRae, Route 1, Scott, Ark.
- London (8)**—E. R. Jarmain, 13 King St., London, Ont., Canada; W. A. Nunn, Radio Station CFPL-TV, London, Ont., Canada.
- Long Island (2)**—E. G. Fubini, Airborne Instrument Labs., 160 Old Country Rd., Mineola, L. I., N. Y.; E. K. Stodola, 118 Stanton St., Northport, N. Y.
- Los Angeles (7)**—J. K. Gossland, 318 E. Calaveras St., Altadena, Calif.; R. G. Kueck, 914 Arroyo Dr., South Pasadena, Calif.
- Louisville (5)**—M. C. Probst, 5067 Poplar Level Rd., Louisville, Ky.; W. J. Ryan, 4215 N. Western Pkwy., Louisville, Ky.
- Lubbock (6)**—E. W. Jenkins, Jr., Shell Oil Co., Admin. Dept., Box 1509, Midland, Tex.; J. J. Criswell, 511 50th St., Lubbock, Tex.
- Miami (3)**—W. H. Epperson, 5845 S.W. 108 St., Miami 43, Fla.; R. S. Rich, 7513 S.W. 54 Ct., S. Miami, Fla.
- Milwaukee (5)**—J. E. Jacobs, 6230 Hale Park Dr., Hales Corners, Wis.; F. J. Lofy, 2258 S. 56 St., West Allis 19, Wis.
- Montreal (8)**—R. E. Penton, 6120 Cote St., Luc Rd., Apt. 6, Montreal, Quebec, Canada; R. Lumsden, 1680 Lepine St., St. Laurent, Montreal 9, Quebec, Canada.
- Newfoundland (8)**—J. B. Austin, Jr., Hq. 1805th AACPS Wing, APO 862, c/o PM, New York, N. Y.; J. A. Willis, Canadian Marconi Co., Ltd., Pinetree-NEAC Depot, Pepperrill AFB, St. John's Newfoundland, Canada.
- New Orleans (6)**—M. F. Chapin, 8116 Hampson St., New Orleans, La.; G. A. Hero, 1102 Lowerline St., New Orleans 18, La.
- New York (2)**—J. S. Smith, 3717 Clarendon Rd., Brooklyn, N. Y.; Joseph Reed, 52 Hillcrest Ave., New Rochelle, N. Y.
- North Carolina-Virginia (3)**—F. E. Brooks, Box 277, Colonial Ave., Colonial Beach Va.; E. S. Busby, Jr., 1608 "B" St., Portsmouth, Va.
- Northern Alberta (8)**—J. E. Sacker, 10235—103rd St., Edmonton, Alberta, Canada; Frank Hollingworth, 9619—85th St., Edmonton, Alberta, Canada.
- Northern New Jersey (2)**—T. N. Anderson, 1539 Deer Path, Mountainside, N. J.; G. D. Hulst, 37 College Ave., Upper Montclair, N. J.
- Northwest Florida (3)**—G. C. Fleming, 579 E. Gardner Dr., Fort Walton Beach, Fla.; W. F. Kirlin, 67 Laurie Dr., Fort Walton Beach, Fla.
- Oklahoma City (6)**—Nicholas Battenburg, 2004 N.W. 30th St., Oklahoma City 6, Okla.; E. W. Foster, 5905 N.W. 42 St., Oklahoma City 12, Okla.
- Omaha-Lincoln (5)**—J. S. Petrik, c/o KETV, 27 & Douglas Sts., Omaha, Neb.; H. W. Becker, 1214 N. 34 St., Omaha 3, Neb.
- Ottawa (8)**—L. H. Doherty, 227 Barclay Rd., Ottawa 2, Ont., Canada; R. S. Thain, 54 Rossland Ave., Box 474, City View, Ont., Canada.

* Numerals in parentheses following section designate region number. First name designates Chairman, second name, Secretary.

- Philadelphia (3)**—Nels Johnson, Philco Corp., 4700 Wissahickon Ave., Philadelphia 44, Pa.; W. A. Howard, WRCV, 1619 Walnut St., Philadelphia 4, Pa.
- Phoenix (7)**—G. L. McClanathan, 509 E. San Juan Cove, Phoenix, Ariz.; E. S. Shepart, 5716 N. 19 St., Phoenix, Ariz.
- Pittsburgh (4)**—Gary Muffly, 715 Hulton Rd., Oakmont, Pa.; H. R. Kaiser, WHC-WWSW, Sherwyn Hotel, Pittsburgh 22, Pa.
- Portland (7)**—D. C. Strain, 7325 S.W. 35 Ave., Portland 19, Ore.; W. E. Marsh, 6110 S.W. Brugger St., Portland 19, Ore.
- Princeton (2)**—L. L. Burns, Jr., RCA Labs., Princeton, N. J.; Sylvan Fich, College of Eng'g., Rutgers Univ., New Brunswick, N. J.
- Regina (8)**—J. A. Funk, 138 Leopold Crescent, Regina, Saskatchewan, Canada; E. C. Odling, 1121 Minto St., Regina, Saskatchewan, Canada.
- Rio de Janeiro, Brazil**—M. P. De Britto Pereira, Caixa Postal 562, Rio de Janeiro, Brazil; J. A. Hertz, Caixa Postal 97 Lapa, Rio de Janeiro, Brazil.
- Rochester (1)**—B. L. McArdle, Box 54, Brighton Station, Rochester 10, N. Y.; L. D. Smith, 27 Landing Park, Rochester, N. Y.
- Rome-Utica (1)**—Edward R. Orear, Ch., 36 Herthum Rd., Harts Hill Heights, Whitesboro, N. Y.; Sidney Rosenberg, V. Ch., 907 Valentine Ave., Rome, N. Y.; Robert A. Zachary, Jr., Sec., 11 Arbor Drive, New Hartford, N. Y.
- Sacramento (7)**—E. W. Berger, 3421—58 St., Sacramento 20, Calif.; P. K. Onnigian, 4003 Parkside Ct., Sacramento, Calif.
- St. Louis (6)**—C. E. Mosley, 8622 St. Charles Rock Rd., Overland 14, Mo.; R. D. Rodenroth, 7701 Delmont, Affton 23, Mo.
- Salt Lake City (7)**—J. S. Hooper, 1936 Hubbard Ave., Salt Lake City 5, Utah; A. L. Gunderson, 3906 Parkview Dr., Salt Lake City 17, Utah.
- San Antonio (6)**—F. A. Brogan, 433 Brees Blvd., San Antonio 9, Tex.; W. L. Donaldson, 129 El Cerrito, San Antonio, Tex.
- San Diego (7)**—E. J. Moore, 3601 Eighth St., San Diego 3, Calif.; R. J. Cary, Jr., 4561 Normandie Place, La Mesa, Calif.
- San Francisco (7)**—Meyer Leifer, Electronic Defense Lab., Box 205, Mountain View, Calif.; V. B. Corey, 385 Gravatt Dr., Berkeley 5, Calif.
- Schenectady (1)**—A. E. Rankin, 833 Whitney Dr., Schenectady, N. Y.; Sec.-Treas. to be appointed later.
- Seattle (7)**—R. H. Hoglund, 1825 E. Lynn St., Seattle 7, Wash.; L. C. Perkins, Box 307, Des Moines, Wash.
- Shreveport (6)**—H. H. Moreland, 11q. 2nd Air Force, Barksdale AFB, La.; M. C. Benson, P.O. Box 1316, Shreveport, La.
- South Bend-Mishawaka (5)**—R. D. Ewing, 3755 Terry Lane, Mishawaka, Ind.; H. E. Harry, Bendix Prod. Div.-Missiles, 400 S. Beizer St., Mishawaka, Ind.
- Southern Alberta (8)**—W. K. Allan, 2025 29th Ave., S.W., Calgary, Alta., Canada; R. W. H. Lamb, Radio Station CFCN, 12th Ave. and Sixth St. E., Calgary, Alberta, Canada.
- Syracuse (1)**—J. B. Russell, Salt Spring Rd., Fayetteville, N. Y.; R. N. Lothes, General Electric Co., Bldg 3—Industrial Park, Syracuse, N. Y.
- Tokyo**—Yasujiro Niwa, Tokyo Elec. Engineering College, 2-2 Kanda-Nishikicho, Chiyoda-Ku, Tokyo, Japan; Fumio Minozuma, 16 Ohara-Machi, Meguro-Ku, Tokyo, Japan.
- Toledo (4)**—H. L. Nevert, 3534 Woodmont Rd., Toledo 13, Ohio; K. P. Herrick, 2516 Fulton St., Toledo 10, Ohio.
- Toronto (8)**—H. W. Jackson, 352 Laird Dr., Toronto 17, Ont., Canada; R. J. A. Turner, 66 Gage Ave., Scarborough, Ont., Canada.
- Tucson (7)**—P. E. Russell, Elec. Engrg. Dept., Univ. of Ariz., Tucson, Ariz.; C. L. Becker, 4411 E. Sixth St., Tucson, Ariz.
- Tulsa (6)**—R. L. Atchison, 415 E. 14 Pl., Tulsa 20, Okla.; B. H. Keller, 1412 S. Winston, Tulsa 12, Okla.
- Twin Cities (5)**—E. W. Harding, 5325 Colfax Ave., S., Minneapolis, Minn.; S. W. Schulz, 3132 Fourth St., S.E., Minneapolis 14, Minn.
- Vancouver (8)**—R. A. Marsh, 3873 W. 23 Ave., Vancouver, B. C., Canada; T. G. Lynch, 739 Edgewood Rd., North Vancouver, B. C., Canada.
- Washington (3)**—A. H. Schooley, 3940 First St., S.W., Washington 24, D. C.; J. E. Durkovic, 10316 Colesville Rd., Silver Spring, Md.
- Wichita (6)**—W. K. Klatt, 2625 Garland, Wichita 4, Kan.; A. T. Murphy, Univ. of Wichita, Dept. of Elec. Engg., Wichita 14, Kan.
- Williamsport (4)**—(No chairman at present); W. H. Bresee, 818 Park Ave., Williamsport, Pa.
- Winnipeg (8)**—C. J. Hopper, 332 Bronx Ave., Winnipeg 5, Man., Canada; T. J. White, Dept. of E.E., University of Manitoba, Ft. Garry, Man., Canada.

Subsections

- Berkshire (1)**—Robert Shechan, Ballou Lane, Williamstown, Mass.; A. K. Hooks, Sprague Elec. Co., N. Adams, Mass.
- Buenaventura (7)**—M. H. Fields, 430 Roderick St., Oxnard, Calif.; D. J. Heron, 1316 Ocean Dr., Oxnard, Calif.
- Charleston (3)**—A. Jonas, 105 Lancaster St., N. Charleston, S. C.; F. A. Smith, Route 4, Melrose Box 572, Charleston, S. C.
- East Bay (7)**—C. W. Park, 6035 Chaboly Terr., Oakland 18, Calif.; Robert Rector, 1425 Edith St., Berkeley, Calif.
- Eastern North Carolina (3)**—Names of officers not yet known.
- Erie (1)**—J. D. Heibel, 310 W. Grandview, Erie, Pa.; D. H. Smith, 3025 State St., Erie, Pa.
- Gainesville (3)**—W. E. Lear, Dept. of Elec. Eng., Univ. of Fla., Gainesville, Fla. (Chairman)
- Hampton Roads (3)**—R. L. Lindell, WTAR Radio Corp., 720 Boush St., Norfolk 10, Va.; J. E. Eller, Waterview Apts., Apt. E-3, Portsmouth, Va.
- Kitchener-Waterloo (8)**—Jules Kadish, Raytheon Canada, Ltd., 61 Laurel St., Waterloo, Ont., Canada; G. C. Field, 48 Harber Ave., Kitchener, Ont., Canada.
- Lancaster (3)**—W. T. Dyall, 1415 Hillcrest Rd., Lancaster, Pa.; P. W. Kaseman, 405 S. School Lane, Lancaster, Pa.
- Las Cruces-White Sands Proving Grounds (6)**—(Chairman to be elected); M. Goldin, 1921 Calle de Suneos, Las Cruces, New Mex.
- Lehigh Valley (3)**—F. W. Smith, E.E. Dept., Lafayette College, Alumni Hall of Eng'g., Easton, Pa.; L. G. McCracken, Jr., 1774 W. Union Blvd., Bethlehem, Pa.
- Memphis (3)**—R. N. Clark, Box 227, Memphis State College, Memphis, Tenn. (Chairman)
- Mid-Hudson (2)**—Altman Lampe, Cramer Rd., R.D. 3, Poughkeepsie, N. Y.; M. R. Marshall, 208 Smith St., Poughkeepsie, N. Y.
- Monmouth (2)**—Edward Massell, Box 433, Locust, N. J.; Harrison Rowe, Box 107, Red Bank, N. J.
- Nashville (3)**—W. W. Stifler, Jr., Aladdin Electronics, Nashville 2, Tenn.; P. E. Dicker, Dept. of Elec. Engrg., Vanderbilt Univ., Nashville 5, Tenn.
- New Hampshire (1)**—M. R. Richmond, 55 Raymond St., Nashua, N. H.; R. O. Goodwin, 86 Broad St., Nashua, N. H.
- Northern Vermont (1)**—Charles Horvath, 15 Iby St., S. Burlington, Vt.; D. M. Wheatley, 14 Patrick St., S. Burlington, Vt.
- Orange Belt (7)**—R. E. Beekman, 113 N. Lillie Ave., Fullerton, Calif.; R. W. Thorpe, 303 S. Louise Ave., Azusa, Calif.
- Palo Alto (7)**—Wayne Abraham, 4256 Los Palos Pl., Palo Alto, Calif.; W. E. Ayer, 150 Erica Way, Menlo Park, Calif.
- Panama City (3)**—C. B. Koesy, 1815 Moates Ave., St. Andrew Station, Panama City, Fla.; M. H. Naeseth, 1107 Buena Vista Blvd., Panama City, Fla.
- Pasadena (7)**—J. L. Stewart, Assoc. Prof. of Elec. Engrg., Calif. Inst. of Tech., Pasadena, Calif.; J. E. Ranks, Electro-Data, Pasadena, Calif.
- Piedmont (3)**—H. H. Arnold, 548 S. Westview Dr., Winston-Salem, N. C.; C. A. Norwood, 830 Gales Ave., Winston-Salem, N. C.
- Quebec (8)**—R. E. Collin, 590 Avenue Mon Repos, Ste. Foy, Quebec, Can.; R. M. Vaillancourt, 638 Avenue Mon Repos, Ste. Foy, Quebec, Canada.
- Richland (7)**—R. E. Connally, 515 Cottonwood Dr., Richland, Wash.; R. R. Cone, 611 Thayer, Richland, Wash.
- San Fernando (7)**—J. C. Van Groos, 21051 Constansto St., Box 425, Woodland Hills, Calif.; F. E. La Fetra, 22700 Erwin St., Woodland Hills, Calif.
- Santa Barbara (7)**—G. J. Maki, 1417 Pacific Drive, Santa Barbara, Calif.; C. P. Hedges, 316 Coleman Ave., Santa Barbara, Calif.
- USAFIT (4)**—I.Cdr. E. M. Lipsey, 46 Spinning Rd., Dayton 3, Ohio; Sec.-Treas. to be appointed later.
- Westchester County (2)**—D. S. Kellogg, 9 Bradley Farms, Chappaqua, N. Y.; M. J. Lichtenstein, 53 Beaumont Circle, Yonkers, N. Y.
- Western North Carolina (3)**—J. G. Carey, 1429 Lilac Rd., Charlotte, N. C.; R. W. Ramsey, Sr., 614 Clement Ave., Charlotte 4, N. C.

Conference on Magnetism and Magnetic Materials

SHERATON PARK HOTEL, WASHINGTON, D. C., NOV. 18-21

MONDAY, NOVEMBER 18

9:30 A.M.

Sheraton Hall

Invited Papers

Opening Remarks, J. E. Goldman, conference chairman. G. T. Rado, presiding. Paper by L. Néel, Institut Fourier, Grenoble, France.

Physical Phenomena Involved in Maser Operation, C. L. Hogan, Harvard Univ.

Masers, C. H. Townes, Columbia Univ.

Time Decrease of Permeability in Iron, G. W. Rathenau, Natuurkundig Laboratorium, Univ. of Amsterdam, Netherlands.

Observations on Magnetism Research in Europe, J. S. Smart, U. S. Office of Naval Research, London, England.

2:00 P.M.

Sheraton Hall

Magnetization Reversal: Mostly in Thin Films

C. P. Bean, presiding.

Magnetic Anisotropy and Relaxation in Thin Films, D. O. Smith, Lincoln Lab. of M. I. T.

Magnetization Reversal in Thin Films of Permalloy, C. D. Olson and A. V. Pohm, Remington Rand Univac.

Rotational Model of Flux Reversal in Square Loop Soft Ferromagnets, E. M. Gyorgy, Bell Tel. Labs.

Transverse Flux Change in Soft Ferromagnets, F. B. Humphrey, Bell Tel. Labs.

The Effects of Heat Treatment of Thin Ferromagnetic Films at Intermediate Temperatures, E. N. Mitchell, Remington Rand Univac.

Reversible Rotation in Magnetic Films, R. M. Sanders and T. D. Rossing, Remington Rand Univac.

Steady-State and Pulse Measurement Techniques for Thin Ferromagnetic Films in the Frequency Range 0.3 to 5000 Mc, D. O. Smith and G. P. Weiss, Lincoln Lab. of M. I. T.

Ferromagnetic Resonance in Ultra-Thin Films, M. H. Seavey, Jr. and P. E. Tannenwald, Lincoln Lab. of M. I. T.

Domain Walls and Patterns in Thin Permalloy Films, E. E. Huber, Jr., D. O. Smith and J. B. Goodenough, Lincoln Lab. of M. I. T.

Motion Pictures of Magnetic Writing on Thin Films of MnBi, H. J. Williams and R. C. Sherwood, Bell Tel. Labs.

Continental Room

Small Particles and Permanent Magnets

W. F. Brown, Jr., presiding.

Electron Microscopical Investigation of the Metallographic Structure of Ticonal-G (Alnico V), J. J. deJong, J. M. G. Smeets and H. B. Haanstra, Philips Research Labs., Eindhoven, Netherlands.

Relation Between Colloid Pattern and Permanent Magnet Precipitate During the Magnetization Reversal in Alnico V, K. J.

Kronenberg and R. K. Tenzer, Indiana Steel Products Co.

Physical and Magnetic Properties of Elongated Single-Domain Fine Particle Iron and Iron-Cobalt Permanent Magnets, R. B. Falk, E. J. Yamartino, and R. C. Lever, Measurement Lab. of General Electric Co.

Effects of Magnetic Fields upon Anisotropic Iron Crystals, J. H. L. Watson, Edsel B. Ford Institute for Medical Research, A. Arrott, Scientific Lab., Ford Motor Co., and M. W. Freeman, M. W. Freeman Co.

Loss of Exchange Coupling in the Surface Layers of Ferromagnetic Particles, F. E. Luborsky, Instrument Dept., Gen. Elec. Co.

Ferromagnetic Resonance Studies of Some Solid State Transformations, D. S. Rodbell, General Electric Research Lab.

Magnetic Determination of Shape Distribution of Single Domain Powders, C. E. Johnson, Jr. and W. F. Brown, Jr., Minnesota Mining and Mfg. Co.

Magnetic Measurements on Some Precipitating Systems, A. E. Berkowitz and P. J. Flanders, Franklin Institute Labs.

Precipitation and Magnetic Annealing in a Copper-Cobalt Alloy, J. J. Becker, General Electric Research Lab.

TUESDAY, NOVEMBER 19

9:00 A.M.

Sheraton Hall

Ferromagnetic Resonance: Line Structures

J. K. Galt, presiding.

Resonant Modes of Ferromagnetic Spheroids, L. R. Walker, Bell Tel. Labs.

Multiplicities of the Uniform Precessional Mode in Ferrimagnetic Resonance, I. H. Solt, Jr., R. L. White and J. E. Marcereau, Hughes Research Lab.

Ferromagnetic Resonance and Nonlinear Effects in Yttrium Iron Garnet, R. C. LeCraw, E. G. Spencer and C. S. Porter, Diamond Ordnance Fuze Labs.

Low Temperature Spin Wave Resonance at 3000 and 4000 Mc/sec in a Permalloy Having Nearly Zero Magnetocrystalline Anisotropy, J. R. Weertman and G. T. Rado, U. S. Naval Research Lab.

Effect of Electronic Mean Free Path on Spin Wave Resonance in Ferromagnetic Metals, G. T. Rado, U. S. Naval Research Lab.

Ferromagnetic Dynamical Response, H. B. Callen, Dept. of Physics, Univ. of Pa.

Dipole Narrowing of Inhomogeneously Broadened Ferromagnetic Resonance Lines, A. M. Clogston, Bell Tel. Labs.

Origin of Ferromagnetic Resonance Line Broadening in Manganese Rich Manganese Ferrites, S. E. Harrison, RCA Labs., and H. S. Belson and C. J. Kriessman, Remington Rand Univac.

Ferromagnetic Resonance in Uniaxial Polycrystalline Materials, C. A. Morrison and N. Karayianis, Diamond Ordnance Fuze Labs.

Ferromagnetic Resonance in Polycrystalline Nickel Ferrite Aluminate, E. Schlomann and J. R. Zeender, Raytheon Mfg. Co.

Damping and the Dispersion Relations in Antiferromagnetic Resonance, E. S. Dayhoff, U. S. Naval Ordnance Lab.

Continental Room

Magnetic Alloys: Mostly Oriented

J. K. Stanley, presiding.

Magnetic Anisotropy Induced by Magnetic Annealing and by Cold Working of Ni₂Fe Crystal, Soshin Chikazumi, Dept. of Physics and Chemistry, Gakushuin Univ., Mejiro, Tokyo, Japan.

The Effect of Sample Thickness on the Field Annealing of 6.5% Si-Fe, P. A. Albert, Magnetic Materials Dev. Section, Westinghouse Electric Corp.

Recrystallization of MnBi Induced by a Magnetic Field, O. L. Boothby, D. H. Wannoy and E. E. Thomas, Bell Tel. Labs.

Effects of Composition and Processing Variables on the Magnetic Properties of the Nominal 50% Nickel, 50% Iron Alloy, M. J. Savitaki, Metals Eng. Dept., Westinghouse Electric Corp.

Orientation Study of Ultra-Thin Molybdenum Permalloy Tape, P. K. Koh, Allegheny Ludlum Steel Corp.

The Development of Preferred Orientations in Silicon-Iron, J. R. Brown, Metal Physics Section, G. K. N. Group Research Lab., Wolverhampton, England.

The (110) 001 Secondary Recrystallization Texture in Silicon-Iron, H. C. Fiedler, General Electric Research Lab.

Magnetic Properties of Cube Textured Magnetic Sheet, J. L. Walter, W. R. Hibbard, H. C. Fiedler, H. E. Grenoble, R. H. Pry and P. G. Frischmann, General Electric Co.

Cube Texture in Body Centered Cubic Magnetic Alloys, G. Wiener, P. A. Albert, and R. H. Trapp, Westinghouse Elec. Corp., and M. F. Littmann, Armco Steel Corp.

Low Magnetic Resonance in the High Aluminum Iron Alloys, D. Pavlovic and K. Foster, Materials Eng. Dept., Westinghouse Electric Corp.

Effects of Elastic Bending on Magnetic Properties of Oriented Silicon-Iron, R. W. Cole, Crucible Steel Co. of America.

2:00 P.M.

Sheraton Hall

Magnetic Moments and Crystal Structures of Oxides

L. R. Maxwell, presiding.

The Effect of Hydrostatic Pressure and Temperature on the Magnetic Properties of a Nickel-Zinc Ferrite, C. Q. Adams and C. M. Davis, Jr., U. S. Naval Ordnance Lab.

The Preferential Volatilization of Cations from Ferrites during Sintering, J. M. Brownlow, IBM Corp. Research Center.

Some Properties of Quenched Magnesium Ferrites, D. J. Epstein and B. Frackiewicz, Lab. for Insulation Research, M. I. T.

Ionic Valences in Manganese-Iron Spinels, A. H. Eschenfelder, IBM Res. Center.

Substitution for Iron in Ferrimagnetic Yttrium-Iron Garnet, M. A. Gilleo and S. Geller, Bell Tel. Labs.

Some Ferrimagnetic Properties of the Sys-

tem $Li_xNi_{1-x}O$, J. B. Goodenough and D. G. Wickham, Lincoln Lab. of M. I. T., and W. J. Croft, RCA Labs.

Effect of Thermal History on the Antiferromagnetic Transition in Zinc Ferrite, D. M. Grimes and E. F. Westrum, Jr., Univ. of Michigan.

Magnetic Germanates Isostructural with Garnet, A. Tauber and H. Kedesdy, U. S. Army Signal Eng. Labs., and E. Banks, Polytechnic Inst. of Brooklyn.

Some Magnetic and Crystallographic Properties of the System $LaMn_{1-x}Ni_xO_3$, A. Wold, R. J. Arnott and J. B. Goodenough, Lincoln Lab. of M. I. T.

Crystal Growth of Magnetic Garnets, J. W. Nielsen, Bell Tel. Labs.

Antiferromagnetic Structures of MnS_2 , $MnSe_2$, and $MnTe_2$, L. M. Corliss, N. Elliott and J. M. Hastings, Brookhaven Nat. Lab.

Continental Room

Applications and Testing

A. D. Franklin, presiding.

Measurement of Losses of Magnetic Materials at High Inductions, at Frequencies up to 100 Megacycles, I. Bady, U. S. Army Signal Eng. Labs.

Measurements of the Property of Various Ferrites Used in Magnetically Tuned Resonant Circuits in the 2.5 to 45 Mc Region, P. P. Lombardini, R. F. Schwartz and R. J. Doviak, Univ. of Pa.

The Behavior of the TE Modes in Ferrite Loaded Rectangular Waveguide in the Region of Ferromagnetic Resonance, W. J. Crowe, Bell Tel. Labs.

Energy Distribution in Partially Ferrite Filled Waveguides, J. E. Tompkins, Diamond Ordnance Fuze Labs.

A Miniaturized Resonant Antenna Using Ferrites, D. M. Grimes, Univ. of Michigan.

An Appraisal of Permanent Magnet Materials for Magnetic Focusing of Electron Beams, M. S. Glass, Bell Tel. Labs.

The Performance of Permanent Magnets at Elevated Temperatures, W. H. Roberts, General Electric Co.

The Micro-Uniformity of Permanent Magnet Materials, L. I. Mendelsohn, General Electric Co.

Understanding and Predicting Permanent Magnet Performance by Electrical Analog Methods, R. J. Parker, General Electric Co.

Method for Measuring Saturation Magnetization in Ring Samples, C. D. Graham, Jr., General Electric Research Lab.

Some Aspects of Tempering $3\frac{1}{2}\%$ Silicon Iron via Time Decay of Permeability, E. S. Anolick and J. Singer, Transformer Labs., General Electric Co.

Materials Problems in Magnetic Suspension Apparatus, J. B. Breazeale, Bill Jack Scientific Instrument Co.

WEDNESDAY, NOVEMBER 20

9:00 A.M.

Sheraton Hall

Ferromagnetic Resonance: Nonlinear Effects and Garnets

C. L. Hogan, presiding.

Origin and Use of Instability in Ferromagnetic Resonance, H. Suhl, Bell Tel. Labs.

A Solid State Microwave Amplifier and

Oscillator Using Ferrite, M. T. Weiss, Bell Tel. Labs.

A New Type of Ferromagnetic Microwave Amplifier, C. L. Hogan, Harvard Univ.

Microwave Frequency Conversion Studies in Magnetized Ferrites, E. N. Skomal, Sylvania Elec. Products.

Spin-Lattice Relaxation Time in Yttrium Iron Garnet, R. T. Farrar, Diamond Ordnance Fuze Labs.

Ferrimagnetic Resonance in Gadolinium Iron Garnet, B. A. Calhoun, W. V. Smith and J. Overmeyer, IBM Corp. Research Center.

Ferromagnetic Resonance in Yttrium Iron Garnet at Low Frequencies, E. G. Spencer, R. C. LeCraw and C. S. Porter, Diamond Ordnance Fuze Labs.

Microwave Properties of Polycrystalline Rare Earth Garnets, M. H. Sirvetz and J. E. Zneimer, Raytheon Mfg. Co.

Ferromagnetic Resonance in Single Crystals of Rare Earth Garnet Materials, R. V. Jones, G. P. Rodrigue and W. P. Wolff, Harvard Univ.

2:00 P.M.

Sheraton Hall

Anisotropy and Magnetostriction

R. M. Bozorth, presiding.

Temperature Dependence of the Magneto-crystalline Anisotropy Coefficients in Cubic Crystals, E. Callen, National Security Agency, J. L. Jackson, National Bureau of Standards, and H. B. Callen, Univ. of Pa.

Temperature Dependence of Ferromagnetic Anisotropy, W. J. Carr, Jr., Westinghouse Elec. Corp.

Magnetocrystalline Anisotropy of Mg-Fer Ferrites: Temperature Dependence, Ionic Distribution Effects and the Crystalline Field Model, V. J. Folen and G. T. Rado, Naval Research Lab.

Magnetic Annealing in Cobalt-Iron Ferrite Single Crystals, L. R. Bickford, Jr., J. M. Brownlow and R. F. Penoyer, IBM Corp. Research Center.

Magnetization Processes in Heat-Treated Single Crystal Cobalt Ferrite, S. Foner, Lincoln Lab. of M. I. T., and J. O. Artman, Harvard Univ.

Crystallographic and Magnetic Studies of the System $NiFe_{2-x}Mn_xO_4$, P. K. Baltzer and J. G. White, RCA.

Origin of Anisotropic Effects in $Co_2Fe_{3-x}O_4$, J. C. Slonczewski, IBM Corp. Research Center.

Theory of Magnetostriction and g-Factor in Ferrites, Noboru Tsuya, Tohoku Univ., Sendai, Japan.

The Relationship Between Single Crystal and Effective Polycrystalline Anisotropy Constants in Ferrites, C. J. Kriessman, Remington Rand Univac, S. E. Harrison, RCA Labs., and H. S. Belson, Remington Rand Univac.

Exchange Anisotropy in the Iron-Iron Oxide System, W. H. Meiklejohn, General Electric Research Lab.

Magnetostriction and Elastic Properties of Ferromagnetic Substances at High Magnetic Fields, H. Sato, Ford Motor Co.

THURSDAY, NOVEMBER 21

9:00 A.M.

Sheraton Hall

Magnetization Processes: Reversals and Losses

J. R. Weertman, presiding.

Domain Wall Motion in Metals, R. W. DeBlois, General Electric Research Lab.

Preparation and Properties of Crystal-Oriented Ferroplana Samples, A. L. Stuijts and H. P. J. Wijn, Philips Research Labs., Eindhoven, Netherlands.

A Rigorous Approach to the Theory of Ferromagnetic Microstructure, W. F. Brown, Jr., Minnesota Mining & Mfg. Co.

The Magnetization Curve of the Infinite Cylinder, A. Aharoni and S. Shtrikman, The Weizmann Institute of Science, Rehovot, Israel.

A Model for Nonlinear Flux Reversals of Square Loop Polycrystalline Magnetic Cores, M. K. Haynes, IBM Corp. Research Center.

Temperature Dependence of Microwave Permeabilities for Polycrystalline Ferrite and Garnet Materials, J. Nemanich and J. C. Cacheris, Diamond Ordnance Fuze Labs.

The Effect of Cobalt on the Relaxation Frequency of Nickel-Zinc Ferrite, F. J. Schnettler and F. R. Monforte, Bell Tel. Labs.

The Switching Properties of Permalloy Cores of Varying Coercivity, T. D. Rossing and V. J. Korkowski, Remington Rand Univac.

Rotational Loss Measurements on Some Ferrites, J. M. Kelly, Armour Res. Found., Illinois Inst. of Technology.

The Temperature Dependence of the Attenuation of Ultrasound in a Nickel Single Crystal from 77° to 650°K, F. West, Texas Instruments, Inc.

Magnetic Fluctuations in Molybdenum Permalloy, J. J. Brophy, Armour Res. Found., Ill. Inst. of Technology.

Burgundy Room

Magnetic Apparatus and Techniques

T. R. McGuire, presiding.

A New Concept in Large Size Memory Arrays—The Twister, A. H. Bobeck, Bell Tel. Labs.

Analysis and Operation of a Ferrite Plate Switch Driven Memory System Using 2 Holes Per Bit, V. L. Newhouse and M. M. Kaufman, Bizmac Eng., RCA.

Recent Advances in the Design of High Field DC Solenoid Magnets, H. H. Kolm, Lincoln Lab. of M. I. T.

Further Development of the Vibrating Coil Magnetometer, K. Dwight, M. Memyuk and D. Smith, Lincoln Lab. of M. I. T.

An Improved Torque Magnetometer, W. S. Byrnes, Westinghouse Electric Corp.

A Transparent Ferromagnetic Light Modulator Using Yttrium Iron Garnet, C. S. Porter, E. G. Spencer and R. C. LeCraw, Diamond Ordnance Fuze Labs.

Design of Optimum Inductors Using Magnetically Hard Ferrites in Combination with Magnetically Soft Materials, J. T. Ludwig, Minneapolis-Honeywell Regulator Co.

Pulse Generator Based on High Shock Demagnetization of Ferromagnetic Material, R. W. Kulterman, Sandia Corp.

A New Magnetic Core Loss Comparator, R. E. Tompkins and L. H. Stauffer, General Electric Co.

The Preparation of Alnico VII Castings

with Improved Physical Properties, D. H. Wenny and K. M. Olson, Bell Tel. Labs.

Skull-Cap Method for Magnetizing Bowl-Shaped Magnetron Magnets, F. X. McDonough, Jr., Bomac Laboratories.

2:00 P.M.

Sheraton Hall

Magnetic Moments and Crystal Structures of Metals

J. J. Becker, presiding.

Magnetometallurgy Applications and Methods, A. Arrott, Ford Motor Co.

Suggestions Concerning the Role of Covalence in Transition Elements and Their Alloys, J. B. Goodenough, Lincoln Lab. of M. I. T.

Transitions from Ferromagnetism to Antiferromagnetism in Iron Aluminum Alloys, A. Arrott and H. Sato, Ford Motor Co.

Some Unusual Magnetic Properties of

Ni_3Mn , J. S. Kouvel, C. D. Graham, Jr. and J. J. Becker, General Electric Research Lab.

Magnetic Properties of Dilute Magnetic Alloys and of the Rare Earth Metals, G. W. Pratt, Jr., Lincoln Lab. of M. I. T.

Further Magnetic and X-Ray Diffraction Studies on Iron-Rich Iron-Aluminum Alloys, A. Taylor and R. M. Jones, Westinghouse Research Lab.

Magnetic Moments and Apparent Molecular Fields in Some Rare Earth Metals and Compounds, W. E. Henry, U. S. Naval Research Lab.

Burgundy Room

Domain Patterns and Theory

T. O. Paine, presiding.

Magnetic Domain Patterns on Iron Whiskers, R. V. Coleman and G. G. Scott, General Motors Corp.

Domain Observations on Iron Whiskers,

R. W. DeBlois and C. D. Graham, Jr., General Electric Research Lab.

Magnetic Domain Wall Motion, P. R. Gillette and K. Oshima, Stanford Res. Inst. A Calculation of the Energy Loss in Magnetic Sheet Materials Using a Domain Model, R. H. Pry and C. P. Bean, General Electric Research Lab.

Growth of MnBi Crystals and Evidence for Subgrains from Domain Patterns, W. C. Ellis, H. J. Williams and R. C. Sherwood, Bell Tel. Labs.

Antiferromagnetic Domain Walls and the Magnetization Process in $\alpha\text{-Fe}_2\text{O}_3$, I. S. Jacobs and C. P. Bean, Gen. Elec. Research Lab.

Optical Properties of Several Ferrimagnetic Garnets, J. F. Dillon, Jr., Bell Tel. Labs.

Contribution to the Study of Ferromagnetic Multidomain Particles, H. Amar, Franklin Inst. Labs.

Constraint Principles in Ferromagnetic Domain Theory, L. Gold, Lincoln Lab. of M. I. T.

Eastern Joint Computer Conference

SHERATON PARK HOTEL, WASHINGTON, D. C., DEC. 9-13, 1957

MONDAY, DECEMBER 9

Morning

Industrial Control Computers and Instrumentation I

Session Chairman: J. F. Reintjes, Massachusetts Institute of Technology.

The Electronic Phase Shift Decoder, G. T. Moore, Concord Controls, Inc.

Systems Design of a Numerically Controlled Machine Tool, E. C. Johnson and Y. C. Ho, Bendix Aviation Corp.

Logical Organization of the Digimatic Computer, J. Rosenberg, Electronic Control Systems, Inc.

The Master Terrain Model System, J. A. Stieber, U. S. Naval Training Device Center.

Afternoon

Industrial Control Computers and Instrumentation II

Session Chairman: E. C. Johnson, Bendix Aviation Corp.

A Coordinated Data Processing System and Analog Computer to Determine Refinery Process Operating Guides, C. H. Taylor, Fisher and Porter Co.

System Characteristics of a Computer-Controller for Use in the Process Industries, W. E. Frady and M. Phister, Jr., Ramo-Wooldridge Corp.

Real-Time Hybrid Computers for Electronic Control Systems, C. T. Leondes, University of California, Los Angeles, Calif.

Real-Time Presentation of Reduced Wind Tunnel Data, M. Bain and W. Hoover, California Inst. of Technology, Jet Propulsion Lab.

Mechanization of Letter Mail Sorting, I. Rotkin, National Bureau of Standards.

Evening

Cocktail Party at the Shoreham Hotel.

TUESDAY, DECEMBER 10

Morning

Traffic Control, Navigation and Surveillance I

Session Chairman: Morris Rubinfeld, Philco Corp.

Preparations for Tracking an Artificial Earth Satellite at the Vanguard Computer Center, D. A. Quarles, Jr., International Business Machines Corp.

Use of a Digital Computer for Airborne Guidance and Navigation, S. Zadoff and J. Rattner, Sperry Gyroscope Co.

Experimentation on the Human Operator Tie-in to an Airborne Navigation Computer Control System, C. A. Bennett, International Business Machines Corp.

Multi-Weapon Automatic Target and Battery Evaluator, A. E. Miller, Burroughs Corp.

Control of Automobile Traffic—A Problem in Real-Time Computation, D. L. Gerlough, University of California, Los Angeles, Calif.

Luncheon

Sheraton Park Hotel

Speaker: R. J. Slutz, National Bureau of Standards.

Topic: IGY and Automatic Data Handling.

Afternoon

Simulation in Real Time

Session Chairman: R. M. Howe, Univ. of Michigan.

Physical Simulation of Nuclear Reactor Power Plant Systems, J. J. Stone, B. B. Gordon and R. S. Boyd, Battelle Memorial Inst.

Applications of Computers to Automobile Stability and Control Problems, R. H. Kohr, General Motors Corp.

Combined Analog-Digital Simulation of Sampled Data Systems, H. K. Skramstad, A. A. Ernst, and J. P. Nigro, National Bureau of Standards.

Facilities and Instrumentation Required for Real-Time Simulation Involving System Hardware, A. J. Thiberville, Convair.

Extending Flight Simulator Time Scale, E. J. McGlenn, Bendix Aviation Corp.

Analog, Digital, and Combined Analog-Digital Computers for Real-Time Simulation, W. W. Seifert, Massachusetts Inst. of Technology.

WEDNESDAY, DECEMBER 11

Morning

Synthesis of Real-Time Systems

Session Chairman: J. W. Carr, III, Univ. of Michigan.

The Place of Self-Repairing Facilities in Computers With Deadlines to Meet, L. Fein, consultant.

Organizing a Network of Computers to Meet Deadlines, A. L. Leiner, W. A. Notz, J. L. Smith and A. Weinberger, National Bureau of Standards.

A Program-Controlled Program Interrupt System, F. P. Brooks, Jr., International Business Machines Corp.

A Transistor Circuit Chassis for High Reliability in Missile Guidance Systems, G. A. Raymond, Remington Rand Univac.

A Method of Coupling a Small Computer to Input-Output Devices Without Extensive Buffers, J. H. Randall, National Cash Register Co.

The Optimum Synthesis of Computer Limited Sampled Data Systems, A. S. Robinson, Bendix Aviation Corp.

Afternoon

Traffic Control, Navigation and Surveillance II

Session Chairman: A. A. Cohen, Remington Rand Univac.

Sage—A Data Processing System for Air Defense, R. R. Everett, C. A. Zraket and H. D. Bennington, MIT Lincoln Lab.

AN/FST-2 Radar Processing Equipment for Sage, H. W. Taylor, E. W. Veitch and J. Wylen, Burroughs Corp.

Operation of the Sage Duplex Computers, P. R. Vance, MIT Lincoln Lab., L. G. Dooley, Rand Corp. and C. E. Diss, IBM Corp.

A Digital System for Position Determination, D. C. Ross, IBM Corp.

Real-Time Data Processing for CAA Air Traffic Control Operations, G. E. Fenimore, CAA Technical Development Evaluation Center.

Evening

Banquet at the Sheraton-Park Hotel.
Speaker: E. R. Quesada, Chairman, Airways Modernization Board.

THURSDAY, DECEMBER 12

Morning

On-Line Business Systems

Session Chairman: R. E. Sprague, Tele-register Corp.

Design Techniques for Multiple Interconnected On-Line Data Processors, F. J. Gaffney and S. Levine, Teleregister Corp.

Reservations Communications Utilizing a General-Purpose Digital Computer, R. A. McAvoy, Eastern Airlines.

Stock Transaction Records, A. H. Payne, Melpar, Inc.

On-Line Sales Recording System, J. S. Baer, A. S. Rettig and I. Cohen, RCA.

The G.E. Integrated Bank Data Processing System Model 2B100, J. Levinthal, J. Weizenbaum and H. Herold, General Electric Co.

Luncheon

Shoreham Hotel

Speaker: Max Woodbury, N.Y.U.

Topic: "The Voters Won't Wait!"

Afternoon

Digital Communications Techniques

Session Chairman: I. L. Auerbach, Auerbach Electronic Corp.

Derivation of Business Machines Data Channels From Standard Telephone Lines for Simultaneous Transmission with Speech, E. Hopner, International Business Machines Corp.

A Self-Checking System for High-Speed Transmission of Magnetic Tape Digital Data, E. J. Casey and D. W. Fritze, Remington Rand Univac.

Communications Between Remotely Lo-

cated Digital Computers, F. P. Forbath, Collins Radio Co.

Communications Switching Systems as Real-Time Computers, A. E. Joel, Bell Tel. Labs.

An Introduction to the Bell System's First Electronic Switching Office, R. W. Ketchledge, Bell Tel. Labs.

Traffic Aspects of Communications Switching Systems, J. A. Bader, Bell Tel. Labs.

FRIDAY, DECEMBER 13

Morning

Document Reading, Pattern Recognition and Character Synthesis

Session Chairman: Howard Engstrom, National Security Agency.

The Use of an IBM 704 in the Simulation of Speech Recognition Systems, G. L. Schultz, International Business Machines Corp.

An Automatic Voice Readout System, C. W. Poppe and P. Suhr, Fairchild Controls Corp.

Experimental Use of Electronic Computers in Processing Pictorial Information, L. Cahn, R. A. Kirsch, L. C. Ray and G. H. Urban, National Bureau of Standards.

Optical Displays for Data Handling System Output, J. Ogle, Burroughs Corp.

Devices for Reading Handwritten Characters, T. L. Dimond, Bell Tel. Labs.

Automatic Registration in High-Speed Character Sensing Equipment, A. I. Tersoff, Intelligent Machines Research Corp.

The NCR High-Speed Electromagnetic Printer, J. M. Seehof, National Cash Register Co.

Abstracts of IRE Transactions

The following issues of "Transactions" have recently been published, and are now available from the Institute of Radio Engineers, Inc., 1 East 79th Street, New York 21, N. Y. at the following prices. The contents of each issue and, where available, abstracts of technical papers are given below.

Sponsoring Group	Publication	Group Members	IRE Members	Non-Members*
Component Parts	Vol. CP-4, No. 2	\$1.20	\$1.80	\$3.60
Information Theory	Vol. IT-3, No. 2	2.45	3.65	7.35

* Public libraries and colleges may purchase copies at IRE Member rates.

Component Parts

VOL. CP-4, NO. 2, JUNE, 1957

Information for Authors

Arc Suppression for Relay Contacts in DC Service—W. J. Godsey

Available relays for control of high-power direct current are seen to be large, heavy, and adversely affected by vibration and shock.

This paper shows how commonly available components of reasonable size can be used with small vibration-resistant relays to control large direct currents at high potential. Thus, control of high-power airborne power supplies on the direct current side has become possible with reasonable equipment.

The Mechanical and Electrical Properties of Polymers: An Elementary Molecular Approach—J. D. Hoffman
Contributors

Information Theory

VOL. IT-3, NO. 2, JUNE, 1957

F. Louis H. M. Stumpers (p. 84)

Information Theory and International Radio Organizations—F. L. H. M. Stumpers (p. 85)

On the Detection of Stochastic Signals in Additive Normal Noise—Part I—David Middleton (p. 86)

The problem of optimum and suboptimum detection of normal signals in additive normal noise backgrounds is examined by the methods of statistical decision theory. Some general results for optimum receiver structure, error probabilities, and average risk are obtained for the case of colored noise backgrounds. A detailed study of threshold reception in white-noise backgrounds is included, along with calculations of Bayes risk, bias terms, and minimum detectable signals for broad-band RC-noise signals and narrow-band, *i.e.*, high-Q, LRC-noise signal processes. Optimum detector structures for signal processes with rational intensity spectra are also determined for the white noise case, and particular attention is paid to optimum receiver design in terms of physically realizable elements. Suboptimum receiver structure and performance are con-

sidered briefly, as well as a number of limiting cases of more special interest. General methods of attack are illustrated, with details given in appendixes I-V. Application of the results to a variety of communication problems is indicated.

The Relationship of Sequential Filter Theory to Information Theory and Its Application to the Detection of Signals in Noise by Bernoulli Trials—Herman Blasbalg (p. 122)

In this paper the problem of detecting signals in noise by the method of sequential filtering is formulated. A slicing operator for converting a given random variable into a Bernoulli random variable is defined. A method for choosing an optimum slicing operator in a certain prescribed sense is given. It is also shown that the Bernoulli sequential test is defined by three parameters $a(p_0, p_1, \alpha, \beta)$, $b(p_0, p_1, \alpha, \beta)$, and $c(p_0, p_1)$ rather than four, as one would normally expect. The significance of these transformations is briefly discussed. Finally, the theory of Bernoulli sequential detection is applied to the detection of a sine-wave carrier in noise when the signal-to-noise ratio is less than one. The efficiency of this detector is calculated and compared with the results of others. Curves of the significant Bernoulli sequential detector characteristics are given for this problem.

A Theory of Weighted Smoothing—L. A. Ule (p. 131)

The problem attacked in this paper is that of a system with a stationary random error input, a nonrandom signal input and a nonrandom error input. The output of the system is required to have a minimum weighted response to the random error and otherwise to consist only of arbitrary functions of time linearly related to the nonrandom signal input. The more general case, which includes a random signal as well, is not considered.

The Response of a Phase-Locked Loop to a Sinusoid Plus Noise—S. G. Margolis (p. 136)

The phase-locked loop is a practical device for separating a sinusoidal signal from additive noise. In this device the incoming signal-plus-noise is multiplied by a noise-free sinusoid generated by a voltage-controlled oscillator (vco). The filtered product is used to lock the phase of the vco output to that of the incoming signal, thus producing a relatively clean version of the incoming signal in which the noise manifests itself as a small phase modulation. Analysis of this noise-produced phase modulation is complicated by the presence of the multiplier at the input to the loop. This paper presents a perturbation method which reduces this inherently nonlinear servo analysis problem to the analysis of a series of linear systems, the first of which is related to the linear model used by previous authors. The perturbation technique permits the phase modulation resulting from an arbitrary noise input to be computed

to any desired accuracy. This analysis is particularly useful in predicting loop performance when it is used as a narrow-band receiver in a phase-comparison angle-measuring system.

A Note on the Sampling Principle for Continuous Signals—A. V. Balakrishnan (p. 143)

Two sampling (integral interpolation) theorems for continuous signals (continuous parameter stochastic processes) are proved. The first of these is the sampling principle introduced by Shannon, precise formulation or proof of which has not appeared hitherto. Obtained as a secondary result in this connection is a generalization of a result on the spectra of sampled signals given by Bennet. The second theorem is a stochastic version of the Newton-Gauss interpolation formula as representative of a different class of sampling theorems.

A Note on Some Statistics Concerning Typewritten or Printed Material—Sid Deutsch (p. 147)

A Note on the Construction of a Multivariate Normal Sample—G. Marsaglia (p. 149)

This note points out the superfluity of a method of Stein and Storer for constructing a multivariate normal sample, and suggests a simple alternative.

A Bibliography of Information Theory (Communication Theory—Cybernetics), (Second Supplement)—F. L. H. M. Stumpers (p. 150)

Correspondence (p. 167)

Contributors (p. 168)



Abstracts and References

Compiled by the Radio Research Organization of the Department of Scientific and Industrial Research, London, England, and Published by Arrangement with that Department and the *Electronic and Radio Engineer*, incorporating *Wireless Engineer*, London, England

NOTE: The Institute of Radio Engineers does not have available copies of the publications mentioned in these pages, nor does it have reprints of the articles abstracted. Correspondence regarding these articles and requests for their procurement should be addressed to the individual publications, not to the IRE.

Acoustics and Audio Frequencies.....	1568
Antennas and Transmission Lines.....	1569
Automatic Computers.....	1570
Circuits and Circuit Elements.....	1570
General Physics.....	1571
Geophysical and Extraterrestrial Phenomena.....	1573
Location and Aids to Navigation.....	1573
Materials and Subsidiary Techniques..	1573
Mathematics.....	1576
Measurements and Test Gear.....	1576
Other Applications of Radio and Electronics.....	1577
Propagation of Waves.....	1578
Reception.....	1579
Stations and Communication Systems..	1579
Subsidiary Apparatus.....	1579
Television and Phototelegraphy.....	1579
Transmission.....	1580
Tubes and Thermionics.....	1580
Miscellaneous.....	1582

The number in heavy type at the upper left of each Abstract is its Universal Decimal Classification number and is not to be confused with the Decimal Classification used by the United States National Bureau of Standards. The number in heavy type at the top right is the serial number of the Abstract. DC numbers marked with a dagger (†) must be regarded as provisional.

ACOUSTICS AND AUDIO FREQUENCIES

- 534.2** **3000**
Formulation of Wave Propagation in Infinite Media by Normal Coordinates with an Application to Diffraction—M. A. Biot and I. Tolstoy. (*J. Acoust. Soc. Amer.*, vol. 29, pp. 381–391; March, 1957.) The mathematical basis of the technique is discussed fully. The method is applied to the example of diffraction by wedges and corners for an idealized point-source transient explosion.
- 534.2** **3001**
Perturbation of a Sound Field by a Rigid Cylinder—O. Brosze. (*Elektronische Rundschau*, vol. 11, pp. 19–22; January, 1957.) A formula is derived for the sound field in the vicinity of a rigid, infinitely long cylinder. Results of acoustic measurements are compared in graphical form with calculated values; good agreement is found.
- 534.2** **3002**
Scattering of Sound Waves by Small Inhomogeneities in a Waveguide—M. A. Isakovitch. (*Akust. Zh.*, vol. 3, pp. 37–45; January–March, 1957.) Analysis is presented for a waveguide 1) which is completely filled with a medium the refractive index of which varies from point to point, and 2) with rough interior walls and filled with a homogeneous medium.
- 534.2-14** **3003**
Phenomenological Theory of the Molecular Absorption and Dispersion of Sound in Fluids and the Relation between the Relaxation Time of the Internal Energy and the Relaxation Time of the Internal Specific Heat—O. Nomoto. (*J. Phys. Soc. Japan*, vol. 12, pp. 85–99; January, 1957.)

The Index to the Abstracts and References published in the PROC. IRE from February, 1956 through January, 1957 is published by the PROC. IRE, May, 1957, Part II. It is also published by *Electronic and Radio Engineer*, incorporating *Wireless Engineer*, and included in the March, 1957 issue of that journal. Included with the Index is a selected list of journals scanned for abstracting with publishers' addresses.

- 534.2-8** **3004**
Note on Finite-Amplitude Waves in Liquids—R. T. Beyer and V. Narasimhan. (*J. Acoust. Soc. Amer.*, vol. 29, p. 532; April, 1957.) See 1999 of 1957. The frequency dependence of the absorption-coefficient/acoustic-pressure relation is substantiated by other data.
- 534.2-8:539.37** **3005**
Frequency Dependence of Ultrasonic Attenuation and Velocity on Plastic Deformation—A. Hikata and R. Truell. (*J. Appl. Phys.*, vol. 28, pp. 522–523; May, 1957.) The results of measurements at 5 and 10 mc on Al are in accordance with those expected from dislocation damping theory.
- 534.23-14** **3006**
Measurements of the Attenuation of Low-Frequency Underwater Sound—M. J. Sheehy and R. Halley. (*J. Acoust. Soc. Amer.*, vol. 29, pp. 464–469; April, 1957.) Values for the range 20–200 cps were obtained.
- 534.231:534.87** **3007**
Calculations of the Sound Field in the Focal Region of a Cylindrical Focusing System—I. N. Kanevski and L. D. Rozenberg. (*Akust. Zh.*, vol. 3, pp. 46–61; January–March, 1957.) An analysis is made of sound fields with wavefronts of finite or infinite width near the axis of the system, assuming that the wavelength is small in comparison with the focal length of the system. Results show that in a direction normal to the axis of the wavefront and in the focal plane the potential has null points, but in a direction perpendicular to both the axis and the focal plane the potential has minima but no null points.
- 534.232-8:546.431.824-31** **3008**
Barium Titanate Ultrasonic High-Intensity Radiator—I. N. Kogan and L. I. Menes. (*Akust. Zh.*, vol. 3, pp. 62–64; January–March, 1957.) The high-power transducer described comprises a BaTiO₃ plate of 38-mm diameter backed by a 0.01-mm air film and a water-cooled reflector; the transducer is capable of continuous transmission in water at a frequency of 400–800 kc and an intensity of 15 w/cm².
- 534.26** **3009**
On the Diffraction of Sound Waves in a Viscous Medium—J. B. Alblas. (*Appl. Sci. Res.*, vol. A6, pp. 237–262; 1957.) The theory of the diffraction of a sound wave at a half-plane barrier is extended to the case of propagation in a viscous medium.
- 534.26** **3010**
Approximate Methods in High-Frequency Scattering—D. S. Jones. (*Proc. Roy. Soc. A*, vol. 239, pp. 338–348; March 12, 1957.) In considering the diffraction of a high-frequency plane sound wave two approximate methods of deriving the scattering coefficient of two-dimensional obstacles without edges are described. In the first method a simple field which satisfies approximately the boundary condition near the points of glancing incidence is found. Elsewhere the geometrical acoustics field is used. The scattering coefficient is about 7 per cent in error. In the second method Fourier transforms are employed to find a field which satisfies the boundary condition over a wider region. This leads to results which, for the circular cylinder, are in complete agreement with those of the exact theory.
- 534.6:621.395.623** **3011**
Contribution to the Study of the Artificial Ear. The New Model Artificiel Ear at the Centre National d'Études des Télécommunications—P. Chavasse. (*C.R. Acad. Sci., Paris*, vol. 244, pp. 2014–2017; April 8, 1957.) See also 1564 of 1950.
- 534.62** **3012**
Investigation of Sound-Absorbing Constructions for the Anechoic Chamber of the Physical Faculty of the Moscow State University—K. A. Velizhanina and S. N. Rzhievkin. (*Akust. Zh.*, vol. 3, pp. 23–28; January–March, 1957.) Experimental results indicate that the best sound absorber for frequencies down to 80 cps is a glass-fiber cone with a packing density of 0.12–0.14 g/cm³ and with an air gap between the wall and the base of the cone equal to $\frac{1}{2}$ of the cone height. Graphs show the frequency characteristics of the sound reflection coefficient of glass-fiber cones for various packing densities and cone dimensions.
- 534.75** **3013**
Downward Spread of Masking—W. Spieth. (*J. Acoust. Soc. Amer.*, vol. 29, pp. 502–505; April, 1957.) Bands of noise have a considerable masking effect on lower-frequency levels; a pure tone has not.
- 534.75** **3014**
Noise-Masked Thresholds as a Function of Tonal Duration and Masking Noise Bandwidth—P. M. Hamilton. (*J. Acoust. Soc. Amer.*, vol. 29, pp. 506–511; April, 1957.)
- 534.75** **3015**
Remote Masking in Selected Frequency Regions—B. H. Deatherage, R. C. Bilger, and D. A. Eldredge. (*J. Acoust. Soc. Amer.*, vol. 29,

pp. 512-514; April, 1957.) Regular variations in the envelope of the masking sound at say 500 cps produce remote masking in the 500-cps region, while irregular variations produce equal amounts of masking everywhere outside the region.

534.75 **3016**
Simultaneous Two-Tone Pitch Discrimination—W. R. Thurlow and S. Bernstein. (*J. Acoust. Soc. Amer.*, vol. 29, pp. 515-519; April, 1957.) An investigation at frequencies of 200 cps, 1, 4, 6, and 10 kc.

534.75 **3017**
Frequency Difference Limens for Narrow Bands of Noise—R. M. Michlaels. (*J. Acoust. Soc. Amer.*, vol. 29, pp. 520-522; April, 1957.) None of the difference limens for noise approach that of the pure tone, all being at least twice as large.

534.75 **3018**
Signal Detection as a Function of Signal Intensity and Duration—D. W. Green, T. G. Birdsall, and W. P. Tanner, Jr. (*J. Acoust. Soc. Amer.*, vol. 29, pp. 523-531; April, 1957.) An attempt to determine the surface of detectabilities in the space determined by signal duration, intensity, and detectability. Results are consistent with data of previous research.

534.75:621.39 **3019**
Monitoring Task in Speech Communication—J. P. Egan. (*J. Acoust. Soc. Amer.*, vol. 29, pp. 482-489; April, 1957.) A quantitative description of the monitor's behavior in terms of the operating characteristic and the articulation-criterion function.

534.78:621.39 **3020**
Estimates of the Maximum Precision Necessary in Quantizing Certain "Dimensions" of Vowel Sounds—J. L. Flanagan. (*J. Acoust. Soc. Amer.*, vol. 29, pp. 533-534; April, 1957.) A discussion of quantization based on formant frequencies, formant amplitudes, and fundamental vocal frequency for reduced-bandwidth transmission of speech.

534.78:681.613 **3021**
The Phonotograph and Subformants—J. Dreyfus-Graf. (*Tech. Mitt. schweiz. Telegr. Teleph. Verw.*, vol. 35, pp. 41-59; February 1, 1957. In French.) Details of the latest model and outline of future development of the phonetic speech-transcription equipment described earlier (1568 of 1953). Oscillograms resulting from investigations of the information content of various speech components are discussed.

534.844.5 **3022**
Correlation Criterion of the Optimum of Reverberation—V. V. Furduev. (*Akust. Zh.*, vol. 3, pp. 74-80; January-March, 1957.) A discussion. The optimum reverberation time is related to the type of signal rather than to the volume of the auditorium.

534.845 **3023**
Absorption of Sound by Patches of Absorbent Materials—R. K. Cook. (*J. Acoust. Soc. Amer.*, vol. 29, pp. 324-329; March, 1957.) Exact solutions are found for plane waves incident on piston-like absorbers in the form of long strips or circles.

621.395.623.7:534.32 **3024**
Contribution to the Subjective Appreciation of Music Reproduction by means of Loudspeaker Combinations—G. Kaufmann. (*Tech. Hausmitt. Nordw. Dtsch. Rdfunks*, vol. 8, pp. 93-102; December 4, 1956. A series of tests is described in which the quality of reproduction of four pieces of music by three different loudspeaker combinations was judged by a number

of listeners in two rooms of differing reverberation characteristics. The results are analyzed in detail.

621.395.623.741:621.375.13 **3025**
Effect of a Negative-Impedance Source on Loudspeaker Performance—R. E. Werner. (*J. Acoust. Soc. Amer.*, vol. 29, pp. 335-340; March, 1957.) Amplifiers with negative-impedance outputs can greatly improve the lf and transient response of moving-coil loudspeakers.

621.395.623.8:621.396.712.2 **3026**
New High-Grade Monitoring Equipment for [studio] Control Rooms—Enkel. (See 3298.)

621.395.625.3:621.317.76 **3027**
Pulse Method of Measuring Magnetic-Tape Speed Fluctuations—A. G. Al'mukhamedov. (*Akust. Zh.*, vol. 3, pp. 19-22; January-March, 1957.) An oscillographic method is described in which pulses recorded at a given constant repetition rate by the recording head are compared with the pulses arriving at the pickup head. The repetition rate is adjusted so that the interval between pulses equals the average time of travel of the tape from the recording to the pickup head.

621.395.625.3:621.397.6 **3028**
Picture-Synchronized Magnetic Sound Recording in Television—Vollmer. (See 3314.)

ANTENNAS AND TRANSMISSION LINES
621.315.212:621.372.51:621.372.8 **3029**
Simple Technique for Diplexing 10000 Mc/s and Video Signals on Coaxial Cables—M. C. Thompson, Jr. and D. M. Waters. (*Rev. Sci. Instr.*, vol. 28, pp. 206-207; March, 1957.) Constructional details of a diplexer used in an airborne refractometer.

621.372.2 **3030**
Electromagnetic Surface Waves, Guided by a Boundary with Small Curvature—M. A. Miller and V. I. Talanov. (*Zh. Tekh. Fiz.*, vol. 26, pp. 2755-2765; December, 1956.) The theory developed indicates the existence of 1) three-dimensional surface waves which maintain their surface characteristics independent of the radius of curvature, and 2) two-dimensional waves which are partly radiated even at small curvatures of the boundary. Curves showing the decrease of the attenuation of the latter type of wave with the increase in wave retardation and with the decrease in the curvature of the guiding surface are given. Several surface waveguides are illustrated.

621.372.2 **3031**
The Surface Wave on a Dielectric Cylinder: the Method of Launching it and its Characteristics—C. Jauquet. (*Rev. HF, Brussels*, vol. 3, pp. 283-296; 1956.) The radiations produced by a magnetic current flowing in a ring concentric with a loss-free dielectric cylinder of infinite length are considered. The ring forms an ideal coaxial electromagnetic horn and the cylinder behaves as a waveguide for surface waves. The calculated characteristics are verified experimentally. The use of a dielectric cylinder for transmitting electromagnetic power is investigated; the losses of such a system have been measured.

621.372.2 **3032**
Propagation of Microwaves on a Single Wire: Part 2—S. N. Contractor and S. K. Chatterjee. (*J. Indian Inst. Sci.*, sec. B, vol. 39, pp. 52-67; January, 1957.) An experimental investigation of the matching of the surface wave, at 3.2 cm λ , with three different types of termination. Part 1: 16 of 1956 (Chatterjee and Madhavan).

621.372.2.029.6 **3033**
Surface-Wave Propagation along Coated Wires—T. Bercei. (*Acta. Tech. Acad. Sci. hungaricae*, vol. 17, pp. 219-251; 1957. In English.) Propagation along a wire with a coating possessing both dielectric magnetic properties is considered theoretically and the application of the formulas derived is illustrated by the design of a surface-wave transmission line for the 2.5-3.5 kmc band.

621.372.22:621.375.121.2 **3034**
Artificial Transmission Lines—Hudson. (See 3079.)

621.372.22 **3035**
Wave Propagation in a Disk Line—G. Piefke. (*Arch. elekt. Übertragung*, vol. 11, pp. 49-59; February, 1957.) Theoretical investigation of wave propagation in a waveguide consisting of alternate copper disks of thickness D_2 with a central hole and lossy dielectric disks of thickness D_1 , with $D_1 + D_2 \ll \lambda$. A formula is derived for the propagation constants of all possible modes. The attenuation of H_{0n} modes exceeds that of the homogeneous waveguide by the factor $(1 + D_1/D_2)^{1/2}$; the attenuation of all other modes is much greater.

621.372.8 **3036**
Variational Calculation Method for Waveguides with Periodic Inhomogeneities: Part 1—Sh. E. Tsimring. (*Radiotekhnika i Elektronika*, vol. 2, pp. 3-14; January, 1957.) A mathematical analysis is presented of the propagation of electromagnetic waves in a corrugated waveguide, with perfectly conducting walls, filled with a loss-free medium. The method developed is applied to an approximate calculation of the dispersion equation of a system comprising two parallel surfaces one of which has rectangular corrugations of arbitrary dimensions.

621.372.8 **3037**
Propagation of the Circular H_{01} Low-Loss Wave Mode around Bends in Tubular Metal Waveguide—H. E. M. Barlow. (*Proc. IEE*, Part B, vol. 104, pp. 403-409; July, 1957.) Theoretical analysis shows that the required field distribution at a bend is obtained if the wavefront is radial with respect to the center of curvature. This may be achieved 1) by a suitable variation of the permittivity over the cross section of the dielectric medium, or 2) by varying the surface reactance of the guide around its circumference.

621.372.8 **3038**
Propagation of Electromagnetic Waves in a Waveguide, Partly Filled with a Dielectric, with a Helix—V. P. Shestopalov. (*Zh. Tekh. Fiz.*, vol. 26, pp. 2749-2754; December, 1956.) The case is investigated theoretically of the effect of the monoenergetic electron beam of circular cross section moving inside the helix and parallel to the waveguide axis. The dielectric layer covers the internal surface of the waveguide.

621.372.8 **3039**
Directional Coupler for the H_{01} Wave in a Waveguide with Circular Cross-Section—M. V. Persikov. (*Radiotekhnika i Elektronika*, vol. 2, pp. 65-74; January, 1957.) Results of the analysis presented give the conditions for the separation of the H_{01} wave from a mixture of other modes, and formulas are derived for the coefficients of coupling, directivity, and attenuation of unwanted modes. Theoretical calculations have been verified experimentally in the 8.6-9.6-kmc band.

621.372.8.029.65.002.2:621.357.6 **3040**
Techniques for Electroforming of Precision Waveguide Components in the Millimetre Wavelengths—A. A. Feldmann. (*Rev. Sci. Instr.*, vol. 28, pp. 295-296; April, 1957.)

621.396.67.014.1 3041
Integral Equation for Currents in the Theory of Metallic Antennas—A. V. Gaponov and M. A. Miller. (*Zh. Tekh. Fiz.*, vol. 26, pp. 2766–2770; December, 1956.) In the presence of a load in the antenna, or when the finite conductivity of the metal is taken into account, the tangential components of the electric field (E_T) and magnetic field (H_T) in the closed surface Σ are connected by the relation $E_T = f(H_T)$; this relation is taken into account in a discussion of the problem considered by King (2196 of 1955).

621.396.67.029.62:621.397.7 3042
The Crystal Palace Television Transmitting Station—McLean, Thomas, and Rowden. (See 3318.)

621.396.677:621.396.11:551.510.535 3043
The Gain of a Directive Receiving Antenna for Short-Wave Back-Scatter—Beckmann and Vogt. (See 3276.)

621.396.677.32 3044
Directivity of End-Fire Arrays of Isotropic Antennas—J. R. Lignon. (*Ann. Acad. bras. Sci.*, vol. 28, pp. 439–446; December 31, 1956. In English.) Expressions are derived for the theoretical gain under conditions of normal and of increased directivity. The optimum number of elements for maximum gain for a given length of array can then be calculated.

621.396.677.75 3045
The Shape of Dielectric Beam Antennas—G. von Trentini. (*Nachrichtentech. Z.*, vol. 10, pp. 60–64; February, 1957.) Report of experimental investigations made at 3.25 cm λ on various types of radiators consisting of dielectric rods and plates. The dimensions of the models used are given and their relative advantages are discussed. 20 references.

621.372 3046
Randwertprobleme der Mikrowellenphysik [Book Review]—F. H. Borgnis and C. H. Papas. Publishers: Springer-Verlag, Berlin-Göttingen-Heidelberg, 266 pp.; 1955, (*Naturwiss.*, vol. 44, p. 188; March, 1957.) The book provides an introduction, illustrated by examples, to methods of solving microwave field problems arising in the vicinity of antennas, and the interior of waveguides or resonators. Solutions are obtained in the form of integrals.

AUTOMATIC COMPUTERS

681.142 3047
Digital Printer boosts Readout Time—H. W. Gettings. (*Electronics*, vol. 30, pp. 182–185; June 1, 1957.) The system can print 180 lines of 12 characters per line in 1 second.

681.142:511 3048
A System of Mathematical Symbols Suitable for Calculations by [digital] Computers—L. V. Kantorovich. (*C.R. Acad. Sci. U.R.S.S.*, vol. 113, pp. 738–741; April 1, 1957. In Russian.)

681.142:621.318.57:621.3.042 3049
The Reading of Magnetic Stores without Loss of Information—A. Darré. (*Frequenz*, vol. 11, pp. 19–27; January, 1957 and pp. 38–42; February, 1957.) A description and comparison of storage and read-out methods using various forms of the "transfluxor" [see 3509 of 1955 (Rajchman and Lo)] and of toroidal core devices.

681.142:621.383.2 3050
An Electromagnetic Simulator for a Hill's Equation—J. Valat. (*C.R. Acad. Sci., Paris*, vol. 244, pp. 2462–2465; May 13, 1957.) Description of a system based on a mirror galvanometer and twin-anode photocell with application to the calculation of cosmotron orbits. See also 3504 of 1955 (Blet).

681.142 3051
Analog Computer Techniques [Book Review]—C. L. Johnson. Publishers: McGraw-Hill, London, 264 pp.; 1956. (*Nature, London*, vol. 179, p. 1042; May 25, 1957.)

681.142 3052
Electronic Analog Computers [Book Review]—G. A. Korn and T. M. Korn. Publishers: McGraw-Hill, London, 2nd ed., 452 pp.; 1956. (*Nature, Lond.*, vol. 179, p. 1042; May 25, 1957.)

CIRCUITS AND CIRCUIT ELEMENTS

621.3.016.35 3053
A Stability Criterion in the Form of an Integral Equation—I. Gumowski. (*C.R. Acad. Sci., Paris*, vol. 244, pp. 2004–2007; April 8, 1957.) Wallman's criterion of realizability (see; e.g., 1674 of 1957) can be interpreted as a stability criterion more general than those of Bode and Nyquist. Examples of its use are given.

621.319.4:621.315.614.6 3054
Change of Capacitance of a Stack of Capacitor Paper under Compression—I. D. Fainerman and L. M. Vaisnan. (*Zh. Tekh. Fiz.*, vol. 26, pp. 2493–2497. November, 1956.) Results of an experimental investigation are reported. The optimum standard pressure for capacitance measurements is 0.5 kg. cm⁻² or higher.

621.372.4 3055
Equivalence Theorem for Two-Terminal Networks with all Three Types of Impedance R, C and L—K. H. R. Weber. (*Hochfreq. u. Elektroak.*, vol. 65, pp. 126–129; January, 1957.) The equivalence theorem formulated is based on earlier work [see 961 of 1955 (Weber and Schlegel)] and is applicable to series-parallel two-pole networks comprising R, C, and L elements.

621.372.4:537.313 3056
The Calculation of Current Distribution in a Linear Network—J. Vratsanos. (*Arch. elekt. Übertragung*, vol. 11, pp. 76–80; February, 1957.) It is proved that if a current I is flowing in a linear network of impedance R between its two terminals, the current i flowing in any branch of impedance r is given by $i^2 = I^2 R / \delta r$.

621.372.4:621.316.86 3057
Analysis of Electric Circuits containing Nonlinear Resistance—L. A. Pipes. (*J. Franklin Inst.*, vol. 263, pp. 47–55; January, 1957.) Two methods of dealing with varistor circuits are illustrated: the "reversion method" for the solution of nonlinear differential equations (*J. Appl. Phys.*, vol. 23, pp. 202–207; February, 1952) is applied to determine transient response; steady-state analysis is effected using a method of harmonic balance.

621.372.43+621.372.54:012 3058
Application of the Smith Chart to General Impedance Transformations—H. N. Dawirs. (*Proc. IRE*, vol. 45, pp. 954–956; July, 1957.) The use of the chart is extended for unsymmetrical networks having complex image impedances and propagation constant; e.g., filters in the rejection bands.

621.372.5 3059
Differentiating and Integrating Circuits—G. Fodor and G. Teimes. (*Acta Tech. Acad. Sci. hungaricae*, vol. 16, pp. 73–103; 1957. In English.)

621.372.5 3060
Exact Electronic Differentiation—H. Wittke. (*Elektronische Rundschau*, vol. 11, p. 7; January, 1957.) The addition of a feedback amplifier to the basic differentiating RC

quadrupole eliminates inherent phase and amplitude errors. See also 2574 of 1955.

621.372.5:621.318.134 3061
Ferrites at Microwaves—P. E. V. Allin. (*Electronic Eng.*, vol. 29, pp. 292–296; June, 1957.) A review of the principles and applications of nonreciprocal microwave ferrite devices.

621.372.54+621.317.3:621.396.663 3062
Possible Applications of Goniometers in Telecommunications—Fricke. (See 3228.)

621.372.543.2 3063
Design of Filters with Two Coupled Resonators for Wide Relative Pass Bands—G. B. Stracca. (*Alla Frequenza*, vol. 26, pp. 41–89; February, 1957.) Design formulas and curves for Butterworth and Tchebycheff type inductively-coupled double-tuned filters are given. See also 2368 of 1957 (Carassa).

621.372.56.029.6:621.372.8:621.318.134 3064
Nonreciprocal Ferrite Attenuator in a Rectangular Waveguide—M. Vadjal. (*Alla Frequenza*, vol. 26, pp. 3–24; February, 1957.) The increase in reverse loss relative to forward loss caused by a layer of dielectric material adjacent to the ferrite slab is investigated [see also 3675 of 1956 (Weisbaum and Seidel)]. Calculated results agree with experimental findings.

621.373:621.374.42 3065
Mutual Synchronization of Oscillators at Multiple Frequencies—G. M. Utkin. (*Radio-tehnika i Elektronika*, vol. 2, pp. 44–56; January, 1957.) The dependence of the mode of operation of the system, the oscillation frequencies, and the synchronization zone width on the frequency ratio of the two oscillators and oscillator parameters is calculated. Beat-frequency operation is also discussed.

621.373.43:513.83 3066
Study of a Nonlinear Oscillator by Topological Analysis—P. Dagneffe. (*Rev. HF, Brussels*, vol. 3, pp. 275–282; 1956.) The oscillator analyzed is of the universal type capable of producing quasi-sinusoidal, and continuous or discontinuous relaxation oscillations according to the adjustment of two parameters (resistances). The discontinuous solutions of the integral equations of the oscillator are discussed and the theory is verified by experimental measurements in the form of oscillograms.

621.373.431.1:621.387.4 3067
Experimental Investigations of the Dead Time of Univibrators—D. Kiss and J. Szivek. (*J. Sci. Instr.*, vol. 34, pp. 99–100; March, 1957.) The earliest time in which a monostable multivibrator can be triggered after a previous triggering is found to be strongly dependent on the amplitude of the triggering pulse.

621.373.52 3068
Transistor RC Oscillators—M. K. Achuthan. (*Electronic Radio Eng.*, vol. 34, pp. 309–310; August, 1957.)

621.374.32:621.314.7 3069
Decade Counters using Junction Transistors—L. P. Morgan and W. L. Stephenson. (*Mullard Tech. Commun.*, vol. 3, pp. 2–10; February, 1957.) A practical design with a counting speed of 100 kc uses one binary and four asymmetrical bistable circuits.

621.374.32:621.314.7 3070
High-Reliability Transistorized Counter—H. C. Chisholm. (*Electronics*, vol. 30, pp. 171–173; June 1, 1957.) "Cascaded silicon-junction transistor binary stages energize neon-lamp indicators for digital frequency meter at counting rates up to 100,000 per second."

- 621.374.32:621.387.4 3071
A Soft-Valve Scaler for Intermittent Fast Counting—G. W. Hutchinson. (*J. Sci. Instr.*, vol. 34, pp. 109–110; March, 1957.) Counting information is stored as charge on a capacitor and is subsequently read off as evenly spaced pulses by discharging the capacitor with a standard repetitive waveform.
- 621.374.4 3072
Double-Lock Synchronizing Method for Frequency Division—J. B. Ernschaw. (*Electronic Eng.*, vol. 29, pp. 282–283; June, 1957.) Both the maximum and the minimum of the timing waveform of a multivibrator are locked to an incoming signal.
- 621.374.4.029.63/.64 3073
Microwave Mixing and Frequency Dividing—R. W. DeGrasse and G. Wade. (*Proc. IRE*, vol. 45, pp. 1013–1015; July, 1957.) Use of the nonlinearity of an overmodulated electron beam in a traveling-wave tube.
- 621.375.024:538.639 3074
D.C. Amplifier with Converter based on the Effect of Change of Resistance of Semiconductors in a Magnetic Field—V. N. Bogomolov. (*Zh. Tekh. Fiz.*, vol. 26, pp. 2480–2486; November, 1956.) Theoretical and practical details are given of a dc/ac converter (modulator) based on the $\Delta\rho/\rho$ effect in InSb, a Hall-effect mixer, and a Hall-effect demodulator.
- 621.375.029.422/.424 3075
Selective Amplification at Sub-audio Frequencies—F. J. Hyde. (*Electronic Eng.*, vol. 29, pp. 260–265; June, 1957.) Direct transmission systems discussed are the resonant galvanometer and double CR (low-pass, high-pass) filter. Five feedback systems considered are based respectively on the twin-T filter, the Wien bridge, the double CR network, the zero-phase-shift oscillator, and a phase-inversion method due to Schneider (1207 of 1946).
- 621.375.029.63/.64:538.221:538.569.4 3076
Proposal for a Ferromagnetic Amplifier in the Microwave Range—H. Suhl. (*Phys. Rev.*, vol. 106, pp. 384–385; April 15, 1957.) Discussion of a system based on the anomalous absorption effects in ferromagnetic insulators at high signal powers.
- 621.375.029.64:538.569.4:621.396.822 3077
Noise in a Molecular Amplifier—M. W. Muller. (*Phys. Rev.*, vol. 106, pp. 8–12; April 1, 1957.) Extension of theory to systems not in thermal equilibrium.
- 621.375.121.1 3078
The Design of Phase-Linear Intermediate-Frequency Amplifiers—A. van Weel. (*J. Brit. IRE*, vol. 17, pp. 275–286; May, 1957.) Both stagger-tuned single circuits and combinations of band-pass filters are discussed.
- 621.375.121.2:621.372.22 3079
Artificial Transmission Lines—A. C. Hudson. (*Electronic Radio Eng.*, vol. 34, pp. 297–299; August, 1957.) Relations are derived between coil dimensions and constants for lines of the negative-mutual-inductance type.
- 621.375.121.2:621.372.6 3080
Amplifier with Distributed Constants as a System of Multipoles—Yu. N. Prozorovski. (*Radiotekhnika i Elektronika*, vol. 2, pp. 57–64; January, 1957.) Analysis is presented of an amplifier with distributed parameters considered as a system of a finite number of multipoles. Matrices connecting the input and output voltages and currents are derived and the transmission coefficient of the amplifier is determined.
- 621.375.132.3 3081
Multivalve Cathode-Follower Circuits—J. G. Thomason. (*Wireless World*, vol. 63, pp. 310–313; July, 1957 and pp. 373–377; August, 1957.) Methods of approaching the ideal buffer-stage performance are discussed and practical feedback circuits and their application are described. Examples include a precision differential amplifier.
- 621.375.2 3082
Alternatives to Cathode Bias for Vacuum Tubes—H. L. Armstrong. (*Proc. IRE*, vol. 45, pp. 1011–1012; July, 1957.) Resistive feedback stabilizes negative grid operating potential.
- 621.375.4.039.3:621.314.7 3083
A 200-mW Amplifier employing Transistors Operated from a 6-V Supply—O. T. Edwards. (*Mullard Tech. Commun.*, vol. 3, pp. 32–33; February, 1957.) Modification of the circuit described earlier (3324 of 1956) operating on 4.5 volts.
- 621.376.222.209.5 3084
A 16-kc/s Amplitude Modulator employing Envelope Feedback—K. G. Corless. (*Electronic Eng.*, vol. 29, pp. 287–290; June, 1957.) Using a greater degree of feedback, modulation linearity within 1 per cent is achieved for any frequency component in the range 0–30 cps.
- 621.376.23:621.396.822 3085
Effect of Differentiation and Integration of Fluctuations on the Mean Number of Peaks—V. I. Tikhonov. (*Radiotekhnika i Elektronika*, vol. 2, pp. 23–27; January, 1957.) An analysis is presented.
- 621.376.23:621.396.822 3086
Transformation of Amplitude and Phase Fluctuations of Oscillations by Tuned Systems—G. S. Gorelik and G. A. Elkin. (*Radiotekhnika i Elektronika*, vol. 2, pp. 28–33; January, 1957.) A theoretical investigation is reported of the transmission of signals with randomly varying phase and amplitude by systems comprising a linear (tuned) and a nonlinear (detector) unit. Formulas are derived relating the statistical characteristics of phase and amplitude at the input of a tuned system with those at the output.
- 621.376.5:621.3.016.352 3087
Stability of Linear Pulse Systems with Variable Parameters—G. P. Tartakovski. (*Radiotekhnika i Elektronika*, vol. 2, pp. 15–22; January, 1957.) The stability conditions for pulse systems with constant parameters are extended to systems with variable parameters and an equation is derived for the transmission function in pulse systems with variable parameters and feedback. The application of results is illustrated in a discussion of a pfm signal in a variable-parameter system with pulse feedback.
- GENERAL PHYSICS**
- 535.566:539.23 3088
Calculation of the Amplitude of a Plane Wave Reflected by a Homogeneous Metal Lamina with Parallel Faces—P. Dumontet. (*C.R. Acad. Sci., Paris*, vol. 244, pp. 2234–2236; April 24, 1957.) The work of previous authors; e.g., 1354 of 1949 (Reuter and Sondheimer) is generalized to allow for finite thickness of film. Calculated values of complex wave amplitude for light reflected from metals such as Ag, Au, Al, whatever the film thickness, are in agreement with classical theory.
- 537.226 3089
Dipole Moment Fluctuations of a Dielectric Body—B. K. P. Scaife. (*Proc. Phys. Soc. B, London*, vol. 70, pp. 314–319; March 1, 1957.) The particular case of a dielectric which has two mechanisms of polarization (orientational and displacement) is considered. It is shown that Fröhlich's free-energy method of computing the fluctuations is independent of the dynamic properties of the dielectric.
- 537.226 3090
Theory of Dielectric Relaxation for the Three-Dimensional Polar Rotator: Lattice Models Leading to Bimodal Loss Curves—J. D. Hoffman and B. M. Axilrod. (*J. Res. Nat. Bur. Stand.*, vol. 58, pp. 61–73; February, 1957.)
- 537.226.33 3091
Relaxation Processes and Inertial Effects: Part 1—Free Rotation about a Fixed Axis; Part 2—Free Rotation in Space—R. A. Sack. (*Proc. Phys. Soc. B, London*, vol. 70, pp. 402–413, 414–426; April 1, 1957.) The dielectric properties of systems of rigid dipoles are determined.
- 537.311.62 3092
Surface [skin] Effect in a System of Conductors with Rectangular Cross-Sections—L. A. Tseitlin. (*Zh. Tekh. Fiz.*, vol. 26, pp. 2771–2777; December, 1956.) Analysis is presented for 1) very thin bars and 2) bars with finite thickness.
- 537.52:621.385.13 3093
Filiform Anode in a Gas Discharge—B. N. Klyarfeld and A. A. Frid. (*Zh. Tekh. Fiz.*, vol. 26, pp. 2541–2547; November, 1956.) An experimental investigation is reported of a Hg-vapor discharge ($p=10^{-3}$ mm Hg) in a long narrow cylindrical tube containing a cylindrical anode at one end, a hot oxide cathode surrounded by another cylindrical anode in the bulbous other end of the tube, and a filiform molybdenum electrode along the axis of the tube.
- 537.525.029.64 3094
Microwave Gas Discharge Breakdown in Air, Nitrogen, and Oxygen—D. J. Rose and S. C. Brown. (*J. Appl. Phys.*, vol. 28, pp. 561–563; May, 1957.) The breakdown field for pure air, without contamination by oxides of nitrogen, is higher than previously observed and lies between the fields for nitrogen and oxygen. The results are now in accordance with theory.
- 537.533+535.215 3095
Electron Emission from Complex Surfaces—P. V. Timofeev. (*Radiotekhnika i Elektronika*, vol. 2, pp. 85–91; January, 1957.) Photoelectric secondary and field emission from complex cathodes are discussed. Conclusions indicate that 1) the surface electron energy levels play an important part in electron emission, 2) the photoelectric emission from Cs photocathodes is largely determined by the distribution of free Cs in the surface layer, 3) high values of secondary electron emission are always observed in cases when particles with low conductivity are present in the surface layer, and 4) field and secondary emission depend on the presence of positive charges in the surface layer.
- 537.533 3096
The Electron Emission from Mechanically Worked Metal Surfaces under Oxygen Pressures Variable with Time—J. Lohff. (*Naturwiss.*, vol. 44, p. 228; April, 1957.) Curves have been plotted of electron emission from an aluminum surface which had been treated with a steel brush and subjected to varying pressures in an atmosphere of O₂. Further tests are necessary to resolve contradictions with theory based on earlier oxidation experiments (see 1723 of 1957).
- 537.533 3097
Electron Emission from Vapour-Deposited Metal Films—J. Wüstenhagen. (*Naturwiss.*, vol. 44, pp. 228–229; April, 1957.) Emission

/time curves for aluminum films in an atmosphere of oxygen show a decrease of emission with decreasing O_2 pressures; a temporary evacuation of O_2 , although stopping emission, does not affect the continued decay of the emission after the O_2 pressure has been restored (see also 3096 above). Tests were also made on Be and Al films in the presence of inert gases.

537.533:537.226 3098

Mechanism of Electron Emission from Thin Dielectric Layers under the Influence of a Strong Electric Field (Malter Effect)—M. I. Elinson and D. V. Zernov. (*Radiotekhnika i Elektronika*, vol. 2, pp. 75-84; January, 1957.) Discussion of the Malter effect. (*Phys. Rev.*, vol. 50, pp. 48-58; July 1, 1936.)

537.56 3099

On Bohm-Pines' Theory of Plasma—W. Schützer. (*Ann. Acad. bras. Sci.*, vol. 28, pp. 419-422; December 31, 1956. In English.) The method of treatment of electron interaction in a dense electron gas developed by Bohm and Pines (1375 of 1954 and back references) is modified so that media of finite extent can be dealt with.

537.56 3100

Derivation of the Fokker-Planck Equation for Plasma—S. V. Temko. (*Zh. Eksp. Teor. Fiz.*, vol. 31, pp. 1021-1026; December, 1956.)

537.56 3101

Hydrodynamic Description of Plasma Oscillations—B. B. Kadomtsev. (*Zh. Eksp. Teor. Fiz.*, vol. 31, pp. 1083-1084; December, 1956.) Brief discussion restricted to electron oscillations assuming ions and molecules to be of infinitely large mass; the amplitude of oscillations is assumed to be small so that the electron velocity distribution function is nearly Maxwellian.

537.56:538.6 3102

Stability of Plasma in a Strong Magnetic Field—Yu. A. Tserkovnikov. (*Zh. Eksp. Teor. Fiz.*, vol. 32, pp. 67-74; January, 1957.)

537.56:538.63 3103

The Lateral Diffusion of an Electron Swarm in a Magnetic Field—R. J. Bickerton. (*Proc. Phys. Soc. B, London*, vol. 70, pp. 305-313; March 1, 1957.) The diffusion of electrons, moving through a gas under the influence of parallel electric and magnetic fields has been measured. Results are presented for the gases He and H_2 and currents between 10^{-10} and 10^{-6} A.

537.56:538.63 3104

On a Generalized Theory of a Lorentz Plasma under a Nonperiodic Force and taking Account of Inelastic Collisions—R. Jancel and T. Kahan. (*C.R. Acad. Sci., Paris*, vol. 244, pp. 2583-2586; May 20, 1957.) First- and second-order approximations are made for a solution of Boltzmann's transport equation by the method described earlier (2420 of 1957).

537.56.083:621.372.413.029.63/.64 3105

Limitations of the Microwave Cavity Method of Measuring Electron Densities in a Plasma—K. B. Persson. (*Phys. Rev.*, vol. 106, pp. 191-195; April 15, 1957.)

537.56.083:621.372.413.029.63/.64 3106

Microwave Measurements of High Electron Densities—S. J. Buchsbaum and S. C. Brown. (*Phys. Rev.*, vol. 106, pp. 196-199; April 15, 1957.)

538.112.083.2 3107

Determination of the Value of the Bohr Magneton by a Method of Resonance in Ionized Air—S. Procopiu and C. Papusoi. (*C.R. Acad. Sci., Paris*, vol. 244, pp. 1905-1907; April 1, 1957.)

538.221 3108

On the Propagation of Waves of the Classical Magnetic Form in a Fluid of Magnetic Doublets—G. Karpman and J. P. Vigiér. (*C.R. Acad. Sci., Paris*, vol. 244, pp. 2577-2580; May 20, 1957.) Application of theory proposed earlier [2421 of 1957 (Karpman)].

538.23:538.221 3109

Interpretation of the Creep of Hysteresis Cycles—L. Néel. (*C.R. Acad. Sci., Paris*, vol. 244, pp. 2668-2674; May 27, 1957.) If a magnetizing field varies cyclically about a mean value which is not zero, successive cycles are displaced and creeping is said to occur. Principal experimental results can be interpreted by supposing that successive hysteresis cycles described between the same limits and identical macroscopically, differ microscopically and give rise to random coupling fields between elementary domains. See also 3110 below.

538.24:538.221 3110

Action of Successive Magnetic Fields of a Random Character on the Magnetization of Ferromagnetic Substances—L. Néel. (*C.R. Acad. Sci., Paris*, vol. 244, pp. 2441-2446; May 13, 1957.) The idea of irreversible susceptibility is recalled and the variation of magnetization produced by n successive applications of a magnetic field of random character is calculated. The results of this research are applied to thermal fluctuations.

538.3 3111

Interaction between a Moving Current-Carrying Filament and a Conducting Wall—A. I. Morozov. (*Zh. Eksp. Teor. Fiz.*, vol. 31, pp. 1079-1080; December, 1956.) The forces acting on the filament, which is moving with a velocity $v \ll c$ parallel to the plane surface of the conducting medium are calculated.

538.311 3112

Note on Production of Strong Magnetic Fields of Short Duration and Measurement of their Intensity—A. Piekara, J. Malecki, M. Surma, and J. Gibalewicz. (*Proc. Phys. Soc. B, London*, vol. 70, pp. 432-434; April 1, 1957.)

538.311:621.317.441 3113

Compensation of the Earth's Magnetic Field—G. G. Scott. (*Rev. Sci. Instr.*, vol. 28, pp. 270-273; April, 1957.) A system for reducing and holding the magnetic fields in a working space to 0.01 per cent of the earth's horizontal component.

538.566:535.42]+534.26 3114

Diffraction by an Aperture—J. B. Keller. (*J. Appl. Phys.*, vol. 28, pp. 426-444; April, 1957.) Diffraction by an aperture of any shape in a thin screen is treated by an extension of geometrical optics introducing diffracted rays produced when incident rays hit the aperture edge. Explicit formulas and numerical results are given for slits and circular apertures.

538.566:535.42]+534.26 3115

Diffraction by an Aperture: Part 2—J. B. Keller, R. M. Lewis, and B. D. Seckler. (*J. Appl. Phys.*, vol. 28, pp. 570-579; May, 1957.) The method described in Part 1 (3114 above) is compared with the Kirchhoff method (Huyghen's principle) and modifications of this [see 2909 of 1954 (Bouwkamp)].

538.566+534.2]:535.43 3116

A New Method of Calculating Scattering with Particular Reference to the Circular Disc—D. S. Jones. (*Commun. Pure Appl. Math.*, vol. 9, pp. 713-746; November, 1956.) A comparatively simple physical picture of the low-frequency problem is developed. In the mathematical formulation the field is split into a nonradiating field which becomes the static field in the limit of zero frequency and the

remainder of the field. By the use of a Fredholm integral equation the use of an iteration scheme is avoided. Sixteen references.

538.566:535.43 3117

Back-Scattering from Dielectric-Coated Infinite Cylindrical Obstacles—C. C. H. Tang. (*J. Appl. Phys.*, vol. 28, pp. 628-633; May, 1957.) The back-scattering properties were investigated both theoretically (using eigenfunction expansion) and experimentally; very close agreement was obtained. A parallel-plate region enclosing a disk-shaped obstacle to represent a section across the theoretically infinite cylinder was used. The disk was rotated eccentrically and the back-scatter detected by the Doppler-shift principle.

538.569.4:538.2:538.54 3118

The Effect of Eddy Currents on Nuclear Magnetic Resonance in Metals—A. C. Chapman, P. Rhodes, and E. F. W. Seymour. (*Proc. Phys. Soc. B, London*, vol. 70, pp. 345-360; April 1, 1957.) The power absorption from a rf magnetic field is calculated as a function of the off-resonance absorption and the complex susceptibility for a material in the form of a plate, cylinder, or sphere. The results thus obtained are confirmed by measurements on aluminum foil.

538.569.4:538.221:621.375.029.63/.64 3119

Proposal for a Ferromagnetic Amplifier in the Microwave Range—H. Suhl. (See 3076.)

538.569.4:621.375.029.64:621.396.822 3120

Noise in a Molecular Amplifier—Muller. (See 3077.)

539.11:061.3 3121

Physics of the Solid State—(*Nature, London*, vol. 179, pp. 1004-1005; May 18, 1957.) Brief report of a meeting of the Physical Society held at the University of Nottingham, April, 1957. Some twenty papers were given, the majority referring to magnetism or semi-conduction. No full report is being prepared.

548.0:539.11 3122

Theory of Excitons in Ionic Crystals—I. P. Ipatova. (*Zh. Tekh. Fiz.*, vol. 26, pp. 2786-2788; December, 1956.)

548.0:539.11 3123

The Interaction of Electrons with Lattice Vibrations—P. G. Harper. (*Proc. Phys. Soc. B, London*, vol. 70, pp. 390-392; April 1, 1957.) Equations are derived for the frequency and zero-point energy of normal modes of lattice motion.

548.0:539.11 3124

Field Mass of Polarizing Excitons in Ionic Crystals—I. M. Dykman, E. I. Kaplunova, and K. B. Tolpygo. (*Zh. Tekh. Fiz.*, vol. 26, pp. 2459-2466; November, 1956.) The effective mass is calculated assuming that it possesses a field characteristic and depends on the interaction of the exciton with lattice vibrations. For excitons with a large radius, the calculation is made in a macroscopic approximation, for those with a small radius, the calculation is made with reference to NaCl and KCl crystals taking into account the discrete structure of the crystal and the dispersion of natural vibrations.

548.0:539.11:537.311.1 3125

Capture of Conduction Electrons by Charged Defects in Ionic Crystals—Yu. E. Perlin. (*Zh. Eksp. Teor. Fiz.*, vol. 32, pp. 105-114; January, 1957.) The probability of capture is calculated as a function of polaron velocity and the temperature dependence of the lifetime of the current carriers is determined.

- GEOPHYSICAL AND EXTRATERRESTRIAL PHENOMENA**
- 523.16:621.396.822 3126
Cosmic Radio-Noise Intensities below 10 Mc/s—G. R. Ellis. (*J. Geophys. Res.*, vol. 62, pp. 229–234; June, 1957.) The increase in intensity with decreasing frequency ceases near 10 mc and the spectrum is flat from 10 mc down to 2 or even 0.9 mc. The flux density is about 2×10^{-19} /wcm² per cps.
- 529.77(470) 3127
New Boundaries of Time Zones in the U.S.S.R.—P. N. Dolgov. (*Priroda, Moscow*, pp. 57–61; January, 1957.) Historical introduction and map of new standard-time zones which came into effect on March 1, 1957 at midnight, Moscow time.
- 55 3128
I.G.Y. World Warning Agency—(*Tech. News. Bull. Nat. Bur. Stand.*, vol. 41, pp. 65–66; May, 1957.)
- 550.385:523.74 3129
The Geomagnetic Influence of the Northern and Southern Solar Hemispheres—W. Gleissberg. (*Naturwiss.*, vol. 44, pp. 176–177; March, 1957.) An analysis of solar data for the period 1889 to 1943 shows that the northern hemisphere of the sun has a predominant effect on geomagnetic disturbances. This is probably due to more intensive particle emission from that part of the sun.
- 551.51 3130
The Theory of Molecular Diffusion in the Atmosphere—P. Mange. (*J. Geophys. Res.*, vol. 62, pp. 279–296; June, 1957.) Existing theory is extended to include a linear variation in scale height and other refinements. The application to particular problems is discussed.
- 551.51 3131
On the Atmospheric Dynamo Theory—M. L. White. (*J. Geophys. Res.*, vol. 62, pp. 329–330; June, 1957.) Methods of avoiding earlier simplifying assumptions are suggested.
- 551.510.535 3132
Ionospheric Problems—T. W. Bennington. (*Wireless World*, vol. 63, pp. 365–368; August, 1957.) The future application of IGY data may help radio communication by providing information on sporadic E and nighttime E layers and on ionospheric disturbances.
- 551.510.535 3133
Physical Properties of the Atmosphere from 90 to 300 km—G. J. Simmons, H. K. Kallman, W. B. White, and H. E. Newell, Jr. (*J. Geophys. Res.*, vol. 62, pp. 327–328; June, 1957.) Comment on 436 of 1957, giving a preferred formula for (16). See also *ibid.*, vol. 62, p. 168; March, 1957, for correction to original paper.
- 550.510.535 3134
Effective Recombination Coefficient in the Ionosphere—V. I. Krasovskii. (*Bull. Acad. Sci. U.R.S.S., sér. géophys.*, no. 4, pp. 504–511; April, 1957. In Russian.) Discussion of theoretical and experimental results. Conclusions are: 1) the coefficient depends on the electron concentration and rate of ion production and therefore cannot be assumed to be constant in time or symmetrical relative to noon, sunrise, and sunset; 2) the coefficient depends on the nature of the primary ions and therefore is not necessarily identical with the coefficient for photoionization when ionization is produced by corpuscles, meteorites, or gas discharges. The presence of infrasonic waves would cause an increase in the coefficient.
- 551.510.535 3135
Recombination Coefficient and Electron Production Rate from Total Electron Content in Unit Column below the Level of Maximum Ionization—S. Datta. (*Indian J. Phys.*, vol. 31, pp. 43–52; January, 1957.)
- 551.510.535 3136
Drift Measurements of the E Layer—L. Harang and K. Pedersen. (*J. Geophys. Res.*, vol. 62, pp. 183–198; June, 1957.) The Mitra method of recording drifts in the diffraction pattern was used at Kjeller, Norway from June, 1953 to September, 1955. The diurnal and seasonal changes in drift are discussed and compared with results elsewhere. There is some evidence for a small lunar component.
- 551.510.535 3137
Anomalies in Ionosonde Records due to Travelling Ionospheric Disturbances—G. H. Munro. (*J. Geophys. Res.*, vol. 62, pp. 325–326; June, 1957.)
- 551.510.535:550.385 3138
Relations among Radio Absorbing Regions, Geomagnetic Bay Disturbances and Slant E_s in Auroral Latitudes—S. Matsushita. (*J. Geomag. Geoelec.*, vol. 8, pp. 156–160; December, 1956.)
- 551.510.535:550.385 3139
Disturbances in the Ionospheric F₂ Region associated with Geomagnetic Storms: Part 1—Equatorial Zone—T. Sato. (*J. Geomag. Geoelec.*, vol. 8, pp. 129–135; December, 1956.) The ionospheric disturbances are explained in terms of the vertical drift of electrons caused by the electric field arising from the disturbed component of the geomagnetic field. The ionospheric data for Huancayo during several disturbances are in accordance with the magnetic data.
- 551.510.535:621.396.812.3 3140
Fading and Random Motion of Ionospheric Irregularities—Mitra and Srivastava. (See 3283.)
- 551.594.5 3141
The Geometry of Auroral Ionization—T. R. Kaiser. (*J. Geophys. Res.*, vol. 62, pp. 297–298; June, 1957.) The pattern of radio echoes from auroral ionization agrees with the hypothesis that the ionization occurs “in blobs” distributed along an arc which follows a parallel of magnetic latitude, and not in narrow columns aligned along the magnetic lines of force.
- 551.594.5 3142
Radar Reflections from Aurorae—Ya. G. Birkfeld. (*Bull. Acad. Sci. U.R.S.S., sér. géophys.*, no. 4, pp. 543–547; April, 1957. In Russian.) Report on experimental results obtained at the Loparskaya station near Murmansk. A frequency of 72 mc was used and echoes were recorded from auroras up to 1000 km distant. Typical cro traces are shown and are briefly described.
- 551.594.6 3143
Lightning Mechanism and Atmospheric Radiation—H. Isikawa. (*J. Geomag. Geoelec.*, vol. 8, pp. 136–146; December, 1956.) A discussion of the discharge processes as deduced from electric-field measurements. Particular attention is paid to the leader discharges.
- 551.594.6:523.75 3144
An Observation of Audio-Frequency Electromagnetic Noise during a Period of Solar Disturbance—J. M. Watts. (*J. Geophys. Res.*, vol. 62, pp. 199–206; June, 1957.) An analysis of hiss recorded during a magnetic storm shows 1) a peak in the frequency spectrum near 3 kc, 2) that the high-frequency limit was variable, 3) a procession of narrow-bandwidth tones gliding upwards occurred during part of the period.
- LOCATION AND AIDS TO NAVIGATION**
- 621.396.933 3145
Vortac Beacons for Rho-Theta Navigation—P. Caporale. (*Electronics*, vol. 30, pp. 156–159; June 1, 1957.) A short-distance navigation system providing information on azimuth and distance when challenged by beacon equipment in approaching aircraft.
- 621.396.933.1 3146
Doppler Navaid for Civil Aircraft—(*Wireless World*, vol. 63, p. 396; August, 1957.) Brief description of a self-contained air navigational system entirely independent of ground station cooperation.
- 621.396.933.2 3147
Applying the Doppler Effect to Direction-Finder Design—J. A. Fantoni and R. C. Benoit, Jr. (*Electronic Ind. Tele-Tech.*, vol. 16, pp. 75–77, 147, 66–67, 128; January–February, 1957.) A circular array of fixed antennas is scanned in sequence to produce a direction-dependent phase. The IF from the receiver is applied to a discriminator and the resultant signal with scanning-switch modulation frequency of 42 cps is applied to a cr-tube bearing display.
- 621.396.96.001.4 3148
Flight Simulator tests Fire-Control Radars—D. L. DeMyer. (*Electronics*, vol. 30, pp. 168–170; June 1, 1957.) Target speeds of 200 to 1000 mph in either direction can be simulated at distances of 800–24,000 yards.
- 621.396.963.3:621.396.822 3149
Detection of Pulse Signals in Noise: Trace-to-Trace Correlation in Visual Displays—D. G. Tucker. (*J. Brit. IRE*, vol. 17, pp. 319–329; June, 1957.) Experiments show that side-by-side presentation of traces gives superior detection to that obtained by true integration. The theoretical reasons are discussed and previously published data are reviewed.
- 621.396.963.3:621.396.822 3150
Detection of Pulse Signals in Noise: the Effect on Visual Detection of the Area of the Signal Paint—J. W. R. Griffiths. (*J. Brit. IRE*, vol. 17, pp. 330–338; June, 1957.) Available experimental data are reviewed in terms of physiological optics. Improvements in detection using side-by-side presentation may be explained by the increase in the solid angle subtended at the eye by the signal “paint.”
- 621.396.969 3151
Rate-of-Climb Meter uses Doppler Radar—S. H. Logue. (*Electronics*, vol. 30, pp. 150–152; June 1, 1957.) The direct-reading instrument uses a 10-kmc cw radar with the ground as reflecting surface. The equipment operates up to 2300 feet.
- 621.396.969:061.3 3152
The International Annual Conference on Radio- and Sound-Location in Hamburg 1956—H. Köppen. (*Nachr.-Tech.*, vol. 7, pp. 34–39; January, 1957.) Summaries of most of the lectures delivered at this conference. See also *Elekt. Rund.*, vol. 10, pp. 343–348; December, 1956; and vol. 11, pp. 27–29; January, 1957.
- MATERIALS AND SUBSIDIARY TECHNIQUES**
- 531.788.7 3153
A New Electronic Circuit for a Hot-Cathode Ionization Gauge—J. Schutzen. (*Appl. Sci. Res.*, vol. B6, pp. 276–284; 1957.) A circuit is described for measuring pressures in the range 10^{-3} – 10^{-10} mm Hg. The quotient of ion current over emission current is measured, and at pressures below 10^{-4} mm Hg the meter indication varies by not more than 3 per cent for emission currents between 10 μ a and 1 ma.

- 535.21:546.23 3154
Structural Changes of Selenium under the Influence of Light—H. Stegmann. (*Naturwiss.*, vol. 44, pp. 108-109; March, 1957.) Experimentally observed changes in the transmission of light through Se films are briefly reported and discussed.
- 535.215:537.311.33 3155
The So-Called 'Secondary' and 'Through' Photocurrent in Semiconductors—S. M. Ryvkin. (*Zh. Tekh. Fiz.*, vol. 26, pp. 2439-2447; November, 1956.)
- 535.215:[546.681.23+546.681.24] 3156
Temperature Dependence of the Spectral Distribution of the Photoconductivity of Gallium Selenide and Telluride—S. M. Ryvkin and R. Yu. Khansevarov. (*Zh. Tekh. Fiz.*, vol. 26, pp. 2781-2783; December, 1956.) Results of an experimental investigation on polycrystalline GaSe and GaTe specimens with conductivities in the range 10^{-4} – 10^{-2} Ω⁻¹cm⁻¹ are reported. Graphs showing the special characteristics at temperatures between about -100° C and +100° C are given.
- 535.215:546.817.221:539.23 3157
Investigation of the Photoconductive Effect in Lead Sulphide Films using Hall and Resistivity Measurements—J. F. Woods. (*Phys. Rev.*, vol. 106, pp. 235-240; April 15, 1957.) Measurements were made of the fractional change of Hall coefficient and of resistivity occurring under illumination of chemically deposited PbS films. Using a model of photoconductivity [1774 of 1957 (Petritz)] the results show that the effect is due to an increase in majority-carrier density, with no modulation of barrier potentials.
- 535.37:534-8 3158
Luminescence Changes in Continuously Excited Zinc-Sulphide Fluorescent Screens under the Influence of Ultrasonic Radiation—M. Leistner and L. Herforth. (*Naturwiss.*, vol. 44, p. 59; February, 1957.) Brief preliminary note on tests carried out on ZnS-Cu and ZnS-Ag screens subjected to ultrasonic radiation at 800 kc and excited by ultraviolet light.
- 535.37:621.385.832:621.397.5:535.623 3159
Luminophores based on ZnS and ZnSe for Colour Television—E. I. Blazhnova, A. I. Mokrintseva, and V. I. Kas'yanova. (*Zh. Tekh. Fiz.*, vol. 26, pp. 2784-2785; December, 1956.) Spectral intensity and brightness/electron-beam-density curves are shown of green, red, and blue luminophores the compositions of which are given. The brightness decreased by less than 5 per cent after 400 h at an anode potential of 15 kv and beam density of 1 μa.cm⁻². The effect of heat treatment in vacuum and in air on the colorimetric coordinates was also investigated and the results are tabulated.
- 537.226/.228.1:546.431.824-31 3160
Improved Barium Titanate Composition—D. Schlofeld and R. F. Brown. (*J. Acoust. Soc. Amer.*, vol. 29, pp. 394-395; March, 1957.) Typical values of dielectric constant, radial coupling coefficient, and piezoelectric constant are given for BaTiO₃ samples containing a small percentage of Co, the addition of which increases the power-handling capacity of the material.
- 537.226/.227:546.431.824-31 3161
Thermodynamic Theory of Ferroelectricity—I. A. Izhak. (*Zh. Eksp. Teor. Fiz.*, vol. 32, pp. 160-162; January, 1957.) Results of measurements on polycrystalline BaTiO₃ in the paraelectric range confirm some predictions of the thermodynamic theory. In the ferroelectric range satisfactory agreement was obtained only at temperatures not more than 10-12°C below the Curie point.
- 537.226/.227:546.431.824-31 3162
Theory of Phase Phenomena in Barium Titanate—L. P. Kholodenko. (*Zh. Eksp. Teor. Fiz.*, vol. 31, pp. 1034-1045; December, 1956.) The "temperature hysteresis" in phase transitions is discussed and the temperature dependence of the permittivity near the phase transition points is calculated. The coefficients occurring in the thermodynamic theory are expressed in terms of measurable quantities.
- 537.226/.227:546.431.824-31:539.185 3163
Fast Neutron Effects in Tetragonal Barium Titanate—M. C. Wittels and F. A. Sherrill. (*J. Appl. Phys.*, vol. 28, pp. 606-609; May, 1957.) An experimental study of the lattice properties of irradiated barium titanate. The neutron flux transformed the tetragonal form into the cubic form normally stable only above the Curie point. The control of ferroelectric properties by varied amounts of irradiation is suggested.
- 537.226:537.224 3164
New Inorganic Dielectric Electrets—A. N. Gubkin and G. I. Skanavi. (*Zh. Eksp. Teor. Fiz.*, vol. 32, pp. 140-142; January, 1957.) The 14 different materials investigated include several titanates, stearite, porcelain, glass, quartz, and KBr. For BaTiO₃ the surface charge density, σ , is 15.4×10^{-9} C/cm², 30 minutes after polarization in a field of 10 kv/cm, falling to 1.1×10^{-9} C/cm² after 7 months. MgTiO₃ with $\sigma = 1.9 \times 10^{-9}$ C/cm² and 0.5×10^{-9} C/cm² after 7 months was shown to have a "lifetime" of over 1.5 years. The variations of σ with time are tabulated for periods up to 7 months after polarization.
- 537.226+537.311.33]:537.29 3165
Influence of an Electric Field on the Properties of Thin Dielectric and Semiconductor Layers—Yu. M. Volokobinski. (*C.R. Acad. Sci. U.R.S.S.*, vol. 113, pp. 1023-1024; April 11, 1957. In Russian.) The electrical conductivity and electrical strength of several oxides, sulphides, and other compounds were investigated. Results indicate that the electrical breakdown is connected with the disruption of the layer by the heating produced by the passage of a current through the layer.
- 537.226:546.42.824-31 3166
Single Crystals of Strontium Titanate—A. L. Khodakov, M. L. Sholokhovich, E. G. Fesenko, and O. P. Kramarov. (*Zh. Tekh. Fiz.*, vol. 26, pp. 2506-2507; November, 1956.) Brief note on the dielectric-constant/temperature characteristics of single crystals of SrTiO₃ prepared by two different methods.
- 537.226:621.315.612 3167
Classification of Perovskite and Other ABO₃-Type Compounds—R. S. Roth. (*J. Res. Nat. Bur. Stand.*, vol. 58, pp. 75-88; February, 1957.) A partial survey of the reactions occurring in binary oxide mixtures of the types AO:B₂O₃ and A₂O₃:B₂O₃ has been conducted as part of a program of fundamental research on ceramic dielectrics.
- 537.226:621.315.612 3168
Breakdown of Ceramic Specimens under a High-Frequency Voltage at Different Temperatures—I. E. Balygin. (*Zh. Tekh. Fiz.*, vol. 26, pp. 2498-2505; November, 1956.) Various commercial-type ceramic materials were tested at a frequency of 1.5 mc and the effects of porosity, chemical composition, and structure of the material on the breakdown characteristics were noted.
- 537.226.2:546.331.31 3169
Influence of Dislocations of the Crystal Lattice on the Permittivity of Rock-Salt Crystals—Yu. A. Sikorski. (*Zh. Tekh. Fiz.*, vol. 26, pp. 2487-2492; November, 1956.)
- 537.227 3170
Phase Transitions in Ferroelectric Solid Solutions based on Strontium Pyrotantalate—G. A. Smolenski, V. A. Isupov, and A. I. Agranovskaya. (*C.R. Acad. Sci. U.R.S.S.*, vol. 113, pp. 803-805; April 1, 1957. In Russian.) The dielectric-constant/temperature characteristics were determined experimentally in solutions of Sr₂Nb₂O₇, Ba₂Ta₂O₇, and Ca₂Ta₂O₇ in Sr₂Ta₂O₇ at a frequency of 500 kc. Results are presented graphically.
- 537.227:546.431.824-31 3171
Solid Solutions of Barium Metaniobate and Metatantalate in Barium Titanate with Ferroelectric Properties—G. A. Smolenski, V. A. Isupov, and A. I. Agranovskaya. (*C.R. Acad. Sci. U.R.S.S.*, vol. 113, pp. 1053-1056; April 11, 1957. In Russian.) Results are reported of an experimental investigation of the dependence of the dielectric constant and loss angle on temperature in the range from -100°C to +200°C in solid solutions with various compositions. The measurements were made at a frequency of 1 kc. A composition/temperature phase diagram is also given.
- 537.227:547.476.3 3172
The Ferroelectric Domain Structure of Rochelle Salt—E. Straubel-Fischer. (*Naturwiss.*, vol. 44, pp. 230-231; April, 1957.) Brief report of optical tests.
- 537.228.1:548.0].001.4(083.7) 3173
IRE Standards on Piezoelectric Crystals—the Piezoelectric Vibrator: Definitions and Methods of Measurement, 1957—(Proc. IRE, vol. 45, p. 1010; July, 1957.) Correction to 1788 of 1957.
- 537.311.31 3174
Electrical Resistivity of Nickel-Palladium Alloys—A. W. Overhauser and A. I. Schindler. (*J. Appl. Phys.*, vol. 28, pp. 544-546; May, 1957.) Experimental data for alloys of different relative concentrations are quoted. The results are discussed in terms of the electronic structure of the alloy.
- 537.311.33 3175
Evaporation of Impurities from Semiconductors—K. Lehovec, K. Schoeni, and R. Zuleg. (*J. Appl. Phys.*, vol. 28, pp. 420-423; April, 1957.) The impurity distribution arising by evaporation from the surface is derived assuming the rate of evaporation to be proportional to the surface concentration. The proportionality constant is derived experimentally.
- 537.311.33 3176
A Contribution to the Recombination Statistics of Excess Carriers in Semiconductors—P. T. Landsberg. (*Proc. Phys. Soc. B, London*, vol. 70, pp. 282-296; March 1, 1957.) For interband transitions the conditions under which a recombination coefficient exists are investigated and the effect of degeneracy of hole and electron gas is discussed. For transitions involving traps, degeneracy, and the case of impurities having several trapping levels are considered.
- 537.311.33 3177
Relation between Ratio of Diffusion Lengths of Minority Carriers and Ratio of Conductivities—S. S. L. Chang. (Proc. IRE, vol. 45, pp. 1019-1020; July, 1957.)
- 537.311.33 3178
Breakdown of Transition Layers in Semiconductors—B. M. Vul. (*Zh. Tekh. Fiz.*, vol. 26, pp. 2403-2416; November, 1956.) The electrical, thermal, and thermoelectric factors in the breakdown of a p-n junction are discussed theoretically.
- 537.311.33 3179
Measurement of Surface Recombination

- Velocity in a Thin Semiconductor with Qualitatively Differing Sides**—O. V. Sorokin. (*Zh. Tekh. Fiz.*, vol. 26, pp. 2467–2472; November, 1956.) Formulas are derived from the solution of the continuity equation connecting the effective length of diffusion of nonequilibrium current carriers, L_{α} , in a plane semiconductor filament with the surface recombination velocities S_1 and S_2 of the upper and lower sides, respectively. The relations derived allow S_1 and S_2 to be calculated from the result of measurements of L_{α} .
- 537.311.33:538.83 3180
Measurement of the Lifetime, Diffusion Coefficient and Surface Recombination Velocity of Non-equilibrium Current Carriers in a Thin Semiconductor Specimen—O. V. Sorokin. (*Zh. Tekh. Fiz.*, vol. 26, pp. 2473–2479; November, 1956.) A thin, plane semiconductor specimen illuminated by a narrow beam of light moving with constant velocity along it is considered. Formulas are given connecting the experimentally determined distribution of non-equilibrium current carriers with lifetime, diffusion coefficient and the velocities of surface recombination.
- 537.311.33:53.083 3181
Comparator Method for Optical Lifetime Measurements on Semiconductors—H. L. Armstrong. (*Rev. Sci. Instr.*, vol. 28, p. 202; March, 1957.) An analog comprising a vacuum photocell with a cr load is used to interpret the cro display in the light-pulse method described by Stevenson and Keyes (2008 of 1955).
- 537.311.33:535.215 3182
Measurement of Carrier Recombination Velocity by Conductivity Modulation—K. D. Glinchuk, E. G. Miselyuk, and E. I. Rashba. (*Zh. Tekh. Fiz.*, vol. 26, pp. 2607–2613; December, 1956.) A photoconductivity-modulation method is described for the determination of minority-carrier life time τ and surface recombination velocity S . A 200-cps square-wave-modulated beam of light of 40,000 lx intensity and about 0.7×0.1 mm² cross section was used. The method is suitable for measurements of $S \approx 10^4 - 10^5$ cm/sec and $\tau \approx 10^{-1} - 10^{-2}$ μ s. Preliminary experimental results show fair agreement with results obtained by other methods.
- 537.311.33:535.215:[546.28 + 546.289] 3183
The Properties of Semiconductor Devices—A. A. Shepherd. (*J. Brit. IRE*, vol. 17, pp. 255–273; May, 1957.) A survey of recent trends in design including the production of germanium and silicon junctions during crystal growth and by alloying and solid-state diffusion. Semiconductor photocells are described. Thirty-three references.
- 537.311.33:538.63 3184
Theory of Galvanomagnetic Phenomena in Semiconductors—M. I. Klinger. (*Zh. Eksp. Teor. Fiz.*, vol. 31, pp. 1055–1061; December, 1956.)
- 537.311.33:539.16/18 3185
The Effect of Nuclear Radiation on Selected Semiconductor Devices—G. L. Kleister and H. V. Stewart. (*Proc. IRE*, vol. 45, pp. 931–937; July, 1957.) A range of commercial Ge and Si transistors and diodes has been exposed to neutron and gamma radiation. Deterioration of performance ensues. Both the surface- and bulk-controlled properties of the devices suffer change. In general, surface changes are of a transient nature whereas bulk changes (*i.e.*, decrease of lifetime and change of resistivity) are permanent.
- 537.311.33:539.16.08:621.387.462 3186
Mechanism of the Forming of Pulses in Semiconductor Crystal Counters (Motion of Charges in Pulse Ionization in Semiconduc-
- tors)**—S. M. Ryvkin. (*Zh. Tekh. Fiz.*, vol. 26, pp. 2667–2683; December, 1956.)
- 537.311.33:546.24:538.63 3187
Investigation of Influence of Pressure on Galvanomagnetic Properties of Tellurium at Low Temperatures—N. E. Aleksevski, N. B. Brandt, and T. I. Kostina. (*Zh. Eksp. Teor. Fiz.*, vol. 31, pp. 943–946; December, 1956.) An experimental investigation of the effect of 1700 atm pressure on Te specimens with various impurity concentrations, at temperatures in the ranges 1.4–4.2, 14–20.4, and 60–78°K, and magnetic fields up to 20,000 oersted.
- 537.311.33:546.28 3188
Carrier Concentration Changes in p Si Induced by Heat Treatment—Y. Matukura. (*J. Phys. Soc. Japan*, vol. 12, pp. 103–104; January, 1957.) The effects of heat treatment (400°–1000°C) on carrier concentration are given, including dependence on heating and cooling times, and on the ambient gas.
- 537.311.33:[546.28 + 546.289]:539.169 3189
Etching Behaviour of Pile-Irradiated Germanium and Silicon Single Crystals—R. Chang. (*J. Appl. Phys.*, vol. 28, pp. 385–387; April, 1957.) Etching behavior changes after pile irradiation, and preliminary work suggests a new experimental approach to the study of radiation damage.
- 537.311.33:546.289 3190
Effective Mass of Electrons and Holes in Germanium—Z. Kopets. (*Zh. Tekh. Fiz.*, vol. 26, pp. 2451–2458; November, 1956.) The effective mass is calculated from experimental data on the thermo-emf α , Hall constant, and electrical conductivity, for the case when α increases with temperature. At a temperature of 125°K and electron concentration of 2.7×10^{16} the effective electron mass is 0.47, and the effective mass of the hole is 0.23 at a hole concentration of 1.3×10^{17} . Results of effective electron and hole mass calculations are tabulated for concentrations of 2.7×10^{15} – 6.6×10^{17} and 1.3×10^{17} – 5.5×10^{18} , respectively, at temperatures between 125 and 250°K.
- 537.311.33:546.289 3191
Precipitation of Cu in Ge—A. G. Tweet. (*Phys. Rev.*, vol. 106, pp. 221–224; April 15, 1957.) Results of an experimental study are expressed in terms of the exponential decay with time of the unprecipitated fraction of Cu. The dependence of the time constant on temperature and dislocation density in the samples is discussed.
- 537.311.33:546.289 3192
Effect of Heavy Doping on the Self-Diffusion of Germanium—M. W. Valente and C. Ramasastri. (*Phys. Rev.*, vol. 106, pp. 73–75; April 1, 1957.) Measurements of the self-diffusion coefficients for intrinsic, heavily-doped n - and p -type Ge suggest that self-diffusion occurs by the vacancy mechanism.
- 537.311.33:546.289 3193
Influence of Electric Field in Diffusion Region upon Breakdown in Germanium n - p Junctions—E. M. Pell. (*J. Appl. Phys.*, vol. 28, pp. 459–466; April, 1957.) The electric field arising from the IR drop in the diffusion region can 1) decrease the voltage at which a junction breaks down, 2) increase the photocurrent if the junction current is increased by any mechanism. An allied phenomenon of "soft breakdown" has also been observed.
- 537.311.33:546.289 3194
Study of Injecting and Extracting Contacts on Germanium Single Crystals—L. Y. Lin. (*Rev. Sci. Instr.*, vol. 28, pp. 187–188; March, 1957.) The preparation of reliable contacts for determining lifetimes by the Many bridge method is described. Rectifying and ohmic contacts to a single crystal must be considered together.
- 537.311.33:546.289:538.6 3195
Oscillatory Magneto-absorption on the Direct Transition in Ge—S. Zwerdling and B. Lax. (*Phys. Rev.*, vol. 106, pp. 51–52; April 1, 1957.) Measurements on intrinsic Ge at $\lambda 1.4 - 1.6 \mu$, in magnetic fields up to 36,000 G.
- 537.311.33:546.289.241 3196
Electrical Properties of GeTe—Y. Moriguchi and Y. Koga. (*J. Phys. Soc. Japan*, vol. 12, p. 100; January, 1957.) Measurements of the Hall coefficient, resistivity, and thermoelectric power of polycrystalline and single-crystal specimens of GeTe show that this material does not conform well to ordinary semiconductor theory, but shows semimetallic properties.
- 537.311.33:546.482.21 3197
Ohmic and Rectifying Contacts to Semiconducting CdS Crystals—W. C. Walker and E. Y. Lambert. (*J. Appl. Phys.*, vol. 28, pp. 635–636; May, 1957.)
- 537.311.33:[546.57.23 + 546.57.24] 3198
Rectification Properties of Silver Selenide and Telluride—N. G. Klyuchnikov. (*Zh. Tekh. Fiz.*, vol. 26, p. 2603; November, 1956.) The rectifiers prepared possess a high forward/reverse current ratio. In Ag_2Te this ratio is approximately 18,000:1. With a potential difference 1.4 v the forward current is 40 a.cm^{-2} ; the reverse current is 12 ma.cm^{-2} for 12 v. For Ag_2Se the forward current is 17 a.cm^{-2} for 2 v, the reverse current 16 ma.cm^{-2} for 12 v. The rectifiers are unsuitable for rectification of an alternating current owing to the unstable nature of the barrier layer under forward current. Weak rectifying properties were also observed in other selenides and tellurides.
- 537.311.33:546.682.86:621.396.822 3199
Current Noise in Indium Antimonide—D. J. Oliver. (*Proc. Phys. Soc. B, London*, vol. 70, pp. 331–332; March 1, 1957.) Measurements in the frequency range 20 cps–20 kc showed that excess noise was not detectable. It is estimated that the noise ratio (total-noise/thermal-noise) was less than 7 at 20 cps, and less than 2 above 1 kc, for currents up to 500 ma through a 1- Ω filament. See also 1142 of 1957 (Suits, *et al.*).
- 537.311.33:546.817.241 3200
Diffusion of Lead in Lead Telluride—B. I. Boltaks and Yu. N. Mokhov. (*Zh. Tekh. Fiz.*, vol. 26, pp. 2448–2450; November, 1956.) Results of preliminary experiments are reported. The temperature dependence of the diffusion coefficient is given by the relation $D = 2.9 \times 10^{-6} \exp(-0.6/kT) \text{ cm}^2 \cdot \text{sec}^{-1}$ at temperatures well below the melting point of PbTe (905°C). The small activation energy (0.6 ev) and the high diffusion velocity indicate that the diffusion by migration of positively charged lead ions is of the interstitial type, similar to that of the diffusion of Cu in Ge.
- 537.311.33:546.817.241 3201
Influence of Impurities on the Electrical Properties of Lead Telluride—T. L. Koval'chik and Yu. P. Maslakovets. (*Zh. Tekh. Fiz.*, vol. 26, pp. 2417–2431; November, 1956.) A considerable increase of the concentration of free electrons in PbTe can only be obtained by the introduction of two impurities; *e.g.*, Br and excess Pb. Introduction of single Br atoms, by substituting a $PbBr_2$ group for a $2PbTe$ group, may result in the production of lattice vacancies and a consequent decrease in current-carrier mobility. Different heat treatments of p -type PbTe give different current-carrier numbers. The relation between the carrier concentration and annealing temperature is given by

- $n_+ = A \exp(-\Delta E/2kT)$, where ΔE is near the value of the forbidden zone width for PbTe as determined from the temperature characteristic of the Hall constant.
- 537.311.33:621.314.7 3202**
On the Injection of Carriers into a Depletion Layer—W. G. Matthei and F. A. Brand. (*J. Appl. Phys.*, vol. 28, pp. 513-514; April, 1957.) Results are given of experiments which verify and extend the concept of injection into a depletion layer of a reverse-biased $p-n$ junction.
- 537.311.33:621.385.833 3203**
Image of $p-n$ Junctions in Semiconductors Obtained by a Reflection Electron Microscope—G. Bartz and G. Weissenberg. (*Naturwiss.*, vol. 44, p. 229; April, 1957.) Micrograms are shown which were obtained by electron reflection and secondary emission from a Si $p-n$ junction subjected to different bias voltages affecting the visibility and contrast of the transition zone.
- 538.2:539.23 3204**
Magnetic Domain Patterns on Thin Films—H. J. Williams and R. C. Sherwood. (*J. Appl. Phys.*, vol. 28, pp. 548-555; May, 1957.) The films were deposited in the presence of a magnetic field to establish a uniaxial direction of easy magnetization. This direction could be changed by reheating in a magnetic field with a new orientation, contrary to the behavior with bulk specimens.
- 538.22 3205**
Magnetic Properties of MnAu₃—A. J. P. Meyer. (*C.R. Acad. Sci., Paris*, vol. 244, pp. 2028-2031; April 8, 1957.)
- 538.22 3206**
Neutron Diffraction Study of the Magnetic Structures for the Perovskite-Type Mixed Oxides La(Mn,Cr)O₃—U. H. Bents. (*Phys. Rev.*, vol. 106, pp. 225-230; April 15, 1957.) Investigation of the series La $[x$ Mn, $(1-x)$ Cr]O₃ with x varying from 0 to 1.
- 538.221 3207**
The Transformation of Haematite(α -Fe₂O₃) into Ferromagnetic Iron Oxide (γ -Fe₂O₃)—F. J. Lęcznar. (*Acta Tech. Acad. Sci. hungaricae*, vol. 16, pp. 383-398; 1957.) The different properties of the two varieties are outlined and experimental methods of producing the ferromagnetic form are described.
- 538.221 3208**
Orientation of the Precipitations of Cobalt in a CuCo Alloy—L. Weil, L. Gruner, and A. Deschamps. (*C.R. Acad. Sci., Paris*, vol. 244, pp. 2143-2146; April 15, 1957.) Magnetic measurements made at low temperatures show the segregated masses of Co in a drawn specimen to be oriented.
- 538.221 3209**
Orientational Superstructures in Fe-Ni Alloys—E. T. Ferguson. (*C.R. Acad. Sci., Paris*, vol. 244, pp. 2363-2366; May 6, 1957.) Uniaxial anisotropy induced in Fe-Ni alloys by reheating in a magnetic field is determined as a function of composition and of temperature and duration of reheating. See 1101 and 2983 of 1954 (Néel).
- 538.221:621.318.134 3210**
Domain Patterns on Ferrite Single Crystals—R. F. Pearson. (*Proc. Phys. Soc. B, London*, vol. 70, p. 441, plates; April 1, 1957.) Powder patterns for BaFe₁₂O₁₉ (magnadur) and Ba₃Zn₂Fe₂₄O₄₁ are shown.
- 538.221:621.318.134 3211**
Effects of Annealing on the Saturation Induction of Ferrites containing Nickel and/or Copper—L. G. Van Uitert. (*J. Appl. Phys.*, vol. 28, pp. 478-481; April, 1957.) Real deviations from the smooth functions usually described occur in ferrites subjected to differing annealing treatments when the induction measurements are made at room temperature.
- 538.221:621.318.134 3212**
Mechanism of Magnetization Processes in Very Weak Fields in some Ni-Zn Ferrites—L. A. Fomenko. (*Zh. Eksp. Teor. Fiz.*, vol. 31, pp. 1092-1093; December, 1956.) Comment on paper by Rathenau and Fast (2136 of 1956).
- 538.221:621.318.134 3213**
Form of Polder Tensor for Single-Crystal Ferrite with Small Cubic-Symmetry Anisotropy Energy—H. Seidel and H. Boyet. (*J. Appl. Phys.*, vol. 28, pp. 452-454; April, 1957.) The tensor is derived for the 110 plane, and its elements are given as a function of several parameters.
- 538.221:621.318.134 3214**
Ferrimagnetic Resonance of Gadolinium Garnet at 9300 Mc/s—J. Paulevč. (*C.R. Acad. Sci., Paris*, vol. 244, pp. 1908-1910; April 1, 1957.) Experimental results were obtained for temperatures from 4°K to 700°K. The compensation temperature is 290°K at which there is a discontinuation in the value of the field strength H . See 183 of 1956.
- 538.221:621.318.134:538.569.4 3215**
Domain Structure Effects in an Anomalous Ferrimagnetic Resonance of Ferrites—R. C. LeCraw and E. G. Spencer. (*J. Appl. Phys.*, vol. 28, pp. 399-405; April, 1957.) Measurements of the intrinsic tensor permeability of unsaturated Ni ferrite at 9.3 kmc have revealed an anomalous resonance for negative (anti-Larmor) circularly polarized fields. Effects are explained by theory. Since the anomalous resonance depends on domain structure and appears to occur generally, it is useful for studying magnetization processes and hf phenomena in ferrites.
- 538.63:546.59 3216**
Galvanomagnetic Properties of Gold—N. E. Alekseevski and Yu. P. Gađukov. (*Zh. Eksp. Teor. Fiz.*, vol. 31, pp. 947-950; December, 1956.) Electrical conductivity and the effect of magnetic fields up to 23,000 oersted were determined experimentally in the temperature range 0.05-20.4°K.
- 538.632:546.87 3217**
On the Hall Effect in Bismuth at Low Temperature—H. Hasegawa, S. Nakano, and N. Hashitsume. (*J. Phys. Soc. Japan*, vol. 12, p. 104; January, 1957.) Theoretical discussion and reanalysis of the experimental data of Reynolds, *et al.* (*Phys. Rev.*, vol. 96, pp. 1203-1207; December 1, 1954).
- 538.652:534.232 3218**
Dynamic Magnetostrictive Properties of Ni-Fe Alloys—C. M. Davis, Jr., H. H. Helms, and S. F. Ferebee. (*J. Acoust. Soc. Amer.*, vol. 29, pp. 431-434; April, 1957.) The suitability of Ni-Fe alloys containing from 35 to 67.3 per cent Ni for use in electromechanical transducers is investigated.
- 539.234:546.26 3219**
Electrical Properties of Arc-Evaporated Carbon Films—M. D. Blue and G. C. Danielson. (*J. Appl. Phys.*, vol. 28, pp. 583-586; May, 1957.) The electrical properties of the films before heat treatment indicate that they are more truly amorphous than any other form of carbon.
- 621.3.032.12:[621.387+621.372.56.029.64 3220**
On Processing Titanium Hydride Replenishers—D. Walsh and P. M. Shearman. (*J. Sci. Instr.*, vol. 34, pp. 161-162; April, 1957.) Methods of processing replenishers are described, with particular reference to their use in microwave coaxial-diode attenuators.
- 669.046.5:537.533.9 3221**
The Floating-Zone Melting of Refractory Metals by Electron Bombardment—A. Calverley, M. Davis, and R. F. Lever. (*J. Sci. Instr.*, vol. 34, pp. 142-147; April, 1957.) See 2147 of 1956.

MATHEMATICS

517.3 3222
The Fermi-Dirac Integrals $\mathcal{F}_p(\eta) = (p!)^{-1} \cdot \int_0^\infty e^{\eta-x} (e^x + 1)^{-1} dx$ —R. B. Dingle. (*Appl. Sci. Res.*, vol. B6, pp. 225-239; 1957.) Complete expansions are developed and values are tabulated for orders -1 and 0 for positive and negative arguments, and for orders 1, 2, 3, 4 for positive arguments.

517.3 3223
The Bose-Einstein Integrals $\mathcal{B}_p(\eta) = (p!)^{-1} \cdot \int_0^\infty e^{\eta-x} (e^x - 1)^{-1} dx$ —R. B. Dingle. (*Appl. Sci. Res.*, vol. B6, pp. 240-244; 1957.) Complete expansions are developed so that integrals of all orders can be calculated without numerical integration.

517.3 3224
The Integrals $E_p(x) = (p!)^{-1} \int_0^\infty e^{-x} (1+x)^{-1} dx$ and $F_p(x) = (p!)^{-1} \int_0^\infty e^{-x} (1+x)^{-2} dx$ and their Tabulation—R. B. Dingle, D. Arndt, and S. K. Roy. (*Appl. Sci. Res.*, vol. B6, pp. 245-252; 1957.) The applications and properties of the integrals are discussed and integrals are tabulated for arguments $x=0(0.002)0.01, 0.02(0.02)0.1(0.1)1(0.2)2(0.5)5(1)10(2)20$ at half-integer spacings of the order p .

517.9 3225
Sufficient Conditions for Non-oscillation and Oscillation of the Solution of the Equation $y'' + p(x)y = 0$ —V. A. Kondrat'ev. (*C.R. Acad. Sci. U.R.S.S.*, vol. 113, pp. 742-745; April 1, 1957. In Russian.)

51:621.3 3226
Mathematics for Electronics with Applications [Book Review]—H. M. Nodelman and F. W. Smith. Publishers: McGraw-Hill Book Co. Inc., New York, N. Y., 391 pp., 1956. (*J. Franklin Inst.*, vol. 263, pp. 84-85; January, 1957.) The book is divided into five parts including equation testing, circuit analysis, and series.

MEASUREMENTS AND TEST GEAR

53.087:519.25:621.396.822 3227
The Analysis of Finite-Length Records of Fluctuating Signals—M. J. Tucker. (*Brit. J. Appl. Phys.*, vol. 8, pp. 137-142; April, 1957.) The problem is that of estimating the characteristics of a signal by Fourier-type analysis or by direct measurement, and its fundamentals are presented with the simplest possible mathematics. The paper is concerned mainly with the accuracy of estimates of the power spectra and rms amplitudes of stationary random Gaussian processes.

621.317.3+621.372.54]:621.396.663 3228
Possible Applications of Goniometers in Telecommunications—H. Fricke. (*Nachrichtentech. Z.*, vol. 10, pp. 65-73; February, 1957.) Survey of applications including methods of measuring frequency, admittance (see 806 of 1955), line reflection coefficients, and quadrupole characteristics, and the use of goniometers in frequency separating networks and as band-pass filters.

621.317.32:537.311.4 3229
An Improved Technique for the Measurement of Contact Potential Differences—K. A. Macfadyen and T. A. Holbeche. (*J. Sci. Instr.*

- vol. 34, pp. 101-105; March, 1957.) A development of the vibrating-capacitor method is described. It is used for the measurement of contact potential differences between metals immersed in an insulating liquid to an accuracy of 0.1 mv.
- 621.317.335.2 3230
A Bridge Network for the Precise Measurement of Direct Capacitance—A. C. Lynch. (*Proc. IEE*, Part B, vol. 104, pp. 363-366, discussion, pp. 366-367; July, 1957.) This comparison bridge, with both oscillator and detector connected to earth, is suitable for use at frequencies from 4 cps to 20 mc. The balance point is independent of frequency and of stray capacitance and conductance to earth.
- 621.317.35.029.3 3231
Construction and Investigation of a Spectral Analyzer of High Selectivity in the Low-Frequency Region—M. Savelli and J. C. Solera. (*C.R. Acad. Sci. Paris*, vol. 244, pp. 2020-2023; April 8, 1957.) A note on the theory and performance of an analyzer for noise measurements in which the signal after heterodyning is filtered at near-zero frequency. The output voltage is applied to a thermocouple followed by a dc amplifier.
- 621.317.352.029.5/.6:621.315 3232
Measurement of Line Attenuation in the Frequency Range from 20 to 250 Mc/s—J. F. Bornhardt and G. Buhmann. (*Elektrotech. Z., Edn. A*, vol. 78, pp. 6-12; January 1, 1957.) Two test methods of universal application based on the use of the line resonance characteristics are described.
- 621.317.39 3233
The [present] State of Electrical Measuring Techniques with Particular Reference to their Application for the Measurement of Non-electrical Quantities—W. Hunsinger. (*Elektrotech. u. Maschinenb.*, vol. 74, pp. 49-57; February 1, 1957.)
- 621.317.42 3234
Instrument for Relative Measurements of Alternating Magnetic Fields—I. S. Shpigel, M. D. Raizer, and E. A. Myae. (*Radiotekhnika i Elektronika*, vol. 2, pp. 111-119; January, 1957.) The instrument described is based on the principle of magnetic resonance absorption, and is designed for relative measurements of weakly inhomogeneous magnetic fields with maximum differences of field strength between a pair of points in the field of $\Delta H_{max} = 3$ per cent H_0 . The errors of the instrument do not exceed ± 3 per cent ΔH_{max} at $H_0 \approx 160$ oersted.
- 621.317.42 3235
Some Possibilities of Measuring Magnetic Field Strength with Film-Type Hall-E.M.F. Generators prepared from HgSe, HgTe and their Solid Solutions—O. D. Elpat'evskaya and A. R. Regel'. (*Zh. Tekh. Fiz.*, vol. 26, pp. 2432-2438; November, 1956.)
- 621.317.616+621.317.77 3236
A Phase-Characteristic Wobbulator for the Video-Frequency Range—E. Legler. (*Rundfunktech. Mitt.*, vol. 1, pp. 20-23; February, 1957.) The instrument described has a range of about 0.3-10 mc for phase angles up to 1440° . The phase characteristics are displayed on a cro screen. Frequency response curves are also obtainable.
- 621.317.616:621.373.42:621.376.3 3237
A Simple F.M. Signal Generator and Wobbulator with Very Large Frequency Deviation—E. G. Woschni. (*NachrTech.*, vol. 7, pp. 51-55; February, 1957.) A relative frequency deviation of about 50 per cent in the lf and mf range is obtainable with the single-stage oscillator circuit described.
- 621.317.7:621.372.8:538.569.4 3238
Directional-Coupler Arrangement for Paramagnetic-Resonance Apparatus using Circularly Polarized Waves—A. Charru. (*C.R. Acad. Sci., Paris*, vol. 244, pp. 2146-2147; April 15, 1957.) Description of apparatus for operation at 3 kmc making use of a coupled rectangular-waveguide section perpendicular to the axis of a circular waveguide, whereby measurement can be made of the reflected-wave energy alone. Measurements on-diphenyl picryl hydrazyl indicate a gain in sensitivity of the order of 30 over that of apparatus previously described (*ibid.*, vol. 243, pp. 652-654; August 13, 1956.).
- 621.317.725:621.397.62 3239
Line Timebase Measurements: E.H.T. Rectifier Heater Voltages—A. Ciuciura. (*Mullard Tech. Commun.*, vol. 3, pp. 25-29; February, 1957.) A thermocouple method gives accuracy within 1 per cent.
- 621.317.729 3240
Flux Plotting Analogue for an Axially Symmetric Potential Field—W. L. Beaver. (*J. Appl. Phys.*, vol. 28, pp. 579-582; May, 1957.) The use of an electrolyte tank is described.
- 621.317.733.029.3:621.314.7 3241
Simple Transformer Bridge for the Measurement of Transistor Characteristics—W. F. Lovering and D. B. Britten. (*Proc. IEE*, Part B, vol. 104, pp. 368-373, discussion, p. 373; July, 1957.) The real and imaginary components of the impedance parameters of point-contact or junction transistors at 1 kc, connected in the common-base circuit, may be quickly measured.
- 621.317.755 3242
A Versatile Oscilloscope—(*Electronic Applic. Bull.*, vol. 17, pp. 1-10; October, 1956.) The instrument described uses a timebase generator that can be converted into an amplifier for horizontal deflection.
- 621.317.755 3243
The Ultimate Performance of the Single-Trace High-Speed Oscillograph—M. E. Haine and M. W. Jervis. (*Proc. IEE*, Part B, vol. 104, pp. 379-384, discussion, pp. 390-392; July, 1957.) An improvement of 10-100 times the present resolution is possible theoretically, without loss of deflection sensitivity.
- 621.317.755 3244
The Design and Performance of a New Experimental Single-Transient Oscillograph with Very High Writing Speed—M. E. Haine and M. W. Jervis. (*Proc. IEE*, Part B, vol. 104, pp. 385-390; discussion, pp. 390-392; July, 1957.) The oscillograph has a limiting resolution of 2×10^{-13} sec per spot width.
- 621.317.755:621.385.832 3245
A New Type of Multibeam Cathode-Ray Oscillograph—Fert, Lagasse, and Clot. (See 3363.)
- 621.317.755.089.6 3246
Line Timebase Measurements: Oscilloscope Calibration Unit—P. L. Mothersole. (*Mullard Tech. Commun.*, vol. 3, pp. 30-31; February, 1957.) Provides square waves variable in amplitude from 100 mv to 100 v.
- 621.317.784 3247
Logarithmic Wattmeter—J. A. Bennet. (*Electronic Eng.*, vol. 29, pp. 266-271; June, 1957.) An electronic wattmeter using logarithmic and antilogarithmic circuits for the measurement of arc loss in mercury-arc rectifiers is described.
- 621.385.001.4:534.1 3248
Standardized White-Noise Tests—J. Robbins. (*Electronic Ind. Tele-Tech.*, vol. 16, pp. 68-69, 122; February, 1957.) A noise generator is used to operate an accelerometer to produce wide-frequency, high-g vibrations for performance tests on tubes and circuit components.
- 621.385.032.216.001.4:621.317.018.75 3249
A Pulse Method for Measuring the Interface Layer of Oxide Cathodes—Lieb. (See 3355.)

OTHER APPLICATIONS OF RADIO AND ELECTRONICS

- 526.2:621.396.9 3250
Surveying Instrument for the Precise Measurement of Length—(*Engineer, London*, vol. 203, p. 538; April 5, 1957.) Description of the "tellurometer," which has a range of about 35 miles and probable error 1 part in 300,000 ± 2 in. Measurement is based on the phase shift between the outgoing and incoming modulation of a wave transmitted by the "master" station, and reradiated from the "remote" station. The wavelength used is 10 cm, with "pattern" modulation frequencies of 10, 9.99, 9.9 and 9 mc.
- 531.78.087.252:621.314.7 3251
Transistorized Strobe measures Shaft Torque—J. Patraiko. (*Electronics*, vol. 30, pp. 147-149; June 1, 1957.) An improved stroboscope for torque measurements on shafts rotating up to 60,000 rpm. For a more detailed account, see IRE TRANS., vol. IE-3, pp. 3-11; March, 1956.
- 621-52:621.314.7:623.98 3252
Transistors Stabilize Missile Ships—R. Scheib, Jr. (*Electronics*, vol. 30, pp. 138-143; June 1, 1957.) A description of measuring, computing, and servomechanism techniques used in controlling underwater fins to reduce roll of a missile-launching ship.
- 621-57:537.228.4 3253
High-Speed Electrostatic Clutch—C. J. Fitch. (*Product Eng.*, vol. 28, pp. 189-191; February, 1957.) Description and performance details of a 3-clutch unit based on the Johnson-Rahbeck effect.
- 621.317.39.082:621.38 3254
Electromechanical Devices—L. A. Goncharski. (*Uspekhi Fiz. Nauk.*, vol. 61, pp. 227-302; February, 1957.) See also 613 of 1957 and back references.
- 621.317.79:531.7 3255
Transducer Indicator System—W. C. Vaughan. (*Electronic Radio Eng.*, vol. 34, pp. 286-290; August, 1957.) Theoretical analysis of a displacement indicator using an inductance transducer and moving-coil dynamometer indicating instrument. See also 895 of 1957 (Spratt).
- 621.365.5:621.385.3 3256
The Design and Operation of High-Power Triodes for Radio-Frequency Heating—Pohl. (See 3359.)
- 621.373.029.4/.51:621.383.2 3257
Generation of Oscillations in Photocells and Photomultipliers—P. V. Makovetski. (*Zh. Tekh. Fiz.*, vol. 26, pp. 2652-2660; December, 1956.) Stable ultrasonic-frequency oscillations can be produced within narrow ranges of illumination intensities and electrode potentials; the frequency of oscillations is a function of the circuit time constant. Experimental results are presented graphically.
- 621.384.6 3258
Envelope Method for Investigating Free Oscillations in Accelerators—A. M. Baldin, V. V. Mikailov, and M. S. Rabinovich. (*Zh. Eksp. Teor. Fiz.*, vol. 31, pp. 993-1001; Decem-

ber, 1956.) The envelope of particle trajectories for a large number of revolutions is used in the calculations, rather than the individual trajectories themselves. The method is illustrated by an application to accelerators with a sectional magnet and with strong focusing.

621.384.612 3259
Excitation of Betatron Oscillations by Synchrotron Momentum Oscillations in a Strong-Focusing Accelerators—Yu. F. Orlov. (*Zh. Eksp. Teor. Fiz.*, vol. 32, pp. 130-134; January, 1957.)

621.384.7 3260
An Application of a Difference-Type Electrostatic Field in the Spectroscopy of Beams of Charged Particles—M. I. Korsunski and V. A. Bazakutsa. (*C.R. Acad. Sci. U.R.S.S.*, vol. 113, pp. 1029-1031; April 11, 1957. In Russian.)

621.385.833 3261
Electron-optical Systems, the Fields of which are Independent of One Coordinate—Yu. V. Vandakurov. (*Zh. Tekh. Fiz.*, vol. 26, pp. 2578-2594; November, 1956.) Electron-optical systems with cylindrical or rotationally symmetrical fields are considered. In these systems one of the two differential equations determining the deviation of the trajectory of any given particle from the axial trajectory can be replaced by a first-order equation. The results obtained are applied to the investigation of fields for which electric potential is symmetrical and the scalar magnetic component antisymmetrical to the central plane. In particular, fields of 1) a linear current, 2) a spherical capacitor, 3) a cylindrical capacitor and 4) a combination of an inhomogeneous magnetic field with that of a cylindrical capacitor, are considered. In the latter case fields with large dispersion are found in the absence of second-order aberrations depending on the divergence angle of the beam in the central plane.

621.385.833 3262
Third-Order Paths in Electron Mirrors—P. Schiske. (*Optik, Stuttgart*, vol. 14, pp. 34-45; January, 1957.)

621.385.833 3263
Experimental Study of the Velocity Spectrum of Electrons Transmitted by the Diaphragm of an Emission-Type Electron Microscope—F. Pradal and R. Simon. (*C.R. Acad. Sci., Paris*, vol. 244, pp. 2150-2152; April 15, 1957.) The velocity spectrum becomes narrower as the diaphragm diameter is reduced. See also 2264 of 1957 (Fert and Simon).

621.385.833:537.533.72 3264
Investigations of a Special Deflection System for Electron Beams—R. Gain. (*Optik, Stuttgart*, vol. 14, pp. 49-71; February, 1957.) The system described, which has the deflection characteristics of an inhomogeneous prism, consists of a wire and a flat plate at a potential different from that of the adjacent electrodes. The equipotential lines are plotted for various electrode arrangements and analytical formulas are derived. Calculations of deflection and aberration are in good agreement with results of tests on an experimental or tube incorporating this system; comparisons with a normal or tube are also made.

621.385.833:537.533.72 3265
Mechanically Adjustable Electrostatic Unipotential Lenses—B. Rajewsky and W. Lipfert. (*Optik, Stuttgart*, vol. 14, pp. 72-73; February, 1957.) In the lens system outlined one of three cylindrical electrodes is movable in the direction of its axis to change magnification.

621.385.833:537.533.72 3266
Asymptotic Image Distortions—F. Lenz. (*Optik, Stuttgart*, vol. 14, pp. 74-82; February, 1957.) A modified theoretical treatment of aberrations is developed which takes account of the interaction between the lenses; e.g., in an electron microscope.

621.387.4:612 3267
Some Nucleonic Instruments for Clinical Use—E. W. Pulsford and N. Veall. (*J. Brit. IRE*, vol. 17, pp. 299-307; June, 1957.) Detailed descriptions are given of a four-channel logarithmic ratemeter, a portable Geiger-counter-type clinical monitor, a recording ratemeter for observing transient phenomena, and a β - γ ionization chamber.

621.387.462:539.16.08:537.311.33 3268
Mechanism of the Forming of Pulses in Semiconductor Crystal Counters (Motion of Charges in Pulse Ionization in Semiconductors)—S. M. Ryvkin. (*Zh. Tekh. Fiz.*, vol. 26, pp. 2667-2683; December, 1956.)

621.398:551.46 3269
Buoy telemeters Ocean Temperature Data—R. G. Walden, D. D. Ketchum, and D. N. Frantz, Jr. (*Electronics*, vol. 30, pp. 164-167; June 1, 1957.) On reception of an appropriate tone-modulated signal a transistor receiver triggers a transmitter in the buoy. A 15-second transmission cycle includes low and high reference tones and a tone determined by a thermistor indicating water temperature. A range of 600 miles has been obtained under favorable conditions.

621.398:621.317.361.029.4 3270
Methods of Telemetry L. F. Oscillatory Phenomena—W. Nicolai. (*Elekt. Rund.*, vol. 11, pp. 8-12; January, 1957.) A comparison shows fm methods to be superior to AM methods for telemetry frequencies ranging from zero to about 1 kc. Details are given of single-channel experimental equipment and of a two-channel telemetry system used for medical applications.

681.188:413:8.03 3271
Automatic Programming of Operations in Translation from One Language into Another—S. N. Razumovski. (*C.R. Acad. Sci. U.R.S.S.*, vol. 113, pp. 760-761; April 1, 1957. In Russian.)

621.398+621.317.083.7 3272
Radio Telemetry [Book Review]—M. H. Nichols and L. L. Rauch. Publishers: John Wiley & Sons, Inc., New York, N. Y. and Chapman & Hall, Ltd., London, 2nd ed. 461 pp.; 1957 (*Electronic Eng.*, vol. 29, p. 301; June, 1957.) "... a comprehensive treatment of the basic theory of radio telemetry together with a review of current equipment." Originally published for the U.S.A.F.

PROPAGATION OF WAVES

538.566.2 3273
On the Theory of Reflection from a Wire Grid Parallel to an Interface between Homogeneous Media—J. R. Wait. (*Appl. Sci. Res.*, vol. B6, pp. 259-275; 1957.) The plane-wave solution for arbitrary incidence is generalized for cylindrical wave excitation. The problem of energy absorption from a magnetic line source by a grid situated on the surface of a dissipative half-space is examined, this being a two-dimensional analogy of a vertical antenna with radial wire earth system.

621.396.11 3274
Fading of Radio Waves Scattered by Dielectric Turbulence—R. A. Silverman. (*J. Appl. Phys.*, vol. 28, pp. 506-511; April, 1957.) Fading is attributed to 1) time variation of the scattering eddies as seen in a coordinate system

moving with the local wind velocity, and 2) Doppler shifting produced by the convection of the scattering eddies by the mean wind and by the macroeddies.

621.396.11:551.510.535 3275
Influence of Collisions on Ionospheric Reflection—P. Poincelot. (*C.R. Acad. Sci., Paris*, vol. 244, pp. 2031-2033; April 8, 1957.) Further analysis of the propagation of plane waves in a stratified medium for linear variation of ionization with height (see 3510 of 1956). An expression for viscous damping is introduced representing the effect of collisions. See also, *ibid.*, vol. 244, pp. 2298-2299; April 29, 1957.

621.396.11:551.510.535:621.396.677 3276
The Gain of a Directive Receiving Aerial for Short-Wave Back-Scatter—B. Beckmann and K. Vogt. (*Nachrichtentech. Z.*, vol. 10, pp. 90-91; February, 1957.) The antenna gain measurements briefly reported were made in West Germany with rhombic antennas of 115-m sides for normal reception of Ankara and New York and for back-scatter reception of transmissions of the nearby station at Bonames. A comparison of results obtained confirms the coherent nature of back-scatter radiation. See also 1888 of 1957.

621.396.11:621.396.96 3277
Back-Scattering from Water and Land at Centimetre and Millimetre Wavelengths—C. R. Grant and B. S. Yapple. (*Proc. IRE*, vol. 45, pp. 976-982; July, 1957.) Describes measurements of the average radar cross section of echo per unit area of surface, made at various angles of incidence at wavelengths of 3.2 cm., 1.25 cm, and 8.6 mm using vertical polarization. Over sea, the cross section was found mostly to increase with frequency and wind velocity; a considerable specular component being present at normal incidence. Over land, it varied in a complex manner with the type of terrain, but usually increased with frequency and a specular component was sometimes present. Dry vegetation was practically an isotropic scatterer.

621.396.11.029.6 3278
Influence of the Form of the Structural Function of Inhomogeneities of the Permittivity of Air on Long-Distance Tropospheric Propagation of Ultra Short Waves—V. N. Troitski. (*Radiotekhnika i Elektronika*, vol. 2, pp. 34-37; January, 1957.) Expressions are derived for the median field strength and the possible transmission bandwidth for tropospheric propagation, assuming a structural inhomogeneity function of the form $(\epsilon_1 - \epsilon_2)^2 = Bga^a$, where ϵ_1 and ϵ_2 are the dielectric constants at points 1 and 2, respectively, a is the distance between the points, and B and β are constants. The influence of the form of this function on field strength and distribution is analyzed; results indicate that it is small for the former, but considerable for the latter.

621.396.11.029.62 3279
Evidence Regarding the Mechanism of Long-Range Propagation at Metre Wavelengths by Measurements of Tropospheric Drift—L. Klinker. (*Z. Met.*, vol. 11, pp. 43-49; February, 1957.) A comparison of propagation measurements beyond optical range over a sea path and records of wind speed and direction at various altitudes appears to indicate that propagation is due predominantly to partial reflections at free inversions.

621.396.11.029.62 3280
Contribution on V.H.F. Propagation over the Sea—B. Abild. (*Tech. Hausmitt. Nordw.-Dtsch. Rdfunks.*, vol. 8, pp. 103-108; December 4, 1956.) Measurements in the 3-m band made in the period from 1952 to 1954 for both sea and land paths in North Germany

are used for a comparison of daily and yearly variations of field strength. Over land, particularly in summer, daily variations are large; over the sea only slight variations occur. The seasonal fluctuation over the sea is greater than over land. The difference is explained by climatic conditions.

621.396.11.029.62 3281
Forward-Scatter Observations at 50 Mc/s
 K. Bihl, H. A. Hess, and K. Rawer. (*Arch. elekt. Übertragung*, vol. 11, pp. 59-62; February, 1957.) Report on field strength measurements over two paths of vhf scatter propagation at 51.3 mc. A 10-kw cw transmitter at Kootwyk (Netherlands) and a special receiver of 70 cps bandwidth distant 500 km (Neuershäuser near Freiburg) and 1000 km (Toulon) were used. The mean propagation loss compared with free-space propagation was 90-100 db for either path; short bursts due to meteor trails were also observed. Some typical records are shown.

621.396.11.029.62:551.510.535 3282
Diurnal Variations of Signal Level and Scattering Heights for V.H.F. Propagation—A. D. Wheelon. (*J. Geophys. Res.*, vol. 62, pp. 255-266; June, 1957.) Scattering in the lower ionosphere is due to turbulent fluctuations of the electron plasma. The theory of gradient mixing is applied to the afternoon and early evening periods when solar control is probably more important than meteoric influences. The theory is used to explain observational data.

621.396.812.3:551.510.535 3283
Fading and Random Motion of Ionospheric Irregularities—S. N. Mitra and R. B. L. Srivastava. (*Indian J. Phys.*, vol. 31, pp. 20-42; January, 1957.) An analysis of the fading observed on transmissions at 1020 kc shows that the rms velocity in the line-of-sight of the ionospheric irregularities varied between 4 and 25 m.

RECEPTION

621.376.23 3284
Low-Distortion A.M. Demodulation—U. Köhler. (*Nachr. Tech.*, vol. 7, pp. 56-60; February, 1957.) Considerations, such as the choice of detection system, underlying the design of a high-grade test receiver are discussed.

621.376.23:621.396.822 3285
Analysis of a General System for the Detection of Amplitude-Modulated Noise—E. Parzen and N. Shiren. (*J. Math. Phys.*, vol. 35, pp. 278-288; October, 1956.) Various statistics of the output, with and without modulation, are computed for a system involving square-law detectors, and a criterion for the design of detection systems is considered.

621.376.333 3286
Dynamic Testing of Ratio Detectors—G. Rösler. (*Funk-Technik, Berlin*, vol. 12, pp. 68-71; February, 1957.) Description of method and circuits which use pulsed AM for checking the characteristics of ratio detectors.

621.396.621:621.376.33 3287
Limiters and Discriminators for F.M. Receivers: Part 5—G. C. Johnstone. (*Wireless World*, vol. 63, pp. 378-384; August, 1957.) The measurement of the AM suppression ratio and various types of limiter are described. Part 4: 2580 of 1957.

621.396.621.029.53/55 3288
Unconventional Communications Receiver—(*Wireless World*, vol. 63, pp. 388-389; August, 1957.) A description of the Racial Type-RA17 receiver which gives continuous coverage from 500 kc to 30 mc without band switching.

621.396.621.54:621.376.2/3 3289
I.F. Amplifiers in F.M./A.M. Receivers—L. W. Hampson. (*Mullard Tech. Commun.*, vol. 3, pp. 11-24; February, 1957.) Circuit design is discussed with particular reference to the Type—EF89 variable—mu rf pentode.

621.396.82:621.376.3 3290
V.H.F. Broadcasting—R. D. A. Maurice. (*Electronic Radio Eng.*, vol. 34, pp. 300-309; August, 1957.) The problem of impulsive noise and man-made interference to vhf broadcasting is discussed and methods of improving signal/noise ratio with particular reference to fm reception are described. A practical illustration of the problem shows field strengths required to protect a given reception from motor-car ignition interference.

STATIONS AND COMMUNICATION SYSTEMS

621.376.3 3291
Distortion in FM Systems—A. Dittl. (*Hochfreq. u. Elektroak.*, vol. 65, pp. 136-148; January, 1957.) Following on theoretical investigation of transient characteristics of fm systems (*ibid.*, vol. 64, pp. 184-193; May, 1956) the signal distortion is calculated with reference to bandwidth limitations particularly in relaying television signals. An approximate formula for calculating the maximum permissible frequency shift for a given amplifier characteristic and amount of distortion is obtained.

621.39.011.1 3292
Coding and Compression of Codes—L. N. Korolev. (*C.R. Acad. Sci. U.R.S.S.*, vol. 113, pp. 746-747; April 1, 1957. In Russian.)

621.391.5.029.45 3293
Selective A.F. Induction Signalling—L. E. Philipps. (*Electronics*, vol. 30, pp. 180-181; June 1, 1957.) A one-way signalling system operating in the range 6-20 kc.

621.394.441 3294
The Voice-Frequency Telegraphy System WT24/1—H. H. Voss and J. Arnold. (*Nachrichtentech. Z.*, vol. 10, pp. 81-87; February, 1957.)

621.396.001.11 3295
Improvement of Binary Transmission by Null-Zone Reception—F. J. Bloom, S. S. L. Chang, B. Harris, A. Hauptschein, and K. C. Morgan. (*PROC. IRE*, vol. 45, pp. 963-975; July, 1957.) Single-null zone (3-level) detection in a binary system of equal and opposite signals is shown theoretically to be capable of achieving about one-half of the improvement in information rate attainable by an infinite number of levels. Double-null (4-level) detection offers only a slight additional increase in rate, but may be better in practice because it is much less sensitive to variations in null level.

621.396.2:621.372.5 3296
Bandwidth Occupied in Pulse Transmission—M. S. Gurevich. (*Radiotekhnika i Elektronika*, vol. 2, pp. 38-43; January, 1957.) Analysis of the distribution of the pulse energy in a given frequency band is presented. The spectral distribution energy is calculated for rectangular, trapezoidal, triangular, cos, and cos² pulses.

621.396.65 3297
Some Information on the Radio Link Monte Erice [Sicily]—Bou Kornine [Tunisia]—(*Poste e Telecomun.*, vol. 25, pp. 157-159; February, 1957.)

62196.712.2:621.395.623.8 3298
New High-Grade Monitoring Equipment for [studio] Control Rooms—F. Enkel. (*Elek. Rund.*, vol. 11, pp. 51-54; February, 1957.)

The installation described has characteristics closely corresponding to those of modern high-fidelity domestic receivers. A spherical loud-speaker system is used for the upper frequencies. Associated matching, correcting, and compensating devices are briefly outlined.

621.396.931 3299
Recent Developments in Mobile Radio in Britain—J. R. Brinkley. (*J. Brit. IRE*, vol. 17, pp. 287-293; May, 1957.) Some comments on the relation between modulation systems and channel spacing are included.

SUBSIDIARY APPARATUS

621-52 3300
The Inductosyn and its Application to a Programmed Coordinate Table—L. H. R. Harrison, B. A. Horlock, and F. D. Hunt. (*Electronic Eng.*, vol. 29, pp. 254-259; June, 1957 and pp. 331-335; July, 1957.) Description of a new control element developed for the U.S.A.F. with an accuracy within 5 seconds of arc in its rotary form and within 0.0001 inches in its linear form. Its application to position control systems is described, particularly for machine tools. For a similar description, see *J. Brit. IRE*, vol. 17, pp. 369-383; July, 1954 (Finden and Horlock).

621-526:621.375.088.7 3301
A Zero-Correcting Servo for Use with D. C. Amplifiers—B. Shackel and M. Beaney. (*Electronic Eng.*, vol. 29, pp. 284-286; June, 1957.) This device is designed primarily to compensate drift voltages which have developed in the external output circuit.

621.314.63:537.311.33 3302
Tunnel Effect in Sulphide Rectifiers—Yu. M. Volokobinski. (*C.R. Acad. Sci. U.R.S.S.*, vol. 113, pp. 1239-1242; April 21, 1957. In Russian.) Results of a series of experiments on Cu₂S/Al and Cu₂S/Mg rectifiers confirm some fundamental conclusions of the tunnel-effect theory developed by Frenkel (*Phys. Rev.*, vol. 36, pp. 1604-1618; December 1, 1930.) and others.

621.316.72:621.314.7 3303
A Regulated Power Unit with Transistor Control—R. E. Reynolds. (*Mullard Tech. Commun.*, vol. 3, pp. 34-36; February, 1957.) A transistor controls the series tube element eliminating the necessity for a negative rail.

621.316.9:621.396.61:621.385 3304
Electronic Crowbar Protects Transmitter—R. G. Wenner. (*Electronics*, vol. 30, pp. 174-176; June 1, 1957.) Details of an electronic switch for protecting high-power cw transmitting tubes against flash-arc destruction.

621.318.57 3305
Electronic Time-Delay Relay with Ionization Chamber as Timing Device—H. Jucker. (*Elek. Rund.*, vol. 11, pp. 13-14; January, 1957.)

TELEVISION PHOTOTELEGRAPHY

621.397.5:389.6 3306
The New Television Standards of the C.C.I.R.—H. A. Laett. (*Tech. Mitt. Schweiz. Telegr.-Teleph. Verw.*, vol. 35, pp. 1-6; January, 1957.) The standards applicable to the 625-line system as established or revised by the Warsaw conference (August/September, 1956) are summarized.

621.397.5:535.623 3307
Colour Television Transmission—K. Teer. (*Electronic Radio Eng.*, vol. 34, pp. 280-286; August, 1957 and pp. 326-332; September, 1957.) Further details of principles and circuits of a system [see 1224 of 1956 (Haantjes and Teer)], using two subcarriers combined with a luminance signal, originally demonstrated be-

fore CCIR Study Group XI in 1955. Subsequent modifications and improvements are also described.

621.397.5:535.623 3308

Colour Television Marks Time—(Wireless World, vol. 63, pp. 354-355; August, 1957.) Research trends from the Paris International Symposium suggest the NTSC system is the most suitable for European use.

621.397.5:535.623 3309

An Alternative Colour TV System—E. J. Gargini. (Wireless World, vol. 63, pp. 361-364; August, 1957.) The signal is compatible for monochrome receivers in a similar manner to the NTSC system, but no brightness information is carried by the color signal. This is achieved by instantaneously dividing the chrominance signal by a brightness signal which is the mean of the three-color component signals.

621.397.5:535.623:621.385.832:535.37 3310

Luminophores based on ZnS and ZnSe for Colour Television—Blazhnova, Inskrintseva, and Kas'yanova. (See 3159.)

621.397.5:535.7 3311

Television Images—T. G. Crookes. (Nature, London, vol. 179, pp. 1024-1025; May 18, 1957.) A viewer 6 feet away from a screen 10½ inches X 8 inches rolls his eyes rapidly first in a horizontal and then in a vertical arc. Pictures are seen, which, although displaced from their place of origin, are first images not after-images. They are due to the method by which a television image is formed on the cr-tube screen, and are not seen with cinematograph or still pictures.

621.397.5:621.396.4 3312

Study of Multichannel Sound Transmission from a Single Transmitter: Application to Bilingual Television—L. Bourassin. (Électronique, Paris, pp. 15-20; January, 1957.) Two methods of modulation suitable for French standards are discussed. See also 2605 of 1957 (Puzol(s)) and 2300 of 1957 (Dubec).

621.397.5:621.396.4 3313

Simple Device for Sound Reception of the Bilingual Television System of Algeria—P. Rogues. (TSF et TV, vol. 57, pp. 16-17; January, 1957.) Brief outline of system. See also 3312 above and Télévision, no. 70, pp. 22-23; January, 1957.

621.397.6:621.395.625.3 3314

Picture-Synchronized Magnetic Sound Recording in Television—H. Vollmer. (Elek. Rund., vol. 11, pp. 33-37; February, 1957.) Problems arising from the use of a pilot frequency on magnetic recording tape are discussed, and some suitable equipment is described.

621.397.611 3315

Slow-Scan Adapter for Conventional TV Signals—S. K. Altes and H. E. Reed. (Electronics, vol. 30, pp. 153-155; June 1, 1957.) A description of a converter providing a slow-scan video output signal with a bandwidth compression of 800 to 1.

621.397.621.2 3316

Improvements in Television Receivers: Part I—Stabilization of the Line and Frame Deflection Circuits—(Electronic Applic. Bull. vol. 17, pp. 12-25; October, 1956.)

621.397.621.2:535.623:621.385.832 3317

Deflection and Focusing in Local [post-deflection] Spot Position Control for Electron Beams—U. Pellegrini. (Alta Frequenza, vol. 26, pp. 25-40; February, 1957.) Further investigation of the two systems previously discussed

(2616 of 1957). For the Lawrence grid system the deflection and focusing characteristics are determined separately by an approximation method. For the other system the differential equations of electron motion are solved numerically to obtain the deflection sensitivity.

621.397.7:621.396.67.029.62 3318

The Crystal Palace Television Transmitting Station—F. C. McLean, A. N. Thomas, and R. A. Rowden. (Proc. IEE, Part B, vol. 104, pp. 392-393; July, 1957.) Discussion on 3895 of 1956.

621.397.7.029.63/.64:621.396.65 3319

Study of the Television Link Monte Generoso—Monte Ceneri [Switzerland]—F. Grandchamp. (Tech. Mitt. schweiz. Telegr.-Teleph Verw., vol. 35, pp. 14-22; January, 1957. In French and Italian.)

621.397.8 3320

The Problem of Assessing Picture Quality, particularly of Television Pictures—W. Kroebe and F. Below. (Rundfunktech. Mitt., vol. 1, pp. 2-6; February, 1957.) On the basis of amount of detail recognizable, as a function of object size with the contrast between object and background as a parameter, the assessment of quality can be made independent of aesthetic considerations or picture content. For descriptions of such methods, see 3321 and 3322 below.

621.397.8 3321

An Objective Method of Determining Television Picture Quality—F. Below, W. Kroebe, and H. Springer. (Rundfunktech. Mitt., vol. 1, pp. 7-11; February, 1957.) The effect of contrast and other objectively measurable parameters on the recognizability of picture detail is discussed. A method of determining picture sharpness is outlined but requires experimental confirmation. Twenty-two references.

621.397.8 3322

Measurements for the Investigation of Picture Quality of Television Systems in the Case of Moving Objects—F. Arp and H. Baurmeister. (Rundfunktech. Mitt., vol. 1, pp. 12-16; February, 1957.) A method is described of objectively testing an observer's recognition of moving detail in a television picture. The test picture of moving circular disks is produced by projecting an optical or television image of black spheres rolling over an inclined illuminated screen. Results are shown in graphical form and discussed.

621.397.8:535.61 3323

Contrast and Grey Scale in the Television Image—R. Suhrmann. (Elek. Rund., vol. 11, pp. 43-46; February, 1957.) The influence of room lighting on contrast and gradation is examined; the effectiveness of compensating gradation losses by an increase in control voltage or brightness was checked by subjective tests.

621.397.813 3324

Delay Distortions in Vestigial-Sideband Television Transmission and their Elimination—F. Kirschstein. (Hochfreq. u. Elektroak., vol. 65, pp. 119-126; January, 1957.) The effects of phase-delay errors on the quality of received pictures is investigated. The merits of remedies such as phase pre-correction at the transmitter [see also 584 of 1956 (Peters)] and phase-linear receivers [2235 of 1956 (van Weel)] are discussed.

621.397.5 3325

Television Engineering Principles and Practice: Vol. 3—Waveform Generation [Book Review]—S. W. Amos and D. C. Birkinshaw. Publishers: Iliffe, London, 226 pp.; 1957. (Electronic Eng., vol. 29, p. 301; June, 1957.)

TRANSMISSION

621.396.61.029.62 3326

Radio Transmitter for Ionospheric Scatter—J. L. Hollis, W. H. Collins, and A. R. Schmidt. (Electronics, vol. 30, pp. 144-146; June 1, 1957.) The transmitter operates in the range 30-65 mc with an output power of 60 kw. A neutralized triode driver operates as a linear amplifier to deliver 8-12 kw to an 8-tube grounded grid power amplifier.

TUBES AND THERMIONICS

621.314.63 3327

Exact Current/Voltage Relation for the Metal/Insulator/Metal Junction with a Simple Model for Trapping of Charge Carriers—G. H. Suits. (J. Appl. Phys., vol. 28, pp. 454-458; April, 1957.)

621.314.63:546.289 3328

Very-Narrow-Base Diode—R. H. Rediker and D. E. Sawyer. (Proc. IRE, vol. 45, pp. 944-953; July, 1957.) The method of construction of a Ge planar-alloy-junction diode, having an active base width of the order of microns, is described. The theoretical treatment includes the effect of the nonideal "ohmic" contact, which is essential to its performance as a rectifier, but limits its high-frequency performance.

621.314.63+621.314.7:621.396.822 3329

Theory of Shot Noise in Junction Diodes and Junction Transistors—A. van der Ziel. (Proc. IRE, vol. 45, p. 1011; July, 1957.) Note of correction and comment on 600 of 1956.

621.314.632:537.311.33:546.289 3330

On the Current/Voltage Characteristics of Metal/Germanium Rectifying Contacts—G. Mesnard and A. Dolce. (C.R. Acad. Sci., Paris, vol. 244, pp. 2025-2028; April 8, 1957.) A rapid increase of current for high reverse voltages is deduced theoretically from known characteristics of n-type Ge.

621.314.632:537.311.33:546.289 3331

The Variation of the Inverse Current of Metal/Germanium Rectifying Contacts when the Carrier Concentrations in the Interior of the Semiconductor Deviate from Thermal-Equilibrium Values—G. Mesnard and A. Dolce. (C.R. Acad. Sci., Paris, vol. 244, pp. 2141-2143; April 15, 1957.)

621.314.7 3332

A Study of High-Speed Avalanche Transistors—J. R. A. Beale, W. L. Stephenson, and E. Wolfendale. (Proc. IEE, Part B, vol. 104, pp. 394-402; July, 1957.) Transistors operated above a critical supply voltage appear as a 2-terminal negative resistance and give a relaxation oscillation at a much higher speed than achieved in conventional use. The design, application, and static and dynamic properties of transistors operated in this way are discussed.

621.314.7:537.311.33 3333

On the Injection of Carriers into a Depletion Layer—Matthei and Brand. (See 3202.)

621.314.7:621.317.733.029.3 3334

Simple Transformer Bridge for the Measurement of Transistor Characteristics—Lovering and Britten. (See 3241.)

621.314.7:621.385.4 3335

High-Frequency Circuits use Meltback Tetrodes—D. W. Baker. (Electronics, vol. 30, pp. 177-179; June 1, 1957.) A description of the design and application of the tetrode-type transistor [see 677 of 1953 (Wallace, et al.).]

621.314.7:621.385.4:546.28 3336

High-Performance Silicon Tetrode Transistors—R. F. Stewart. (Proc. IRE, vol. 45, p. 1019; July, 1957.)

- 621.314.7:621.396.822 3337
Behaviour of Noise Figure in Junction Transistors—E. G. Nielsen. (Proc. IRE, vol. 45, pp. 957–963; July, 1957.) The work is based on a simplified version of a noise equivalent circuit developed by van der Ziel (600 of 1956). Calculations show that for minimum noise figure the ohmic base resistance and emitter current should be small, while the current gain and its cutoff frequency should be large.
- 621.383.27 3338
Fluctuations in Photomultipliers—P. Moatti. (C.R. Acad. Sci., Paris, vol. 244, pp. 2366–2368; May 6, 1957.) Previous theoretical work (2948 of 1951) is modified to allow for incomplete electron capture by the different dynodes.
- 621.383.5 3339
Improving the Linearity of Barrier-Layer Photocells—D. G. Wyatt. (J. Sci. Instr., vol. 34, pp. 106–108; March, 1957.) "A modification of the Campbell-Freeth circuit is described, whereby the effective series resistance of a barrier-layer photocell, insofar as it is constant, may be eliminated. The results suggest that the series resistance includes part of the barrier layer."
- 621.385(083.74) 3340
IRE Standards on Electron Tubes: Definitions of Terms, 1957. (Proc. IRE, vol. 45, pp. 983–1010; July, 1957.) Standard 57 IRE 7.S2.
- 621.385:621.395.64 3341
Electron Tubes for the Transatlantic Cable System—J. O. McNally, G. H. Metson, E. A. Veazie, and M. F. Holmes. (P.O. Elec. Engrs' J., vol. 49, pp. 411–419; January, 1957.) See 1951 of 1957.
- 621.385.001.4:534.1 3342
Standardized White-Noise Tests—Robbins. (See 3248.)
- 621.385.029.6 3343
International Congress on Microwave Valves—(Onde élect., vol. 37, pp. 86–193; February, 1957.) Further selection of papers presented at the 1956 Congress in Paris. See also 2643 of 1957.
- 621.385.029.6 3344
Analysis of the Energy Interchange between an Electron Stream and an Electromagnetic Wave—V. N. Shevchik. (Radiotekhnika i Elektronika, vol. 2, pp. 104–110; January, 1957.) Analysis is presented of the electron bunching process in a traveling wave, which is identical with that occurring in a klystron. The maximum of the first harmonic of the current in the traveling wave was calculated and the efficiency of the interaction between the electron stream and the traveling wave was determined. The concept of synchronization was clarified. The calculations have been extended to the traveling-wave tube, and the optimum small-amplitude working conditions were found for a backward-wave generator.
- 621.385.029.6 3345
High-Frequency Oscillations in Electron Beams with a Periodically Varying Velocity—P. V. Bliokh. (Radiotekhnika i Elektronika, vol. 2, pp. 92–103; January, 1957.) The interaction of em waves with a compensated electron beam in a longitudinal periodic electric field is examined by means of kinetic equations. Dispersion equations, derived for small signals, are used in determining the stability conditions of the electron beam.
- 621.385.029.6 3346
Barkhausen Electron Oscillations as the Basis of Velocity-Modulated Values—H. E. Hollmann. (Hochfreq. u. Elektroak., vol. 65, pp. 112–119; January, 1957.) A phenomenological survey of the history of this type of microwave tube. Over 24 references, mainly to German literature.
- 621.385.029.6 3347
Space-Charge Effects in Beam-Type Magnetrons—R. W. Gould. (J. Appl. Phys., vol. 28, pp. 599–605; May, 1957.) A small-signal theory for magnetron-type traveling-wave tubes is developed assuming a thin electron beam. The starting conditions for an M-type backward-wave oscillator are deduced. If the tube is long in space-charge wavelengths, the starting current is appreciably reduced.
- 621.385.029.6 3348
Widening of Oscillation Zones of Decimetre-Waveband Magnetrons—G. M. Gershtein and G. L. Vitel's. (Radiotekhnika i Elektronika, vol. 2, pp. 120–121; January, 1957.)
- 621.385.029.62:621.376.32 3349
A Frequency-Modulated Magnetron—E. Petrasco and I. I. Vasilescu. (C.R. Acad. Sci., Paris, vol. 244, pp. 2296–2298; April 29, 1957.) A diagram and performance curves are shown for a special construction of magnetron with a truncated-cone anode. At 110 mc a highly linear frequency excursion approaching 30 mc is obtained for a 30 per cent variation of anode voltage (950–1350 v), a minimum voltage change of 1.5 v gives a 200 kc deviation with negligible amplitude modulation. Output power is about 1 w.
- 621.385.029.63/64:621.374.4 3350
A Travelling-Wave Frequency Multiplier—D. J. Bates and E. L. Ginzton. (Proc. IRE, vol. 45, pp. 938–944; July, 1957.) The tube has two helices in cascade, the output helix being of dispersive, forward-wave type with voltage tuning for selection of a particular harmonic in the range 2–4 kmc. Useful input range is 0.1–1 kmc. Multiplication ratios up to 10 or 15 are feasible with substantial gain. Output of a few milliwatts has been obtained at harmonics as high as the 40th.
- 621.385.029.64 3351
Space Harmonics of an Electron Wave—G. A. Bernashevski. (Radiotekhnika i Elektronika, vol. 2, pp. 124–125; January, 1957.) Brief note on systems of the type described by Kleinwächter (2075 of 1952 and 279 of 1953).
- 621.385.032.2:537.533 3352
Transverse Scaling of Electron Beams—G. Herrmann. (J. Appl. Phys., vol. 28, pp. 474–478; April, 1957.) A discussion of scaling operations and their practical applications, particularly in analyzing beams when actual velocity effects are to be considered.
- 621.385.032.213:621.396.822 3353
On the Cause of the Anomalous Flicker Effect—W. W. Lindemann and A. van der Ziel. (J. Appl. Phys., vol. 28, pp. 448–451; April, 1957.) Experiments are described which indicate that the flicker effect is caused by sudden bursts of positive ions emitted by the cathode in a period much less than 1 μ sec.
- 621.385.032.216 3354
The Effect of Sulphur and Oxygen on the Electrical Properties of Oxide-Coated Cathodes—G. S. Higgins. (Brit. J. Appl. Phys., vol. 8, pp. 148–149; April, 1957.) Poisoning and recovery experiments substantiate the Loosjes-Vink theory of conduction (see 3208 of 1950).
- 621.385.032.216.001.4:621.317.018.75 3355
A Pulse Method for Measuring the Interface Layer of Oxide Cathodes—A. Lieb. (Nachrichtentech. Z., vol. 10, pp. 88–89; February, 1957.) In the method described pulses are applied in turn to the tube under test and to a reference tube without interface layer. From a direct comparison of the resulting pulse shapes on a cro screen and the consequent adjustment of a resistor and capacitor, the layer characteristics can be determined. For an earlier pulse method, see 2052 of 1951 (Eisenstein).
- 621.385.1 3356
A New Method of Investigating the Microphony of Valves: Part 2—Test Arrangements and Results—I. P. Valkó, A. Kemény, and L. Szécsi. (Hochfreq. u. Elektroak., vol. 65, pp. 129–136; January, 1957.) Details of the test apparatus and procedure are given and test results are discussed and compared with those obtained by other methods. Part 1: 1981 of 1957 (Valkó).
- 621.385.2:621.3.011.4 3357
The Capacitance between Diode Electrodes in the Presence of Space Charges—C. S. Bull. (Proc. IEE, Part B, vol. 104, pp. 374–378; July, 1957.) The capacitance of the active area of a space-charge-limited diode is zero; that of a saturated diode varies with a sudden transition from twice the cold value to the cold value as the anode potential is varied from the saturation value to the value at which space charge is negligible.
- 621.385.3 3358
The Determination of the Space-Charge Field, the Space-Charge Capacitances and the Characteristics of a Planar Triode by means of a Resistance Network with Current Sources—G. Čremošnik and M. J. O. Strutt. (Arch. elektr. Übertragung, vol. 11, pp. 63–75; February, 1957.) Results obtained by means of the network analog, particularly applied to the triode-connected tube type EL6, are compared with results of precise calculations and with published data; close agreement is found. Thirty-seven references.
- 621.385.3:621.365.5 3359
The Design and Operation of High-Power Triodes for Radio-Frequency Heating—W. J. Pohl. (Proc. IEE, Part B, vol. 104, pp. 410–416; July, 1957.) A new range of power triodes and the principles of their design.
- 621.385.5 3360
Input Conductance of a Pentode—Yu. N. Prozorovski. (Radiotekhnika i Elektronika, vol. 2, pp. 121–123; January, 1957.) The effect of the heater/cathode capacitance on the input conductance is briefly discussed.
- 621.385.83:537.533.082.7 3361
Electron Beam Analyzer—A. Ashkin. (J. Appl. Phys., vol. 28, pp. 564–569; May, 1957.) The beam is swept across a pinhole in crossed electric and magnetic fields. The charge distribution is shown visually on a cr tube.
- 621.385.832 3362
A Survey of Image Storage Tubes—H. G. Lubszynski. (J. Sci. Instr., vol. 34, pp. 81–89; March, 1957.) Half-tone storage tubes operate either with charge restoration or with charge modulation. The construction, performance, and applications of a representative selection of these tubes are discussed.
- 621.385.832:621.317.755 3363
A New Type of Multibeam Cathode-Ray Oscillograph—C. Fert, J. Lagasse, and J. Clot. (C.R. Acad. Sci., Paris, vol. 244, pp. 2148–2150; April 15, 1957.) A new version of the multibeam cro described in 1624 of 1954 (Fert, et al.) and 2377 of 1955 (Olte). The improvements are low hv consumption, no beam interaction, and automatic time marking.

MISCELLANEOUS

- 061.4:621.396.933+621.396.96 3364
French Air Show—(*Wireless World*, vol. 63, pp. 368-370; August, 1957.) New electronic developments at the 22nd Salon International de l'Aéronautique.
- 538.569.2.047 3365
Eye Protection in Radar Fields—W. G. Egan. (*Elec. Eng., N.Y.*, vol. 76, pp. 126-127; February, 1957.) "Tests on animals indicate that eyes exposed to microwave radiation may develop cataracts. The design of protective goggles, utilizing transparent microwave shielding, is discussed."
- 621.3.002.2:551.58 3366
Climatic Resistance Code of Components for Electronic Equipment—E. Ganz. (*Bull. schweiz. elektrotech. Ver.*, vol. 48, pp. 137-141; February 16, 1957. In French.) The system of coding developed by the Commission Électrotechnique Internationale is briefly explained with examples.
- 621.3.049.75:681.142 3367
Three-Dimensional Printed Wiring—E. A. Guditz. (*Electronics*, vol. 30, pp. 160-163; June 1, 1957.) A new technique, using collimated light sources, for the production of etched wiring in the holes in ferrite cores of storage matrices.
- 621.38.019.3 3368
The Reliability of Electronic Equipment and Installations—E. Ganz. (*Elektrotech. Z. Edn A*, vol. 78, pp. 218-225; March 11, 1957.) The statistical results of typical life and performance tests are discussed.